BRUNEL UNIVERSITY

Advanced Electrospinning Apparatus for Control, Alignment and Coating

PhD Thesis

Thomas Maltby

Many thanks go to my supervisors Dr Antonio Vilches and Dr Wenhui Song for their invaluable support, advice and assistance throughout.

Also thanks to my family and friends for their constant love and support.

Additional thanks must also go to the technicians, staff, students and friends at Brunel University who have been a fountain of knowledge.

Contents

Figures

Tables

Equations

Abstract

The work contained within this thesis is concerned with the further innovation and the development of apparatus for the electrospinning method which in its most basic form is used to produce and deposit small diameter fibres of many polymers and other materials in a mat structure with random orientation of the deposited fibres. The focus of the innovation is concerned with expanding the ways of collecting these fibres by implementing newly developed techniques, building upon the conventional electrospinning technique and literature to create an advanced electrospinning system.

The innovation can be split into the following areas of study: Development of apparatus for the control of the electrospinning process, apparatus for the control of the deposition of the fibres and the development of apparatus for coating conductive wires and other materials with electrospun polymer fibres. Each of the apparatus designed and tested within this work build upon previous examples of experimental apparatus created by other groups as discussed in the following chapters. The apparatus developed and described is a combination of incremental improvement and previously untried combinations of the work that as gone before. All the apparatus developed for use as part of the electrospinning process were designed to be easily improved incrementally and the development cycles to achieve the final apparatus shown have also been included.

The novelty within this work is concerned the development of apparatus for use with the electrospinning process and with the overall supporting systems that have been developed alongside them. The novelty of the apparatus used in conjunction with the electrospinning process includes a remotely controlled fibre printer that can print tracks of electrospun fibres creating shapes and patterns. The development of the apparatus is discussed in detail covering all mechanical and electronic considerations and design decisions. The final apparatus is shown to operate as desired with polymer tracks thicknesses of 20mm in width achieved.

A novel apparatus was developed using multiple ground electrodes that were digitally controlled in conjunction with the electrospinning method to achieve a new

method of layering aligned fibres in layers with alternating orientations. Also the apparatus can be used in an alternate mode which allows the selective electrospinning of aligned bundles of fibres between multiple electrodes in user defined patterns. The apparatus is shown to achieve good polymer fibre alignment between electrodes and also is shown to work as deigned in regard to the layering of the aligned fibres. An alternate way of using the apparatus is successfully demonstrated allowing the selective patterning of deposited fibre bundles between multiple electrodes.

A polymer coating apparatus was also developed to extend the electrospinning method to create core-shell fibres as part of a larger system developed for creating smart textiles and fibrous sensors. The novel electrospinning apparatus is shown to be able to uniformly coat both the circumference and along the length over a comparatively long length of core-shell fibre. A deposition thickness of polymer between 36 µm and 242 µm was achieved by changing the coating speed. An alignment of the electrospun fibres along the length on the core wires is also shown and discussed.

The core-shell fibres developed are used in conjunction with another developed apparatus piece that weaves a series of wires around the outer shell to create a three layer device consisting of an outer electrically conductive layer, an electrospun polymer layer and an electrically conductive core. The system is shown to successfully create these three layer devices.

1 Introduction

1.1 *Overview*

Many advancements are taking place in the development and synthesis of functional polymers for a wide range of uses. One of the most researched functional polymers is Polyvinylidene fluoride (PVDF), which when processed in a specific way can be made into a piezoelectric material. One popular way to achieve such processing is the electrospinning process, which is a well-documented process for the production of thin and thick porous films for a wide range of polymers. Using PVDF with the electrospinning process allows any deposition to be tested as a piezoelectric device once electrodes have been added.

The research presented here consists of the development of a system built upon the conventional electrospinning process containing novel sub-systems for increasing the flexibility of the electrospinning process, focusing on producing thin films, thick films and composite fibres with novel morphology. The improved control over morphology and apparatus automation is being developed to allow the development of novel piezoelectric polymeric devices in the first instance utilising PVDF for potential energy harvesting and sensor applications, however the developed systems have much more flexibility and scope as discussed.

Recent advancements and the development of functional polymers with various material properties such as biocompatibility, piezoelectric, thermal, mechanical and chemical properties allow the creation of advanced devices with unique properties. With an increasingly inter-connected and data driven world sensors and other devices are needed and new polymer technologies are well suited for these applications. As well as the development of new materials it is also essential to develop new processing techniques and apparatus that can leverage the material advancement to facilitate the development of new devices. The described work covers multiple research areas and brings together previous research to create novel apparatus and processing techniques that can be used for a wide range of applications. The need for this has been identified through the literature and study of research already carried out.

The aim of the research was to produce apparatus that could be used to process and produce polymers and enable the development of devices utilising these

functional polymers. The contribution to knowledge within this work is concerned with the development of the apparatus, the testing of the apparatus and the production of samples and devices from this apparatus.

A process called the electrospinning technique was identified as a polymer processing method that that had a large scope for improvement from investigation of the literature. It also allows the production of many different polymers and can be used to achieve a large range of morphologies ranging from producing single polymer fibres of a diameter of a hundred nano-meters [1] and greater to creating porous randomly orientated or aligned fibrous mats [2].

Some research had already been done into improving the basic electrospinning technique which creates the polymer fibres but there was scope to take this work further and combine different aspects to create a more advanced electrospinning process. This became the focus of the research reported here and can be split into distinct areas including controlling and aligning the polymer fibres during the electrospinning process, depositing polymer fibres into patterns and forming polymer depositions of different morphologies.

The research carried out used a single polymer for experimentation and testing of the developed apparatus, Polyvinylidene fluoride (PVDF) was chosen from the many polymers that can be electrospun as when it's processed by the electrospinning technique the polymer exhibits piezoelectric properties. This meant that the apparatus developed created functional devices that could then be tested and evaluated by looking for the piezoelectric response from the deposited electrospun polymer fibres. It also led to the design of systems that exploited the piezoelectric properties of the deposited polymer to create advanced devices that could be used for sensing applications.

The work shown is concerned with the design, development testing of multiple pieces of apparatus which allows improvement of the electrospinning process. Particular focus is on the development of apparatus to align fibres during deposition, including alignment of fibres in alternating layers and along the length of wires. An emphasis on automation was made for the apparatus developed to help with ease of experimentation and use. Another example is a developed piece of equipment that

allows the deposition on randomly orientated fibres into patterns by using a moving electrode bed.

Other apparatus was developed as part of larger systems allowing the collection and testing of substrate free electrospun films. Also a system to coat electrospun fibres around flexible fibres such as wires and then add an outer woven electrode is shown. Together the apparatus becomes a series of accessories for the standard electrospinning method which greatly expands the capabilities of the process.

1.2 *Motivation*

With the current, sustained interest and developing markets for smart personal electronics, low power independent wireless sensing networks and new sensor technologies there is a great need for innovation to meet the upcoming needs for these types of technologies. New energy harvesting technologies are needed for powering low power devices and sensors used in remote and inaccessible positions. Flexible polymer sensors and energy harvesters have the ability to be used in such roles and also have applications for powering low power consumer electronics if utilised intelligently and on the correct scale.

Current commercial electrospinning systems are basic in their design with limited accessories with little automation available to expand the electrospinning process to allow more complex morphologies and devices to be created. For example IME technologies produce an electrospinning system that comes with a range of accessories that allow electrospinning onto a number of different rotating drum electrodes [3] this allows the creation of electrospun deposition morphologies other than those created by the normal process however they are still basic morphologies with little automation. There is a need for improved apparatus in the commercial sector to allow better control of the electrospinning process and to improve the range of deposition morphologies available.

The focus on expanding the electrospinning process with the aim to produce better devices is beneficial for multiple disciplines as the electrospinning process and therefore the advanced electrospinning system developed can be used with most polymers to produce a multitude of devices for different applications [4].

2 Literature

2.1 *Introduction*

This following chapter explores what has already been achieved in regards to electrospinning, materials, supporting apparatus and applications. It also focuses on the polymer PVDF used for experimentation and testing the developed apparatus. Sensors and other devices that utilise PVDF are shown to give an idea of what has already been achieved and also what could be developed in future.

2.2 *Electrospinning*

2.2.1 Electrospinning Process

The electrospinning technique is a process to produce nanoscale and micron diameter fibres that are collected in a randomly orientated fibrous mat. The process first appears in literature in a conference paper in 1993 and published by the same group in 1995 in the Journal of Electrostatics [2]. The conventional electrospinning technique has not changed since then and in its simplest form a polymer solution is slowly fed to the tip of a needle. At the needle tip the solution is held by its surface tension. In most electrospinning experiments the needle is held vertically with the surface tension of the solution preventing the solution dripping from the needle tip by gravity.

The needle itself is used as an electrode by attaching it to the positive output terminal of a high voltage (HV) power supply. Directly below the needle at a distance decided on by experimental procedure is a conductive plate that is connected to the ground terminal of the HV power supply as a base electrode. When the HV power supply is turned on the potential voltage on the needle causes the suspended polymer solution to become positively charged. The charged solution is then attracted towards the base electrode.

At the needle tip the solution is drawn out into a conical shape. This is described as a Taylor cone [5] which is defined by having a half angle of 49.3° and which was initially described in regards to the electrostatic work done by Geoffrey Taylor where the fluid tension and electrostatic forces find an equilibrium [6]. This work led to the electrospraying technique, a precursor to electrospinning. It has been shown in

literature that for electrospinning it is not a true Taylor cone as the cone has been measured with a half angle of 33.5° [7]. However the term is still used for describing the cone formed during electrospinning.

Once the charge in the solution is great enough and a cone has formed then the cone starts jetting fluid from its tip. This jet is initially stable and highly electrically charged so travels in a straight line towards the base electrode. However due to small irregularities of the charge within the jet and because the fluid is moving at speed through the very high electrical field this causes the jet to become highly unstable and undergoes bending instability [8]. This is where the jet moves chaotically and spirals around in an unpredictable motion influenced by the high electrical field and repulsion between different sections of the same fibre in flight, this process is referred to as the whipping effect [9]. This extreme motion causes the rapid evaporation of the solvent causing only the polymer to be left, forming a single small diameter fibre. The movement also causes the fibre to stretch longitudinally along its axis causing it to thin further [1].

The now solid polymer fibre in flight is still being electrostatically attracted towards the grounded base plate electrode. When it reaches the electrode it is deposited onto it and is partially discharged, as the fibre continues to be deposited the fibres overlay each other and due to the unstable movement during flight the fibres are deposited as a randomly orientated mat [2].

Too other factors to be aware of when electrospinning is that even though it is described as an electrostatic process, a charge is carried by the fibre between the positive and ground electrodes and also that the fibrous mat has residual charge as it builds up thickness [10]. This is important to be aware of when designing apparatus to be used in conjunction with the electrospinning process.

Figure 2.1 show the conventional electrospinning apparatus. Note that the syringe is not directly connected to the needle. Piping is used connect the two which allows the investigator to set and change the flow rate of the solution during experimentation as the Syringe pump can be positioned well away from the high voltage connected to the needle itself.

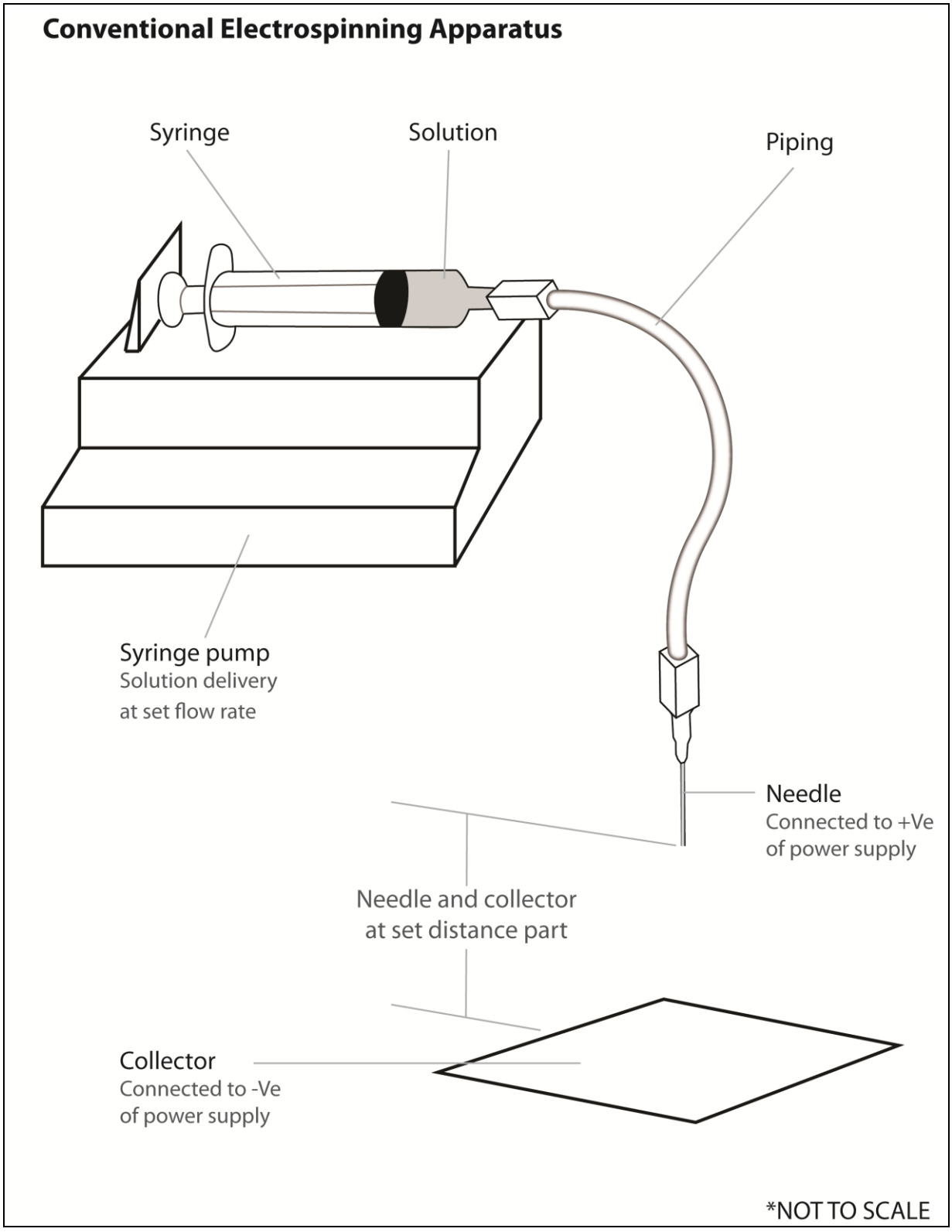

Figure 2.1- Conventional Electrospinning System

2.2.2 *Electrospinning Parameters*

There are certain parameters that are universal for all electrospinning experiments using polymers and these directly affect the quality, diameter and uniformity of the individual fibres produced during electrospinning. These parameters are:

Polymer molecular weight, this has a direct effect on the electrospun fibres diameter with a lower molecular weight giving a smaller diameter. There is a lower limit to this after which polymers of with low molecular weights will not successfully electrospin [11]. Low molecular weight has also been shown to increase the instances of beading where small polymer beads appear on the fibres at intermittent intervals [12].

Solution viscosity effects the electrospinning process since if there is not a high enough concentration of polymer within the solution, causing a low viscosity then polymer chains do not form to create fibres during electrospinning and instead electrospraying takes place depositing individual polymer droplets [13]. There has been found to be a strong relationship between the increasing solution viscosity and the increase in fibre diameter when electrospun due to more polymer in the Taylor cone [14]. A high viscosity solution that can successfully produce fibres during electrospinning may suffer from beading. Reducing the viscosity so there is a higher percentage of polymer in the solution used has been shown to reduce beading as well as increase fibre diameter [13]. However caution is needed when increasing the percentage of polymer to get better fibre morphology because this can decrease the crystallinity of the polymer in the produced electrospun fibres which can then adversely affect many desired material properties such as tensile strength [15]. Crystallinity in regards to polymers is used to describe an ordered molecular polymer chain [15].

The needle used is known to have an effect on the electrospun fibres. This is because it is used as the primary electrode and so has a direct connection to the polarisation of the solution within the needle and to morphology the electric field. It has been found that the average fibre diameter is greater for longer needle lengths. It was also shown in the same study that a longer needle will also produce a deposition area of a smaller diameter [16]. The material the needle is made of is another factor since it is being used as an electrode as it has been shown that using

a glass needle produces smaller average diameter fibres during the electrospinning process when compared to the conventional stainless steel needles commonly used [17].

The distance between the needle as the positive electrode and the collector as the base electrode has an effect on two aspects of the fibres produced during electrospinning, it is known that the distance effects the diameter of deposition on the collector, with larger heights creating larger diameter deposition [16]. There does not seem to be any relationship between the distance and the diameter of the produced electrospun fibres [18]. It is also important to ensure that a suitable or optimum height is found to ensure full evaporation of solvent during electrospinning, if the distance is to small then the polymer will not become fully solid during the electrospinning process [19]. Also using greater distances will require larger voltages, if the distance is too great at a set voltage beading or droplets will be found on the fibres [20].

The temperature that electrospinning is carried out at is believed to have little effect on the morphology of fibres like smoothness or beading. It does though have a small effect on fibre diameter due to the fact that higher temperatures cause a decrease in the viscosity of the polymer solution being used leading to smaller average electrospun fibres [21, 22].

The humidity during electrospinning is known to have a large effect on the formation and morphology of electrospun fibres. The effect of humidity is relative to the polymer being used with hydrophilic polymers interacting more and so being particularly effected [23]. High humidity does not just affect the polymer itself but also can adversely react or mix with the solvents being used too. It has also been shown that the jetting during electrospinning is less stable and less fibres are produced at high relative humidity. It is theorised that this is due to less charging of the solution because of greater electrostatic discharge at higher humidity [24]. It has been found that fibre diameter increases with an increase in relative humidity [22].

Flow rate of the polymer solution being delivered to the needle tip has been investigated to understand its effect. It has been shown that a lower flow rate is desirable as it produces more uniform fibres and reduces beading. It has been theorised that this is due to faster solvent evaporation which is known to reduce the

likelihood of beading [19]. A higher flow rate has also been shown to slightly increase average fibre diameters because of more solution at the needle tip that can be jetted however this extra solution leads to less stable jets and therefore less uniform fibres [25, 26].

The voltage that the electrospinning experimentation is carried out at is the most important parameter since it is the enabling factor to successfully electrospin. The voltage must be high enough that a Taylor cone is formed and a jet expelled from its tip. The voltage should not be too high so that the solution is being jetted faster than the flow rate is delivering solution to the needle tip as this depletes the Taylor cone completely stopping stable electrospinning. This means that finding equilibrium is necessary when choosing an electrospinning voltage [27]. Many studies have been carried out to investigate if the voltage used influences fibre diameter and it has been shown that it does. However to what magnitude and to what effect seems to be dependent on the polymer used with some groups describing a decrease in fibre diameter at higher voltages [19] and some an increase [18]. It has also been shown that relatively high voltage can also increase beading [28].

In summary it has been shown by Yoerdem et al. that to get uniform polymer fibres without beading and with good crystallinity the most important aspects are finding a balance between voltage, solution concentration and the flow for the polymer being used [27]. The ambient temperature should be kept constant and the relative humidity should be kept at a constant, relatively low level. The distance between needle and collector can be adjusted to achieve the desired deposition area and the voltage then adjusted accordingly.

2.2.3 Electrospinning Materials

The electrospinning process can be used with a multitude of materials. Most experimentation has been done with polymers and many polymers and copolymers have been successfully electrospun, a review paper published in 2003 listed 44 different polymers [29] and that number has gone up as the interest in electrospinning has increased. There are also many experiments carried out using a polymer as a carrier for other materials such as carbon nanotubes [30, 31] or colloidal metals [32] and other metal fillers as listed in the review paper by Dong et

al. [33]. This ability to use many different materials makes the electrospinning process versatile for a large range of applications.

2.2.4 Electrospinning Applications

The number of applications and areas that electrospinning has been shown to be a viable technique for, is vast. This is down to its versatility and sheer number of polymers and other materials that can be used with the technique. The most promising and researched areas that electrospinning has been used for are discussed briefly below.

Biomedical research such as drug delivery and release systems, [34] wound dressing [35] and tissue scaffolding [36]. The electrospinning process is especially useful due to the porous nature of the produced thin films and the high number of biocompatible polymers that can be electrospun [37].

When collected the small diameter fibres produced by electrospinning create porous fibre mats. The small fibre diameter of the electrospun fibres and the small pore sizes within the mats make them highly desirable for a range of filtration tasks including water treatment [38], blood filtration [39], and filtration of nanoparticles and smoke [40].

There is great interest in electrospun materials for electrical applications including development of electrospun capacitors, either electrospinning the whole device [41] or just the electrolyte layer/separator [42]. Also electrospun transistors have been developed from both organic [43] and inorganic [44] materials. Transistors made from single electrospun fibres have been successfully produced making their size very small due to only being the diameter of a single electrospun fibre [45, 46]. Other electrical applications include power applications such as the separator layer [47] or anodes [48] in batteries and in the development of novel fibrous photovoltaic solar cells [49, 50]. Piezoelectric actuators have been developed using the electrospinning process for applications that need a small controlled movement [51]. The wide choice of material available to be electrospun has led to actuators that are driven chemically [52] and by temperature [53]; as well as biocompatible actuators [54] to

be electrospun. Active electrical devices such as organic light emitting diodes (OLED) have successfully been produced with the electrospinning process [55].

Electrospinning has been used to produce conductive mats for use as electrodes and for other applications. This has been done using conductive polymers such as PEDOT:PSS creating flexible electrodes [56] and also by doping polymers with metal particles and if necessary using post processing techniques such as calcination to create the conductive fibrous mats [57].

Electrospun films and fibres have been developed for sensor applications. This includes development of chemical gas sensors using doped fibres [58] and also purely polymer fibrous mats [59]. Also water sensors have been developed [60]. The water sensor developed indicates the presence of Hg2+ by producing light through florescence from adding a doping material in the electrospun solution. This florescent means of indication by using doping materials is utilised for gas sensors as well [61] and is well explored within the literature. The fibrous films produced by electrospinning are particularly useful as chemical sensors due to their very large surface area making there sensitivity higher and giving a faster response than conventional techniques [62]. Temperature [63] and humidity [64] sensors have been shown, again exhibiting superior response to environmental changes due to large surface areas. Resistive type strain sensors have been devised and electrospun [65] and also the piezoelectric type of force sensors have been widely investigated [66, 67]. The electrospinning of piezoelectric polymers has been widely looked at for energy harvesting applications as well as sensor applications, where the electrospun piezoelectric films vibrate and convert this wasted mechanical energy to usable electrical energy [68, 69].

As has been shown there are a wide range of applications for devices produced by electrospinning. However, most of the above applications use randomly oriented fibre mats created by conventional electrospinning, the next section will look at electrospinning technologies that have been developed and how they can greatly improve the above applications and even expand the ability of the electrospinning process so it can be used for an even greater range of applications.

2.3 *Electrospinning Apparatus*

Various improvements have been made to the electrospinning process by creating novel apparatus that allows the creation of specialised deposition morphology to further expand the range of applications that the electrospinning process can be used for.

2.3.1 Substrate Free, Control and Alignment Techniques

For many applications electrospinning fibres onto a substrate is not ideal as the deposited fibrous mats are difficult to remove from the substrate post electrospinning. Therefore, various techniques have been developed to allow substrate free electrospinning.

This includes electrospinning onto various types of rotating collectors that suspend the electrospun fibres in free space. The reason for suspension is different due to the different applications presented in the literature but the technique is the same, for instance creating electrospun fibre bundles between multiple collectors made of electrically grounded electrodes. One way is to electrospin between two disks, one of which is rotating to twist the fibres together, this creates tightly packed orientated fibre bundle but the technique limits the fibre bundle length to the distance between the disks [70]. This approach twists the electrospun fibres together adding tension and also restricting the orientation of the fibres as only a twisted structure can be produced.

A more advanced method by electrospinning between multiple, finger like small electrodes which are rotated around a central point. The electrospun fibres are then deposited between the fingers in a suspended mesh. This can then be drawn from the centre into a fibre and onto a spool. The rotation of the collector twists the electrospun fibres together as they are drawn into a long bundle of fibres [71]. The study showed it was possible to use multiple instances of the apparatus to create core-sheaf yarns that could then be woven, knitted or braided using conventional processes. This process allows for long lengths of fibres to be produced however the morphologies of the bundled fibres is fixed due to the twisting and the fibres are put under strain during this process.

Another application that often used to electrospun fibres into free space is for aligning fibres in an oriented mat rather than randomly orientated mats created by conventional electrospinning. This can be done in multiple ways however the simplest is to have parallel electrodes with a gap between them within which the electrospun fibres automatically align [72]. This creates well aligned fibres however the fibre yield is low due to most of the electrospun fibres being deposited onto the two electrodes. An effort has been made to further advance alignment by investigating the electric field and angle of the collector edges to improve the alignment [73]. Secasanu et al. showed that using shaped electrodes could increase the yield of aligned fibres across the gap between the parallel electrodes. However the degree of alignment between fibres was not different between the use of standard parallel electrodes and the shaped electrodes shown in this literature.

This approach has been taken further to obtain an even greater degree of alignment of the fibres by attaching the parallel collectors to a rotating disk which then encourages better alignment as fibres are stretched between the collectors [74]. This idea was expanded upon again by Katta et al. using a drum created with evenly spaced wires around the circumference that collected aligned fibres between each of the parallel wires during electrospinning [75]. All these methods of aligned fibre production are limited due to the fact that only a single axis of alignment can be achieved during electrospinning due to the use of rotating collectors. This limits the morphology of the films being produced. The rotational movement stretches the fibres being aligned across the mounted plates adding extra tension. Collection of fibres is difficult and the yield of fibres comparatively low compared to the conventional electrospinning technique.

The control of the alignment between parallel collectors has been achieved by selectively switching the collectors between ground and a bias voltage from a secondary power supply. This allowed the investigator to control the voltage of either of the collector electrodes. When the collector connected to ground was switched to a positive voltage and the other collector switched to ground a single fibre was deposited between them. By doing this multiple times an exact number of aligned fibres could be deposited across a gap [76]. This led to a large build-up of fibres on the collectors themselves while only producing a few aligned fibres across the gap between collectors. This process is wasteful due to the amount of material deposited

on the electrodes in relation to the few fibres that are electrospun across the gap. Also the process relied on a mechanical switch rather than an automated system which would allow for greater yields as it could be switched faster. For this piece of reported work the deposited fibres were then stretched to reduce diameter. This form of post processing would be undesirable for some polymers as it adds tension to the fibres and also if there are any defects or thin areas on the fibres being stretched then the fibres would stretch more at these points which would lead to a non-uniform elongation.

Alignment and patterning was also achieved by having a grid of needle electrodes as the collector. The fibres were then electrospun between the grounded needle points with multiple fibres aligning between them creating aligned patterns [77]. This was shown for multiple electrode layouts however fibres aligned between all needles and from the images shown many fibres aligned diagonally rather than in the desired grid pattern. The collector needles used also couldn't be individually selected so the layout and pattern was fixed, limiting the patterns possible with this method.

Another approach is to electrospin onto fluid baths and then remove the fibres after. This technique is used for different applications such as producing continuous fibre bundles by electrospinning onto the surface of a liquid in a bath with the base electrode in the bottom of it. The fibres on the surface are collected by drawing the mat out of the fluid. The movement makes the fibres come together to create a bundle of fibres that can then be wound onto a spool collector as a yarn [78, 79]. Smit et al. found using analysis of scanning electron microscope (SEM) images the bulk of the fibres were well aligned and tightly bundled when drawn from the water bath however there is a large number of fibres that are only partially bundled with free ends and lengths of fibre protruding from the yarn creating an area of freely moving disorganised fibres around the yarn. Depending on application this area of fibres could be unwanted and detrimental if the yarn morphology needed to be smooth and well aligned.

Khil et al. expanded on this process by using the water bath to modify the electrospun fibres chemically, in this case by electrospinning onto a water bath containing methanol and water. This coagulated the fibres causing better assembly of fibre yarns when the fibres are drawn from the water bath onto a roller system.

Using the water bath method in this way greatly expands the technique as it adds an additional method of material modification during the electrospinning process [79]. However chemical or mass changes that are shown to occur using this method are polymer specific and may be undesirable for some applications and polymers.

This approach was taken further by using the vortex of water falling through a hole in the bottom of a container to twist the electrospun fibres together to create more uniform fibre bundles. The fibre bundle could then be collected from a container below. The water was pumped back into the top container allowing the process to go on indefinitely creating aligned fibre bundles of great lengths [80]. The experiment also showed that the spooling of the aligned fibres onto the collection mandrill tensioned the bundles straightening the electrospun fibres. Using this method of creating bundles of fibres is not the best production method for some polymers as they have different hydrophobicity and also for some applications the electrospun polymer being under extra tension wouldn’t be desirable.

Alignment techniques have been paired with other technologies such as deposition area control using secondary electric fields created using secondary electrode rings that are biased at a lower voltage than the primary voltage of the electrospinning needle. These rings are placed between the needle and collector below. The electrospun fibres in flight are repelled from the biased electrode rings and controlled by the electric field that these secondary electrodes create. This effectively creates a tunnel that the fibres can travel through allowing control of the deposition area [81]. Dietzel et al. showed through simulation and experimentation that changing the macroscopic electric field using secondary electrode rings caused electric field lines to converge in the centre line of the base electrode. This was shown to dampen the electrospinning jet instability and allow the control of the deposition area. By controlling the fibre deposition using secondary electrodes better control and alignment can be achieved using parallel base collectors [82]. Archarya et al. found that this secondary field improved the alignment of fibres collected between two parallel base electrodes however the cause of the greater alignment is not fully investigated. It was suggested that the focusing of the jet and the shielding of the collector by the secondary field stopped branching fibres being deposited.

The focusing effect was found to dampen and control the whipping effect allowing very small deposition areas to be achieved. With this focusing ability additional steering rings were developed that could then control where the fibre is deposited on a collector allowing patterning of the deposited fibres [83]. This method used a secondary electrode ring split into four parts and by changing the voltage on each of the four parts the modified electric field causes the electrospun fibre in flight to be deflected. Changing the voltages during the electrospinning process allows the jet to be steered quickly enough to direct and deposit fine tracks of electrospun fibres into simple geometries. The geometries that can be produced with the reported apparatus were very basic with limited length of track being able to be deposited and reported issues with the charge dissipation of deposited fibres causing repulsion of fibres in flight close to the deposition area.

Another approach to allow the patterning of electrospun fibres was to use an auxiliary electrode focuser and computer controlled moving stage, to focus the fibres into a small deposition area and then allow the patterning of the fibres on the moving stage [84].The auxiliary electrode that Kim used in this work attached to the electrospinning needle and modified the electric field so that the Taylor cone and initial jet was more stable than during conventional electrospinning. This led to more uniform whipping of the jet and greater control of the process creating a smaller deposition area. A base electrode attached to a moving stage was then moved below the jet to simply deposit tracks of the electrospun fibres into simple shapes. The uniformity of width of the deposited patterns was good however the track width produced was wide at around 30 mm and the edges of the tracks poorly defined. However this was not the focus of the work reported as so isn’t optimised or explained.

An alternative way of patterning electrospun fibres was found by using a voltage biased mask. The electrically conductive mask was biased at a relatively low potential voltage compared to the primary voltage used for electrospinning however the mask still repelled the fibres in flight. The mask was placed slightly above the grounded collector. The gaps in the mask allowed the fibres in flight to reach the grounded base plate and so when the mask was removed there were only fibres where there were gaps in the mask [85].

2.3.2 Coaxial Fibre, Fibre Bundling and Multi-layer Fibre Production

Modifying the electrospinning process so that it can be used to produce long lengths of bundled deposited fibres or coating a wire or other core material to create core-shell fibres rather than mats is an important area of research as it opens up the ability to use the electrospinning technique for a wider array of applications, especially for novel textile development. Some bundling fibre techniques have already been discussed in regards to the other technologies they employ [70, 71, 78, 79, 80]. Now a closer look at the type of bundled fibres and the different methods of achieving these fibres will be discussed in more depth as well as methods of creating multi-layered fibres.

There are two main types of multi-layered fibres. The first is by electrospinning two materials together at the same time to create co-axial fibres that have a core and outer layer. To do this the primary electrode electrospinning needle has a smaller needle inside. Then two solutions are fed to the needle tips where they do not mix in the tailor cone. When the tailor cone jets during electrospinning some solution from the inner needle and the outer is drawn from the cone and as the solvents evaporate a central core fibre is formed from the solution delivered from the inner needle and the solution from the outer needle forms around this central core [86]. Hollow fibres have also been produced using coaxial electrospinning where by in one ceramic fillers are used in the outer shell solution and a polymer only solution in the inner, after electrospinning the core is removed leaving only hollow ceramic fibres [87]. Hollow polymer fibres have also been achieved by using an oil solution with no polymer addition at all delivered to the internal needle with a polymer solution delivered to the outer needle. The outer sheathing forms around the core of oil during the electrospinning process and the oil is then removed after [88].

Improvements to the coaxial electrospinning technique has removed the use of the nested needles and instead utilised free surface electrospinning which used a shaped primary electrode with a reservoir of solution on its top surface. In this setup the electrospun fibres are spun upwards and multiple tailor cones are produced on the liquid surface during electrospinning, greatly increasing the productivity, producing thicker fibre mats faster [89]. Electrospinning upwards has also been

shown to effect the average fibre diameter and increase fibre diameter uniformity potentially due to the now opposing effect of gravity [90]. In this case two solutions were used and naturally separated into layers. During electrospinning multiple tailor cones form and on the surface and due to the layered solutions these tailor cones consisted of a core shell structure which when jetted created core-shell fibres [91].

An additional method to create core-shell fibres is by doping a polymer solution with carbon nanotubes. The carbon nanotubes have been shown to self-assemble into a strand during the electrospinning process because of the high electric field. On deposition this creates a core-shell fibre with a carbon nanotube core and a polymer outer shell [92].

2.4 *Polyvinylidene Fluoride*

Even though the electrospinning process can be used with most polymers Polyvinylidene fluoride (PVDF) was chosen as the polymer to be used for this body of work. It was chosen due to its piezoelectric material properties when electrospun [93]. This makes it an ideal polymer to work with as its piezoelectric properties can be exploited for many different applications including sensor manufacture and energy harvesting applications [66, 68]. See Appendix 10.1 Piezoelectric Theory and Appendix 10.2 Piezoelectric Coefficients for details on the piezoelectric effect.

It was found that PVDF when stretched and poled under a high electric field the materials crystalline structure changes and the resulting beta crystalline formation is piezoelectric, the electrospinning process does this during the fibre production which means that there is no post processing necessary [93]. PVDF is normally found in its alpha and gamma crystalline structure which do not exhibit the piezoelectric effect since the hydrogen and fluorine atoms attached to the carbon chain that make up the molecule are not regularly ordered. Each alternating carbon atom either has two hydrogen atoms bonded with it or two fluorine atoms. When stretched and poled in a high electric field the positively charged hydrogen and the negatively charged fluorine atoms reorient themselves to align appropriately with the electric field, after poling this leaves the material ordered with all the hydrogen atoms on one side of the carbon chain and the fluorine on the other. The atomic charge differential between them creates the materials piezoelectric properties [94].

The piezoelectric coefficients for PVDF are included in Table 1. The important coefficients are d_{33}, d_{31} and g_{33}, which match the input mechanical force with the produced electrical charge and produced voltage respectively. For more information about piezoelectric coefficients see Appendix section 9.2. At around 30 pCN^{-1} PVDF has the largest d_{33} of all the piezoelectric polymers which is why it has been so well researched for various applications such as energy harvesting which needs a higher electrical charge over voltage [95]. However when compared to the conventional piezoelectric ceramics the d_{33} is actually very small. One of the leading and most used ceramic piezoelectric materials Lead zirconate titanate (PZT) has a d_{33} value of 593 pC/N, a d_{31} value of -274 pC/N and a g_{33} value of $23.1x10^{-3}$ Vm/N (PZT-5H). [96]

PVDF however due to being a polymer has material and mechanical properties that are superior to ceramics for some applications especially in regards to its mechanical properties. The mechanical properties for the Kynar 761 grade of PVDF supplied by Arkenma and used in this work is listed in Table 1 [97]. The mechanical properties are for bulk thin films, not electrospun fibrous membranes and the data is from the supplied Kynar datasheet. The polymer is highly suited for a wide range of applications as the material is highly stable, resistant to a high degree against many chemicals and also it is also highly resistant to ultraviolet (UV) light [98].

Physical Properties	Bulk membranes
Molecular weight	440,000
Density (g/mol)	1.77–1.79
Water absorption	0.01–0.03
Mechanical Properties	
Tensile stress at yield (MPa)	45–55
Tensile stress at break (MPa)	34–55
Elongation at yield (%)	5–10
Elongation at break (%)	50–200

Tensile modulus (MPa)	1379–2310
Thermal Properties	
Melting point (°C)	165–172
Glass transition temperature, T_g (°C)	−38
Thermal stability, 1 wt% mass loss/in air (°C)	375
Linear thermal expansion coefficient 10^{-6}/°C	66–80
Electrical Properties	
Dielectric Strength (KV/Mil)	1.7
Dielectric Coefficient	4.5-9.5
Dissipation factor	0.01 – 0.21
Volume resistivity (Ω cm)	$2x10^{14}$
Piezoelectric Coefficients [99]	
d_{31} (pC/N)	-18
d_{33} (pC/N)	30
g_{33} (mV m/N)	340

Table 1 - PVDF Material Properties

2.5 *Conclusion*

The literature shows that the electrospinning process is an established way of creating nanofibres and depositing porous randomly orientated fibrous mats. This process has the potential for a wide range of applications due to its simple method and the large range of polymers and other materials that can be utilised with the technique. The literature shows studies for a range of disciplinary areas such as biomedical, looking at creating scaffolding, wound dressings and drug delivery systems. Sensing and electromechanical technologies such as strain gauges, piezoelectric transducers and also filtration applications have also been shown. Due to the process producing fibres it is also highly suitable for textile applications. The process is limited by its ability to only produce sub-micron size fibres and that due to

the whipping effect it is hard to control the deposition of the fibres produced. The process is not readily suited to manufacturing as due to the fibre diameters it takes a long time to build up thick layers, especially when large areas of deposition are wanted.

The literature also shows that there has been many developments and innovation to the electrospinning process itself allowing greater control of the electrospinning process. This has been achieved using various techniques. Dampening of the electrospinning jet instability and control of the deposition area has been achieved by using secondary electrodes to modify the electric field. Using multiple base electrodes and rotating disks alignment of the deposited electrospun fibres has been achieved. Various methods to create bundled fibres and yarns have also been shown however some of these methods are not suitable for some polymers, such as electrospinning onto water due to the polymers material properties. Also some methods produce fibre morphology that would not be suitable for all applications such as the twisting or tension put into the electrospun fibres during collection after electrospinning.

The apparatus used for each of the three different areas, control of electrospun fibres in flight, alignment of fibres on deposition and the creation of yarns from electrospun fibres mostly lack automation or have little user control. There is scope for these advanced electrospinning methods to be extended to create more adaptable and advanced systems that utilise control methods, advanced circuitry and integration of multiple aspects of the apparatus in literature. This will create more advanced systems which will allow the creation of more advanced devices and allow a greater range of applications to be explored.

PVDF is an appropriate choice of polymer to use for experimentation and the testing of apparatus as the electrospinning process creates the conditions to make PVDF fibres piezoelectric allowing for the production of simple devices from the apparatus developed. This gives more options for testing and evaluation of developed apparatus where applicable.

The aims of the research going forward were decided upon from the literature and are as follows.

Can more automation and the use of digital electronics be used to improve apparatus developed for the electrospinning technique?

Can apparatus be developed that allows for greater control of the electrospinning technique for depositing fibres with different morphologies allowing alignment, patterning and coating in ways not explored already in literature?

Can PVDF be used with any of the developed apparatus to make novel piezoelectric sensors or devices?

3 Methodology

3.1 *Introduction*

From the research already carried out as shown and discussed in the previous chapter, areas of research presented themselves for further investigation. There is a lot of interest in the development of advanced electrospinning techniques for the alignment of fibres and for the structuring of fibres for various applications. The apparatus reported are often simple and not automated, with limited functionality. By increasing the functionality, flexibility and automation of the apparatus more advanced methods of coating and deposited film morphology can be achieved, increasing the scale and complexity of devices produced using the apparatus. Improvements in complexity and automation will move research based techniques towards commercial manufacturing.

Within the literature there is a focus is on smart materials development using PVDF for sensor or energy harvesting applications, with work done on how to best exploit and tailor experimental procedures to the production of potential devices maximising the efficiency of the experimental process and the efficiency of the developed potential device.

The following chapter gives an overview of the different methodology used to create experimental devices that are flexible enough to test multiple areas of interest and develop potential devices as previously discussed. The electronic technology and processes used to create the experimental apparatus is also covered, as is the general experiential techniques used to characterise the samples produced by the apparatus developed. The design and development of all the apparatus developed as part of this work then follows.

The development of the apparatus and how it was built up modularly is shown in Figure 1. Recreating some of the simple apparatus found in literature (Section 2.3) was then iteratively built upon, creating more complex apparatus. This apparatus was then tested, analysed and improved, often a number of times to create the final versions of the apparatus reported. There are three main areas of development. These are the control of the fibres in flight during the electrospinning process, the deposition area and shape of the deposited electrospun fibres and the alignment of fibres on deposition. Figure 1 shows how all the developed apparatus builds upon

the conventional electrospinning apparatus and interacts to create an advanced electrospinning system that can align, pattern and produce devices of different morphology using the electrospinning process.

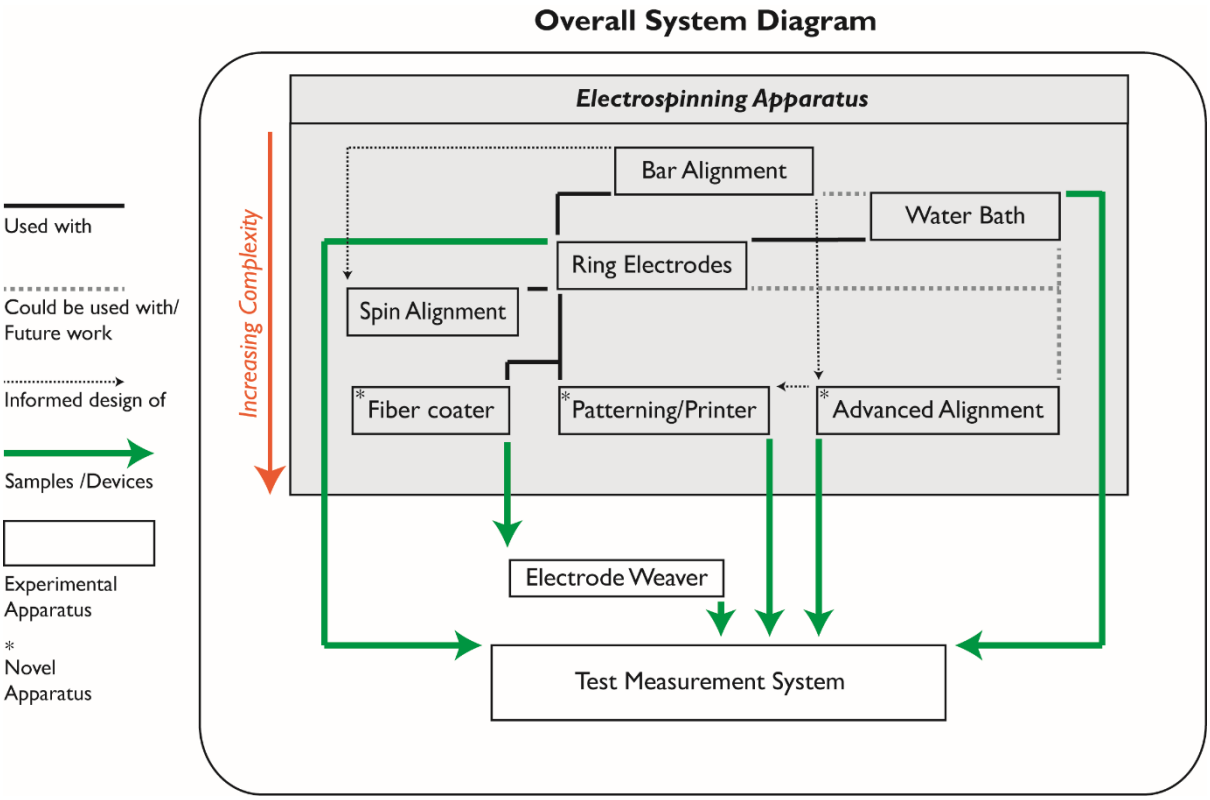

Figure 3.1 - Overall System Design

3.2 *Design Methodology*

3.2.1 Apparatus design

An iterative design process was used throughout the ideation, development and testing phases necessary for the creation of each piece of apparatus. The design process used focuses on continual innovation and evaluation to improve the functionality and extend the applications that each of the apparatus developed can be used for. Figure 3.2 shows the design process graphically showing the feedback loop that allows for continual incremental improvement of the apparatus being developed.

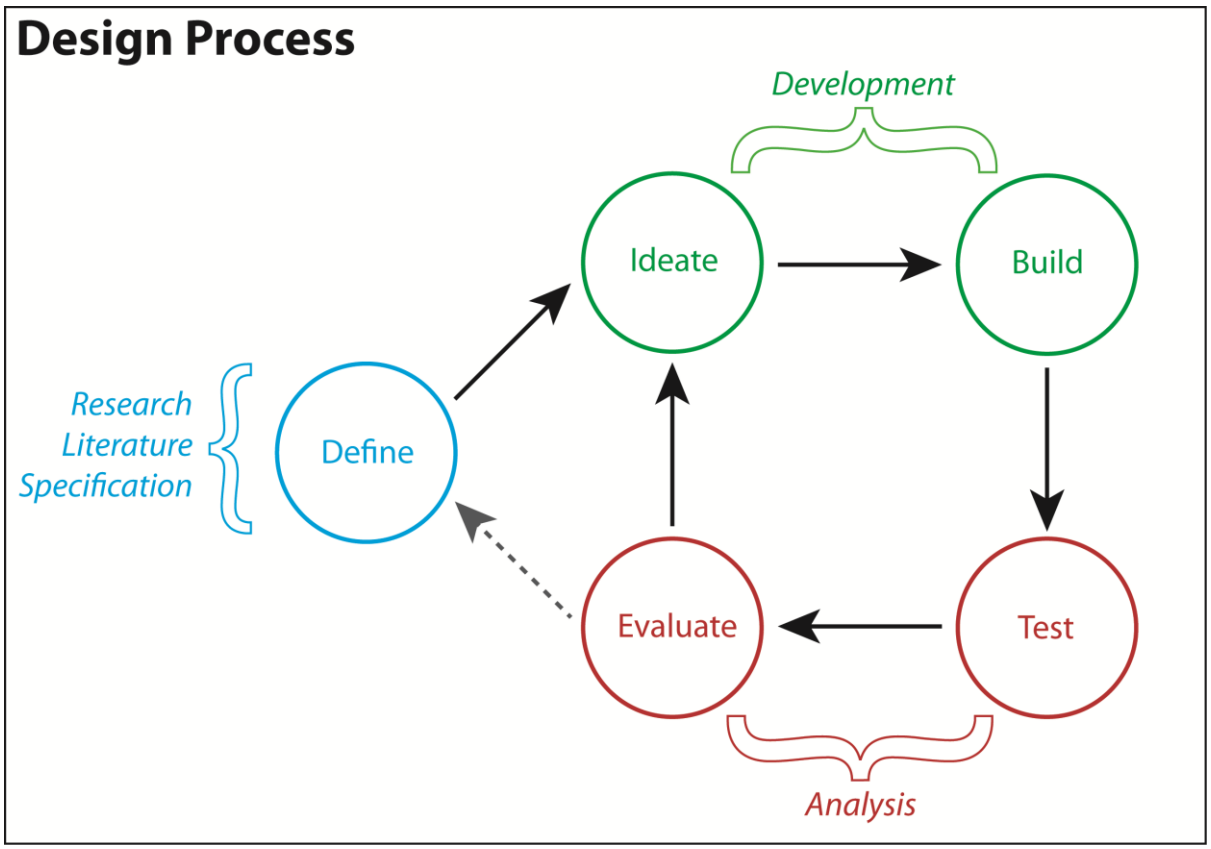

Figure 3.2 - Design Process Diagram

The definition for each of the pieces of apparatus comes from literature and the identified experimental aims for the apparatus that's being designed. Limitations of the reported upon apparatus found in literature are considered and defined creating a specification for development. In the ideation phase the specification is explored and a design developed that satisfies the aims laid out in the specification.

The design is then built and tested in a number of ways to ensure the design is fit for purpose. Testing is done to ensure that the mechanical and electrical operations of the design work as expected and further experimental testing is done to show the design works as intended with the electrospinning process.

The results of the testing are then evaluated and are used to develop an improved version of the apparatus, improving both functionality and usability of the apparatus while fixing any operating problems. In some cases it is necessary to adjust the defined specification to allow for unforeseen problems or to incorporate functionality that increases the scope of the apparatus.

This feedback loop of iterative design is not only used for the overall apparatus or system being developed but also for select parts of the individual apparatus. All the apparatus developed was built to be modular and so the iterative design process was used for select modules within each apparatus design where applicable. Making the apparatus modular meant that it was simple and quick to modify parts such as secondary electrode designs to allow a greater range of experimentation to be completed and also meant that apparatus need not be completely remade for each overall design iteration in most cases.

The material selection for apparatus to be used with the electrospinning process was important as it is within a high electric field, wherever possible acrylic plastic was used as it is not electrically conductive and so can be used while in contact with the electrospinning electrodes without causing issues such as short circuits.

Subtractive manufacturing using a laser cutter was used for producing most parts out of acrylic sheet as this is a quick production technique that allows for rapid apparatus development and makes it simple to create modular parts which can be easily replaced or improved.

During the ideation phase of development parts to be laser cut were built using CAD software and built into a virtual version of the apparatus to be built, this allowed apparatus to be partially tested virtually to ensure that any mechanical parts had appropriate tolerances and would theoretically work as designed. It also allowed easy conversion to cutting outlines to be laser cut, ensuring accurately dimensioned parts to be created and removing the possibility of human error during the manufacture of parts. This method of development and building greatly reduced manufacturing time and increased accuracy.

3.2.2 Electronic Circuit Design and software development

A similar iterative design process was also used for the development of the electronic circuits developed for the automation and control electronics used within the apparatus developed. The development of the digital circuits and the accompanying software happened concurrently.

A specification was first developed to outline exactly what functionality was required for the electronic element of a particular piece of apparatus. This was then expanded to define multiple areas, usually software considerations, hardware considerations and the user interface if applicable. These areas cover the whole scope of the electronics to be developed.

From these plans the electronics were built in stages, again using an iterative feedback process. The most basic hardware was built on breadboard and then any software that was necessary for control of this hardware block was developed, this often consisted of multiple design iterations. Once shown to be stable the hardware complexity was increased and this process was repeated until the final hardware and software had been developed on breadboard that achieved the desired specification. To reduce development times for the circuits developed a minimum number of different electronic components were used, the repeatedly utilised components and modules are detailed in the Appendix section 9.3.2. The microcontrollers, microcontroller hardware blocks and software used for programing them are detailed in Appendix section 9.3.1. The microcontrollers used all come from the Microchip PIC family and have similar hardware on board which was leveraged to provide functionality for the apparatus developed.

Testing of these circuits was done using a combination of standard electrical testing equipment and software debugging methods. Electrical connection issues between components were investigated using a multimeter. Electrical signals were investigated using storage oscilloscopes and logic analysers where appropriate. The software was debugged using the hardware under development and Microchips MPLAB IDE software utilising register watch windows and breakpoints in conjunction with an in circuit debugger to allow the code to be stepped through and the effect of each line of code analysed if appropriate using the actual hardware in development.

From the circuit design built on breadboard a schematic was developed and a printed circuit board (PCB) layout designed. The PCB layout was then produced using a PCB computer numeric controlled (CNC) router and PCB’s were then visually inspected and if necessary tracks checked for continuity using a multimeter, issues found at this stage either meant re-routing the PCB or slight layout adjustments of the PCB artwork. PCB’s were then populated with components

before further testing. See Appendix section 9.3.3 for more detailed information on apparatus used.

The developed and populated PCB and coded microcontroller was then put into the developed physical apparatus for further testing, at this stage the code would then be modified to account for unforeseen operational issues due to the mechanical properties of the apparatus if necessary.

3.3 *Experimental Methodology*

3.3.1 Introduction

Experimental methodology can be split into distinct parts for all experiments carried out. First a solution is prepared, then the electrospinning apparatus is setup and the experiment is then completed. Finally the deposited electrospun film is collected and if appropriate any post processing is carried out before testing and analysis.

3.3.2 Solution Preparation

A polymer solvent solution is necessary for electrospinning and for all experimentation PVDF was used as the polymer. PVDF does not dissolve readily in anything but strong solvent. For all the experiments carried out PVDF supplied by Arkema (Kaynar 761) [100] was used. It was important to keep the PVDF used constant throughout all experimentation as differences in molecular weight changes the electrospinning parameters used for experimentation and also the produced electrospun fibre characteristics [12].

Within literature only a few solvents are used to dissolve PVDF, these are Dimethylacetamide (DMAc) and Dimethylformamide (DMF). At least eight solvents are able to dissolve PVDF but these are the least volatile to work with [101]. For all experiments carried out 1.41 ml of DMAc was used mixed with 2.67 ml of Acetone This was the normal amount of solvent used however if more was needed for longer experimentation the ratio of DMAc to Acetone was kept constant. The acetone is needed to facilitate faster evaporation of the DMAc during the electrospinning

process, reduces the viscosity of the solution and has been shown to help prevent beading on the deposited fibres when the ratio is 1:2 DMAc to Acetone [102].

A glass vial is used to mix the solvent and a magnetic stirrer capsule is added before any of the chemicals. To ensure that there is no contamination the vial and capsule are washed with acetone before use. The solution was prepared by measuring the desired weight of PVDF into the vial using an electronic balance to ensure accurate measurement. The following steps are carried out in a fume cupboard due to the safety risks associated with handling the solvents. The acetone was then added to the vial and the PVDF gently agitated and so dispersed within the acetone. The DMAc is then added to the solution and the vial sealed. The solution is then stirred magnetically at 1100 rpm for approximately 20 minutes at slightly elevated temperatures of around 40-50 °C. The timing is dependent on the amount of PVDF used in the solution. The solution could be seen to be thoroughly mixed when it went clear, showing that the PVDF was fully dissolved and the solution ready for use once cooled to room temperature.

3.3.3 Apparatus Preparation

The experimental apparatus to be used is put into an electrospinning safety enclosure. This enclosure is a locking acrylic box that protects the operator from accidently electrocuting themselves while the experiment is running. The door of the enclosure locks using an electronic lock and to prevent electric shocks from static build up after experimentation the door is on a timer and so cannot be opened within 20 seconds of the high voltage power supplies being operational.

Once the apparatus is inside the collector electrode is connected to the ground connection of the primary HV power supply and if being used the secondary HV power supply's ground connection is also added. Continuity between the power supply leads and the base electrode is checked using a multimeter to ensure a good connection.

Next a length of Polytetrafluoroethylene (PTFE) small diameter piping is cut and has connecters added to both ends. The length of the piping is dependent on the experiment and is approximately the distance between the syringe pump and the top

of the electrospinning apparatus being used. One connecter has a clean 12 gauge blunt luer-lock needle attached to it and at the other end of the PTFE tubing the connector has a 10 ml syringe attached to it. Before the needle and syringe are attached to the piping they are used to draw the previously prepared PVDF/Solvent solution from the vial into the syringe. Figure 3.3 shows the syringe and needle set up described above.

The syringe is then placed into a syringe pump and the needle is attached into the electrospinning apparatus being used. At this point it is ensured that the needle has a good connection to the primary High Voltage power supply because it acts as the positive electrode for all the experiments carried out. If necessary this connection is also checked using the continuity function multimeter.

The collection substrate, for example aluminium foil is then added to the base electrode if applicable to the experiment. Once the system is setup the needle is primed with solution by setting the syringe pump to a relatively high (1ml/h) flow rate to ensure that the syringe is siting correctly in the syringe pump and that the piping assembly isn't restricting solution flow. Once the solution is seen at the needle tip the syringe pump flow rate is changed to the one desired for experimentation.

The door to the safety enclosure is then closed and with the locking mechanisms catch engaged then allows the high voltage power supplies to be used. Once turned on the door to the electrospinning enclosure cannot then be reopened until 20 seconds after the high voltage power supplies have been turned. Now the apparatus could be used as many times as needed as only the collection substrate is removed between experiments.

Between each experiment the needle tip will be cleaned using a dry cloth to ensure the needle tip is free of any dried solution and is clear of obstruction, after cleaning the syringe pump is reset and a small amount of fluid is pumped out of the needle to ensure it is able to flow freely.

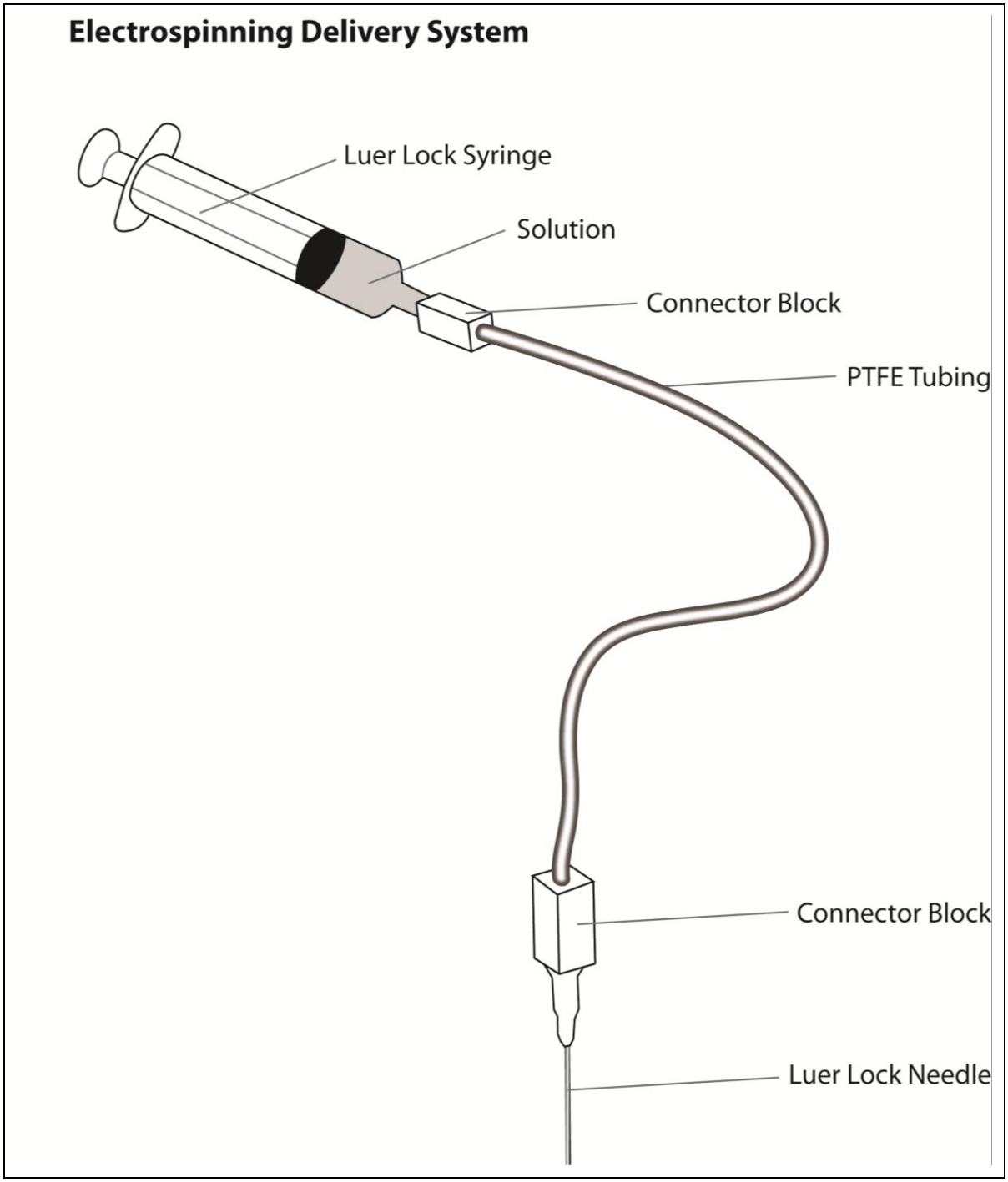

Figure 3.3 - Solution Delivery Diagram

3.3.4 Experimental Parameters

The experimental parameters are dependent on the apparatus being used and external factors such as temperature and humidity [2]. The usual ranges are given in table 2. Note the very high humidity range due to seasonal changes which has been shown to have a large impact on electrospun fibre properties in literature [103]. To correct this silica gel was used to bring down the relative humidity for some of the later experiments which kept the humidity between 8 % and 20 %.

Parameter	**Minimum**	**Maximum**	**Note**
Temperature	18 °c	30 °c	Ambient air – Ave. 25
Humidity	8 %	80 %	Controlled using silica
Primary Voltage	10 KV	25 KV	
Secondary Voltage	2 KV	12 KV	Usually ¼ to 1/3 of PV
Flow Rate	0.2 ml/h	0.4 ml/h	Usual 0.3 ml/h
Height	100 mm	250 mm	Apparatus dependant

Table 2-Electrospinning Parameters

The primary voltage needed was different on an experiment by experiment basis and was found by gradually changing the voltage until a tailor cone was formed with an electrospinning jet that was continuous. Once found then the system was watched to make sure the jet was stable and that the voltage was not depleting the tailor cone of solution faster than the syringe pump was delivering it. Once equilibrium had been achieved then the primary voltage was not changed for the duration of the experimentation.

If the secondary high voltage power supply was being used then the secondary voltage was set at approximately half the usual primary voltage and then the primary

voltage was raised until the tailor cone formed at the needle tip. At this point the secondary and primary voltages were changed until system equilibrium was found.

3.3.5 High Voltage Considerations and Safety

The electrospinning process operates at a high potential voltage, if the positive electrode is grounded at any point then the power supply will short circuit which could damage the power supply. If a person touching the positive electrode to create the short circuit then that person will be electrocuted. There is a high risk associated with high voltage electrocution, this risk was minimized by carrying out all experiments within a custom built plastic box which was large enough to freely electrospin within and fit the developed experimental apparatus inside of. The door to this box had a solenoid safety catch attached which stopped the door of the box being opened during the experiment and due to a timer function the door couldn't be opened for 20 seconds after the power supply had been turned off. This allowed any static charge build up to have partially or fully dissipated by the time the door could be opened. Any remaining static charge was removed by grounding the charged electrodes to the ground electrodes using a metallic rod with an electrically insulated handle after experimentation.

All the experimental apparatus described in the following chapter was built to be electrically safe and all the electrodes utilised had sufficient air gaps between them to stop arcing and short circuits. The minimum air gap between high voltage electrodes was determined by allowing 1mm per 1 kV potential difference and then a 50% safety margin was also added.

3.4 *Testing and Analysis Methodology*

The different electrospun films and composite fibres produced by the apparatus were tested in multiple ways depending on the aims of the experiment. The following procedures were carried out for the corresponding analysis.

3.4.1 Fibre and Film Morphology

To investigate fibre morphology on a macro scale an optical microscope was used, due to the sub-micron scale of the electrospun fibres deposited is not possible to

measure the diameter of the fibres using this technique. However both bright field and dark field microscopy was used to look at bulk alignment of the fibres and for unwanted or unexpected morphologies of the fibres.

Optical microscopy was also used for measuring overall diameter and polymer layer thickness of the produced composite core-shell fibres and also the results of the braiding apparatus developed. In both cases a mounted digital camera captured images of the sample under investigation for analysis.

Dark field microscopy was used to investigate most samples as the technique improves the contrast between the sample and background allowing the electrospun fibres to be seen easily. However for some samples, especially where it was beneficial to observe fibres through the thickness of the deposited fibre layers bright field microscopy was used. Appendix section 9.5 has more information on the microscope equipment used and also the bright field and dark field techniques.

Scanning electron microscope (SEM) imaging was used to look at fibres at higher resolution, this allowed individual fibres to be measured with high accuracy. Measurements were taken using an open source imaging program Fiji, an extended version of imageJ developed by researchers at National Institutes of Health (NIH) for analysis [104].

3.4.2 Piezoelectric Output

The custom designed apparatus covered in section 4.1.5 was used to investigate the piezoelectric output of the electrospun films deposited. To investigate the output of the deposited PVDF films electrodes were added to the top and bottom surface using electrically conductive silver paint. These electrodes were then connected using flying leads to a National Instruments USB 6009 Data Acquisition (DAQ) device. A LABVIEW program controlled the experiment and recorded the voltage that the electrospun films developed.

The user inputs a frequency range to be investigated into the LABVIEW program and the program then outputs a sine wave at the specified frequency to a PC sound card to drive the loudspeaker. This causes the PVDF film to vibrate and the resulting voltage could be recorded by the DAQ. The Program outputs a comma separated

value (.CSV) file that carries three columns of data, time stamp, frequency and recorded voltage. The frequency and output voltage is plotted on a graph to see both piezoelectric output and the resonant frequency of the films produced. As the PVDF films are vibrating with their maximum amplitude at resonance this corresponds to the maximum voltage output. The samples were swept from a low frequency of 20 Hz to a frequency of above 400 kHz for each PVDF sample tested.

3.4.3 Material properties

Differential scanning calorimetry (DSC) is used to find the melting point of a material by investigating how heat flows in and out of the material being tested as the temperature is changed. The equipment used was a Q2000 made by TA Instruments [105]. The samples tested were unprocessed PVDF power. The DSC experimentation was used to look at the melting temperature of the PVDF being used.

The DMA equipment used was a DMA800 by Perkin Elmer [106]. The equipment was used to examine material properties at different temperatures. These properties focus on mechanical properties such as finding the young's modulus but because the analysis is done by changing temperature the specific temperature properties such as the glass transition temperature and melting points were investigated. To test for glass transition of the material liquid nitrogen was used to cool the sample. The temperature ramp was done automatically and incrementally during experimentation going from a starting temperature of -190 °C to a temperature of around 200 °C. The final temperature varied as the apparatus automatically stopped once the material properties had changed to a point that indicated that the material under test had melted. Both DSC and DMA were used to find temperature properties of the PVDF which then gave a minimum and maximum temperature that any developed devices can work within.

4 Experimental Apparatus Design and Development

4.1 *Substrate Free Film Production and Testing*

4.1.1 Introduction

A method of producing and testing substrate free thin and thick films was required to be able to produce and quantify both the voltage output and resonant frequency of the piezoelectric samples produced.

From the literature it can be seen that work has already been completed in regards to using water as a medium for the collection of electrospun fibres [78, 79, 80]. It was identified that to utilise this approach would benefit this research since being able to collect the produced thin films without a supporting substrate such as Aluminium foil would allow for the addition and use of different electrode layers produced using different techniques. Adding custom electrodes gave more flexibility in regards to the mechanical properties and thickness of the electrodes added to the produced electrospun polymer films.

A secondary high voltage electrode was used with the water bath to allow greater control of the deposition area of electrospun fibres as shown in the literature [81]. This in turn allowed the development of a system for quickly producing thin or thick electrospun films of different surface areas. A collection system was devised to collect the free floating electrospun films, these then could have electrodes added to them and tested in a custom built piece of apparatus that looked at the voltage output and resonant frequency of the films. Figure 4.1 shows this particular configuration of the sub-system in relation to the overall system.

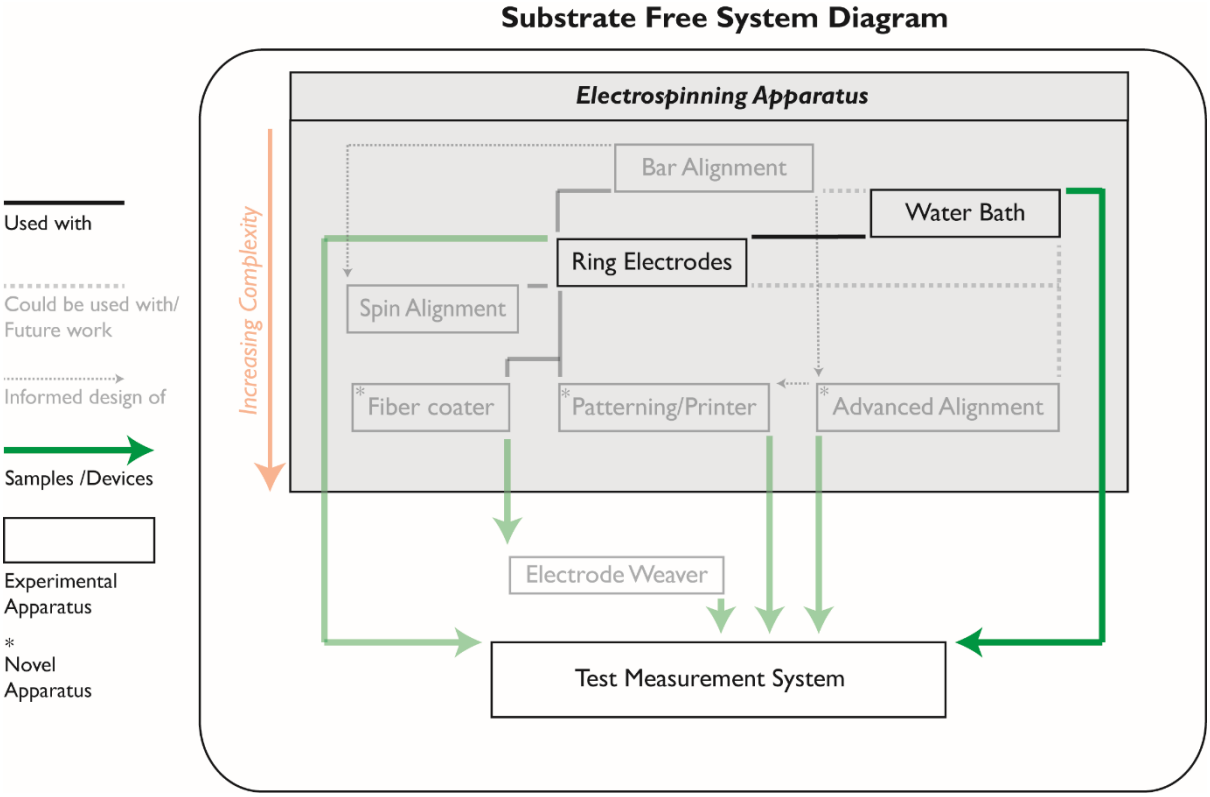

Figure 4.1 - Substrate Free System Diagram

4.1.2 Ring Electrodes

4.1.2.1 Introduction

The following section details the design and development of a piece of experimental apparatus used in conjunction with the conventional electrospinning system as described in section 2.3.1. This allows greater control of the electrospun polymer fibres in flight and the deposition of these fibres. The apparatus itself is not novel however it makes up part of the novel substrate free electrospinning system being described in this subchapter and is also used as part of several other pieces of experimental apparatus that are novel and covered in later subchapters.

4.1.2.2 Design Specification

The aim of this apparatus is to achieve a greater control over the electrospinning process by controlling the area within which the whipping effect takes place on the electrospun fibres in flight, this then allows greater control of the deposition area of the electrospun fibres. This has been shown in the literature [81] and is achieved by

adding a secondary positive electric field to the conventional electrospinning apparatus and set up.

The process is shown in diagrammatic form in Figure 4.2. The primary electrode (needle) is positioned at the top opening of a metal drum which is the secondary electrode. The electrospun fibres are jetted from the Taylor cone into the drum, this means that no material is wasted which is another benefit of using this control technique. The charged fibres in flight are repelled from the positively charged secondary electrode forcing the fibres to travel down the length of the secondary electrode drum in a channel. By changing the potential voltage of the secondary electrode and therefore the electric field strength within the confines of the secondary electrode drum you vary the interaction of the fibres in flight within this electric field. This narrows or widens the diameter that the fibres in flight can move within during the whipping effect. This is the main process that determines the deposition diameter of the fibre mats on the collection substrate/ground electrode.

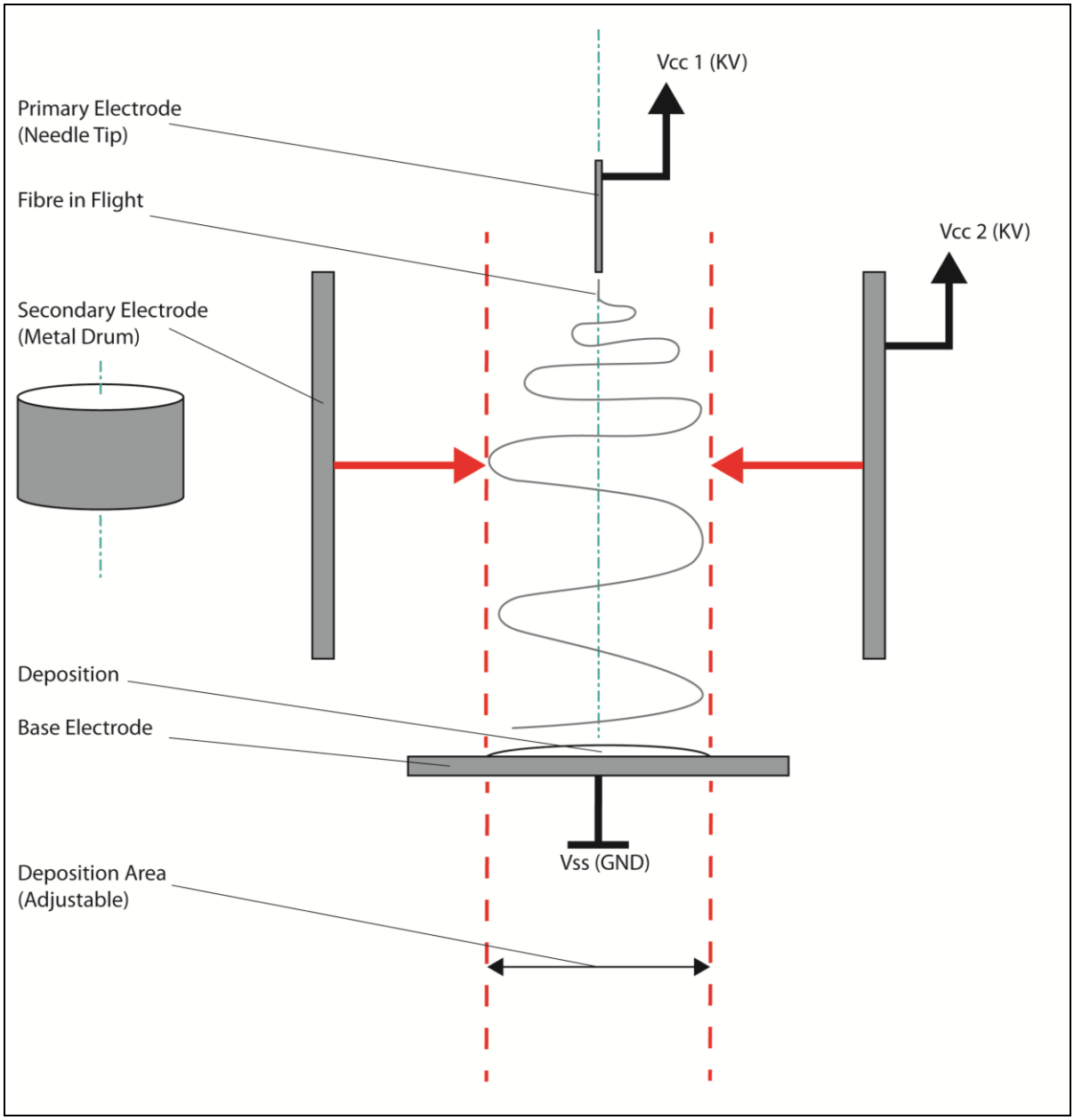

Figure 4.2 - Secondary Ring Electrode Diagram

4.1.2.3 *Physical Design*

The design of this apparatus is a metal drum or metal rings that are supported using an acrylic frame. The number of rings can be increased or decreased to create a secondary electrode of varying height. The metal rings need to be manufactured so that they are as uniform and circular as possible to ensure a uniform electric field and predictable deposition area. They also have a mounting point on them to both mount to the frame and also to allow the connection of the secondary power supply.

The frame needs to be made from plastic, acrylic was chosen, this is because the frame had to be non-conductive so it would not affect the electric fields being produced and also stop any problems with potential electrical short circuit between the positively charged secondary electrode and the electrically grounded base electrode.

4.1.2.4 *Apparatus Integration*

The integration with the conventional electrospinning technique was relatively simple. The apparatus is positioned so that the electrospinning needle is concentric with, and the bottom of the needle is in line with the top of the secondary electrode. The base electrode is then placed below the secondary electrode and centred. The distance between the secondary electrode and the base electrode is decided upon in reference to the minimum safe distance to stop electrical arcing as covered in section 3.3.5.

The primary electrode needle and the base electrode are connected to the high voltage power supply as in conventional electrospinning however the additional secondary electrode is now connected to a second high voltage power supply. This secondary power supply's ground lead is connected to the base electrode so that both high voltage power supplies have their ground leads connected. All the secondary electrode rings used have their own connection to the secondary power supplies high voltage positive lead, putting them effectively in parallel. This is to reduce the effect of the electrical resistance of the rings, which would be greater if connected in series.

4.1.3 Initial Water Bath

4.1.3.1 *Introduction*

The following work described is concerned with initial development of a water bath to test work carried in literature [80] concerning the feasibility of electrospinning onto the surface of water. This work is not in itself novel however it makes up an important component to the novel substrate free collection and testing system being described.

4.1.3.2 *Design Specification*

Very early initial experimentation spun PVDF fibres onto aluminium foil, this substrate is used extensively in electrospinning work as aluminium is highly electrically conductive. However the process electrostatically bonds the PVDF to the surface of the aluminium and the PVDF film layer is difficult to remove from the Aluminium foil. To spin substrate free films that are not bonded to any material a previously studied idea was built upon to electrospin substrate free films.

The aim was to spin onto water which initially only needed a simple piece of experimental apparatus which would hold a depth of water which was deep enough to be able to successfully extract the produced electrospun polymer films after electrospinning. For the electrospinning process to happen a ground electrode is needed that is submerged into the water and is the closest path of least electrical resistance between the primary electrode and the base electrode. As water is not fully conductive and has a high resistance the depth of water used is an important variable. To avoid the fibres in flight being attracted to other grounded areas like the cable going between the Power supply and base electrode the equipment designed is to be used with the secondary electrode drum so that the fibres produced are focused onto the water's surface. This will also allow the control of the film deposition area. See Figure 4.3 which shows this approach in detail.

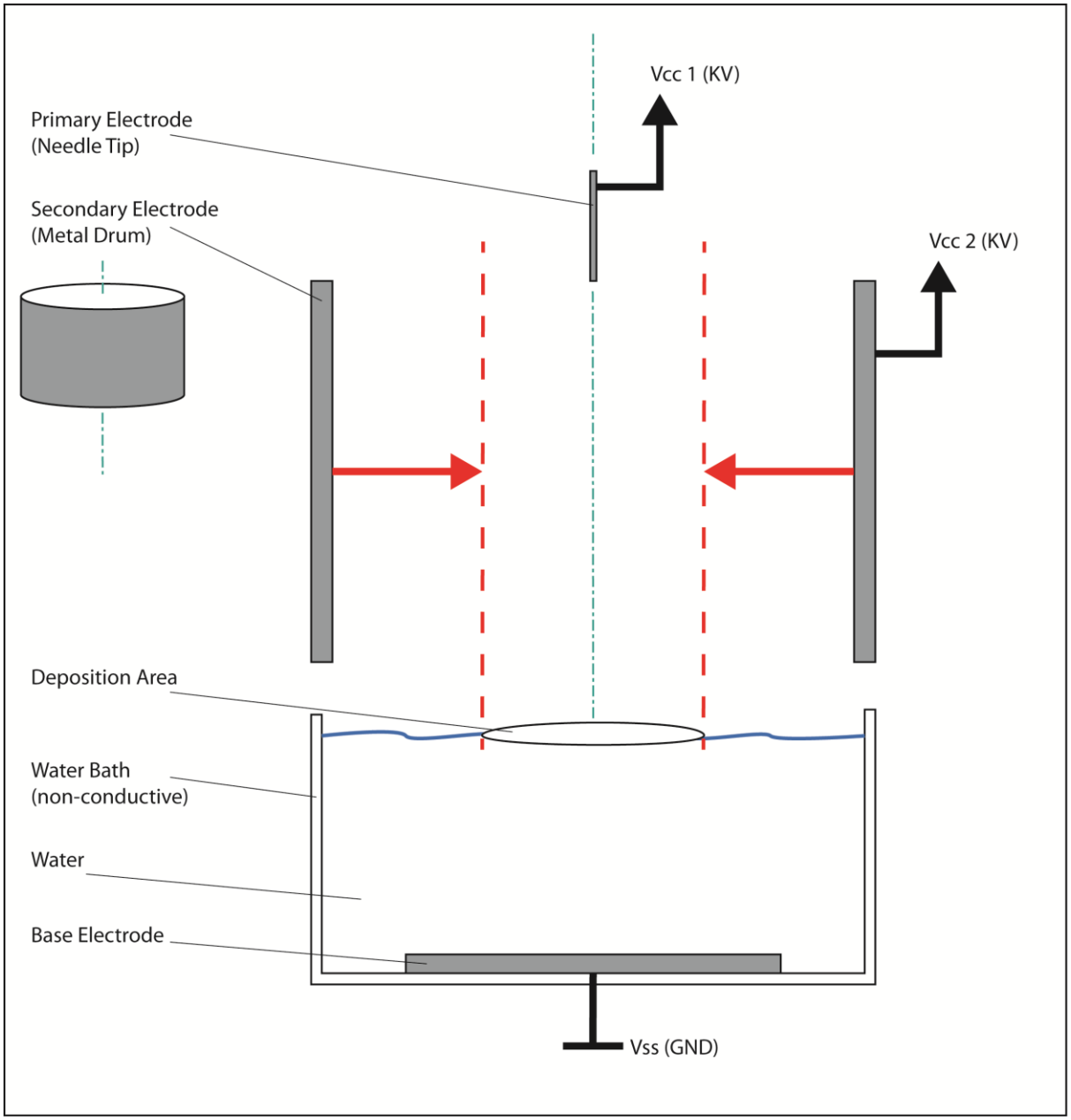

Figure 4.3 - Water Apparatus Diagram

4.1.3.3 *Physical Design*

The design is an acrylic box that is sealed with silicon to make sure it is water tight. The bottom of the box has a hole in it and the circular 100 mm base electrode used has a 15mm long stud of 5mm diameter that is threaded to take a nut. This stud passes through the hole in the bottom of the box allowing the necessary ground cable to be attached and the circular base electrode sufficiently clamped to the

bottom of the box and sealed with a piece of closed cellular foam to prevent leakages. This arrangement is shown in Figure 4.4 showing the produced apparatus.

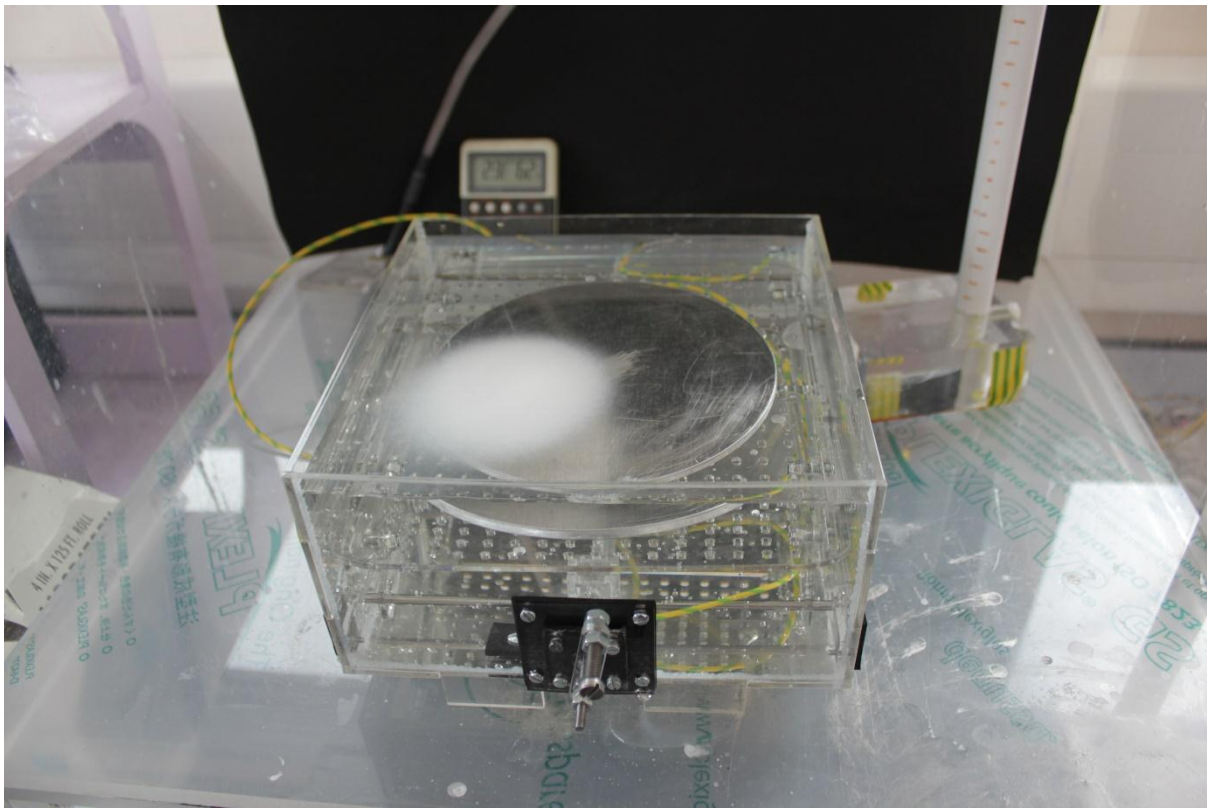

Figure 4.4 - Water Bath

4.1.3.4 *Apparatus Integration*

The secondary electrode ring was placed a short distance from the top of the water bath and connected to the positive output of the Secondary High Voltage power supply. The electrospinning needle was connected to the Primary High voltage power supply and positioned concentrically to the secondary electrode ring with the tip of the needle aligned with the top of the Secondary electrode ring.

The collection of the fibres was completed using specially designed laser cut plastic rings which held the collected fibre mats for easy drying and to give support for adding electrodes to the top and bottom surface of the produced films. The rings were dipped below the water surface and then used to gently lift the film from the water surface. Due to the residual static charge on the films the edges of the films

readily wrapped around the outer edges of the plastic collection rings creating a complete top surface on the collection rings. The rings were then left with the films attached to dry where slight shrinkage of the film was observed. The films then had electrodes produced on their top and bottom surfaces either by masking an area and painting conductive silver ink onto the surface or by masking an area and putting down thin layers of conductive metals by DC Magnetron sputtering. Once the electrodes were added the rings were then mounted straight into the developed test apparatus for testing the voltage output and resonance.

4.1.4 Water Bath Improvements

4.1.4.1 *Introduction*

The following developments build upon the initial water bath detailing the improvements made, the reasoning behind them and how this improves the overall system being described.

4.1.4.2 *Design Specification*

From experimentation and simulation discussed in section 5.3.2.2 an improved apparatus design was developed. The main issues identified were with the distance between the edge of the secondary electrode and the water and also the depth of water covering the base electrode. Ideally the distance between the bottom of the secondary electrode and the top of the base electrode should be as small as possible with the minimum possible depth of water covering the base electrode. The issue with having a small amount of water covering the base electrode is that the films needed to be scooped up from the water onto their frames, which meant that the height of the base electrode in the water had to be adjustable. An improved version of the water bath was developed which allowed this as shown in Figure 4.5.

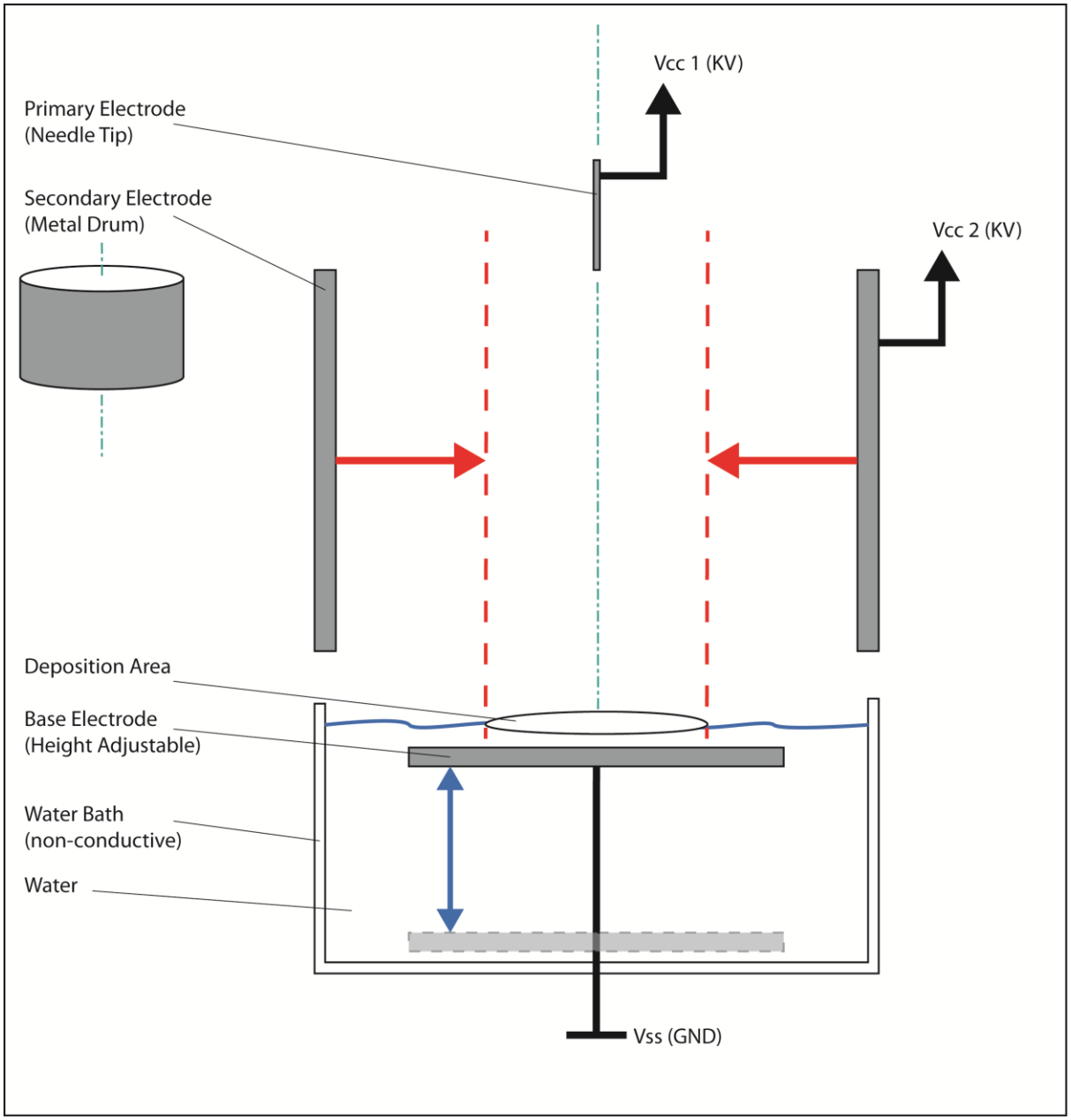

Figure 4.5 - Improved Water Bath Apparatus Diagram

4.1.4.3 *Physical Design*

As the new design had to be more complicated due to needing a mechanical system the physical design was changed accordingly. The apparatus was made from acrylic that was laser cut into parts which were developed before manufacture using CAD software and a virtual version of the apparatus built to ensure good tolerances and appropriate design of both the casing and mechanical elements.

The apparatus was bonded together using Tensol liquid cement and then sealed using silicon sealant. Anywhere that holes needed to go through the casing for the mounting of the mechanism or the control mechanism the bolts used were sealed by adhering closed cell foam around the hole and tightening the bolts washers against the foam making a good water tight seal. Figure 4.6 shows the overall design of the apparatus. Note that the area around the handle and been double sealed with closed cell foam as this is where the handle used to adjust the height of the base electrode comes out through the casing and since this has to be operational while the apparatus is filled with water it is especially important that it is well sealed.

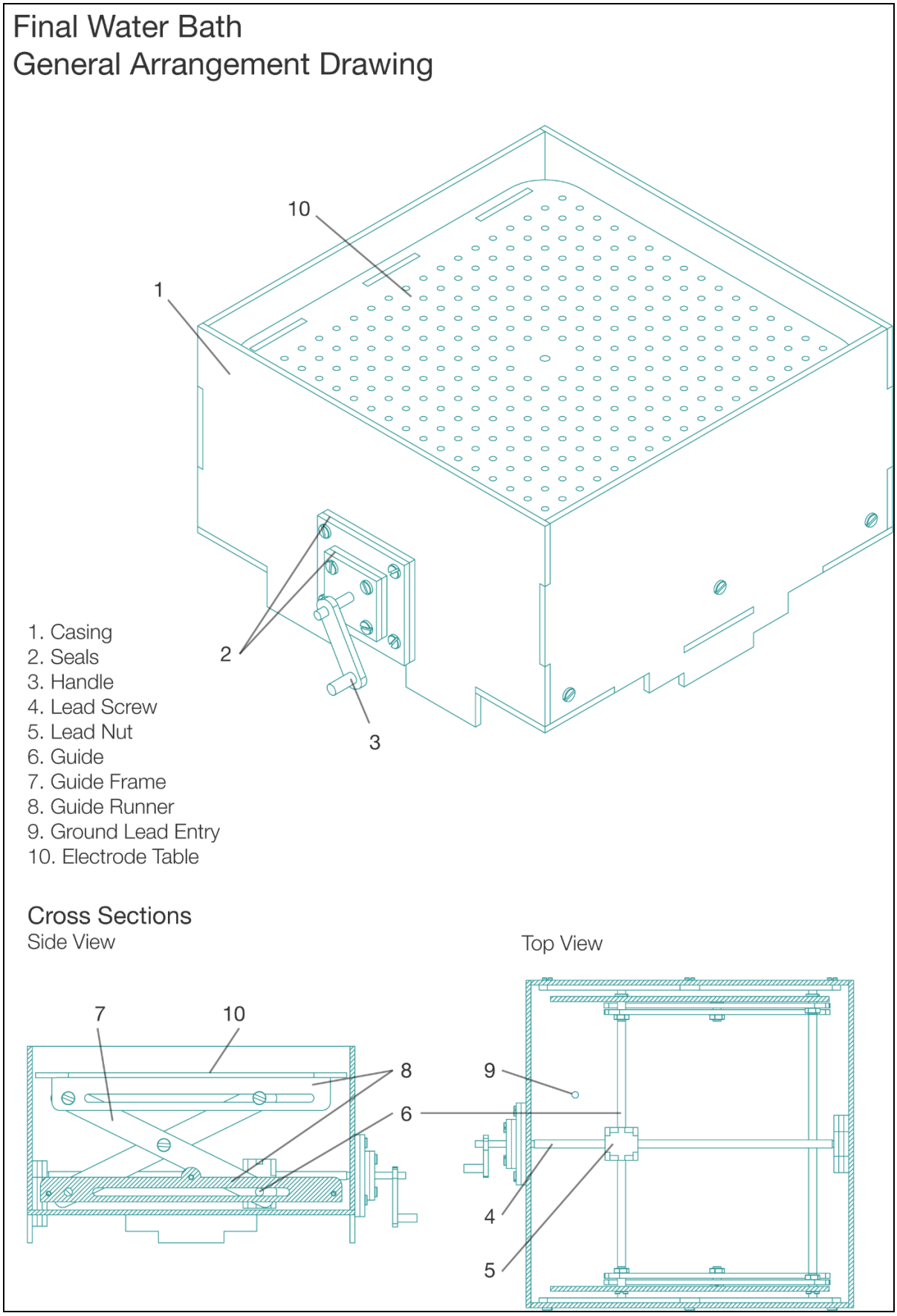

Figure 4.6 - Improved Water Bath General Arrangement Drawing

4.1.4.4 *Mechanical Design*

The mechanical design of the apparatus can be seen in the Cross section views in Figure 4.6. The mechanism itself is made up of two mechanical linkages similar to scissors. A lead screw is used and a nut travels up and down its length attached to a guide which in turn is attached to one part of the mechanical linkage. As the guide moves along the length of the box the mechanical linkages either get closer, forcing the electrode table upwards or they get further apart bringing the electrode table lower. The lead screw attached to the exterior handle is an m4 screw thread which has a pitch of 0.7mm therefore for every turn of the handle the lead nut moves 0.7 mm along the lead screw. This translates into a vertical movement of the electrode table however due to the scissor mechanism the relationship between it and the lead nut is not linear. This mechanism is appropriate for this application as the electrode table is positioned by hand and by eye in proximity to the water's surface.

4.1.4.5 *Apparatus Integration*

The apparatus integration is identical to the initial version of the apparatus however now before the start of the experimentation the electrode table has to be adjusted so that it's just below the water surface. Also when collecting the produced electrospun film it is necessary to move the secondary electrode back away from the apparatus and then use the handle on the water bath to lower the electrode table to a suitable depth to allow the collection of the fibre films by scooping the collection frames underneath them.

4.1.5 Voltage Output, and Resonance Test Facility

4.1.5.1 *Introduction*

A method of testing the produced electrospun PVDF fibre samples was developed, this was necessary to evaluate the samples for expected characteristics such as if they display piezoelectric properties and if they do, what range of voltage and current output they exhibit and also what there resonant frequencies are. These characteristics are important for the development of devices however the piezoelectric coefficients could not be calculated from the results from the developed

test apparatus due to the unknown quantity of force transferred to the samples using the approach developed and detailed in the following sections.

4.1.5.2 *Design Specification*

A method of testing the electrospun films produced was needed as part of the characterisation of the piezoelectric element of the work completed. A method of testing the films for voltage output, current output and also their resonant frequency's was developed. The apparatus needed to energise the films by vibrating them at which point any voltage that is produced can be measured and then analysed.

A system where by audio pressure waves in air was used to energise the produced PVDF films was developed. Audio waves were chosen as it was relatively easy to adjust the amplitude and the frequency of the pressure waves and therefore the amplitude and frequency of vibration of the PVDF films which allowed the resonant frequency of the produced films to be found by looking for the frequency that gave the maximum voltage output from the samples. The method is shown diagrammatically in Figure 4.7.

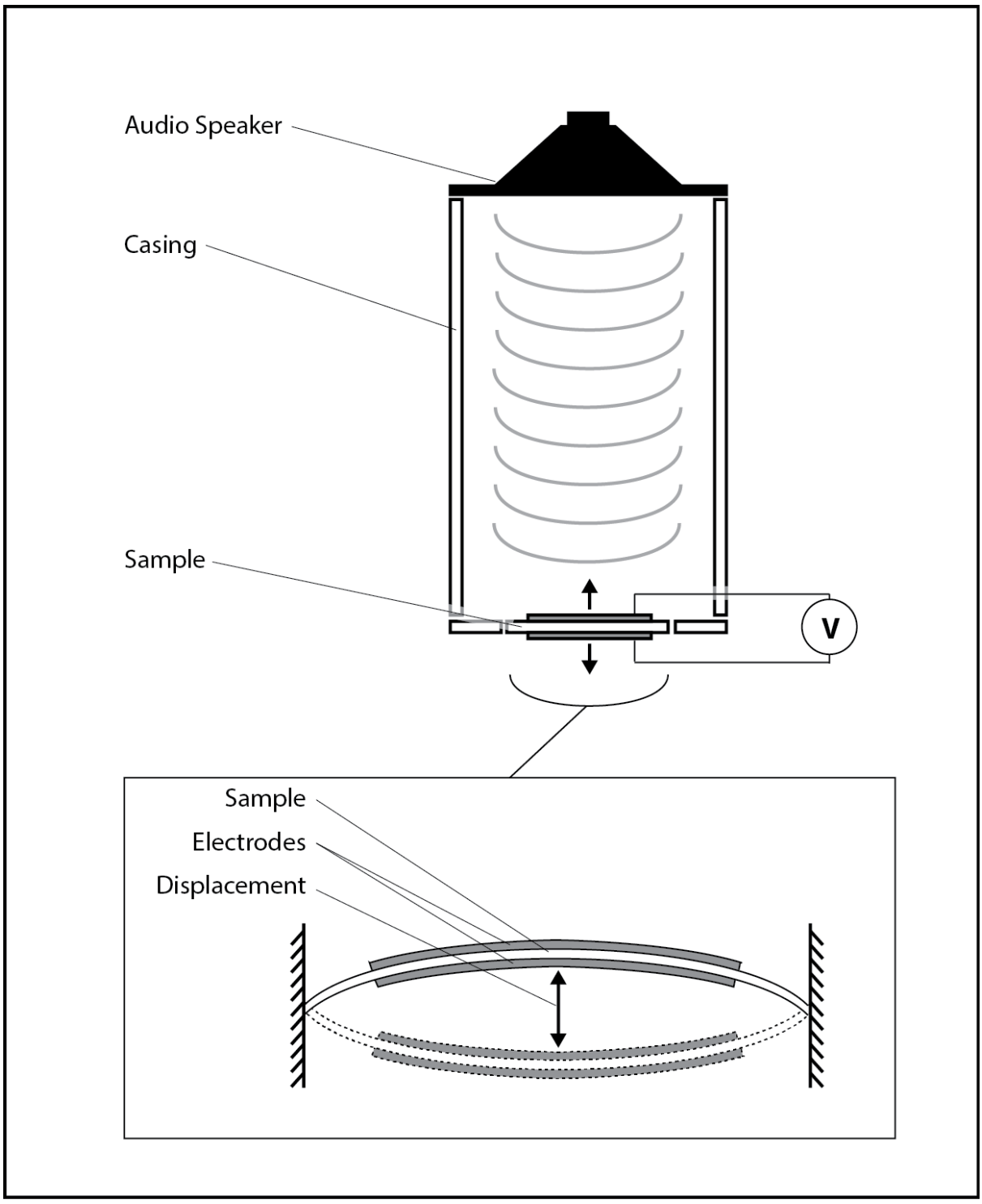

Figure 4.7 - Sample Excitation Method

4.1.5.3 *Physical Design*

The physical design of the apparatus was developed with the following considerations. It was necessary to build this apparatus as a faraday cage to stop any electromagnetic noise from the environment affecting the experimental results. Therefore the casing was exclusively made from mild steel.

The main part of the faraday cage was a metal box which housed the sample holder, where the sample for testing was mounted and the supporting electronics were housed. Protruding from the faraday cage is a metal cylinder and mounted to the top of this cylinder was the audio driver (speaker). There is a plastic layer between the speaker and the metal cylinder and the fastenings are done with nylon bolts. The rationale for having the speaker away from the sample holder and also having the acrylic flange separating the speaker and metallic housing is due to the electromagnetic noise that audio drivers create and the possible interaction of this noise with the sample being tested and electronics housed within the faraday cage.

Inside the metal cylinder is another cylinder made from acrylic, a layer of closed cell foam is around the top edge of this cylinder which makes an air tight seal with the top of the speaker. At the bottom of the acrylic cylinder, within the faraday cage, it friction fits into another seal, again made from closed cell foam, that is mounted to the top of the sample holder.

The sample holder itself is made from acrylic and the sample is mounted into the centre of the system and can be screwed down. The sample holder is in two parts with the sample being mounted in the lower half and then the top half of the sample holder is fastened on top of the lower half. Again an air tight seal is created between the top and bottom half of the sample holder to ensure an air tight fit. In the lower half of the sample holder there is a hole to allow air to move in and out of the bottom chamber, the system between the top of the mounted sample and the speaker itself is fully air tight. A closed, air tight system such as has been described stops dissipation and ensures good propagation of the sound pressure waves, transferring the desired power and frequency to the sample being tested.

4.1.5.4 *Electronic Design*

The electronic design is in four parts: the generation of an audio tone at a set or varying frequency, the amplification of the generated tone, the amplification or

buffering of the piezoelectric voltage response and then the recording of the piezoelectric voltage response.

A National Instruments LabVIEW program was written which generates the tone at specified frequencies and pushes it out to a computers sound card. The program also records the piezoelectric devices voltage response and also the output voltage sine wave from the sound card. Recording both simultaneously ensures that the frequency that the piezoelectric device is vibrating at can be closely matched to the piezoelectric devices output voltage making it possible to determine the resonant frequency of the piezoelectric device being tested. The voltage data is digitised by a Data Acquisition (DAQ) module and read by the LabVIEW program. The LabVIEW program then saves the data into a comma separated value (CSV) file for analysis. The DAQ sample rate used is 24 KS/S (kilo-samples per second) and therefore the amount of data recorded is very high, this is necessary to accurately sample and digitise any analogue wave form as described by the Nyquist theory where the sample rate should be at least twice the maximum expected frequency, in this case twice the expected resonant frequency.

The audio amplifier circuit was built from the application note on page 3 figure 2 of the data sheet for the audio amplifier used which was a LM1875 made by Texas Instruments [107]. The audio amplifier was chosen as it has high power output at 20 W, with low distortion of 0.015% at this power level. This allowed the excitation of the piezoelectric devices at a high amplitude while ensuring the frequency output by the LabVIEW program was not changed during amplification. The schematic and PCB created from it are shown in Figure 4.8.

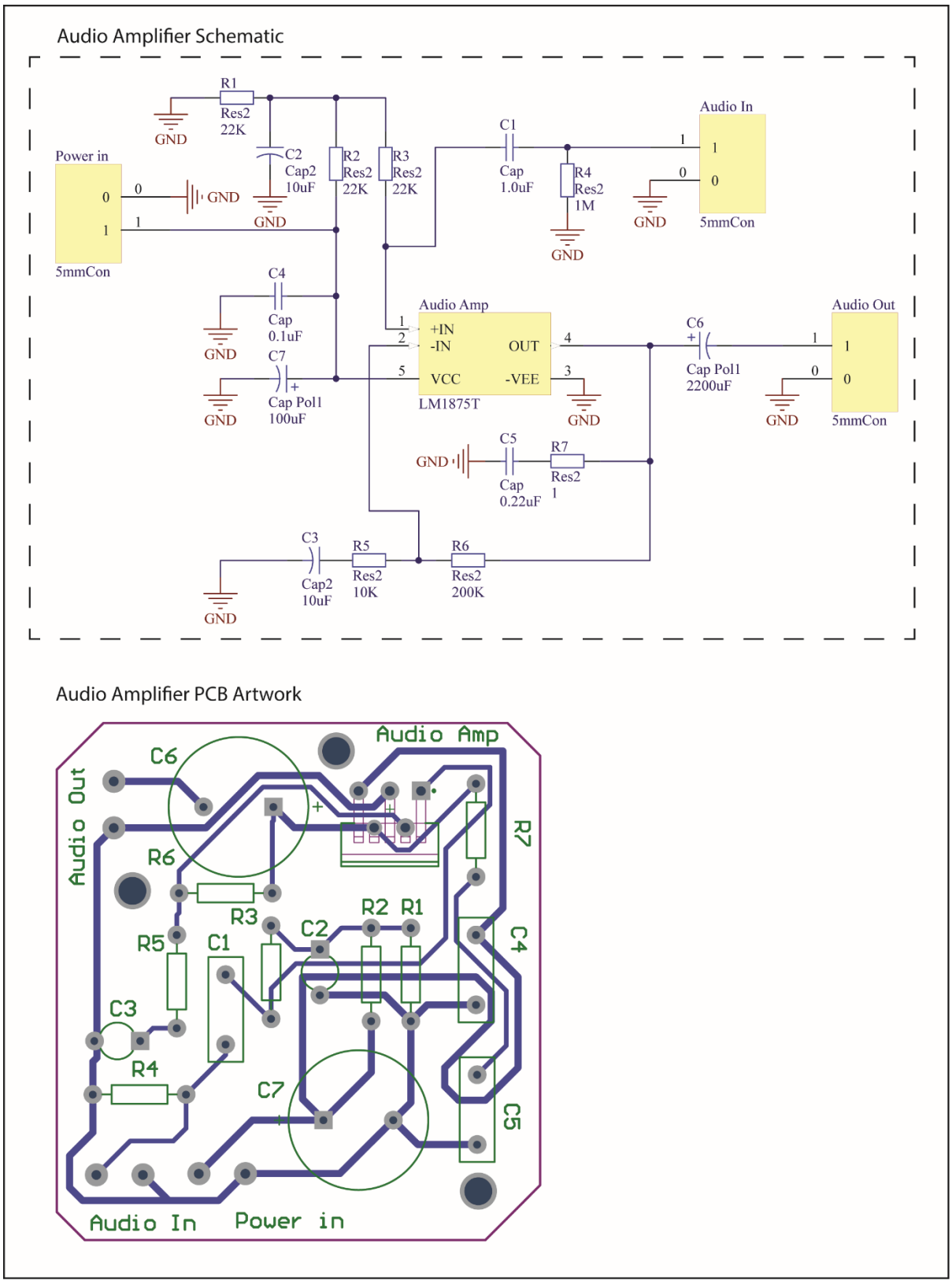

Figure 4.8 - Audio Amplifier Schematic and Board Layout

The amplifier and buffer circuit that was developed for use with the testing apparatus was directly attached to the outputs of the piezoelectric sample being tested. It consisted of a voltage buffer circuit and a more complex amplifier design that had adjustable gain and was developed for use with piezoelectric devices. Both amplifier circuits use the microchip MCP6023 operational amplifier. This op-amp was chosen because it was rail to rail with 10 MHz bandwidth and had a low noise and distortion profile. Other benefits were that it operates between ground and 5 V DC so it could be easily integrated with electronics that use digital logic levels. It also has a stable mid supply voltage output between v_{ss} and v_{dd} which allows you to accurately bias the input from the piezoelectric device so the voltage changes created by the piezoelectric device swing between the mid supply voltage. This allows the full range, both positive and negative voltage from the piezoelectric device to be recorded.

The schematic is shown in Figure 4.9 and depicts the circuit developed and tested on a breadboard. To mimic a piezoelectric device a function generator was used for testing the response of the circuit before it was made into a printed circuit board.

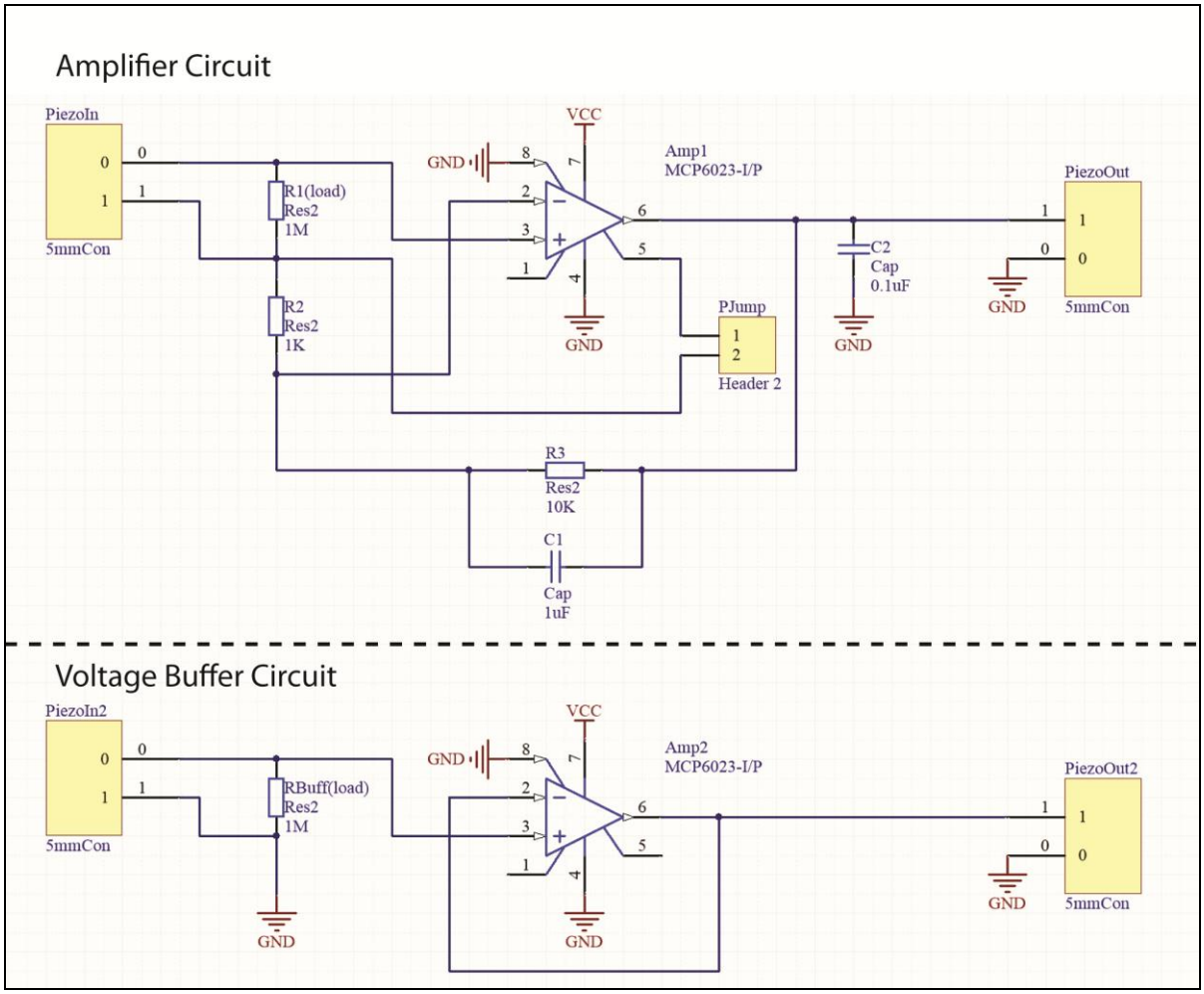

Figure 4.9 - Buffer/Amplifier Circuit Schematic

The schematic shown in Figure 4.9 has been split into three parts for simplicity. The Power management consists of the power connector and a smoothing capacitor. The Amplifier Circuit includes a load resistor (R1) between the piezoelectric devices inputs. This resister is replaced on the PCB itself with a female header so its value can be changed when necessary. Having a changeable load resistor allows the piezoelectric sample being tested to have its impedance measured by comparing its voltage output under no load (with no R1 resistor) to its output with varying values of R1.

Resistor R3 and capacitor C1 are also female headers on the PCB allowing the respective component values to be changed. By being able to change R3 and C1 the gain of the amplifier can be adjusted as necessary. This allows different

morphologies of sensors to be tested as different sensors have different outputs and therefore need different amplification ratios.

The header PJump is to connect the mid supply voltage from the op-amp into the circuit to optionally bias the piezoelectric response. His means that both negative and positive voltages from the piezoelectric film being tested can be seen on a system that uses a digital voltage range, in this case of between 0 v and 5 v. The op-amp was powered by 5 v so with the bias enabled the piezoelectric voltage recorded swings around the 2.5 v level.

The Voltage Buffer or unity gain circuit does not amplify the piezoelectric response, instead it buffers the voltage and is necessary because piezoelectric materials have a high impedance. RBuff is an optional load resistor and is replaced on the PCB by a female header to allow its value to be changed. A voltage buffer was included on this circuit since piezoelectric devices are highly sensitive and a buffer such as this has very high input impedance so that the op-amp effectively isolates the piezoelectric device from any other electronics that could affect the voltage readings when being recorded. Below is Figure 4.10 showing the complete PCB layout for this circuit.

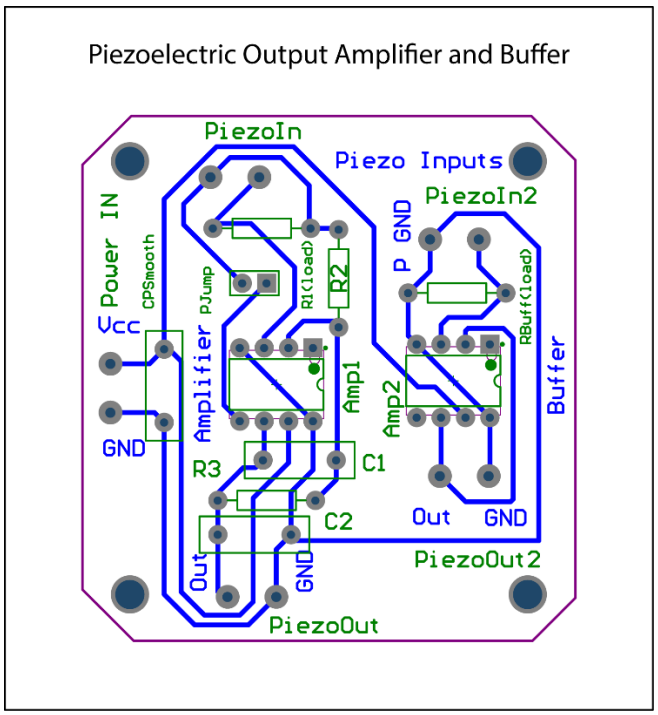

Figure 4.10 - Buffer/Amplifier Board Layout

4.1.5.5 *Apparatus Integration*

The apparatus is connected together with the sample being tested inside the faraday cage with the National instruments DAQ and also the buffer and amplifier circuit. This is necessary to reduce the electrical noise from the external environment which can interfere with the voltage output reading from the sample being tested. This allows for more accurate recording of the voltage output of the sample. Also a DC regulated power supply was used which supplies power for driving the speaker and audio amplifier circuit at 12 - 24 v and also the power for the signal buffer and amplifier at 5 v.

4.2 *Novel Advanced Fibre Alignment*

4.2.1 Introduction

It has been shown and discussed that an area of interest is in controlling the deposition of fibres during electrospinning process. Most of this work is concerned with aligning produced fibres and controlling fibre deposition during the electrospinning process however due to the scale of the fibres produced this is usually done on a small scale using micro x, y stages [84] and statically aligned electrodes [72]. Also layering of aligned fibres was an area that hadn't been fully investigated. Inspiration was taken from literature where parallel electrodes were alternatively switched to encourage selective aligned fibre deposition between them [76] and also the work showing patterning and alignment between grounded needles [77]. Expanding upon that work a novel method of patterning aligned fibres into multiple layers with different orientations during the electrospinning process was developed through two main areas of development by using an initial simple exploratory piece of equipment and then a refined full featured experimental piece of equipment, both of which are detailed in the following work. Figure 4.11 shows the system described here in relation to the other sub-systems and apparatus developed. Note the inclusion of the Bar alignment apparatus that is talked about in chapter 5.4.2 preliminary fibre alignment as this work informed the development of the following system.

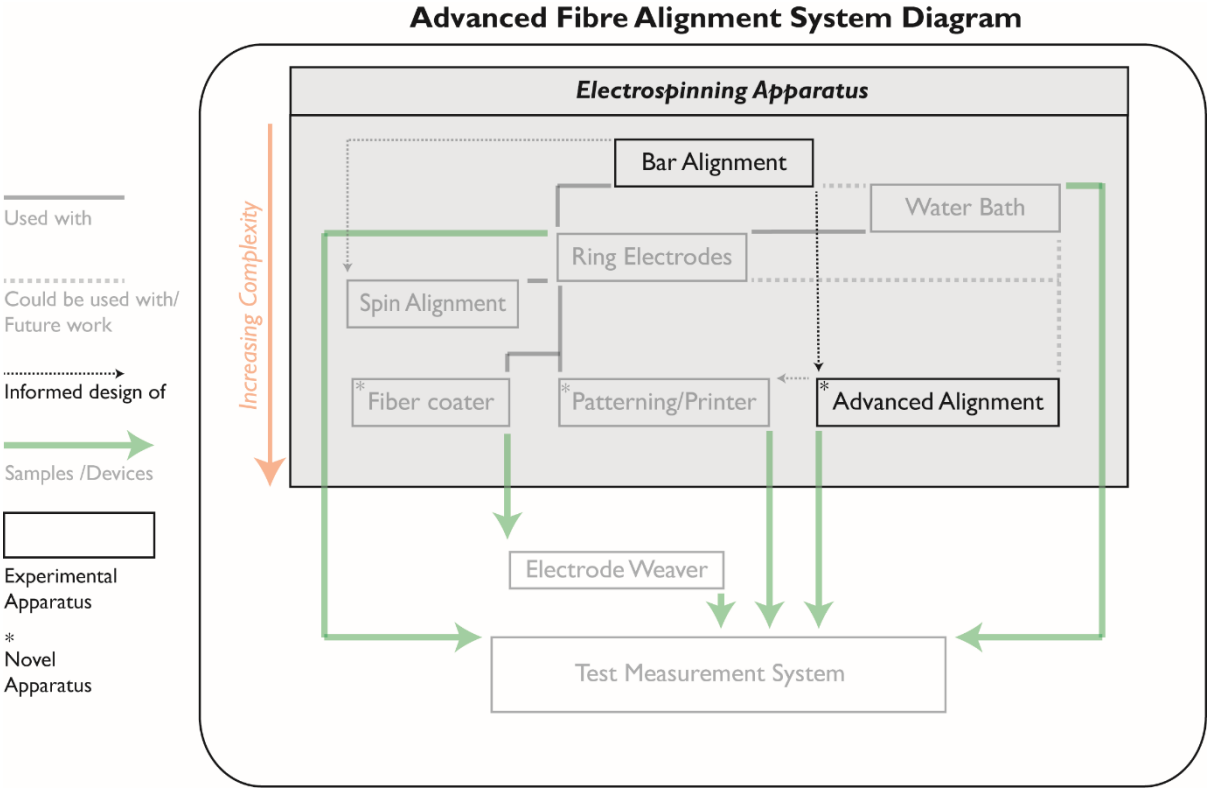

Figure 4.11 - Advanced Fibre Alignment System

4.2.2 *Initial Experimental Apparatus*

4.2.2.1 *Introduction*

The following work details the development of the initial attempt at creating novel experimental apparatus that allows a number of ground electrodes to switch to and from the high voltage power supply ground connection in a predetermined order and timing.

4.2.2.2 *Design Specification*

The aim of this apparatus was to expand the already widely utilised electrospinning method of using separated ground electrodes to encourage the fibres to align across them during the electrospinning process. To expand upon this methodology it was necessary to develop a way of actively changing the state of the ground electrodes between electrically floating and electrically grounded in relation to the high voltage power supply used for electrospinning. By changing which of the electrodes are grounded control can be gained of were the fibres are attracted to in flight and then

how they align at deposition. Figure 4.12 shows a simplified overall view of the system.

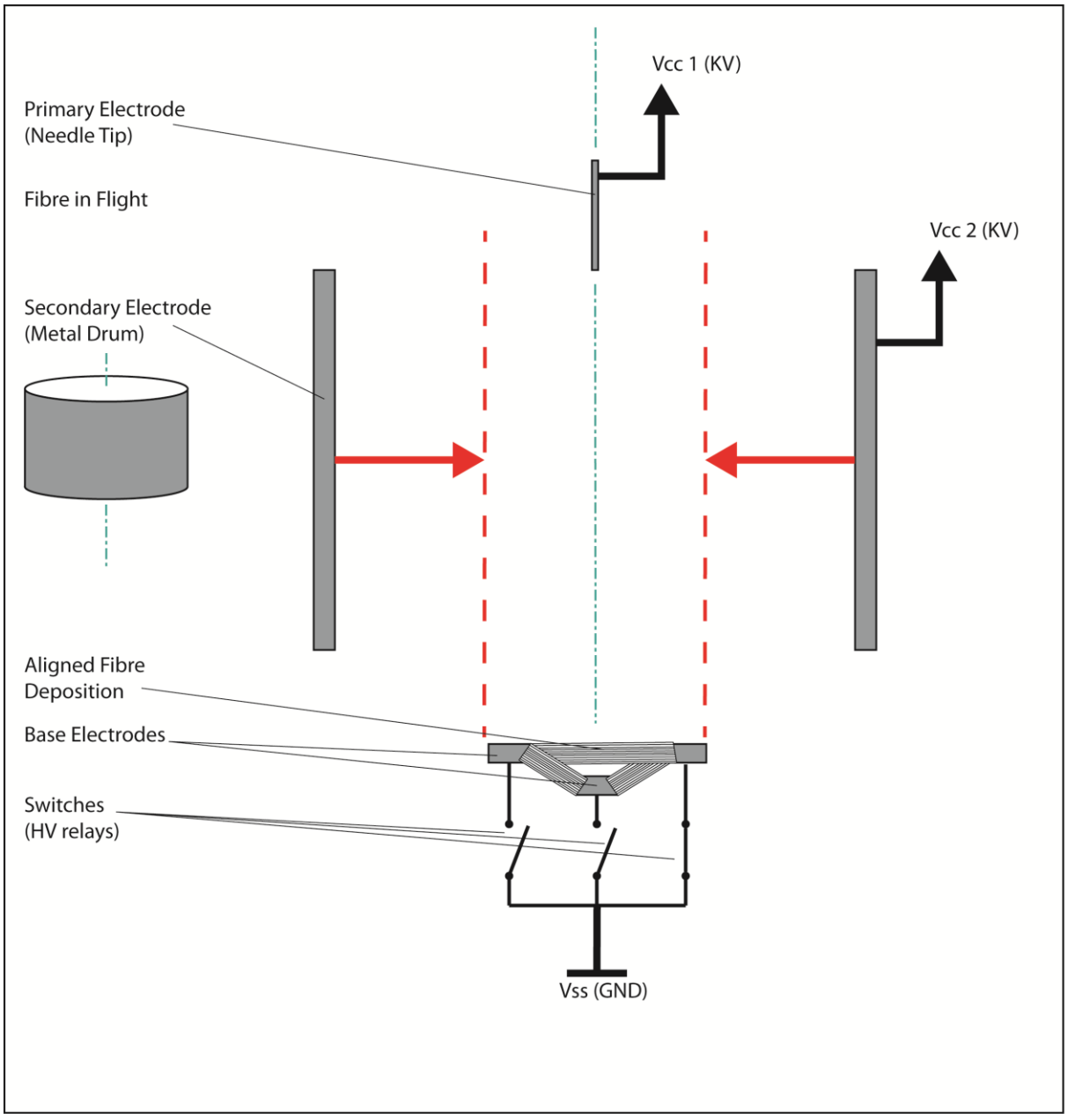

Figure 4.12 - Initial Fibre Alignment System

This could be used in two ways with different electrode configurations. The first possible configuration would be to have small point electrodes where fibres would align between them in a thick bundle and as the electrodes are switched between

floating and ground electrical states. This would allow the creation of geometric patterns made from fibre bundles. The second way to utilise this new technique would be to use bar electrodes in a pattern where the bars are grounded or floated in pairs. The fibres in flight would align across the bars creating an aligned fibre mat and then when the electrode pairs are switched the alignment would change in direction, allowing the build-up of aligned fibres with different layer orientations during the electrospinning process.

4.2.2.3 *Physical Design*

The physical design of this piece of apparatus was much easier to implement than some of the other ideas developed since there was no mechanical component to the apparatus. However it was more important to be aware and design accordingly for the electrical components since some of them are directly linked into the high voltage supply used for electrospinning. This meant that all parts were made from acrylic and fastenings were either bolted using nylon nuts and bolts or Tensol liquid cement was used to bond parts together.

4.2.2.4 *Electronic Design*

4.2.2.4.1 *Aim*

The electronics developed needed to facilitate the control of the experimental parameters for the apparatus being built. For the initial testing of the concept this was limited to a few pre-determined patterns that the High Voltage Relays being used would be activated in and also the timing between the activation of the relays.

As this was an initial proof of concept series of experiments the hardware and software was kept simple to aid the speed of development. This therefore needed a minimum component count and the use of easily implemented hardware.

The control PCB which housed the components such as the microcontroller that would control the experimental parameters was designed so that the relays used, as described in Appendix section 9.4.2, could easily be removed if necessary. This ensured that the control PCB could be easily replaced if there was an issue with the PCB or if the PCB needed updating and improving.

4.2.2.4.2 *Hardware Development*

Figure 4.13 shows the schematic of the PCB marked control board on the block diagram above. This PCB has the microcontroller and user interface that allows the selection and implementation of the pre-coded experimental parameters.

Initial Relay Control Schematic

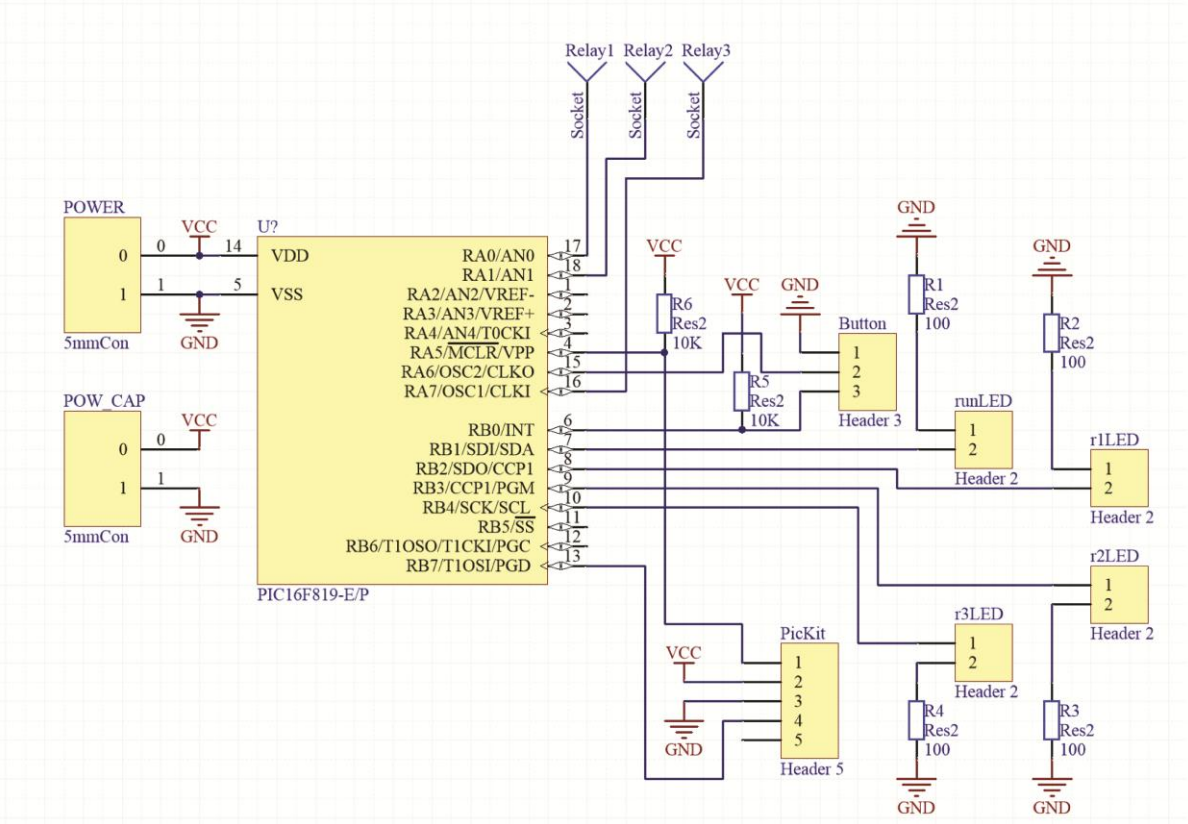

Initial Relay Control PCB Artwork

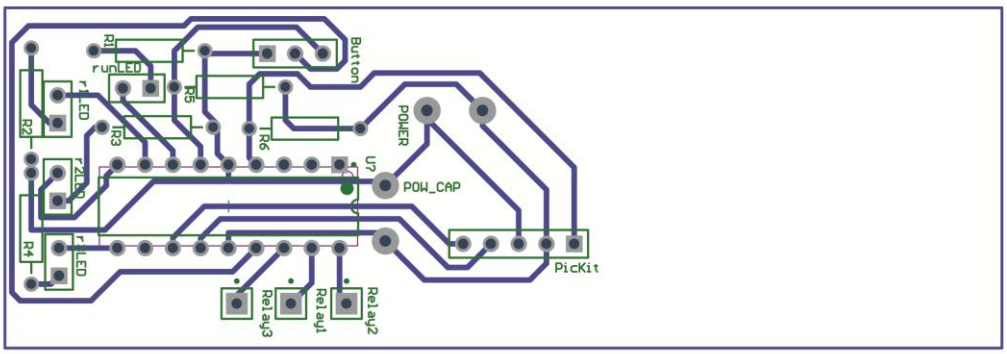

Figure 4.13 - Initial Relay Control Circuit Schematic and Board Layout

4.2.2.4.3 *Software Development*

The microcontroller is used to control the relays during the experimental procedures. The relays are triggered in set patterns and with timing chosen by the user. These patterns were pre-coded so that the user could only choose between 3 experiments and then choose one of 7 timing increments between the relays switching. A simple interface consisting of one button and three LED's was chosen to allow selection of the experiment wanted and the LED's gave feedback on the selection and timing chosen. A full version of this code is in appendix section 9.6.1.1.

4.2.2.5 *Apparatus Integration*

Integration with the conventional electrospinning system is as follows, the ground connection from the High voltage power supply is attached to the common ground lead on the developed apparatus and the positive voltage cable connected to the electrospinning needle as usual. The apparatus was positioned centred in relation to the needle above it.

In line with the bottom of the electrospinning needle and concentric to it is the secondary electrode apparatus. The bottom electrode ring of this is positioned so that it is in line with the electrodes on top of the Fibre Alignment apparatus and also concentric to the secondary electrode rings and also with the primary electrode electrospinning needle.

4.2.3 Final Experimental Apparatus

4.2.3.1 *Introduction*

Building upon the successful initial piece of apparatus this following work shows the development and improvement made to the initial apparatus and the scaling up of the approach to allow for more complex and advanced experimentation to be tried.

4.2.3.2 *Design Specification*

From the experimentation carried out and covered in section 5.4.3.1 the process had been validated however certain elements of the initial design needed changing. The

floating electrical state needed to be made a positive high potential voltage. This added new limitations to both the physical design of the apparatus and also the electrical hardware design. Due to only having two high voltage power supplies it also meant that the way in which the secondary electrode rings were used would be limited. Since the approach had been successful the number of high voltage relays used was increased from 3 to 7, scaling the process up and greatly increasing the scope of the experimentation possible. The improved system is shown in Figure 4.14.

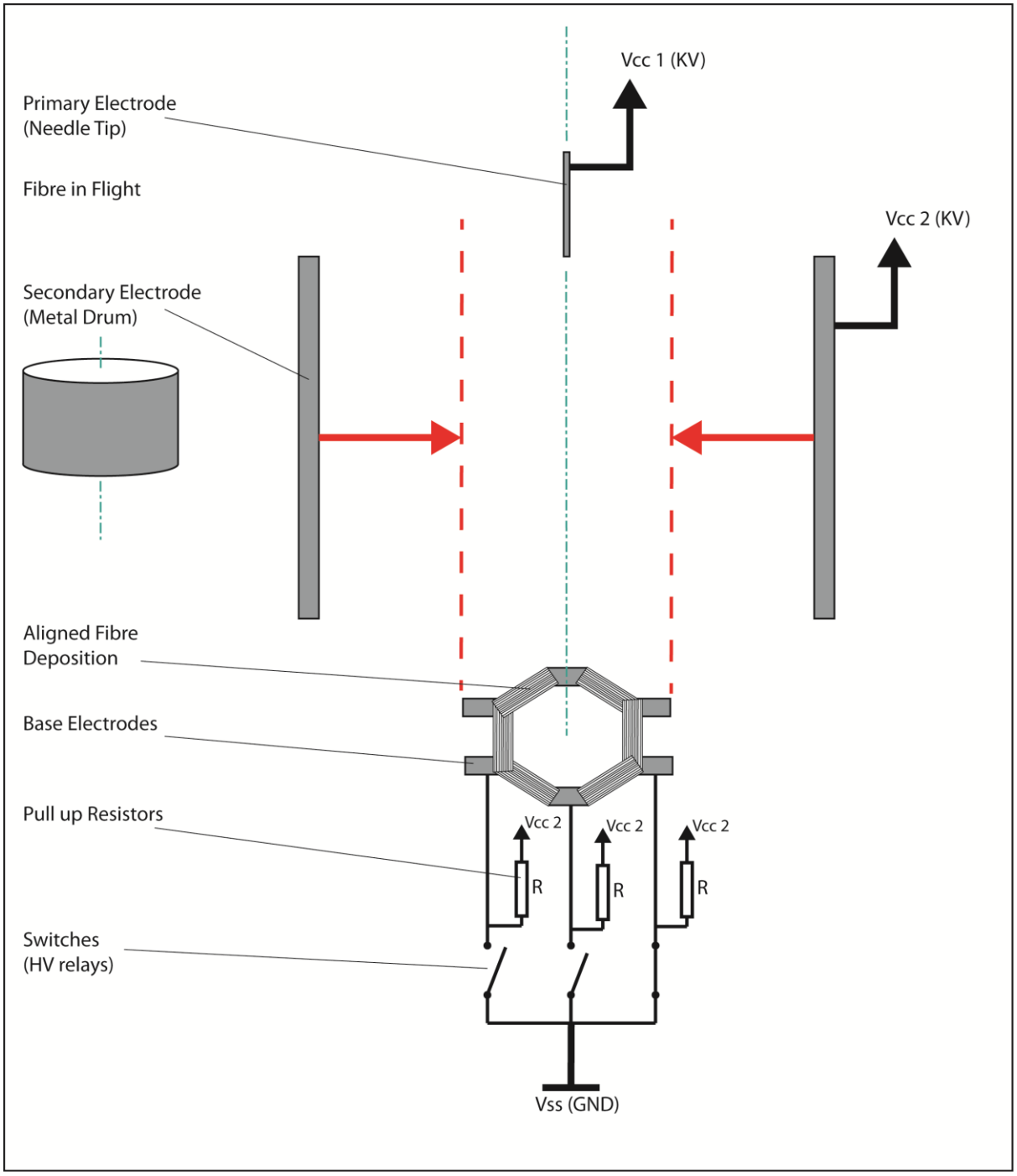

Figure 4.14 - Improved Fibre Alignment Apparatus Diagram

4.2.3.3 *Physical Design*

The physical design wasn't changed greatly from the first version, the casing was made larger due to the extra high voltage relays being utilised and the interior of the casing compartmentalised due to the need of having both a positive potential high voltage and ground potential voltage cabling going into the same housing.

The high positive potential voltage PCB that carried the pull up resistors (See Appendix section 9.4.1) was separated using thick acyclic sheet from the electronic control PCB and high voltage relays below to minimize chances of short circuit. A grounded metal plate was positioned above the electronic control PCB to shield it from any electromagnetic interference which could interfere with the microcontroller.

4.2.3.4 *Electronic Design*

4.2.3.4.1 *Aim*

With the validation of the initial apparatus and the decision to scale up the experiment to use more relays the control PCB had to also be updated. The PCB now needed connection to 7 of the relay boards and also a much more complex software system that allowed full control of which relays are chosen and how they are patterned, as well as the timing of the relays. In addition to this due to the need to keep the apparatus, including the control board inside the electrospinning safety locked box, the method of interface between the control board and the needed changing both for ease of use and safety. Bluetooth connection (See Appendix section 9.3.2.5) was used as it allowed control from an external device.

The other major change introduced is the for the inclusion of the High voltage pull up resistors which make the base electrodes attached to the relays go between ground and a high potential voltage instead of between ground and the floating electrical state. The schematic and PCB are included in Appendix section 9.4.1.

4.2.3.4.2 *Hardware Development*

4.2.3.4.2.1 Control Board

There were multiple versions of this PCB developed due to unforeseen effects that using the High Voltage Pull Up PCB caused such as electromagnetic interference (EMI) talked about in section 5.4.3.1. The schematic shown below in Figure 4.15 is for the final PCB developed. Note the resistance capacitance (RC) circuits attached between each of the Relay headers and Microcontroller outputs to help stop the EMI issues from resetting the Microcontroller when running the experiments.

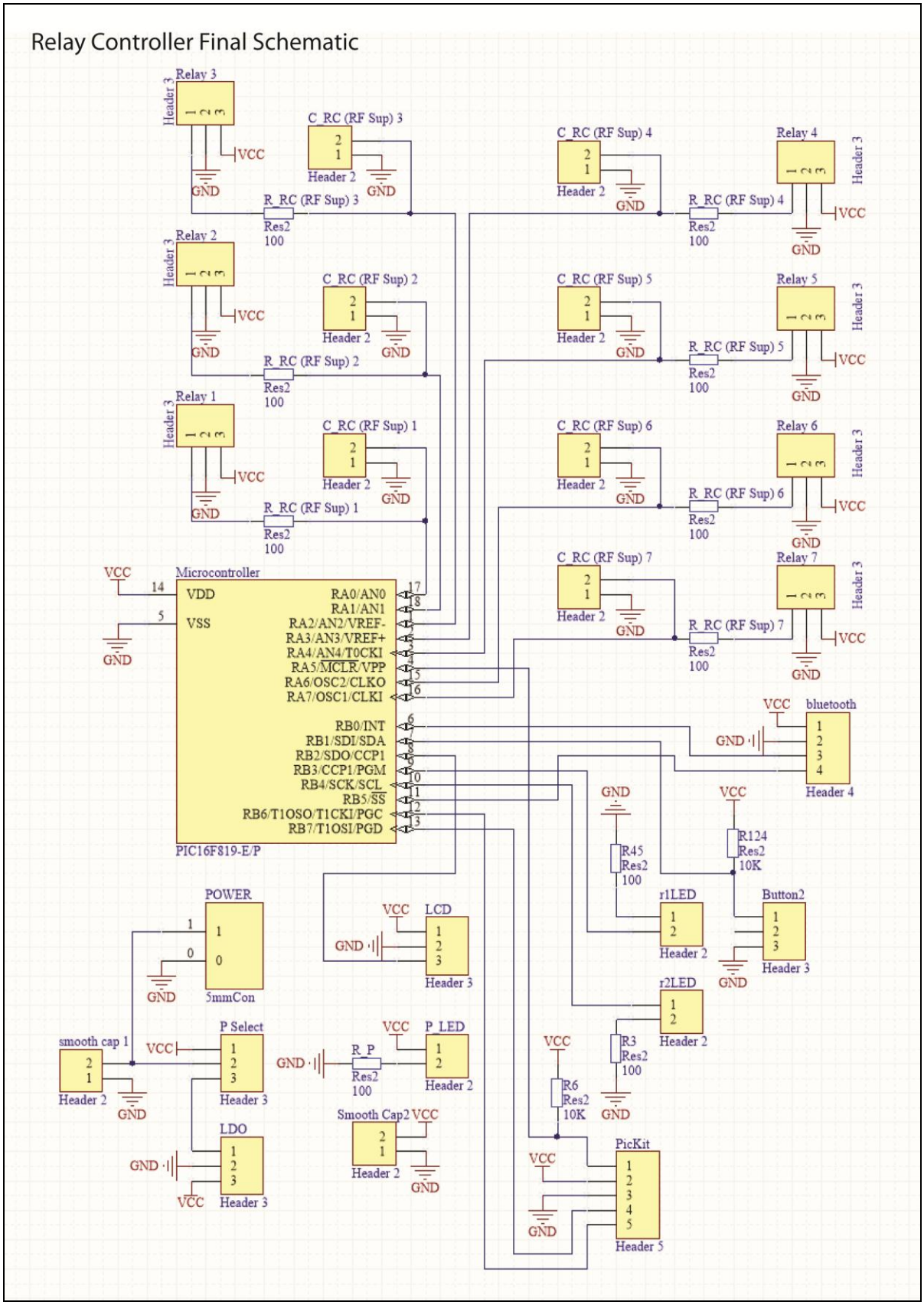

Figure 4.15 - Improved Relay Control Circuit Schematic

The PCB layout has the connectors for the relay PCB's arranged around the outside for ease of connection. Also a ground plane on the top copper layer was included to help elevate some of the EMI issues with intermediate versions of this PCB.

4.2.3.4.2.2 High Voltage Pull Up Resistor Network

A printed circuit board was developed to supply the secondary potential voltage to the base electrodes through a series of high Ohm resistors, the need for these large resistor values is to limit any potential current due to the high potential voltages utilised when the relays are switching. The resistors used are 10 MΩ in value and there are 11 in series for each relay. The board had another two rows of ten 10 MΩ resistors that could be used in series to increase the total resistor values is necessary depending on the experimental parameters used. This circuit board and the high resistor values used was necessary to limit the current flowing through the vacuum reed relays while they were switched to ground. See Appendix Section 9.4.1 for PCB schematic and artwork.

4.2.3.4.3 *Software Development*

The code for the final version of the apparatus developed was quite complex. The structure of the code can be split into the two parts: The menu where the experimental parameters are chosen and the run time where the relays are switched in the desired pattern as set in the menu. Within the menu there are two ways to use the relays either individually or in pairs. In both cases the relays will switch sequentially. You can also chose the duty cycle of the relays and which of the seven relays to use.

Initial versions of this code used an LCD screen, LED's and buttons for the interface however with the integration of the Bluetooth serial module for the final hardware all interaction from the user and feedback is done remotely using a host device. The final version of this code is included as an appendix in section 9.6.1.2.

4.2.3.5 *Apparatus Integration*

Integration is slightly different to the initial apparatus as now the secondary High Voltage power supply's positive lead is attached to the input on the High Voltage Pull

Up PCB. Both high voltage power supplies ground leads are connected together and to the common ground lead of the apparatus. The primary High Voltage Power Supply's positive lead is connected as usual to the electrospinning needle.

Since the secondary power supply is utilised for the apparatus it is not possible to use the secondary electrode control rings with this apparatus (Unless the rings are used with the same potential voltage as the Pull Up PCB), so the apparatus is positioned at the desired height straight under and centred to the electrospinning needle.

4.3 *Patterning Printer*

4.3.1 Introduction

From the literature most of the produced films deposition area when conventionally electrospun were either round or square, an area of research that had not been investigated fully was producing more intricate shapes and patterning of the deposited fibres. Most of the processes that had been utilised to do basic patterning were only on the micro scale such as using a x,y moving stage as already discussed. Developing a technique that can lay down patterns on a macro scale has many benefits especially for the future fabrication of devices. A printing system was therefore developed, improving upon the work already carried out by Kim which used a computer controlled stage to collect and pattern electrospun fibres [84]. The work already presented had already achieved printing however the track thickness was relatively thick, the aim therefore was to produce finer tracks with greater control by using alternative electrode configurations. An iterative process of design and development is shown in the following subchapters leading to the successful creation of a novel piece of equipment that fulfils the needs identified. The proposed system elements are shown in Figure 4.16 building upon the other work already completed.

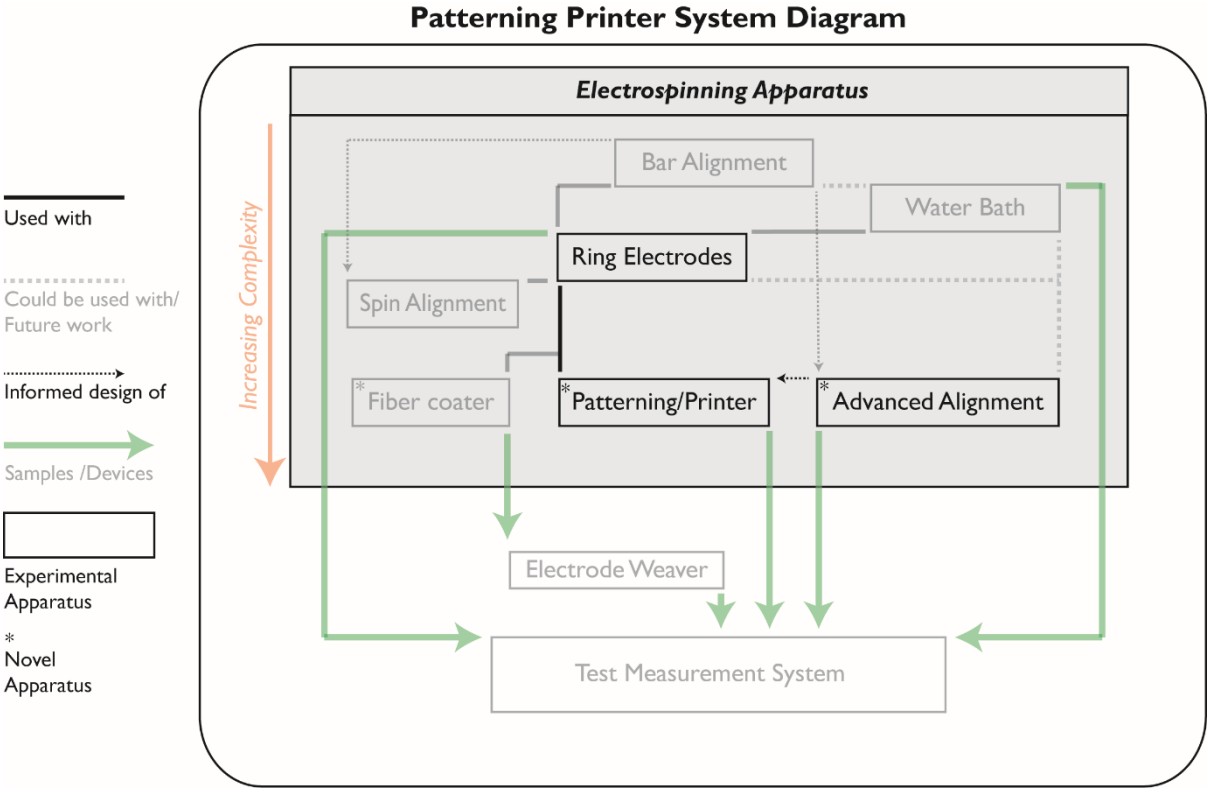

Figure 4.16 - Patterning Printer System Diagram

4.3.2 *Initial Design*

4.3.2.1 *Introduction*

The following section details the necessary design and development necessary to build and test an initial piece of experimental apparatus that allows novel patterning of electrospun polymers using a custom designed printer compatible with the conventional electrospinning system.

4.3.2.2 *Design Specification*

The main aim and the reason to develop this piece of equipment was to allow much greater control of the deposition area during the electrospinning process which will allow the patterning and also variable thickness of deposited fibre mats. The basic methodology devised is shown in Figure 4.17 and shows the use of a secondary conical electrode that is utilised to control and focus the deposition area of the electrospun fibres. A moving stage with the ground electrode attached is placed underneath the secondary electrode and can move in both x, y axis. The z axis or

height is fixed at a height determined by the minimum safe air gap between electrodes as described in section 3.3.5.

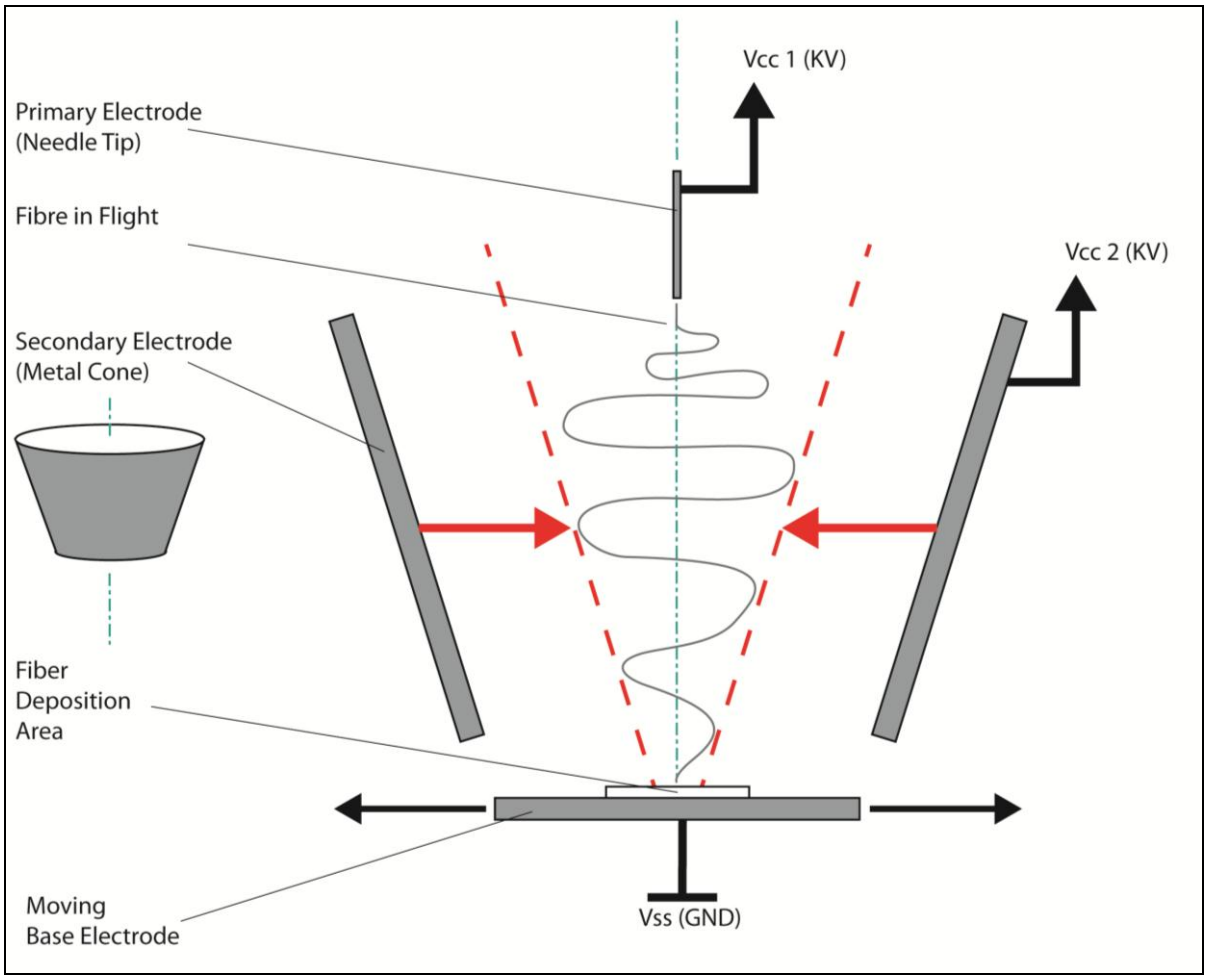

Figure 4.17 - Basic Printer Method

Similar work has been presented which utilises x, y stages and a near field electrospinning process which has been shown to pattern single fibres, this concept is similar however the patterning is on a macro rather than a micro scale. This is because the reported work only has an x, y axis bed movement of a few microns compared to a bed movement of 100 mm or more for this developed apparatus.

It is necessary for the production of piezoelectric fibres using PVDF to both stretch and electrically pole the fibres during the electrospinning process. Using near field electrospinning doesn't allow the whipping effect and so the axial stretching of the

fibres in flight will not occur to the same degree reducing the crystallinity and therefore the piezoelectric effect exhibited by any fibres produced. The apparatus developed uses a cone which controls the deposition area and still allows a greater degree of whipping of the fibres in flight to take place.

The x, y stage developed needed to be controlled accurately and with a high enough resolution of the linear movement that patterns could be deposited accurately and repeatedly. The control for the x,y stage needed to be wireless so that it could be controlled within the existing enclosed electrospinning system with the door lock activated.

4.3.2.3 *Physical Design*

The physical design considerations are similar as for the other experimental apparatus developed. Since the apparatus will be used within a high electric field as much as the structure and other parts as possible must be made from a non-conductive material that is easily worked with and ideally laser cut to reduce manufacturing and development time, clear acrylic was used for the majority of this apparatus.

The overall size of the apparatus was dictated by the length, width and height of the existing electrospinning box. There also had to be clearance allowed for the stepper motors and any wiring.

The apparatus was designed in a modular way with different systems being separate, this allowed for the cyclic testing, development and improvement of the different systems without the need to re-manufacture the whole apparatus on every design iteration. The modular systems was also designed to be highly adjustable for the testing and experimentation necessary to prove the apparatus behaves as required. The general arrangement drawing shown in Figure 4.18 shows the different modular systems and what makes up each of them and a render of the developed apparatus can be seen in Figure 4.19.

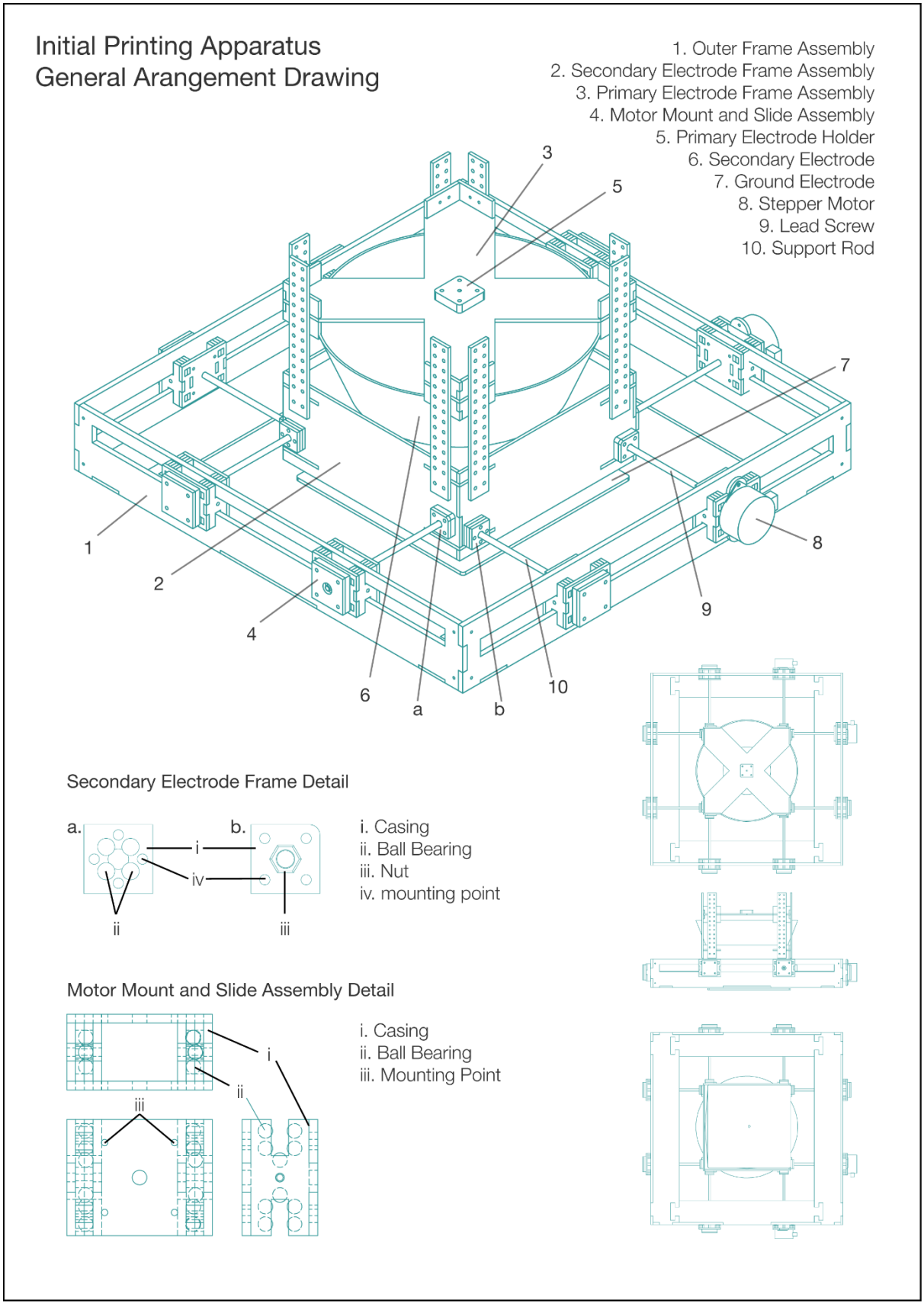

Figure 4.18 – Initial Printing Apparatus General Arrangement Drawing

The designed apparatus can be split into three main parts, the frame, slide assembly and the secondary electrode frame assembly which also incorporates the primary electrode holder and its frame. The frame, marked part 1 on the GA drawing (Figure 4.18), gives support to the whole structure and is designed in such a way so that the Slide Assemblies, marked part 2, can travel along it freely. As can be seen from the Motor Mount and Slide Assembly Detail on the GA drawing there are 20 loose balls incorporated into the Slide Assembly design to reduce friction and encourage smooth movement. The slide Assemblies work in pairs opposite one another. They either have the stepper motor mounted to one and a Bearing set in the one opposite, with a lead screw between the two. Or they just have a support rod between them made from 5 mm diameter silver steel.

The two lead screws are orientated at 90° to each other and they pass through the Secondary Electrode Frame Assembly, part 3 on the GA drawing. The Secondary Electrode Frame Detail image, marked b. shows now the lead nut is incorporated and mounted to the Secondary Electrode Frame, the lead screw passes through the lead nut and therefore supports a portion of the weight of the secondary electrode and frame. For the support rods a bearing assembly shown in the Secondary Electrode Frame Detail image, marked a. is used to transfer the weight from the secondary electrode and frame to the support rod while minimizing the friction to encourage smooth movement.

The primary electrode holder and its frame, marked 3 on the GA drawing, are attached to the top of the Secondary electrode frame on a ladder system which allows for the adjustment of the height of the primary electrode. In this design the primary electrode is kept perfectly concentric in relation to the centre of the second electrode cone, this is important for predictable electrospinning deposition and uniform electric field profiles.

For this design the ground electrode is placed below the apparatus and is separate to it. The aligned primary and secondary electrodes move over the ground plate to pattern the electrospun fibres. The frames and assemblies are made up of 152 laser cut parts made from acrylic. The different frames parts were adhered using Tensol cement or bolted together primarily using M3 bolts. Two ball bearings and 176 loose balls are used to ensure smooth movement during operation.

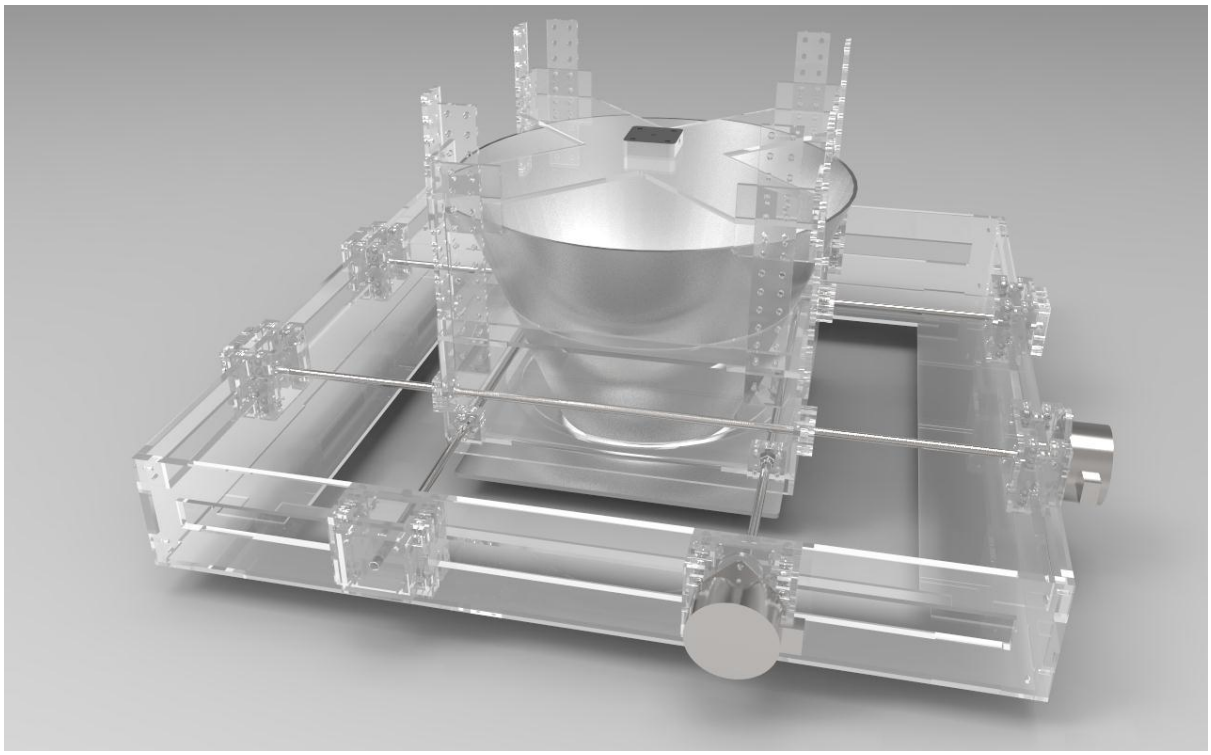

Figure 4.19 - Initial Printing Apparatus Render

4.3.2.4 *Mechanical Design*

The necessary mechanical considerations for the design of this piece of apparatus were mainly concerned with ensuring smooth and repeatable movement of the secondary and primary electrodes and frames. This was achieved through extensive use of ball bearings and loose balls built into parts of the design.

Figure 4.20 shows the slide assembly with the balls in their places. The slide assembly was designed in such a way so that there was a small clearance of 0.2 mm between the balls and the frame they run against to ensure smooth operation. The balls used are 5mm in diameter and are free to move around a small amount in their housing to the degree of 1 mm in the direction of travel and 0.2 mm in the other axes.

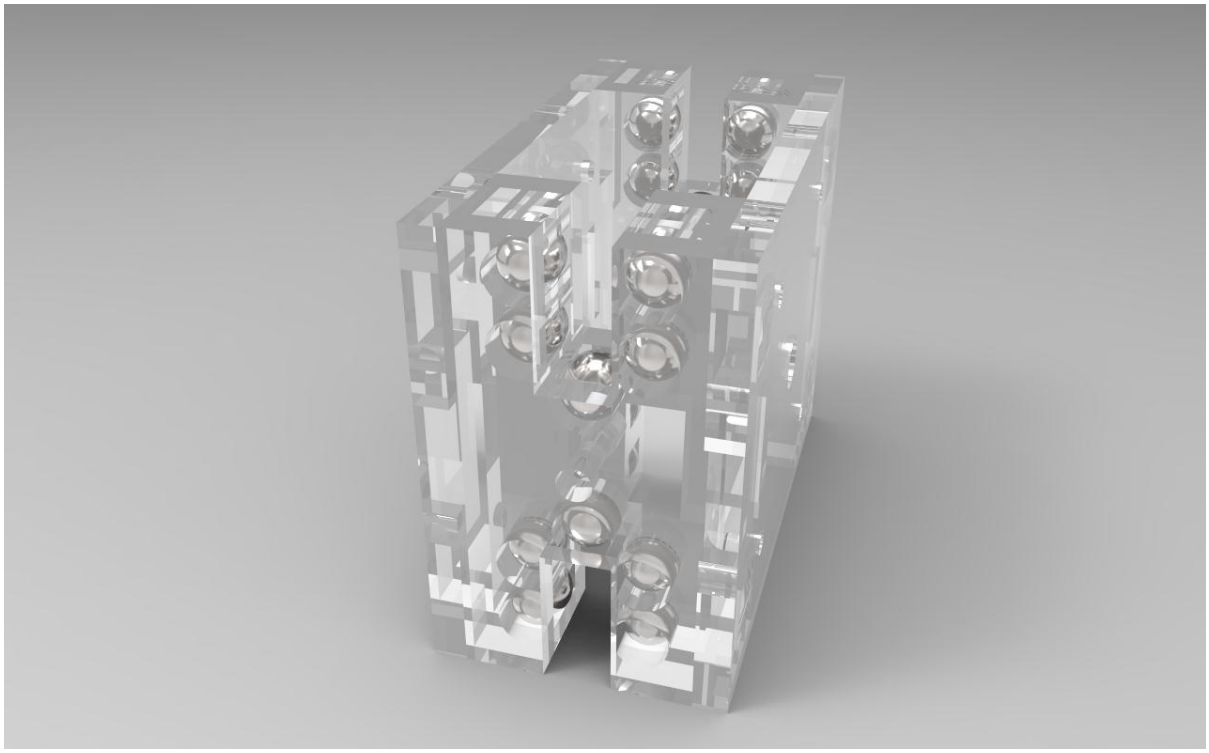

Figure 4.20 - Slide Assembly Render

Two ball bearings were used to support the end of the lead screws not attached to the stepper motors. They help to keep the turning lead screw straight and take some of the pressure off the stepper motors during operation. The lead screws themselves are of a M5 standard thread size, this has a pitch of 0.8 mm so for a full rotation from the driving stepper motor the electrodes and frame assemblies move 0.8 mm, since the stepper motor has 48 steps per 360° rotation this gives a minimum linear movement of 0.017 mm.

4.3.2.5 *Electronic Design*

4.3.2.5.1 *Aim*

The electronics for the initial apparatus developed had to control and drive two stepper motors which controlled the positioning of the stage with collector base electrode on it during experimentation. It was decided that four micro lever switches would be used to detect when the stage was at its maximum and minimum length of travel on the x and y axes. This would stop issues and potentially damage caused by the stage crashing at its travel limits into the frame. It would also allow for the

software that controls the stage to automatically centre itself after finding the limit of the x and y axis and then moving back half way. The electronics developed also needed to have a suitable user interface that would allow the user to input desired morphology, setup and execute the experiments. A connection for a high voltage relay needed to be added as well to allow the electrospinning jet to be selectively turned on and off programmatically.

4.3.2.5.2 *Hardware Development*

The control hardware chosen for this apparatus was the Microchip microcontroller PIC16F819 and a Bluetooth module for user interfacing. The motors were driven using two L293D quadruple half-H drivers. As the stepper motors themselves need 12 v to operate it was necessary to have 12 v on the circuit board so this was chosen to be the primary voltage. The digital components like the microcontroller and Bluetooth module needed 5 v so two low drop out voltage converters stepped down the 12 v input to a 5 v rail. Two were used to ensure that there was enough current available for all the digital components used.

Figure 4.21 shows the schematic developed from the breadboard prototype circuit which was built first to test the circuit. Note the configuration used for the four micro switches where a header connector is used that supplies 5 v and ground lines to the switches and the signal from each of the switches returned. Each switch is connected to the microcontroller directly and then all the switches are connected to one microcontroller pin through 4 diodes. This last microcontroller connection is the external interrupt pin which is used to detect external input such as a switch being pressed and immediately runs a separate piece of code.

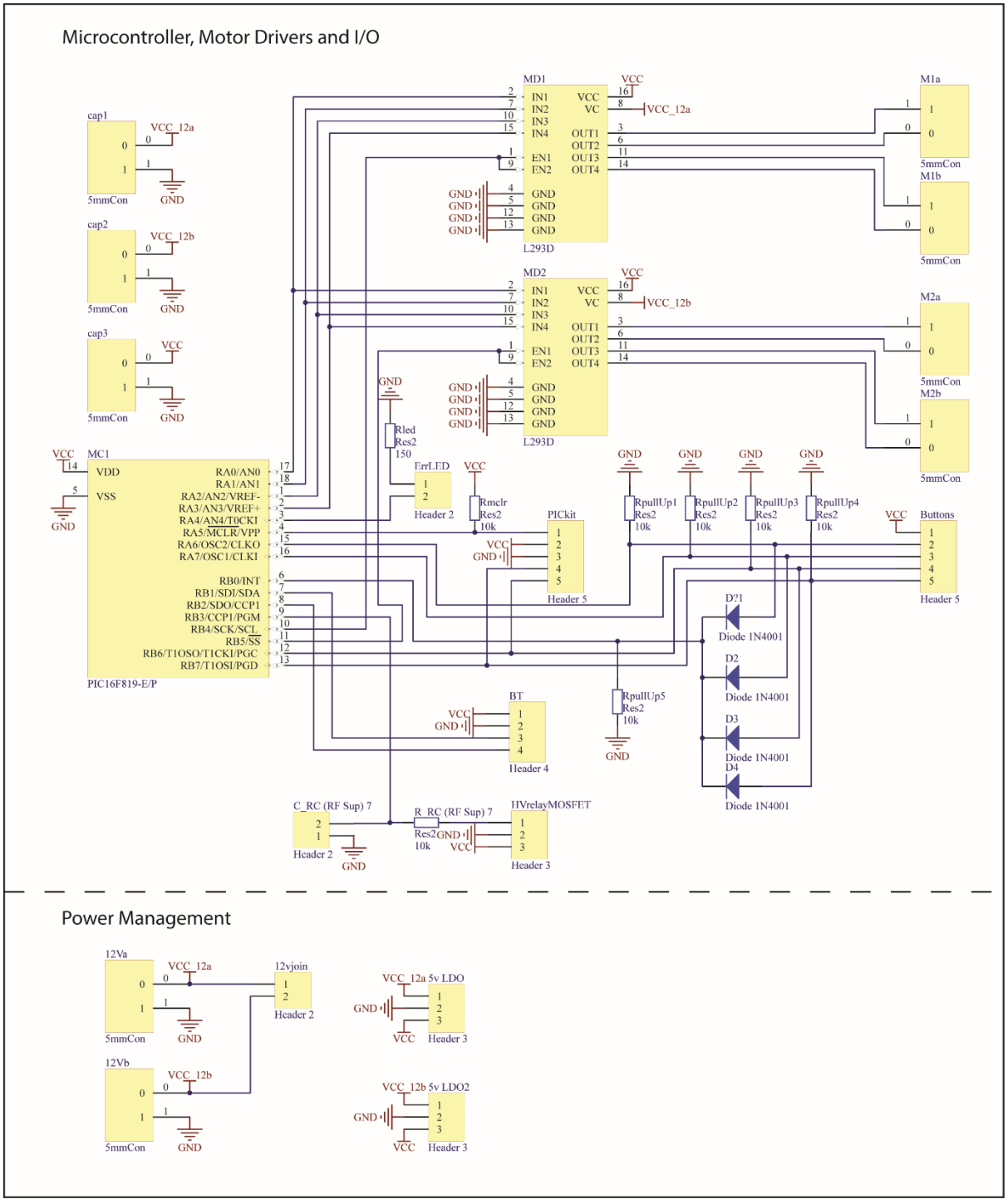

Figure 4.21 - Initial Fibre Printer Schematic

The printed circuit board layout that was developed and then printed from the schematic above is shown in Figure 4.22. Note the different coloured tracks which signify the top and bottom copper layers. Making the PCB double sided was necessary due to the complexity and component count for this piece. Care has also

been taken to ensure that most of the connectors appear on the outer perimeter of the PCB.

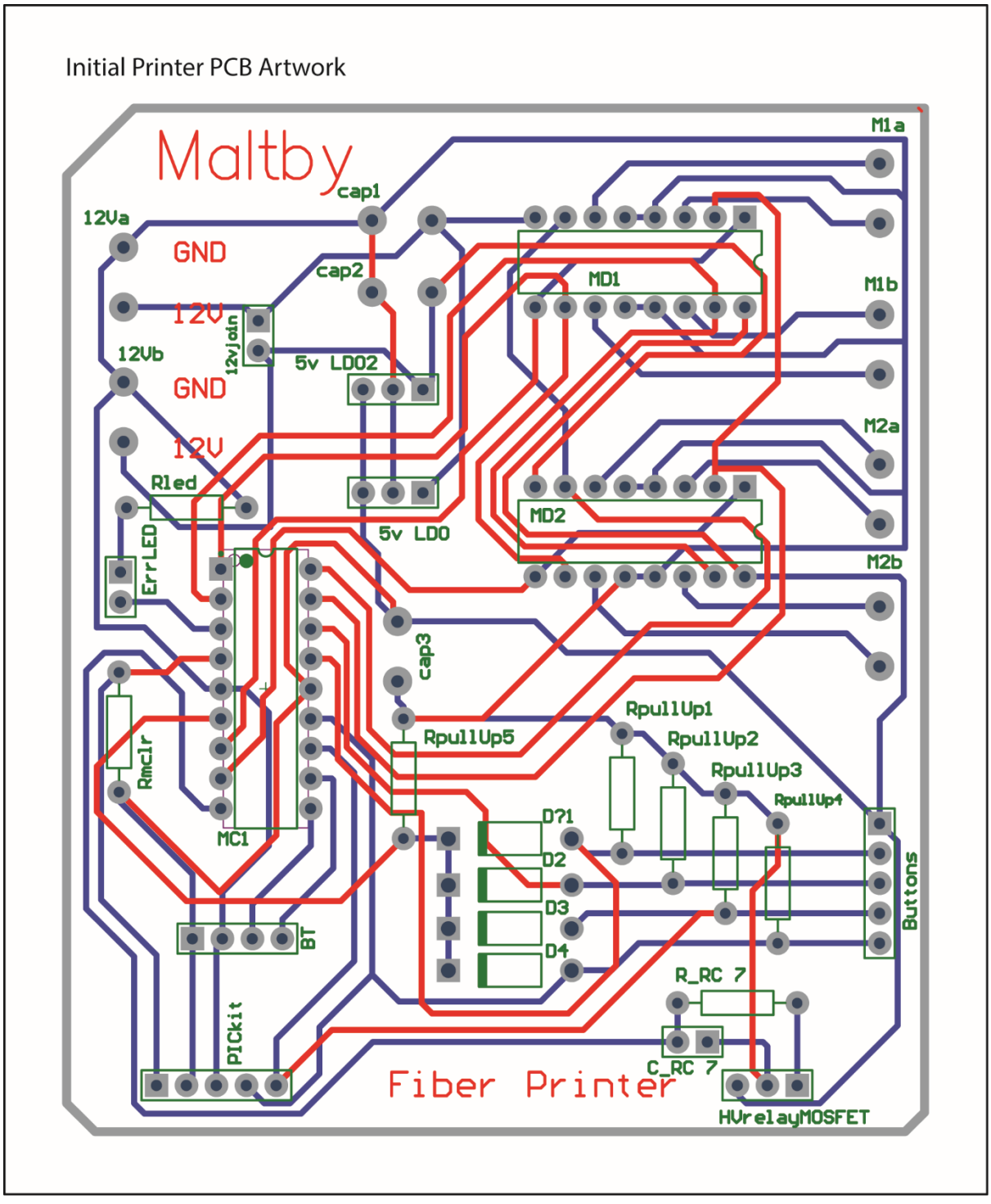

Figure 4.22 - Initial Fibre Printer Board Layout

4.3.2.5.3 *Software Development*

For the development of the software it was necessary to work out a coordinate system based on how many steps of the stepper motor it takes for the stage to fully traverse the x or y axis. This was found by taking the total distance that the stage could travel (250 mm) and then divide by far the stage could travel per step of the stepper motor (0.017 mm per step) this gave the number of steps that the stage could travel in total at 14705 steps.

The software itself is split into a few distinct areas, the initial centring of the stage, the user input and then the execution, driving the stepper motors to produce the desired movement of the stage. There is also the safety routine that watches for the micro-switches being pressed showing the stage is at the end of its travel.

On initialisation the developed program first centres the stage by first stepping the x axis motor until the minimum limit x axis micro-switch is triggered. Then the process is repeated for the y axis so the stage ends up in one corner of the apparatus. The stage is then centred by stepping both motors 7352 steps towards the maximum limit switches.

Once centred, the program sends a menu to a host device such as a mobile phone via Bluetooth. This is done by sending ASCCII characters by UART to the Bluetooth module which in turn sends them over radio to the host device. The program then waits for input from the user in regards to the pattern that the stage is to move in during experimentation. This input data has to be input in a predetermined format to be correctly understood by the program. The format is as follows:

The number of steps is tracked in both axis to ensure that the maximum number of steps has not been reached which would cause the stage to try to move past its travel limit during experimentation.

The input data is stored into arrays and once the program is set running by a final command from the host device this data is then read back and translated into step commands that drive the stepper motors. The pattern will be repeated the amount of times that was desired and then the program will stop and the stage will reset its position to the centre, completing the experiment.

The micro-switches work in conjunction with an interrupt routine that can stop the program above at any point if any of the micro-switches are triggered indicating that the stage has come to the end of its travel in one or both axis. This is possible due to the microcontroller architecture which has an external interrupt (Pin 0 on port B) that can be used to automatically detect a logic level voltage change on that pin. Once a micro-switch is pressed and the change in voltage seen on the pin then the microcontroller comes out of the code it is currently running and then executes a special interrupt routine. In this case the interrupt routine just sends an error message to the phone and permanently stops the program. It should be mentioned that the main code should not allow the input of a geometry that would cause a crash from the stage getting to its maximum or minimum travel however it is still useful in case of any other issues like missed steps or jamming that causes the stage physical position to become unaligned to where the program believes it to be.

It should be noted that the use of a high voltage relay to selectively switch the electrospinning jet on and off was not implemented in the initial code even though the hardware allowed for this innovation. It was planned that it would be implemented in a later version of the code and is seen in the final apparatus developed.

4.3.2.6 *Apparatus Integration*

The electrospinning needle is put through the aluminium block at the top of the apparatus and secured by tightening the screw. The positive lead for the HV power supply is attached to the aluminium block as well. The HV power supply ground lead is attached to the ground lead that is connected to the base electrode on the moving stage. The circuit board for diving the stepper motors and controlling the experiment must be within the electrospinning safety cabinet. The regulated power supply providing 12 v however is kept outside of the cabinet and power leads go from this to the circuit board.

4.3.3 Improvements

4.3.3.1 *Introduction*

From the experiments completed using the initial printing apparatus various changes were identified and they were developed over a period of time as incremental improvements. These following sections give an overview of the final apparatus developed and the technical changes made for all aspects of the final design solution.

4.3.3.2 *Design Specification*

The initial design showed that the approach had merit and worked as expected however the technique needed refinement, please see section 5.5.2. for experimental testing and analysis of the initial apparatus. The improved design tried to reduce the fibre deposition area or as in this application the track width of the printer. A method of selectively turning off the electrospinning jet and synchronising this with the moving stage was wanted to expand the practicality and functionality of the printing technique. The improved system is shown in Figure 4.23.

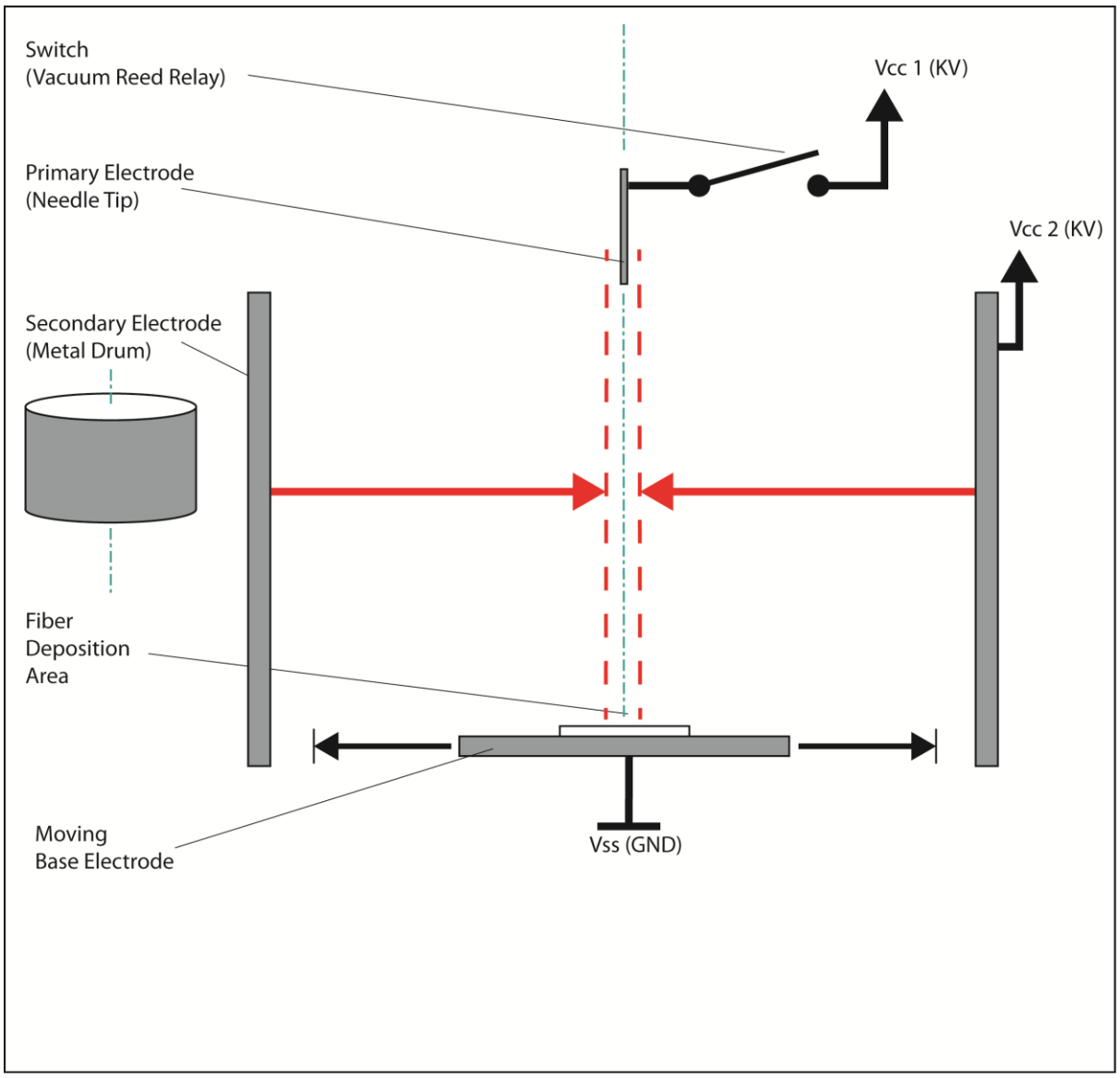

Figure 4.23 - Improved Fibre Printing System Diagram

4.3.3.3 *Physical Design*

The final experimental apparatus is shown in Figure 4.24. The procedure has stayed the same from the initial version however now the grounded plate electrode is now moved in the x and y axes instead of the primary and secondary electrode. This was done for multiple reasons, in summary however mechanically this approach was superior as the weight of the ground electrode and frame is lighter than the previous assembly which reduced strain on the drive mechanism. There had been an issue with the electrodes and frame assembly's not running smoothly and straight but instead becoming jammed or moving erratically in short jerks. It also allowed a

change in the secondary electrode which was found to be prohibitively small during experimentation.

The base electrode has been moved up into the secondary electrode cylinder to adjust the electric field this reduces the movement allowed in the x and y planes to prevent the secondary electrode arcing to the base electrode, this reduces the total travel in the x and y movement range in comparison to the original design.

The changes as previously stated were incremental. With the change from having a stationary base electrode to having the base electrode move rather than the primary and secondary electrode being the first and greatest change. The evolution of the design can be seen in Figure 4.25.

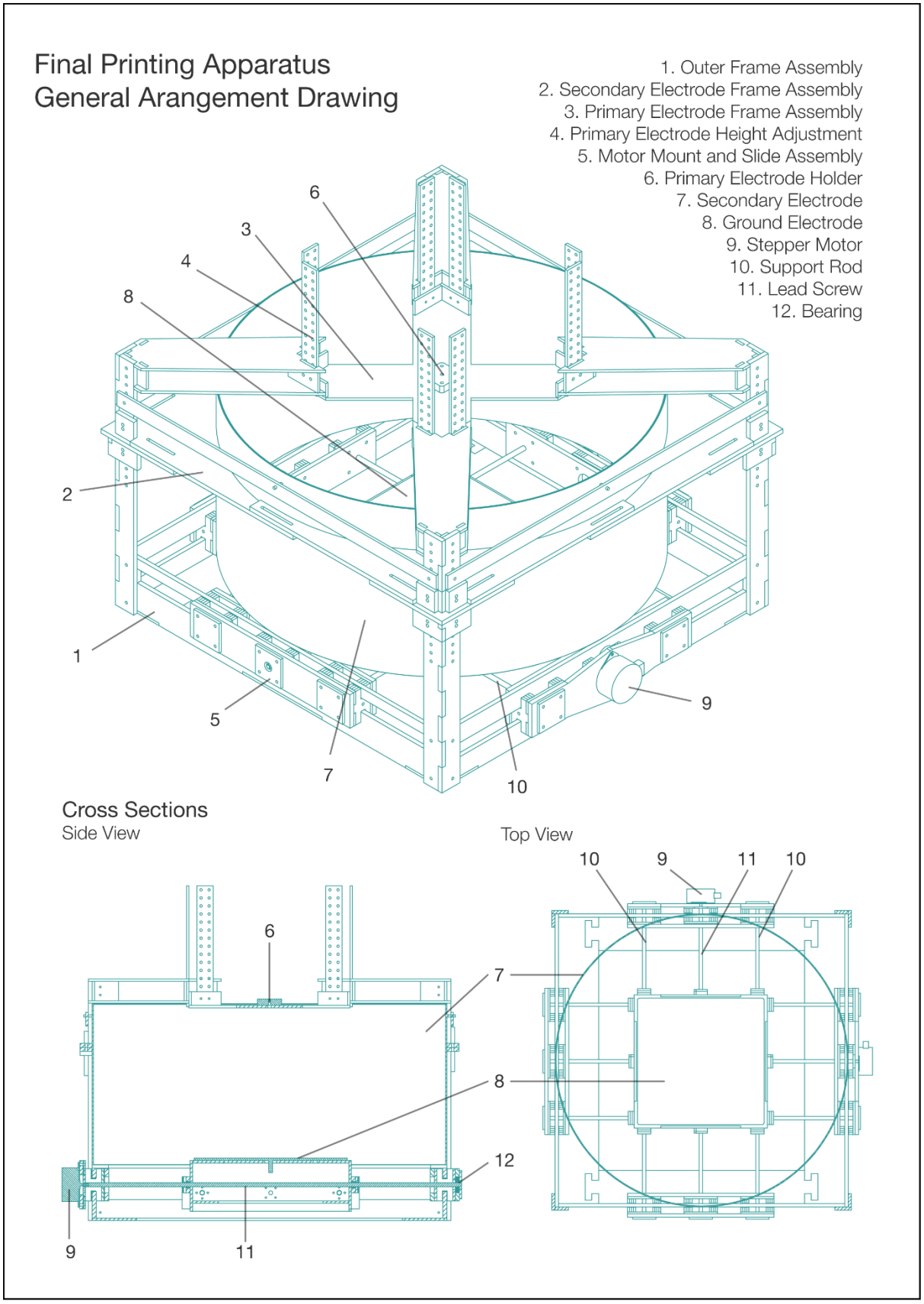

Figure 4.24 - Improved Fibre Printer General Arrangement Drawing

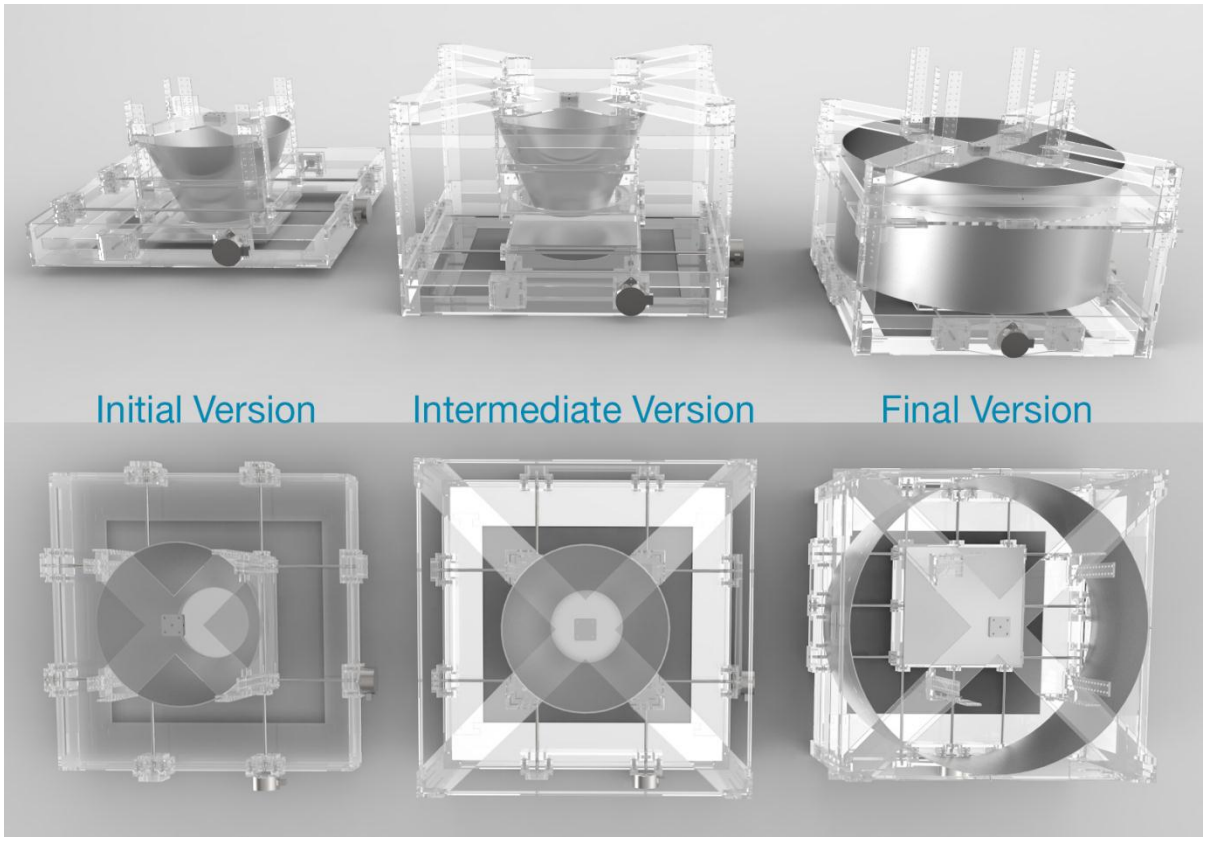

Figure 4.25 - Fibre Printing Apparatus Design Evolution

4.3.3.4 *Mechanical Design*

The mechanical design considerations are similar to the first version however improvements have been made. The drive mode and the resolution are the same as the original version at 0.017 mm even though the base is moved rather than the electrodes and frame assembly. However the rigidity of the movement system needed improvement from experimentation so the lead screw was moved to the middle of the drive mechanism and another support rod was introduced where the lead screw used to be. As shown in Figure 4.26 the final drive mechanism consists of three of the Slider Assembly's on each side, two for supporting the base and base electrode with support rods and one for housing the motor and lead screw. The advantage to this is that the force of the drive mechanism is central and the rigidity of the system is much better with two guide rods.

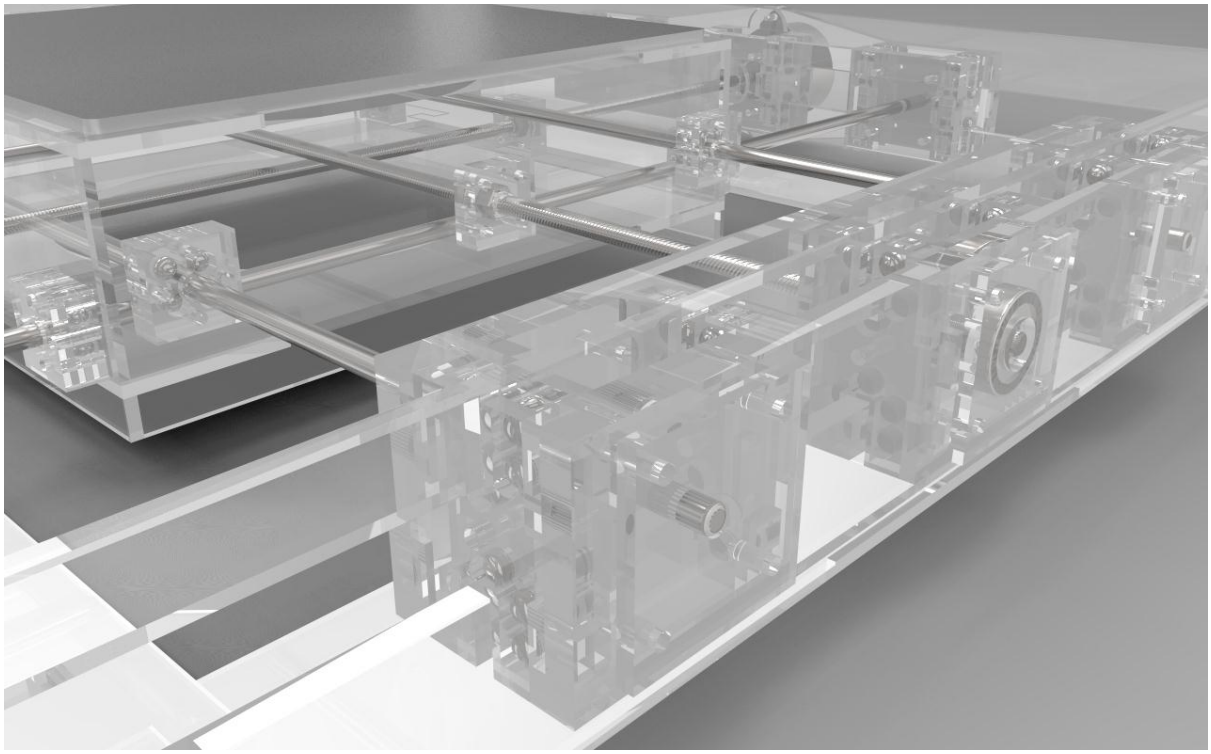

Figure 4.26 - Improved Fibre Printer Drive System Render

4.3.3.5 *Electronic Design*

4.3.3.5.1 *Aim*

The electronic circuit that had been developed needed some slight adjustments and had some protection circuitry added to try and stop the issue found with the initial circuit where the microcontroller would reset interrupting the experiments, this was due to unwanted high voltage noise on the stepper motor input pins during electrospinning. The software needed much greater adjustment than the hardware because of the physical redesign of the apparatus which now has the stage moving within the electrode stopping the ability to use the limit switches for positioning the stage.

4.3.3.5.2 *Hardware Development*

The schematic shown in Figure 4.27 shows the full circuit developed with the added protection circuitry. The protection circuitry consists of limiting resistors and two diodes and a smoothing capacitor that connect to the data lines between microcontroller and L293D driver. See Appendix section 9.3 for information on the

microcontroller and L293D motor driver. The concept here is that any noise that is on these data lines will be absorbed by the circuit shown. If the noise is a high voltage then the diodes will break down shorting the spike to ground protecting the microcontroller.

The rest of the circuit is the same as for the initial circuit developed. The final PCB that was created is shown in Figure 4.28. Note that the header that was used previously for the limit switches was retained on this circuit even though the switches could not be utilised with the physical redesign. This allowed for potential improvement in the future without having to redesign the circuit again.

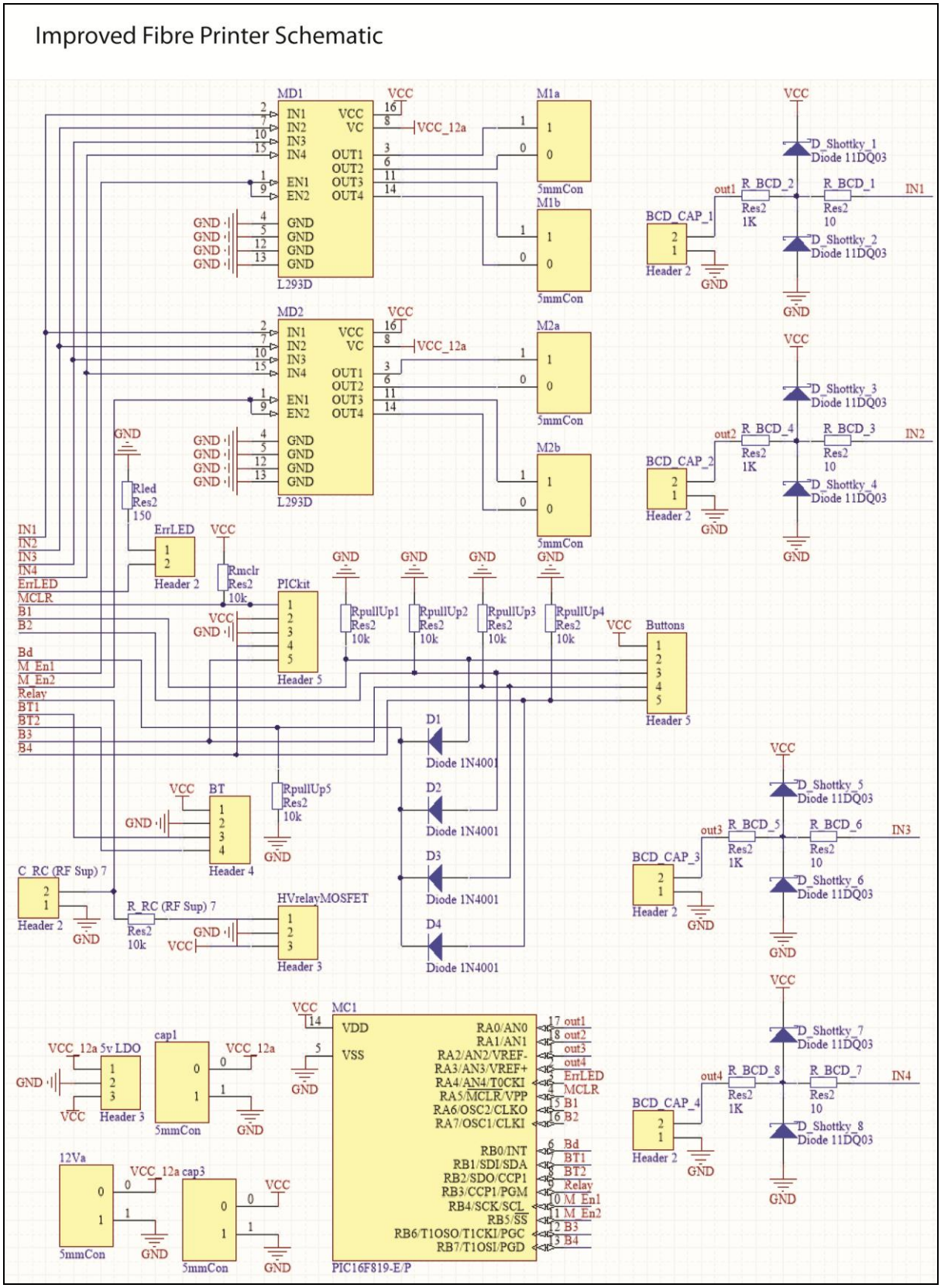

Figure 4.27 - Improved Fibre Printer Schematic

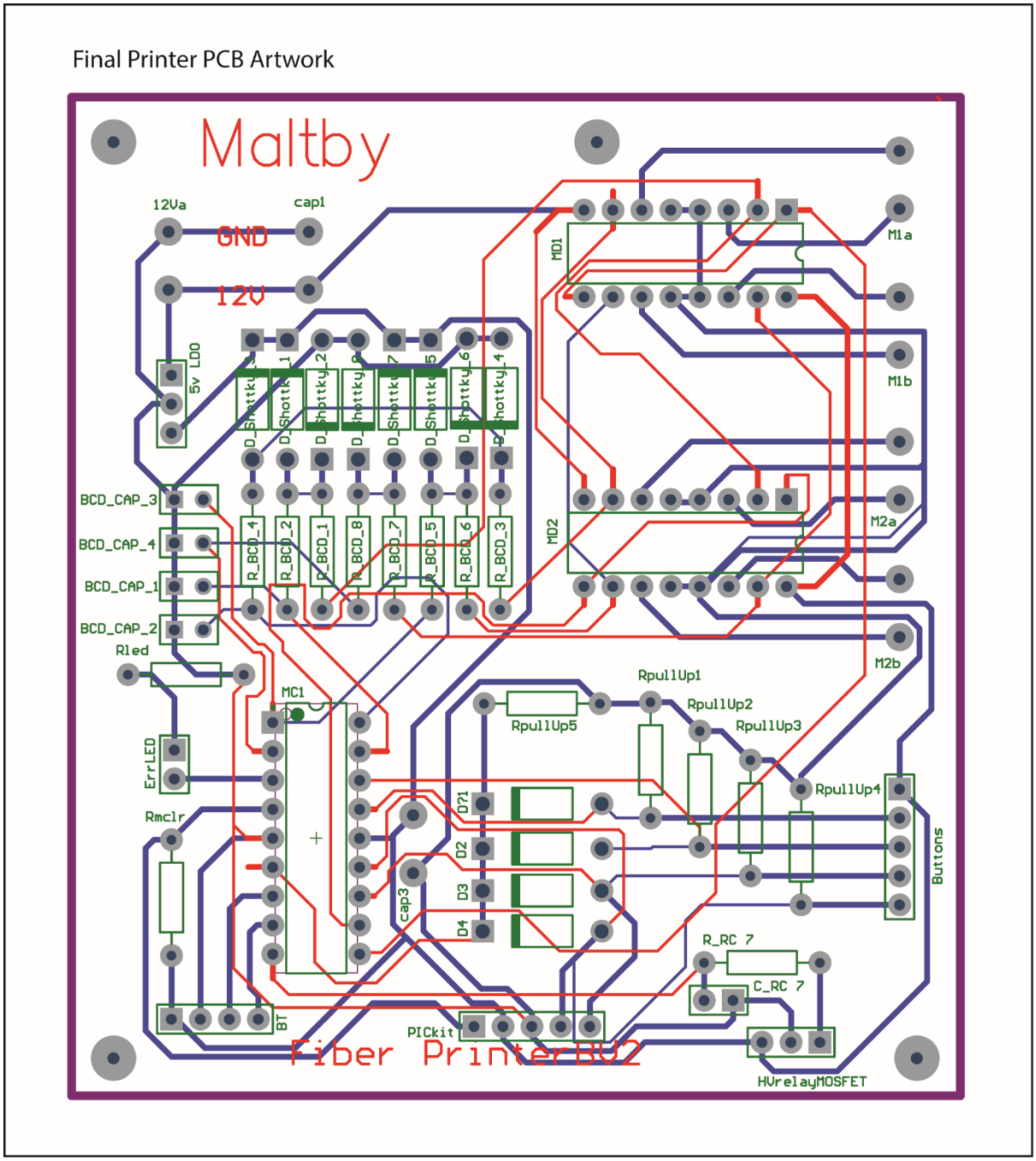

Figure 4.28 - Improved Fibre Printer Board Layout

4.3.3.5.3 *Software Development*

The software for the final developed apparatus was different from the initial code since the limit switches were no longer used. This made the centring code redundant, instead the program had to rely on the user manually centring the stage before use and then the program used the same coordinate system as before based on the distance the stage travels per step. Without the limit switches it was even

more essential that the stage did not try to move past its minimum and maximum limits and so the number of steps move in the x and y axis needed to be closely and accurately monitored by the program to prevent crashing of the stage. This was further complicated by the fact that now the drum electrode had been moved down and the stage moves within the confines of the drum itself. So the x, y axis limits are fluid because of the circumference of the drum which made coding a challenge and so the distance of travel was reduced so that the limits were based on a square.

This improved programme also added the functionality to use the High voltage relay to selectively turn the electrospinning jet on or off. This option was added into the menu system so a line could be drawn with the jet on or off allowing the printing of much more complicated patterns and of multiple different unconnected patterns.

4.3.3.6 *Apparatus Integration*

With the addition of the high voltage relay the primary high voltage power supplies positive lead is connected to one of the HV relays flying leads rather than directly to the aluminium block and electrospinning needle. The other flying lead from the relay is connected to the aluminium block. The remainder of the setup is the same as for the initial apparatus as described in section 4.3.2.6.

4.4 *Multi-Layer Fibre System*

4.4.1 Introduction

As can be seen in section 2.2.4 investigations have already been made in regards to the development of textile like fibres [78, 79] of different morphologies for use in textiles, sensors and energy harvesting. However a full system has never been reported upon and mainly the literature is concerned with the production of composite core-shell fibres. A full system has been developed here including a novel reel to reel core-shell electrospinning coating technique and a reel to reel outer electrode weaving device to create a three layer piezoelectric device. Together these are used to produce functional fibres that could be woven into textiles, used in sensor arrays or in low power energy harvesting applications. Figure 4.29 shows the system and the apparatus used within it.

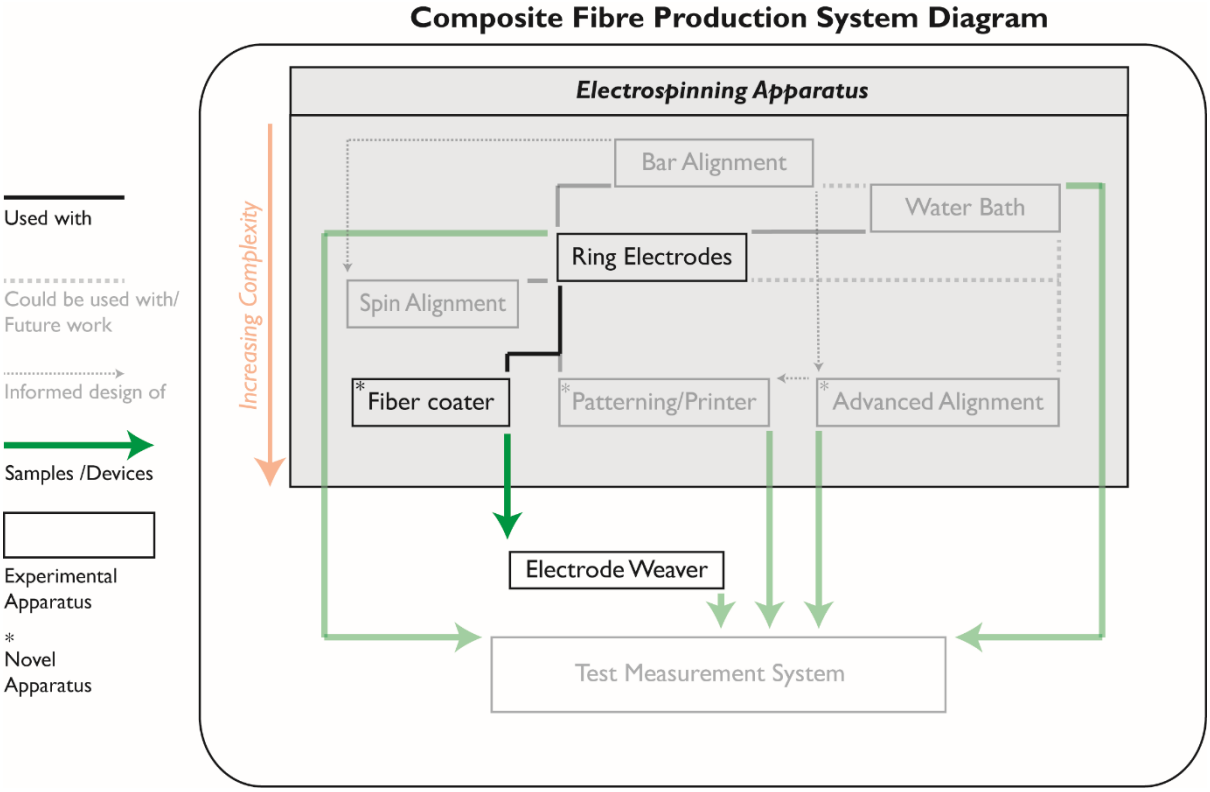

Figure 4.29 - Composite Fibre Production System Diagram

4.4.2 Coating Machine

4.4.2.1 Introduction

The coating machine developed in the following work is the only part of the composite fibre production system that is used to expand the conventional electrospinning technique. It was developed as a way to allow a uniform coating of electrospun fibre deposition around a central core fibre. The mechanical method developed to achieve this is novel in its approach and the reported results as detailed in section 5.6.3 shows novel morphology of the deposited fibres using this system.

4.4.2.2 Initial Version

4.4.2.2.1 Introduction

The initial version of the coating machine was developed to see how the electrospun fibres in flight interacted and formed a deposit on and around a central core fibre. The following work details the design of this initial piece of apparatus.

4.4.2.2.2 *Design Specification*

The design needed to uniformly coat a long length of central core wire. Therefore a system was needed that could move a length of wire through the path of the fibres in flight. To do this a reel to reel system was appropriate as it would allow the coating of long lengths of core fibres.

The initial design incorporated a secondary electrode drum to ensure that the electrospun fibres in flight were only deposited on the central core wire being drawn from reel to reel. This was necessary because the reel which held the central core wire was a metal cylinder attached to the ground lead of the high voltage power supply. This would also ground the central core wire making the fibres in flight be attracted to it while being drawn reel to reel during experimentation. This large grounded metal mass would readily attract the fibre in flight and so the electrospun deposition would be onto the reel rather than onto the core fibre. The design as shown in Figure 4.30 would therefore allow experimentation to see the effect of the feed rate of the fibre being drawn reel from reel to reel. Also the effect of changing the secondary voltage to the drum electrode could be investigated to see how it affected the deposition area on the wire.

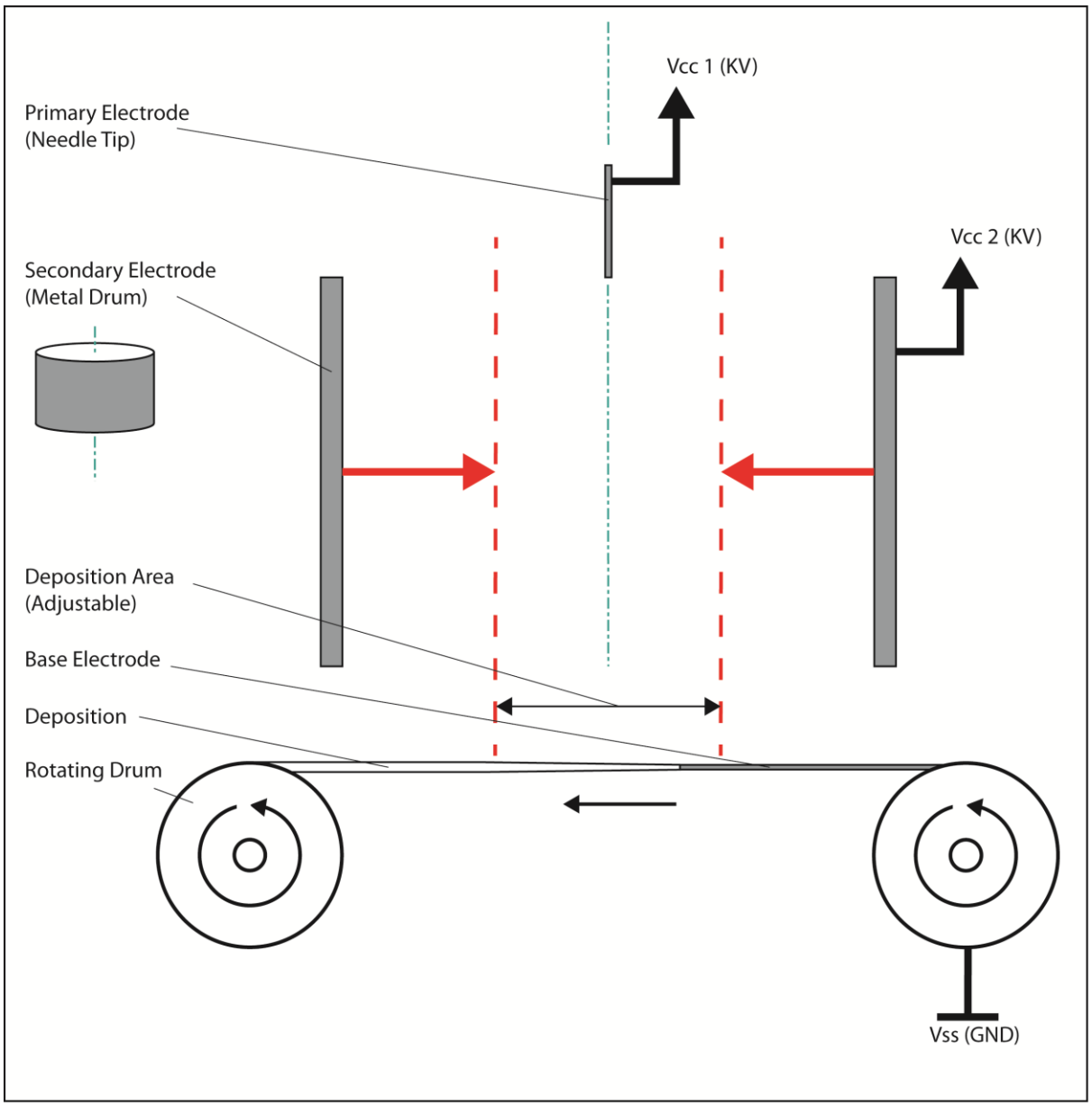

Figure 4.30 - Initial Fibre Coating Apparatus Diagram

4.4.2.2.3 *Physical Design*

The produced initial apparatus is shown in Figure 4.31. As with the other apparatus developed the bulk of the fibre coater was made out of acrylic plastic with the parts to make up the apparatus designed using CAD and then laser cut and then either bonded or bolted together.

The design can be split into different parts, reels, gearbox, risers and separator. The two reels were made out of different materials, one from an acrylic cylinder of diameter 90 mm and the other out of steel also with a diameter of 90 mm. The gear

box was designed so that the stepper motor could be geared so to reduce or increase the linear distance the central core fibre moved per step of the stepper motor, which was important to allow experimentation to find a good feed rate for the technique. The risers lifted the central core fibre between the reels to allow the height between the secondary electrodes bottom edge and the central core fibre to be adjusted. The risers also had pulley wheels mounted on the top to ensure the central core fibre stayed in the centre of the secondary electrode drum. The separators allowed length adjustment by keeping the two reels at a set distance apart. It also kept the reels and risers aligned.

A method of electrical connection was needed between the ground lead of the high voltage power supply and the metal reel. To do this the mild steel axel of the reel was also grounded by attaching a wire from the reel to the axel. On the axel two brass slip rings which could rotate freely were placed and then a wire was attached to them. The other end of this wire could then be attached to the HV power supplies ground lead. This setup stopped the wiring interfering with the ability of the axel to rotate while ensuring a good electrical connection at all times.

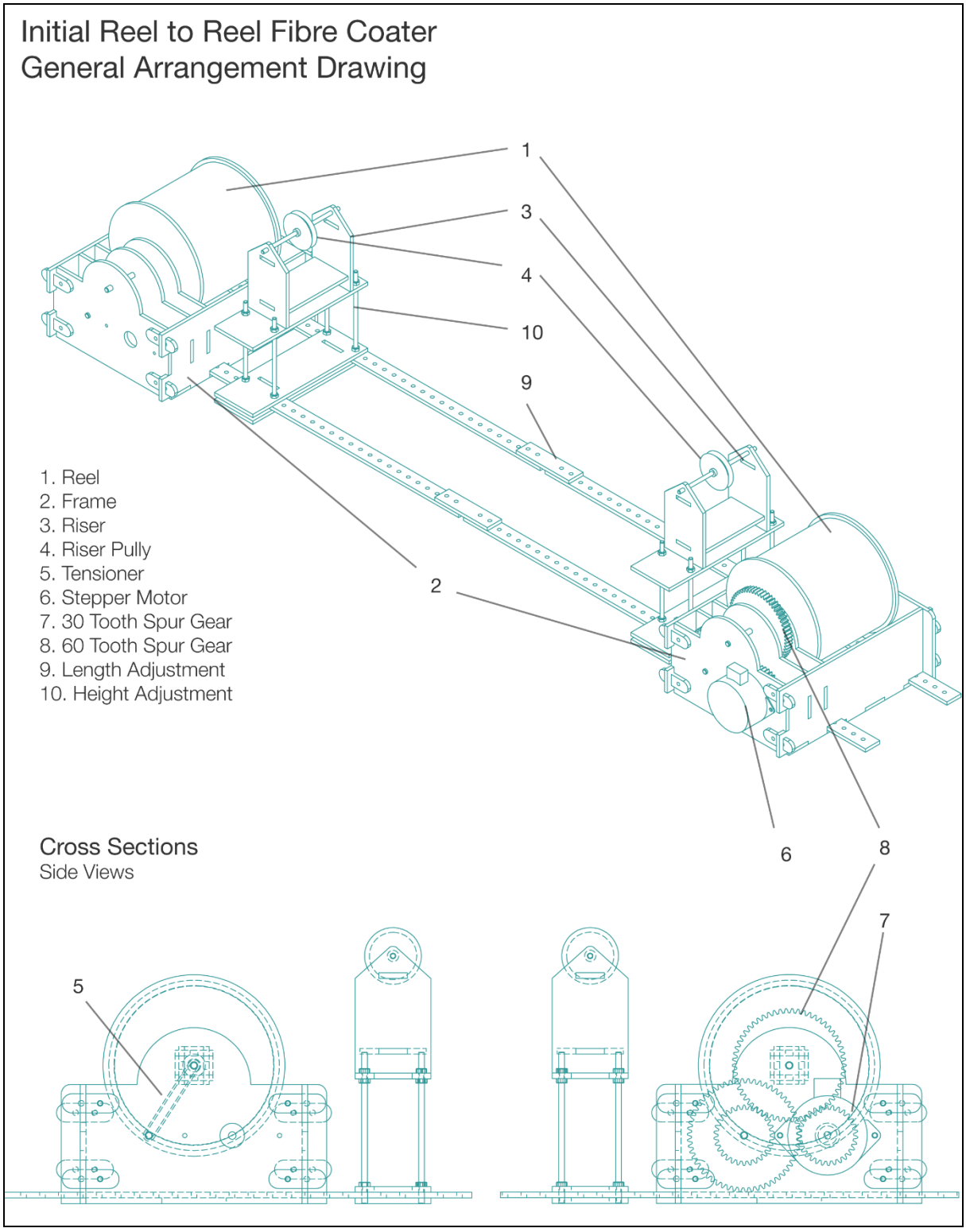

Figure 4.31 - Initial Fibre coating Apparatus General Arrangement drawing

4.4.2.2.4 *Mechanical Design*

The mechanical design is centred on the gear box for the apparatus. The design used 30 tooth and 60 tooth gears allowing the gear ratios to be 1:1, 4:1 or 1:4. The used stepper motor as described in Appendix section 9.3.2.3 has a maximum rotational velocity of 412.5 rpm so using this table 3 shows the possible maximum linear velocity's of the central core wire depending on the different gear ratios.

Gear ratio	Maximum angular velocity of reel (rpm)	Maximum linear velocity of central core wire (m/s)
4:1	103.125	0.486
1:1	412.5	1.943865
1:4	1650	7.77546

Table 3 - Fibre coating apparatus possible maximum velocities

The linear velocity is found using equation 1. Where v is the linear velocity in meters per second, r is the radius, in this case the radius of the reel at 45 mm and ω is the angular speed in radians per second.

$$v = r \times \omega \quad (1)$$

It is highly unlikely that the linear speed needed would ever need to be as high as that maximum given with the 1:4 gear ratio. The minimum feed rates are set by the time waited between steps of the stepper motor and in theory that means that there is no lower limit to this. If a slow feed rate is required it would be beneficial to use the 4:1 gear ratio as this reduces the step size from an angle of 7.5° to 1.875°. This gives a much smoother motion at lower speeds as the linear distance travelled per step is now less than if no gear ratio was used.

The other reel is not driven and to ensure the central core wire is kept taut a simple friction based tensioning system was used using an elastic band that is tight onto the

axel of the reel. The friction between the axel and surface of the elastic band provides a small amount of resistance to the pull of the driven take up reel keeping the central core wire tight.

4.4.2.2.5 *Electronic Design*

4.4.2.2.5.1 Aim

The aim of the electronics is to control the stepping speed of the stepper motor to allow control over the feed rate of the take up reel. The electronics for this needed a stepper motor driver circuit and a microcontroller circuit for the user input and control. As with the other apparatus developed the user interface was wireless utilising a Bluetooth module.

4.4.2.2.5.2 Hardware Development

For this initial apparatus it was possible to reuse the initial circuit board developed for the patterning printer apparatus as this was also concerned with stepper motor control. Please see section 4.3.2.5.2 for details on the circuit and developed printed circuit board.

4.4.2.2.5.3 Software Development

The software was initially very simple as it only needed to move the fibre along at a steady rate. The software allowed the choice of various feed rates which were then converted to the necessary time delay between stepper motor steps to achieve the desired feed rate. The initial code can be found in the Appendix section 9.6.2.1.

4.4.2.2.6 *Apparatus Integration*

Setting up the apparatus for experimentation consists of transferring a length of conductive wire that is to be used as the central core fibre onto the metal reel. The end of the wire is then drawn by hand across the apparatus onto the plastic take up reel ensuring that the suspended wire in under sufficient tension.

The secondary electrode drum is placed so that it is centred above the apparatus, the electrospinning needle is above this and centred so that it is concentrically aligned. The tip of the needle is at the same height as the top of the secondary electrode drum.

The coating apparatus is then positioned so that the wire is directly across the centre of the secondary electrode drum and the height of the central wire adjusted using the risers so that there is an air gap of sufficient distance to prevent electrical arcing between the bottom of the secondary drum electrode and the central core wire.

4.4.2.3 *Final Experimental Apparatus*

4.4.2.3.1 *Introduction*

After analysing the results obtained from the first coating apparatus problems with the technique being utilised were identified as discussed in section 5.6.3.1. This necessitated a full redesign of the experimental apparatus which needed a much more complicated and involved piece of design. This redesign and the development that was undertaken is detailed in the following sections.

4.4.2.3.2 *Design Specification*

Uniform concentric co-axial fibres are achieved using the electrospinning method by using the central wire as the ground electrode. The electrospun fibres are attracted to the grounded central core wire and uniform coating is ensured by rotating the wire at a constant rate.

The system is designed to produce many meters of coated core-shell fibres with an even coated thickness along the length of the core wire. This is achieved by implementing a steady linear rate which draws the wire between two reels. The deposition area of the electrospun fibres onto the slowly moving central core is also controlled using a secondary electrode. This increases the evenness of the coating by ensuring that all the electrospun fibres are directed on the central core wire, stopping unwanted fibre deposition on other areas of the system. This reduces material wastage but also encourages greater uniformity as fibre deposition is controlled onto a desired area.

Other design considerations include offsetting the two reels by 180° to balance the mechanical system to give a constant angular velocity to the core wire. The off-set reels are rotated around the central core wire which ensures that the core wire does not move up and down during electrospinning but only rotates and moves linearly as desired around its own central axis, as shown in Figure 4.32 with the axis of rotation marked. Both reels are also rotated to draw the core wire linearly, by turning both this ensures that the tension on the wire remains constant throughout the coating process as well as the linear speed the wire moves at. This effort should ensure that no stretching or twisting of the central wire happens during the coating process which could introduce unwanted stress into the resulting core-shell fibres.

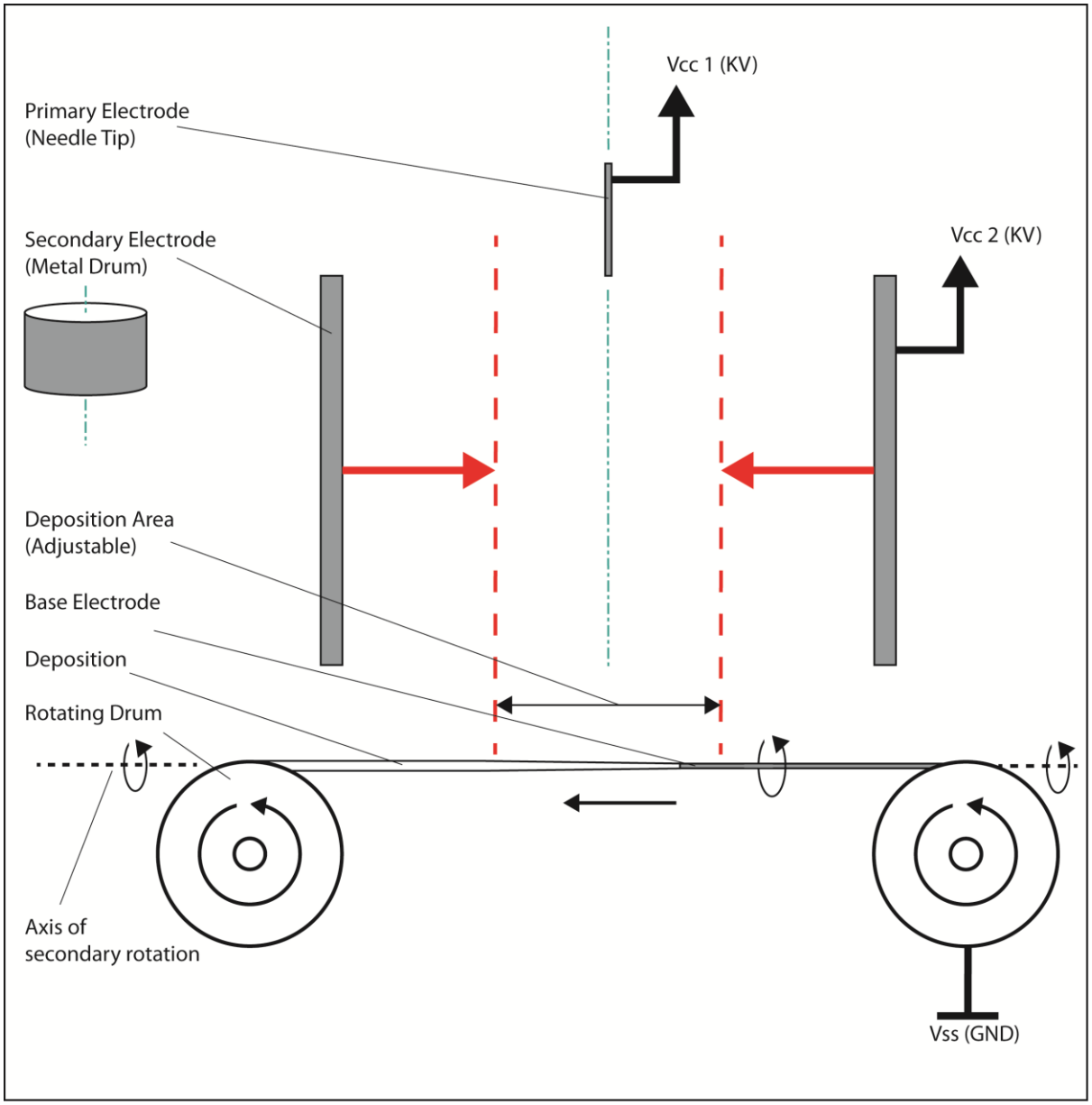

Figure 4.32 - Improved fibre coating apparatus diagram

4.4.2.3.3 *Physical Design*

The physical design of the improved apparatus is similar to the initial apparatus, with the design and individual parts being developed on CAD before being laser cut from acrylic. Due to the identified need for a greater mechanical complexity an emphasis was put on being able to disassemble the apparatus either for maintenance or future improvement. This led to a design with minimal bonded parts with almost all building being done by bolting together parts. This meant that greater care was taken with the minimising of tolerances for the whole system which was especially important due to

the increased mechanical complexity and integration of drive belts and ball bearings which needed careful attention to spacing and alignment.

The developed design is shown in Figure 4.33 and can be split into two areas. The base and motor mountings with associated gearing and drive elements and the two reel mountings including the mechanical systems that allows rotation of the central core wire as well as the linear movement from reel to reel.

As with the initial apparatus one of the reels is made from acrylic and the other made from mild steel and is connected to the high voltage power supplies ground lead. This creates a good connection to ground for the central core wire wrapped around the reel. The ground connection on the reel is made by attaching a wire lead to the shaft that goes through the centre of the large 90 tooth gear. This is done using brass bushes that the shaft can rotate in while still making a good electrical contact. The central shaft also has bushes at its other end near the reel itself and a wire connects these bushes to bushes placed on the axel of the reel. A wire then connects the axel to the reel itself completing the circuit.

The design is such that both reels can easily be removed by unscrewing the side part of the reel mount. This allows the easy removal of reels for both loading with wire and removing completed experiments.

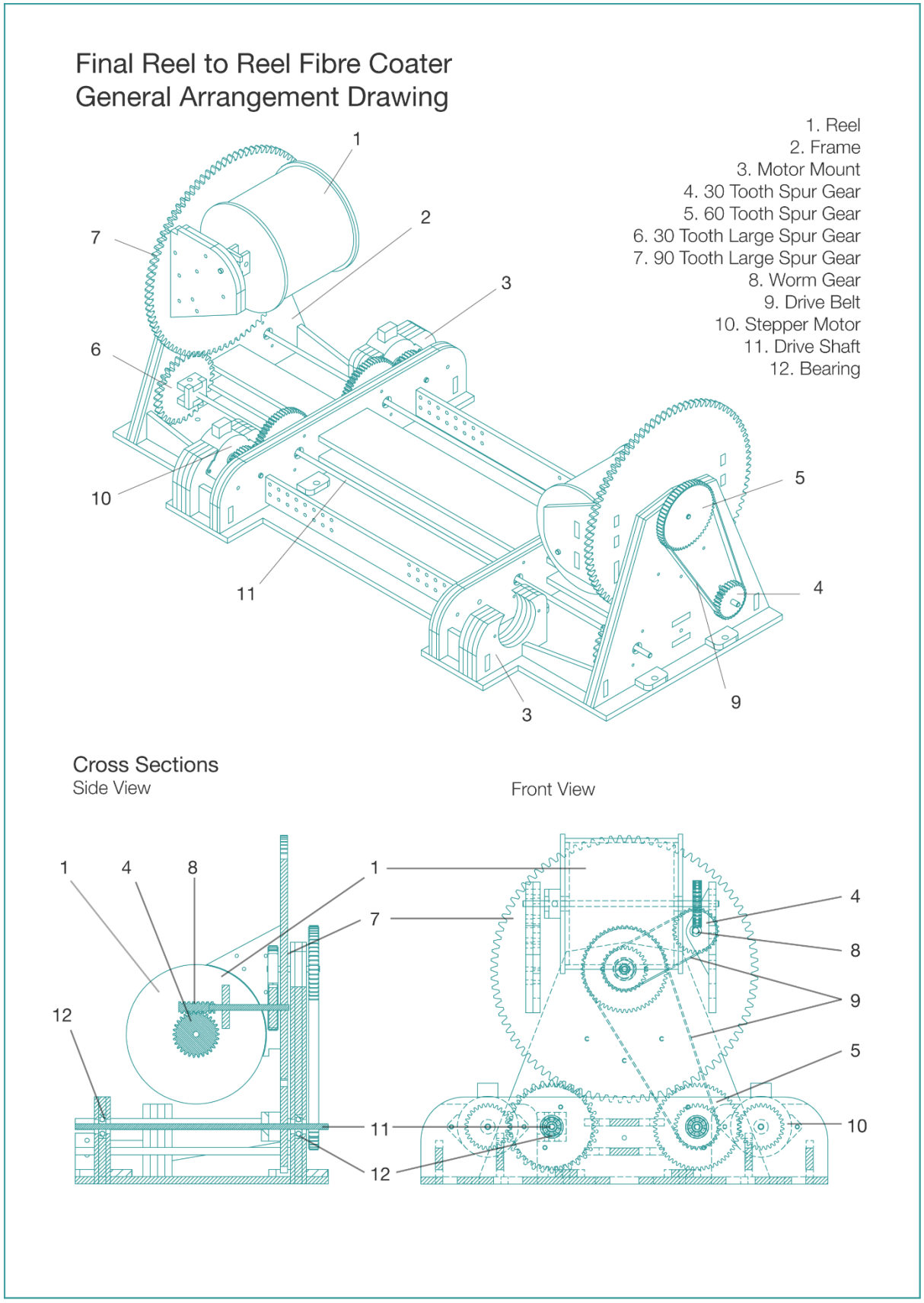

Figure 4.33 - Improved fibre coating apparatus General Arrangement drawing

4.4.2.3.4 *Mechanical Design*

The mechanical design was developed in two parts, one to achieve the rotation of the central core wire allowing its angular velocity to be controlled and the other system to control the feed rate or linear velocity of the central core wire being transferred from reel to reel. To ensure smooth mechanical operation a multitude of bearings were used to reduce friction and ensure alignment of the various shafts and mechanical elements.

The angular velocity system consists of a 90 tooth spur gear onto which the reels are mounted so that the whole reel rotates. This gear is meshed with a 30 tooth spur gear and is driven by a stepper motor which is also geared. The gear ratios of the system developed for the rotation of the reels reduce the step size of the stepper motor to 2.5 ° at a gear ratio of 3:1.

The linear velocity system consists of the stepper motors connected to a gear set that drives a shaft, at the ends of the shaft a 30 tooth gear is connected by a belt to a 60 tooth gear that is concentric to the large 90 tooth gear that the reels themselves are mounted to. The shaft attached to this gear passes through the centre of the larger gear via a bearing allowing them to turn at different speeds. At the end of this shaft a 30 tooth gear is then attached to another 30 tooth gear by a belt. This gear is placed towards the edge of the 90 tooth gear and the shaft that comes from it extends to just below the axel of the reel itself. At the end of the shaft a worm gear is meshed with another 30 tooth gear that is mounted to the axel of the reel itself. This completes the gearing that rotates the reels creating the linear movement of the central core wire between the reels. This gear train is used to drive both reels at the same time making sure they move in unison. The reels turn in the same direction as the gearing is effectively mirrored from one reel to the other reel. The linear velocity gear train that moves the central core wire from reel to reel has to a step size of 0.125 ° with a gear ratio of 60:1.

To achieve the desired angular velocity and linear velocity three stepper motors are used. Two motors are used for the angular velocity which needs more torque due to the weight of the reel system and a lower gear ratio. One stepper motor was used for creating the linear velocity of the core fibre as this required less torque. This gives a

smooth linear and rotational movement, ensuring even coating of the electrospun fibres around the central core wire.

When considered together the mechanical design of the whole system is such that depending on the rotational velocity set a proportional linear velocity is also applied to the central wire at the same time. This is due to the necessary off-set of the gearing that drives the rotation of the reels that draw the wire linearly. As the reels and central wire rotate, to allow coating of the whole surface of the central wire, the offset gearing also rotate, even though they are not being driven causing the linear movement of the central wire. To then change the linear velocity of the core wire to a desired rate another linear velocity is added in the same or opposite direction to the linear velocity from the rotation of the system. For example at an angular velocity of 12 rpm there is an applied linear velocity of 1.885 mm/s and so to achieve a linear velocity of 0.5 mm/s, a linear velocity of 1.385 mm/s is used in the opposite direction as the applied linear velocity. The natural linear velocities that are created from the applied rotational velocity at the different RPM rates used for experimentation are listed in Table 4.

Angular velocity (rpm)	Applied linear velocity (mm/s)
12	1.88496
24	3.76992
36	5.65488
48	7.53984

Table 4 - Linear velocities produced at different RPM rates

4.4.2.3.5 *Electronic Design*

4.4.2.3.5.1 Aim

Due to the issues outlined in section 5.6.3.1 in regards to intermittent microcontroller resets the circuitry for the initial fibre coating apparatus had already been improved with the use of circuit protection in the form of a series of diodes, resistors and smoothing capacitors in the same format as used for the fibre printing apparatus and explained in section 4.3.3.5.2. As the only real difference between the initial apparatus and this is the need to drive an extra stepper motor, two boards were used from previous designed apparatus instead of a complete PCB redesign. One

board was used to drive the angular rotation of the central core wire and one to drive the linear velocity of the central core wire. This had additional benefits as driving two stepper motors at once would have put timing pressure on the program to ensure that the stepper motor steps were executed with exactly the right timing complicating the code further. A single Bluetooth module was then used connecting the two boards and a software protocol was used to address data to one or other of the boards when the user was inputting experimental parameters.

4.4.2.3.5.2 Hardware Development

The developed circuit schematic for this apparatus is shown in Figure 4.34. The setup is similar to the other developed boards using a L293D chip for driving the stepper motor and low drop out regulators to provide 5 v logic level for the microcontroller and Bluetooth module.

As the circuit was initially designed as an improvement to the initial coating apparatus there are a few peripheral and user interface elements that are on the circuit but not utilised in the later code such as a header to attach a liquid crystal display (LCD) screen.

Although the schematic specifies a Microchip PIC16F819 microcontroller this was changed to a PIC16F1827 due to the better clock speed of 32 MHz this allowed a greater accuracy of control over the timing between steps of the stepper motors leading to a greater accuracy in regards to the velocities during operation of the apparatus. Both microcontrollers have the same pin configurations and so nothing else had to be changed on the hardware to facilitate this change.

Figure 4.35 shows the printed circuit board layout for this apparatus with the connectors populating the perimeter of the board for easy access and setup. The alternate user interface items that were not utilised were also laid out to produce an easy to use user interface on the board such as alignment of LEDs button and potentiometer.

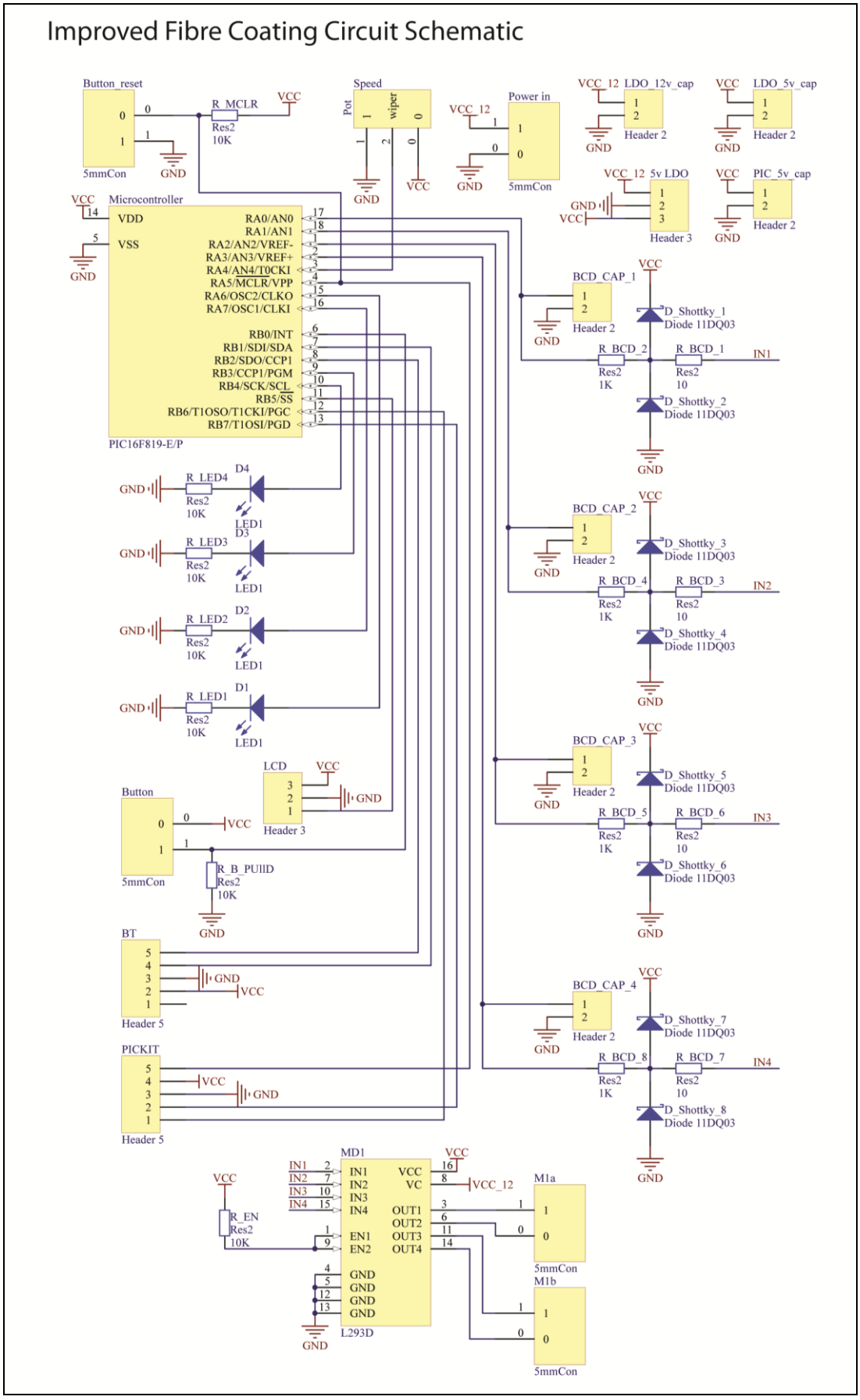

Figure 4.34 - Improved fibre coating circuit schematic

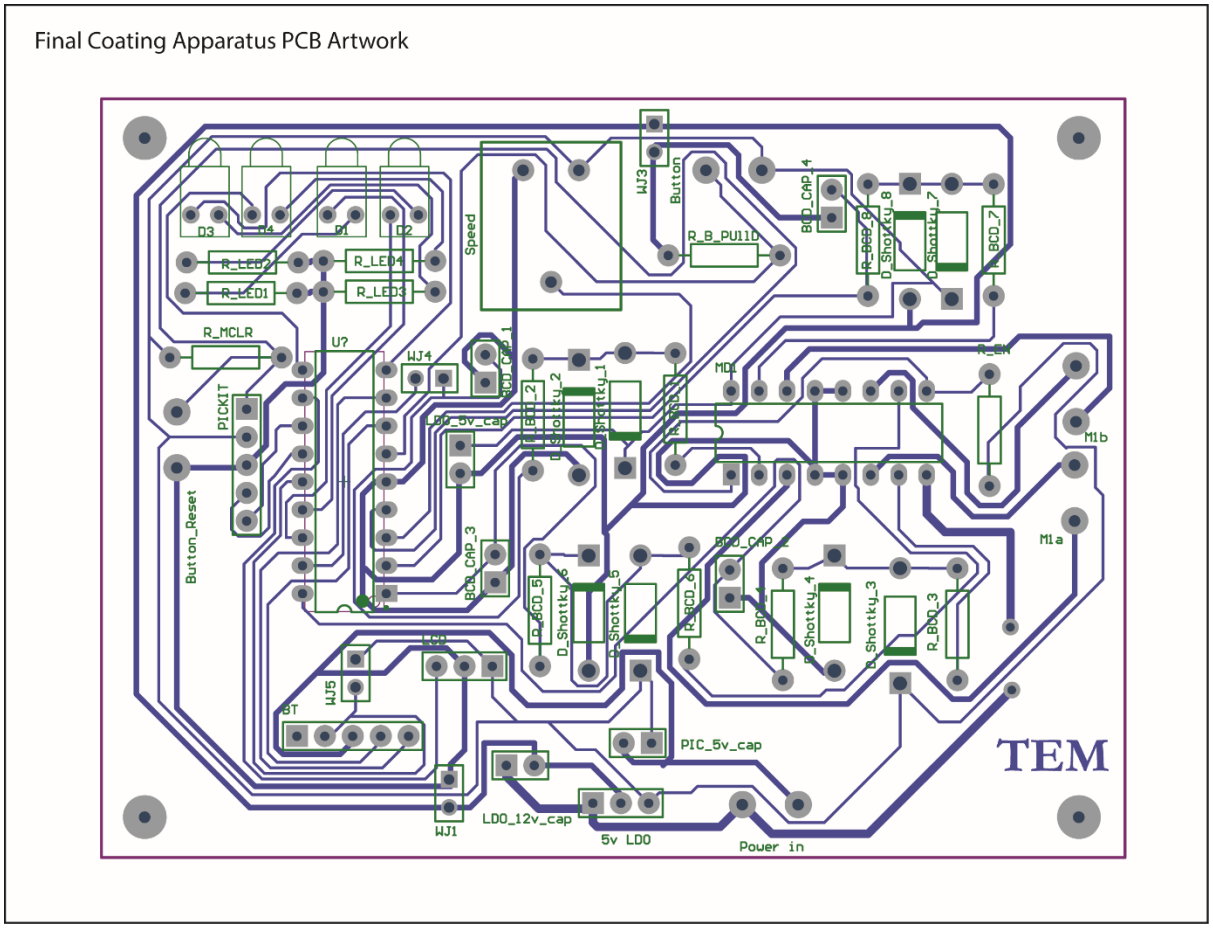

Figure 4.35 - Improved fibre coating board layout

4.4.2.3.5.3 Software Development

Since two microcontrollers were used two different sets of software were developed. They are similar in nature as they both concern driving stepper motors and so share some algorithms. Where they differ however is in regards to conversion of the desired rotational velocity to microcontroller step rate and desired linear velocity to microcontroller step rate. This is due to the difference in gear ratios used and the equation necessary to convert from angular velocity produced by the stepper motor to linear velocity of the central core fibre.

Since both microcontrollers share the Bluetooth module it was necessary that the correct data input from the host device is read by the right microcontroller. This was done in a basic way where one programme acts as master and initiates user input by sending a menu to the host device. Once data input for that device has been sent by

the user an ASCII character is then sent that the other programme is waiting for. This initiates the data collection for the second microcontroller. Once all the necessary data has been input and the linear and angular velocities are set and the experimentation can begin.

For the angular rotation the speed is built up slowly until the desired rotational velocity is reached as this takes advantage of the better torque profile that the stepper motor exhibits at lower speeds. This is necessary due to the weight of the reel systems and the effect that the gearing has on the torque profile. Once the system is at the desired speed, less torque is needed due to the momentum that the system has allowing smooth operation. The code for the microcontroller that controlled the linear velocity of the central core wire can be found in Appendix section 9.6.2.2.1 and the code for the microcontroller for the angular velocity of the apparatus is in section 9.6.2.2.2.

4.4.2.3.6 *Apparatus Integration*

The apparatus is setup in the same way as for the initial version of this apparatus by first spooling a length of the wire to be used onto one of the reels. For this apparatus care has to be taken when suspending the wire between the reels as the tension on the wire needs to be carefully considered as it is prone to slight tightening during experimentation due to the slight diameter changes between the two reels as the wire being spooled crosses over itself.

The secondary electrode drum is positioned with the suspended wire directly perpendicular to its central axis at a safe distance below the bottom edge of the secondary electrode. The reels sit outside of the central electrode drum so when positioning them an equal distance between each reel and the edge of the secondary electrode is found which again is at a distance that ensures that electrical arcing cannot happen between the grounded wire and reels and the secondary electrode drum.

4.4.3 Electrode Weaver

4.4.3.1 *Introduction*

The methods available for adding a top electrode to the core-shell fibres produced by the coating system were not well suited to allow a high level of flexibility of the final device. Painting or dip coating the core-shell fibres results in an uneven, inflexible electrode layer and DC magnetron sputtering either uses expensive materials like gold and only deposits very thin layers of material which are not resilient enough to allow a long device lifespan. A method of adding inexpensive, flexible and long lasting electrodes was required to create an outer electrode for the produced composite core-shell fibres. Taking inspiration from traditional weaving processes that are used to create sheathing for ropes a scaled down version was developed especially to facilitate the weaving of fine metal wire around the produced composite fibres. These composite fibres are created with the Fibre coating apparatus the design of which has been detailed in the previous sections and then the apparatus detailed in the following sections add the outer electrode.

4.4.3.2 *Initial Experimental Apparatus - Mechanical system*

4.4.3.2.1 *Introduction*

Creating a flexible outer electrode shell around a composite core-shell fibre is a complicated task, initial tests as shown in results section 5.6.2 with painted silver electrodes around the composite fibres found that the paint added an uneven and stiff layer once dry. Designing an apparatus that weaves an outer shell electrode around the core-shell fibres these issues would be reduced. The following section details the initial mechanical approach tried to add woven outer electrodes to the electrospun core-shell fibres.

4.4.3.2.2 *Design Specification*

The design of the electrode weaving apparatus is mechanically complex as it needs to ensure that a number of bobbins move in a set pattern while a number of other bobbins move in the same pattern but in the opposite direction. Each of the bobbins moving in opposite directions has to cross each other's path to weave the fibres on

the bobbins together. This is shown in Figure 4.36. The number of bobbins chosen for experimentation is 8, with 4 moving clockwise and 4 anticlockwise creating an 8 strand weave as shown in the diagram. A maximum of 16 bobbins and a minimum of 4 bobbins can be used with the design developed to make weaves with different numbers of strands in them.

The chosen design is based on larger scale weaving machines that are used for applications such as weaving sheathings for ropes [108]. This design uses 8 carousels which rotate carrying the bobbins around with a pivoting catch mechanism that transfers bobbins between carousels.

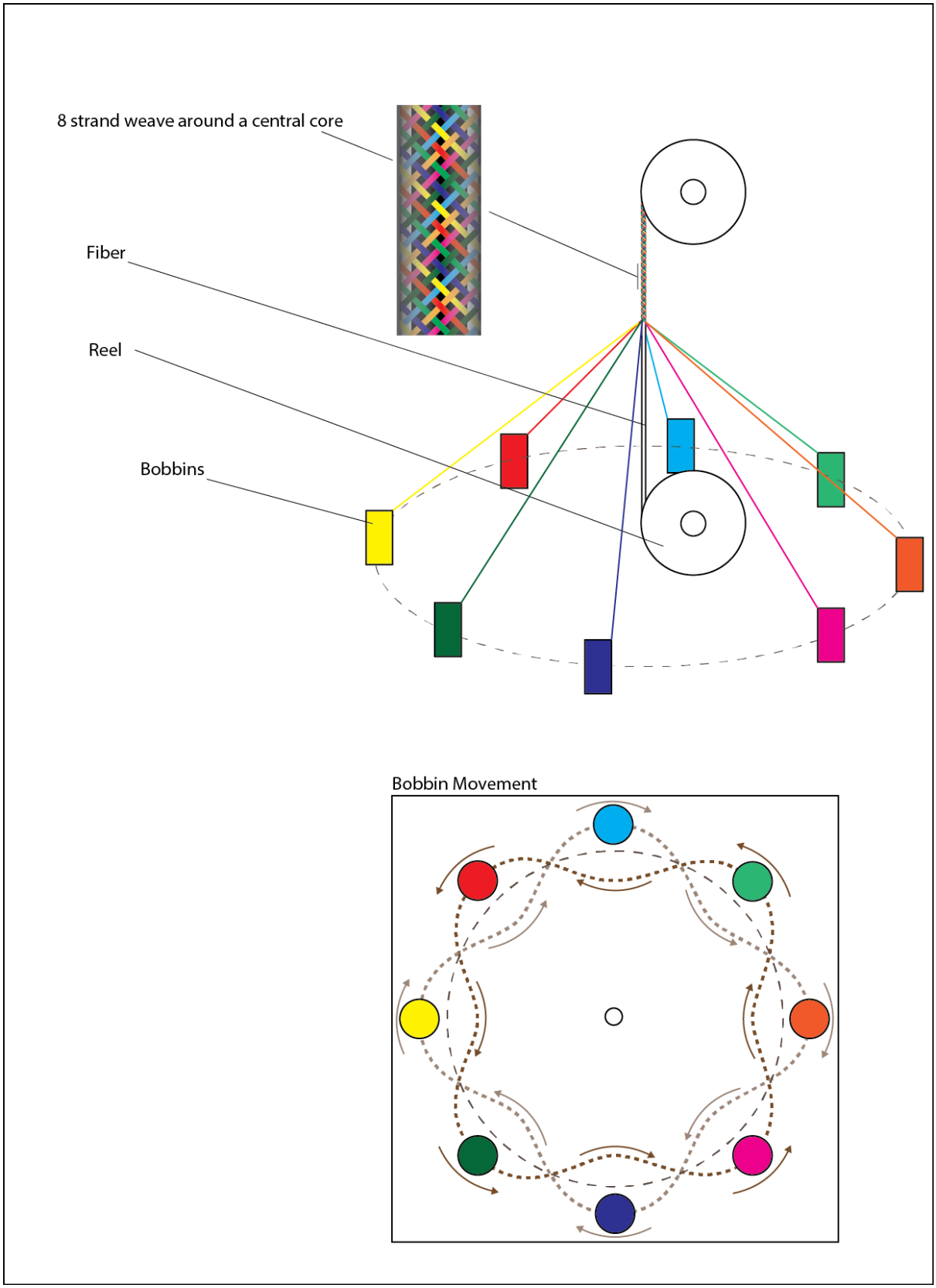

Figure 4.36 - Weaving method diagram

4.4.3.2.3 *Physical Design*

The size and design of the apparatus was built around the mechanism that used a series of meshed gears to rotate the carousels. It was initially designed, developed and tested using CAD before being built and the CAD model was designed so that the parts could be directly laser cut to shorten the time it took to build this prototype. As it was laser cut the material used for the apparatus was acrylic.

The design is shown is Figure 4.37. The design consists of a layered base that houses the gearing and above them the carousels. A top piece aligns with the top of the carousels to constrain the bobbins. Above this the pivoted catches known as wobblers are mounted that facilitate the moving of the bobbins between carousels. In the centre of the apparatus a reel can be mounted on which the core-shell fibres to have electrode added by the weaving process are kept. Rising from the top surface a gantry is placed with the take up reel and stepper motor mounted to it. The height of the gantry is adjustable. This allows the core-shell fibre to have its outer electrode woven around it and then taken up onto the top reel.

The whole apparatus was designed so that parts could easily be replaced or improved upon and so it was mainly assembled by bolting parts together. The carousels parts were bonded together but were attached to their shafts by grub screws which meant they could be easily removed so the bobbins could be inserted into and taken out of the system as needed.

The bobbins themselves were built around the pulley wheel which was to have the wire used for the woven electrodes spooled onto them. The bottom of the bobbin has a three pronged design to add stability with a wider base and facilitate the clean transition from one carousel to another without jamming. A thread guide was necessary above the pulley to ensure the spooled wire was pulled at a suitable angle to stop the wire from unspooling and becoming entangled when the wire goes slack.

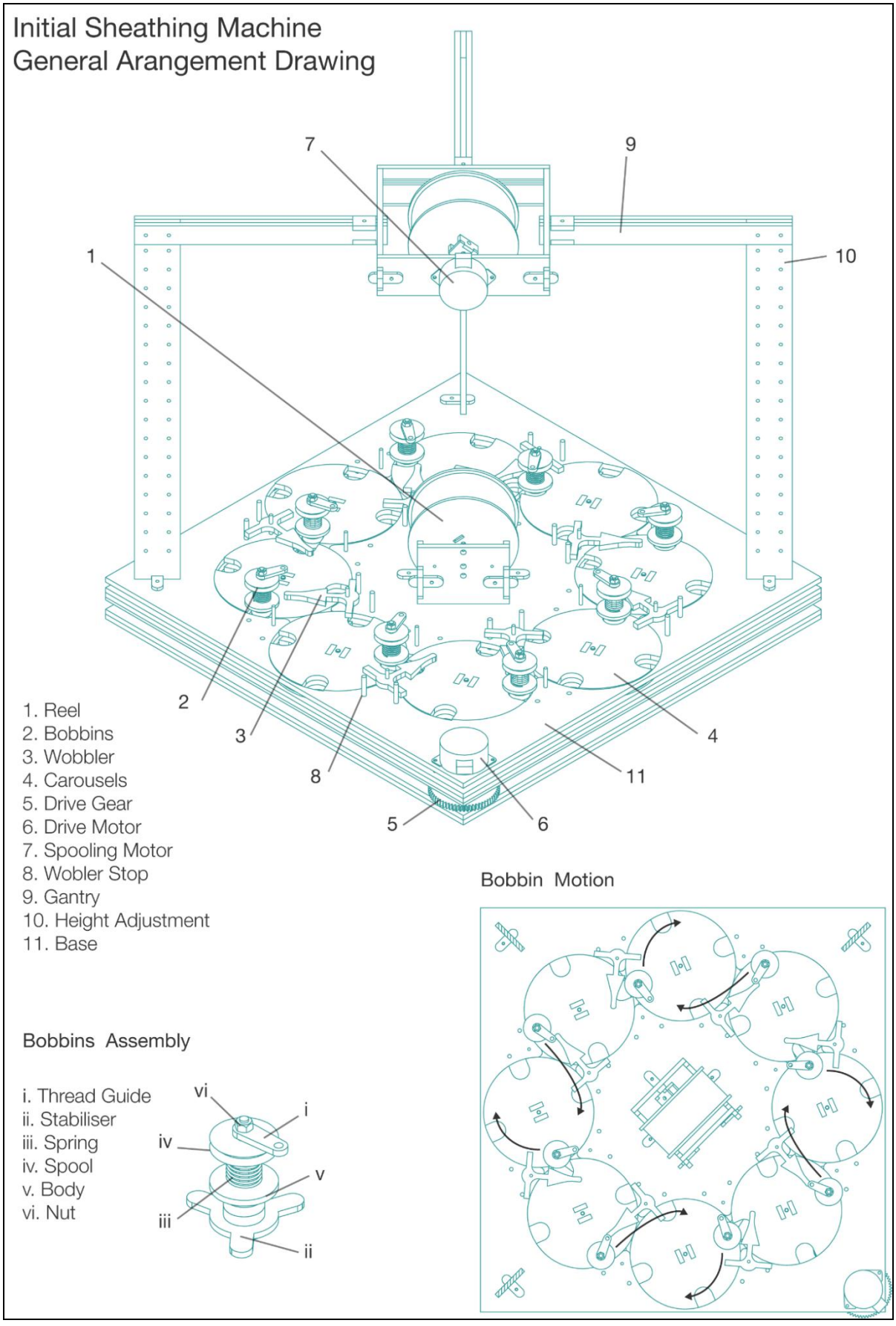

Figure 4.37 - Initial braiding apparatus general arrangement drawing

4.4.3.2.4 *Mechanical Design*

A mechanical system is used to turn the carousels in unison. Figure 4.38 shows how this has been done using a combination of different sized gears. The larger 60 tooth gears are connected by shafts to the carousels above. Each sequential carousel gear needs two idle gears between them to ensure that they turn in the alternating directions. To reduce the overall size of the apparatus smaller 30 tooth gears were used for these idler gears. All carousels rotate at the same speed and as the carousels are fixed to the larger gears they rotate in alignment.

The carousels have four slots cut into them that are just slightly larger in size than the bobbins diameter. These slots carry the bobbins around when the carousel rotates. Since the meshed gearing below causes the carousels to be aligned, the slots in the different carousels align at the point where the bobbin is passed from one carousel to another.

The pass itself uses a system were a pivoted guide (wobbler) is positioned at the bobbin passing point. As the carousel rotates the bobbin at the passing point, the bobbin is pushed against the guide that slides along the guide out of the slot in the carousel and into the aligned slot of the next carousel. As the bobbin then rotates on the next carousel an arm that protrudes from the guide is pushed, pivoting the guide so that now as a bobbin comes in the opposite direction it will be successfully passed onto the first carousel. This allows the bobbins to weave between and pass each other creating the desired woven electrode structure on the core-shell fibres.

To ensure that this motion is as smooth as possible bearings were used above and below the gearing to ensure alignment of both the meshing gears and also above them the correct alignment of the carousels. The Idler gears did not have any bearings however they were loose on their shafts and greased to reduce friction.

The bobbins themselves were designed with a tensioning system inbuilt. This was necessary to stop excess wire from coming from the reel causing an excess of slack which affects the uniformity of the weave and also can lead to entangling of the wires. As the bobbins move around at their orbits at certain points they are further away from the central core-fibre being woven. At this time it is necessary for the weaving wire to be pulled tight which in turn tightens and closes the woven structure

creating the desired uniformity and a close packed weave. The tensioning system ensures that this necessary tightening of the wires happens.

The method of tensioning is by adding a spring below the spool so that it adds resistance when the wire being pulled from the spool. The tensioning can be adjusted by changing the compression of the spring which increases the force exerted onto spool. This increases the force necessary to rotate the spool due to the added friction between the spring and spool.

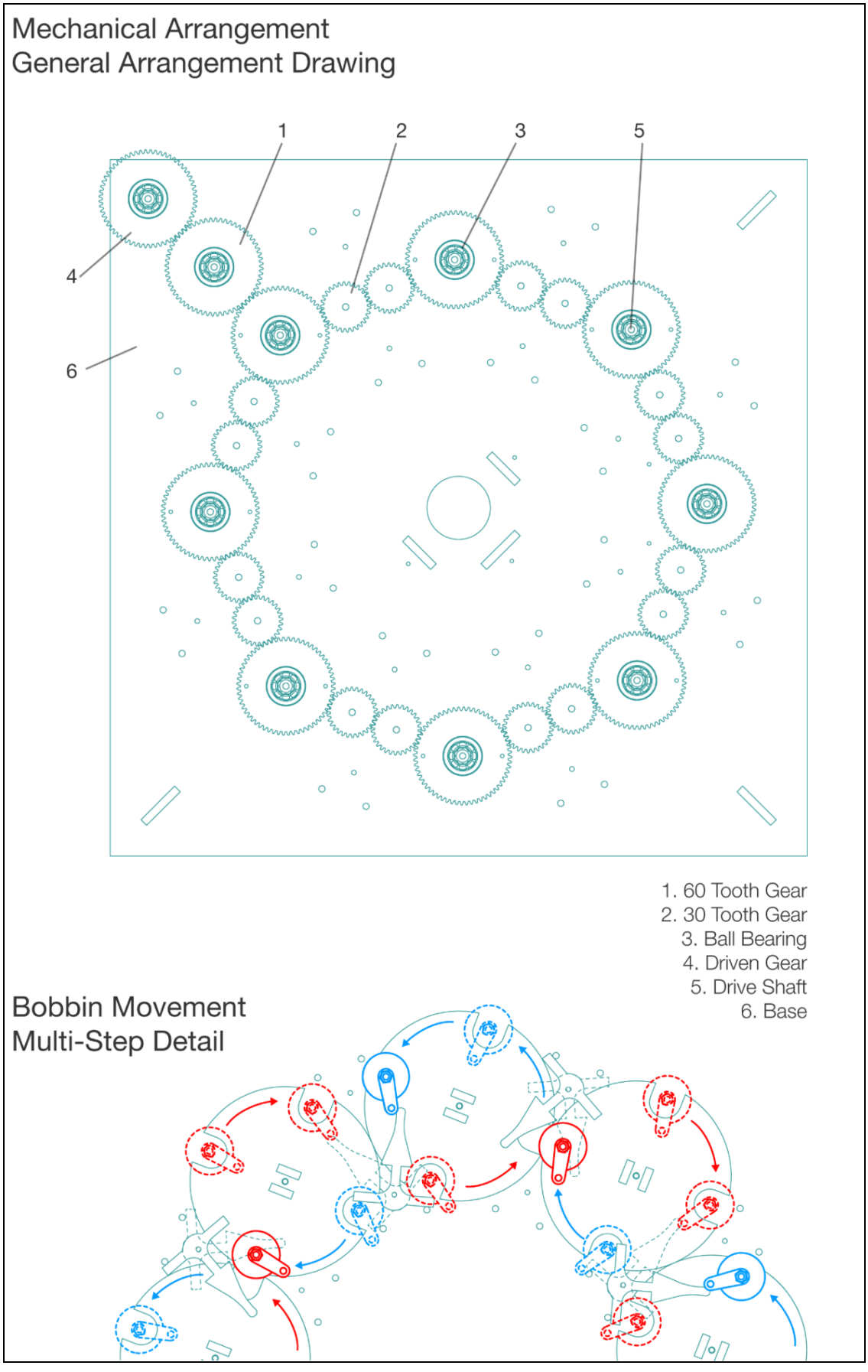

Figure 4.38 - Initial Weaving apparatus mechanical system

4.4.3.2.5 *Apparatus Integration*

As this apparatus is not used within the electrospinning system so its integration with the overall system is in regards to its ability to take the product of the reel to reel coating process and then add an external woven sheathing, creating a multilayer fibre device.

The reel with the core-shell fibres collected on it from the coating apparatus can be taken straight after electrospinning and the reel then attached to the bottom part of the braiding apparatus without having to remove or disturb the core-shell fibres. The end of the core-shell fibre is found and then pulled up to the top reel and securely fastened.

Below the reel a piece of nonconductive tread is tired around the core shell fibre with a loop in it. To this loop the wires from each of the 8 bobbins are attached. It is necessary to attach to a nonconductive thread so that if any damage to the core-shell fibre happens when it is tied on there is no chance of it causing a short circuit between the central core wire and the outer woven electrode. Once all the braiding fibres are attached then the weaving apparatus can be used to weave an external sheath.

4.4.3.3 *Final experimental Apparatus - Embedded System Solution*

4.4.3.3.1 *Introduction*

The issues found with the initial weaving apparatus especially in regards to the problems with the tolerances, gearing other mechanical aspects as discussed in section 5.6.4.1 meant that the apparatus underwent a series of modifications and improvements to make it fully functional. The final apparatus is presented in the following sections and the incremental improvements made to achieve the final apparatus are discussed.

4.4.3.3.2 *Design Specification*

The main change needed to be the individual control of the carousels to better achieve alignment for passing the bobbins. This necessitates a change from a mostly mechanical system to an electrical system which added complexity such as

driving each carousel individually using stepper motors and then having sensors in place to detect the correct alignment of carousels. These changes were added first and then changes were made incrementally after this.

Gearing was also found to be needed for rotating the carousels accurately so each stepper motor then needed a gear box. To achieve a more uniform weave and also to help prevent tangling of the wires a guide was placed above the bottom reel which causes the wires to approach the core-shell fibre at a more obtuse angle.

4.4.3.3.3 *Physical Design*

The physical design underwent few changes and the majority of the initial apparatus was reused for the improved version. The main changes were the addition of the gearboxes which were designed to mount to existing points on the base and the addition of additional bearings to increase reliability of the system.

Other improvements included the addition of the thread guide and improvements to the wobblers were made so that the shape was optimised to facilitate a smoother bobbin transition between carousels. The shape of the slots in the carousels were changed so they flared out towards the edges, widening the slot and also a 5 mm rounded edge was added so that the bobbins could move more easily into the slots and the possibility of the bobbins jamming on the edge of the slots removed. The carousels also had mounting points for four magnets added that were used in conjunction with the developed alignment sensor system. Figure 4.39 shows this design and the improvements made.

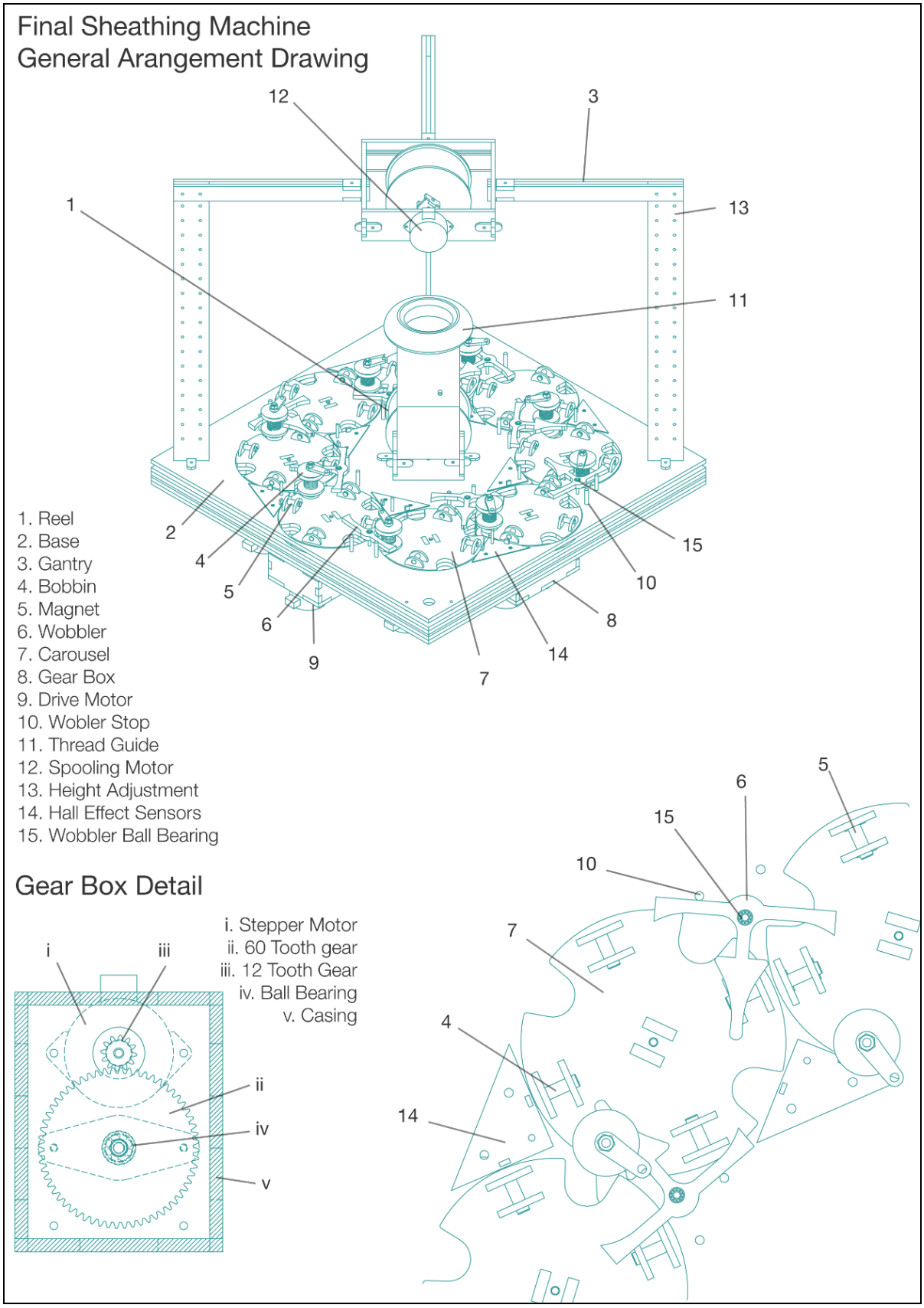

Figure 4.39 - Improved braiding machine general arrangement drawing

4.4.3.3.4 *Mechanical Design*

The mechanical design saw most changes as the focus was moved from a fully mechanical system to a predominately electronic controlled system. Stepper motors were used to drive each individual carousel and a gear box between each motor and carousel used to reduce the step size of the stepper motor, reducing the rotational distance the carousel moved per step. A 60 tooth and a 13 tooth gear were used for each gear box giving a gear ratio of 4.6:1. This changed the step angle of the carousel to 1.63° giving a more accurate control over the positioning of the carousel allowing a better degree of alignment between carousels. Bearings were added at the bottom of the gear box and below the carousels to ensure a good vertical alignment and ease of motion.

Changes were made to the wobblers as well such as the addition of a bearing on the pivot that improved the ease of motion. As well small bar magnets were bonded to the edge of the protruding arms which magnetically kept the wobbler in the correct place between bobbin passes because of attraction between the magnet and the metallic stop behind the wobbler used to limit its range of movement.

4.4.3.3.5 *Electronic Design*

4.4.3.3.5.1 Aim

The electronic system developed had to drive nine individual stepper motors, one for the reel to reel feed and eight for the rotation of the carousels. For this nine L293D half H drivers were used. It also needed to detect the correct alignment of the eight carousels, 16 magnetic unipolar Hall Effect sensors were used to do this. The sensors themselves were mounted on the apparatus base by the carousels and so as the carousels rotated the magnets mounted on them would trigger the Hall Effect sensors when the carousels are correctly aligned. See Figure 4.39 for a diagram including the Hall Effect sensor boards. LEDs for indicating alignment were added by each Hall Effect sensor, so there were also 16 LEDs in the electronic system. Headers were used to connect both LEDs and Hall Effect sensors to the control board.

On the control board itself a small user interface was needed, the chosen design of which consisted of an LCD screen, three LEDs, a potentiometer and button. With such a large amount of necessary inputs and outputs a larger Microcontroller was needed. The PIC16F1789 was chosen with 40 pins for this purpose, the large pin count and the ability to have multiple ports with interrupt on change functionality made it suitable for this project. As with the other microcontrollers used the chosen microcontroller also had multiple on-board timers which were useful for this particular project [109].

4.4.3.3.5.2 Hardware Development

Even with the large pin count there were not enough pins to drive each stepper motor independently as this would have used 36 pins going from the microcontroller to each stepper motors L293D driver, four pins for each stepper motor. To reduce the pin count necessary for the circuit the stepper motors were multiplexed whereby they all shared the four outputs of the stepper motor. This meant that all the L293D drivers inputs were connected together so all the stepper motors could be stepped in unison from the microcontroller. To then allow the selection of individual stepper motors the L293D's enable pins were utilised so that the driver chips themselves could be turned off, therefore stopping the signal from the microcontroller causing the stepper motor to make a step. This would have meant that in total 13 pins were needed to individually drive all the stepper motors however this number was reduced even more with the addition of a CD4028B binary to decimal decoder (BCD) [110] where by addressing the chip using changing logic levels on four inputs selects one of ten outputs from the BCD to go to a high logic level. This meant that in total only 8 pins were needed to drive 9 stepper motors independently.

Even with this reduction in needed pins there were still not enough for both the alignment indicator LEDs, Hall Effect sensors and user interface. The pins necessary to drive the LEDs was reduced using a 4 to 16 line decoder CD4514B [111] which allows any one the LEDs to be driven at any time and only needs 5 pins from the microcontroller. The downside to this is that only one of the LEDs can be on at a time however the code was developed to strobe all the LED's that were indicating correct

alignment which made it highly useful during the development and testing of the circuitry and apparatus.

The Hall Effect sensors were attached to ports A and C on the microcontroller as these had interrupt on change functionality allowing the instant detection of the alignment of the carousels. This meant they took up 16 pins. The developed circuit schematic is shown in Figure 4.40 and Figure 4.41, with the PCB layout in Figure 4.42. An image of the competed printed and populated board and connections to the apparatus is shown in Figure 4.43. Note on the PCB layout the space at the centre of the board for the mounting of the LCD screen and below it the user interface layout.

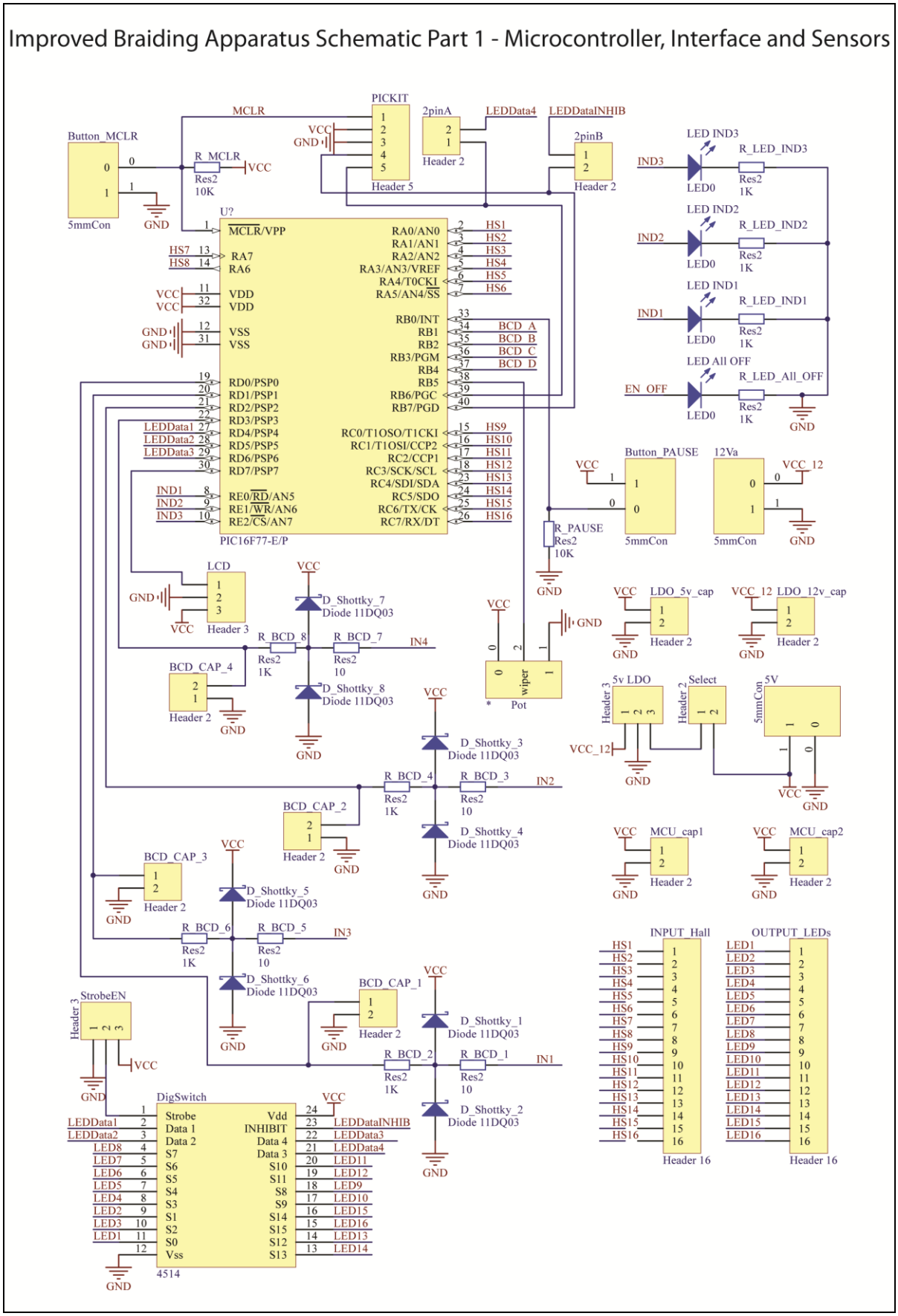

Figure 4.40 - Improved braiding apparatus schematic part 1

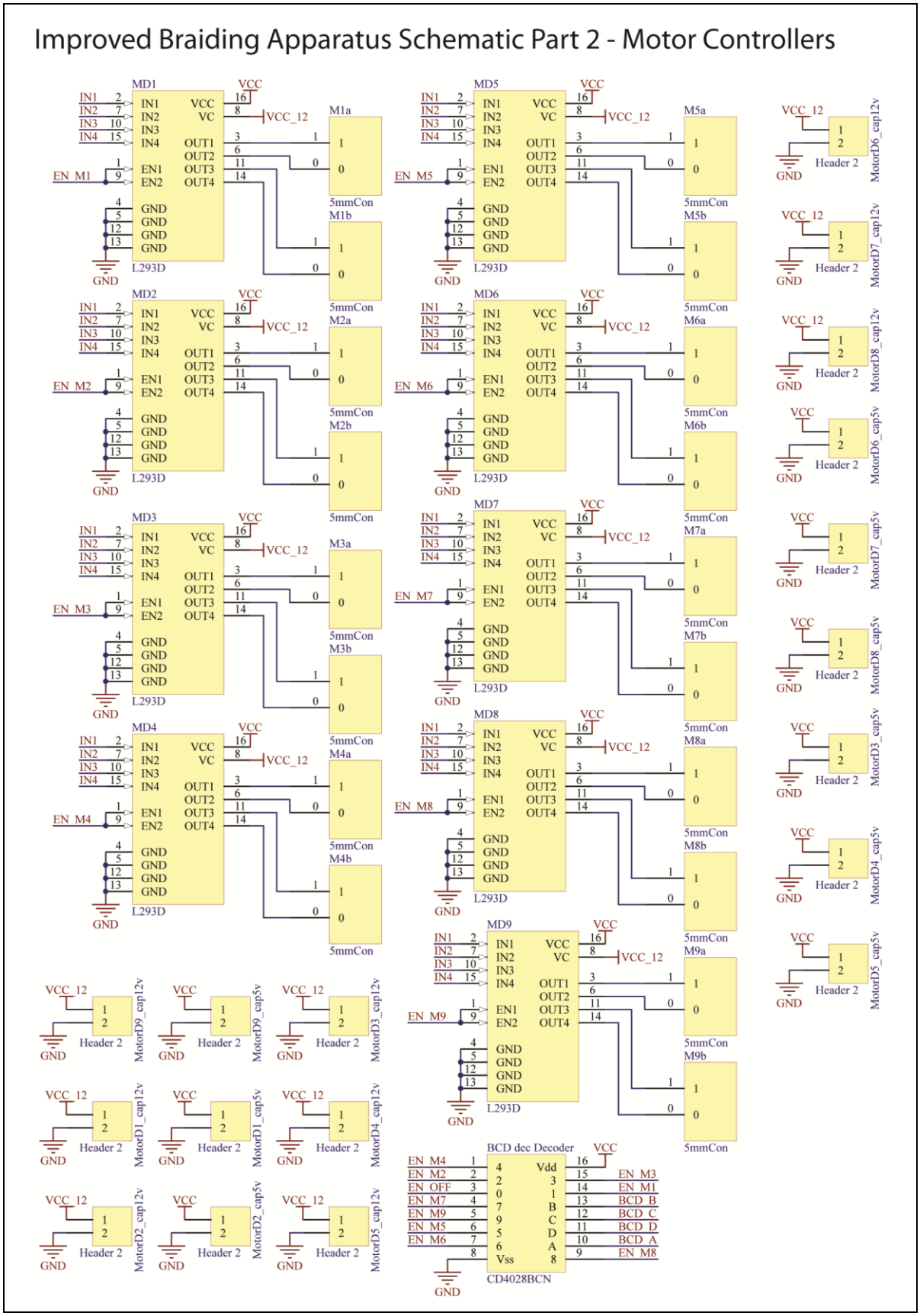

Figure 4.41 - Improved braiding apparatus schematic part 2

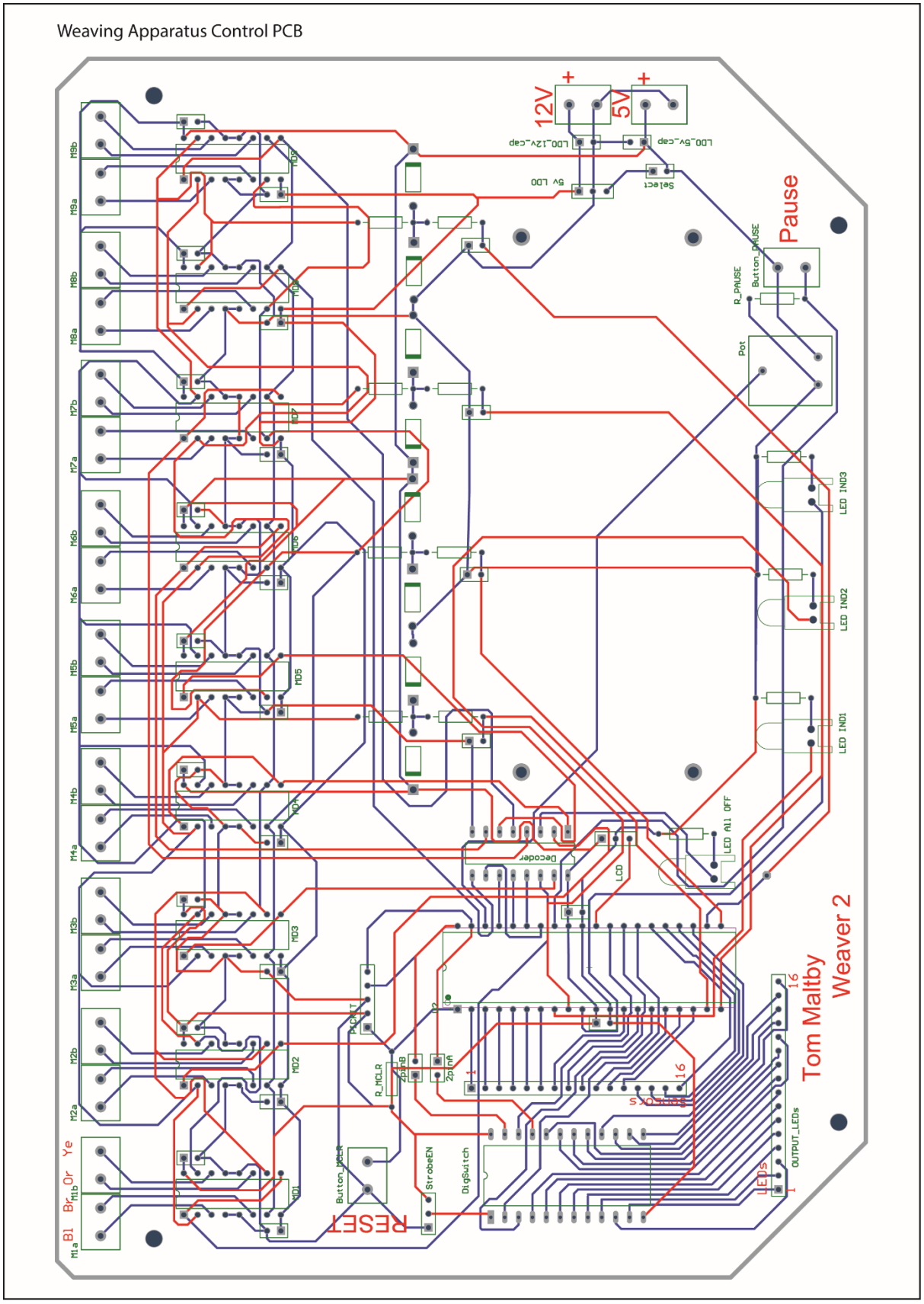

Figure 4.42 - Improved weaving apparatus circuit board layout

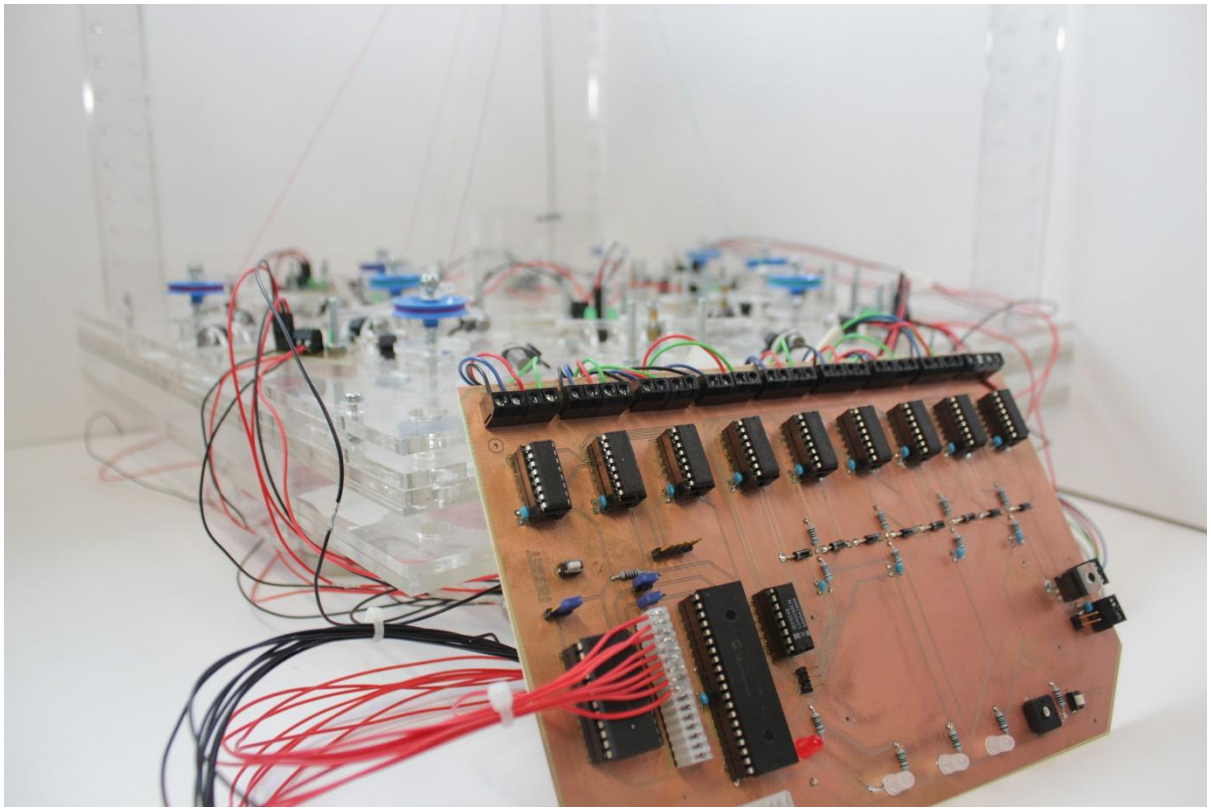

Figure 4.43 - Improved weaving apparatus populated printed circuit board

4.4.3.3.5.3 Software Development

The software developed was complex due to the necessary interaction between the Hall Effect sensors and the driving of the steeper motors. The full code can be broken down as follows.

During operation each stepper motor is turned one step sequentially. This goes on until a change is detected on one of the Hall Effect pins. The program then moves to an interrupt routine that detects the interrupt on change on either port A or C when the Hall Effect sensor is triggered indicating correct carousel alignment. When the interrupt is triggered the routine goes through each pin and detects the one that has been triggered. Once detected it changes a flag in an array that corresponds to the carousel that has achieved alignment.

The program then goes back to the stepper motor run code which now no longer steps the motor for the previously detected aligned carousel. This process carries on until all the Hall Effect sensors have been triggered and all carousels are correctly aligned. As it is known which 8 of the 16 Hall Effect sensors should be triggered at

the same time if one of the wrong Hall Effect has been triggered the program then reverses this carousel until the correct alignment is achieved. Once full alignment occurs then all the stepper motors are stepped in unison to achieve the bobbin pass.

The program then resets the alignment array and goes back to the initial code that steps the motors until full alignment. To stop any issues associated with the program continuing to step the motors if one of the bobbins has jammed a timing function has been implemented that uses a timer interrupt that monitors the time between full alignments. If this times out then a jam or another issue has happened to stop the alignment process and the programme stops the hardware and sends an error to the LCD screen along with an error indicated using one of the LEDs.

Another timer is utilised for the ninth stepper motor which controls the feed rate so that the central core fibre being braided moves in exact intervals. Due to the slow nature of the weaving process this stepper motor steps infrequently. The code produced for the final version of this apparatus can be found in section 9.6.3 of the Appendix.

4.4.3.3.6 *Apparatus Integration*

Setting up the apparatus was the same as for the initial version of the apparatus however care has to be taken as to the initial alignment of the carousels in regards to their positioning in relation to the Hall Effect sensors. This was because there was no way for the software to know the exact positioning of the carousels and bobbins, only when they were correctly aligned so the user had to align them manually before use.

5 Results

5.1 *Introduction*

The following sections details the results from the testing of the different experimental apparatus developed. The focus is on the apparatus that extends the conventional electrospinning technique and the majority of the results are concerned with, in the first instance proving the concept put forward and then identifying improvements and additions to the developed technique that need to be made. Following this the improved upon apparatus is analysed and results looking at morphology and usability of the produced electrospun polymer fibres and devices are presented and discussed.

Even though the focus is on the expansion of the conventional electrospinning technique this upcoming chapter is structured so that the overall systems developed are discussed together in the order which they are used experimentally, the order being: pre-electrospinning, electrospinning, collection of electrospun material, post processing and testing of produced material. Not all systems developed have all the stages listed above.

In addition to this some basic material characterisation and conventional electrospinning results are presented first to help show and put the material properties of PVDF and conventional electrospinning into context for comparison with the samples produced by the developed apparatus.

5.2 *Initial Experimentation*

5.2.1 Introduction

Initial experimentation was carried out to investigate the properties of the PVDF powder (Kynar 761) kindly provided by Arkema [100]. It including looking at the melting point, glass transition temperatures and crystallinity as this shows the quality and shows what the working temperature ranges of any developed devices would be.

5.2.2 Differential Scanning Calorimetry (DSC)

The graph in Figure 5.1 shows a DSC plot with three cycles of heating, cooling and heating. The graph can be split into three parts with the top trace showing the cooling phase. The large peak seen at 125 °C is where the previously melted polymer is re-crystallising during which time it is giving out heat.

The two lower traces show a substantial dip at around 155 °C which indicates the polymers melting point. This is lower than the temperature range given by Arkema of 165 – 172 °C [100] however the sample was shown to be completely melted at around these temperatures as the traces flatten off. This shows that the upper temperature limit for PVDF is less than 140 °C as above this temperature changes in the polymer will begin to occur.

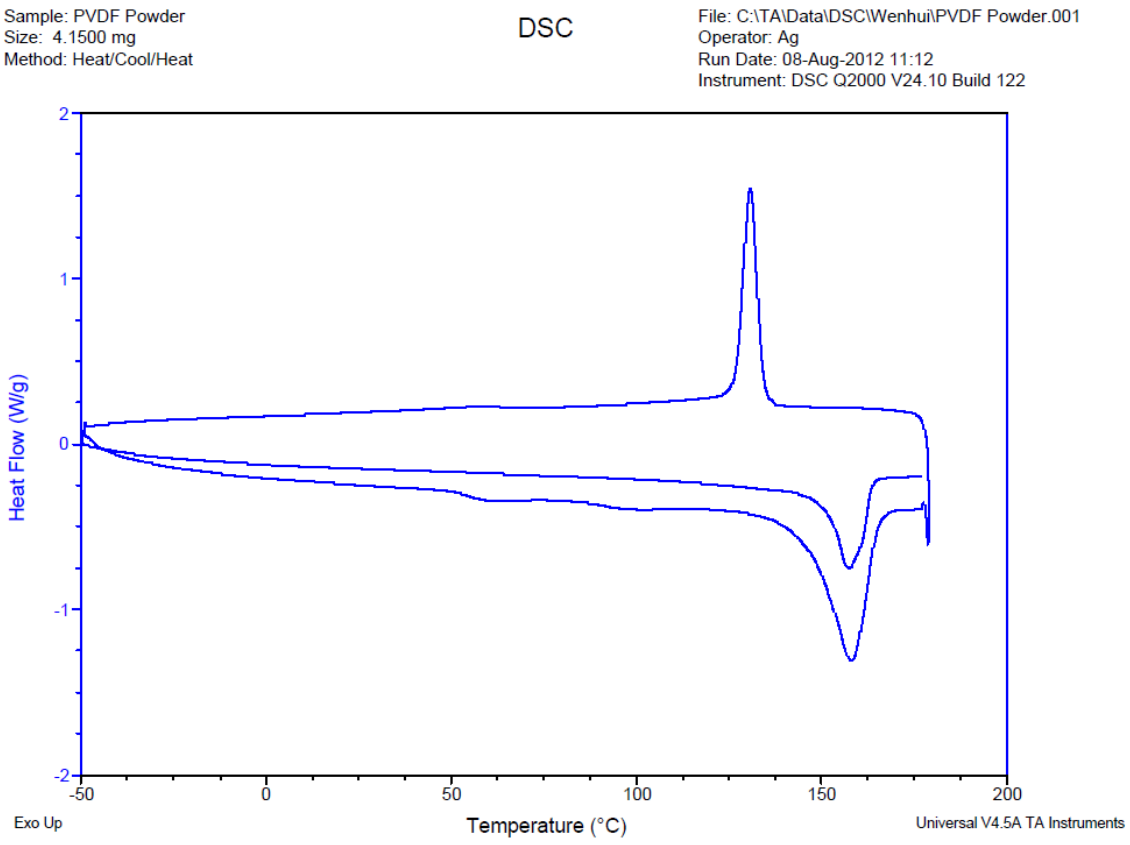

Figure 5.1 – DSC graph showing melting and crystallisation point of PVDF

5.2.3 Dynamic Mechanical Analysis (DMA)

The samples tested were thick films (>100 µm) produced by electrospinning. The equipment can be used in two modes, extension/tension and cantilever. Figure 5.2 shows a graph of a PVDF sample tested in tension mode. This test involved fixing the sample so it was not under tension but tightly held in the apparatus. During experimentation the equipment oscillates the sample to a set distance measuring the force required to do so. As the temperature changes and the material goes through structural changes the force differs.

The Tan Delta trace in red shows the energy dissipation in the material and shows clearly the glass transition temperature at the first peak at around -36 °C which corresponds well to the value given in literature. The region between 0 and 100 °C is relatively linear and clean showing material stability in this region. After 100 °C there are unexpected fluctuations. The possible reasons for this are either slippage between the fibres in the electrospun sample or shrinking of the PVDF as suggested in literature [112]. The trace ends abruptly at around 162 °C when the apparatus detects that the sample has broken or stretched past an acceptable limit. In this case the sample has started to melt and the value matches very well with the expected melting point given in literature [100].

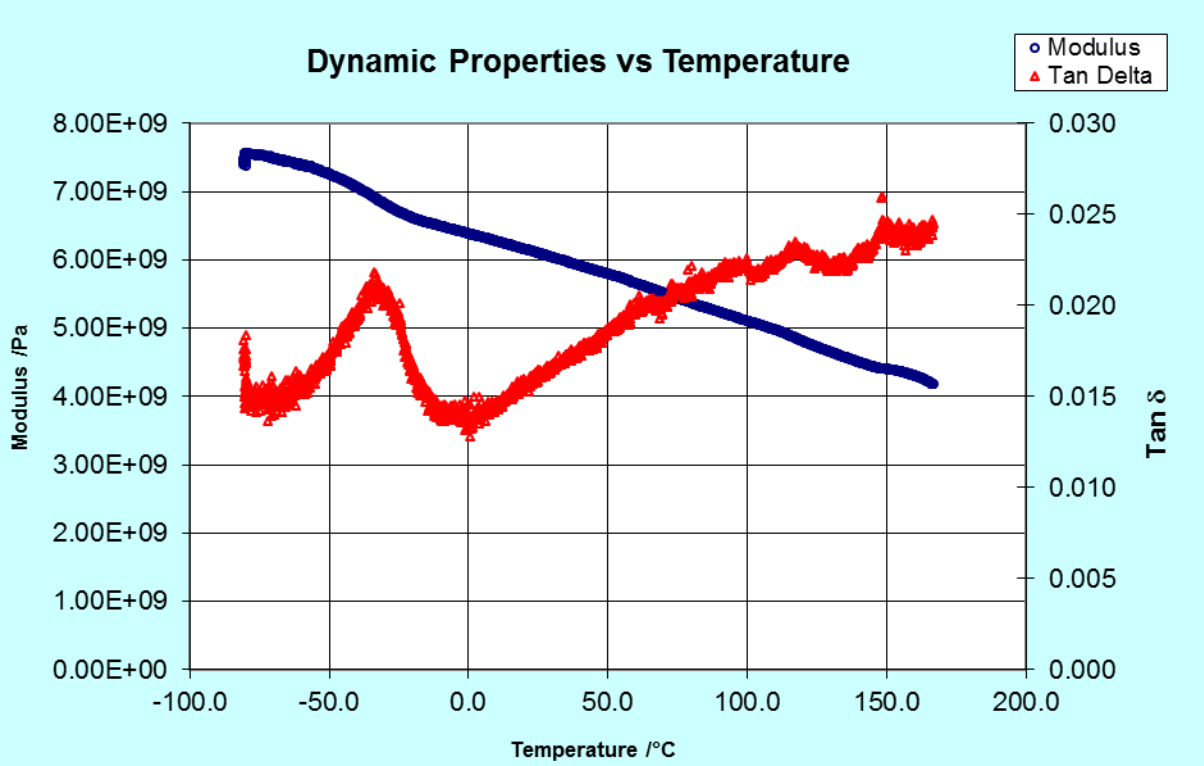

Figure 5.2-DMA of PVDF film sample tested in tension mode

Due to the unexpected changes in Tan Delta over 100 °C the experiments were run again but this time using the single cantilever mode. In this mode the sample is contained in a stainless steel pocket and one end of the pocket is clamped and the other end is attached to the shaker and force sensor. In this setup the sample is bent as a cantilever rather than put under tension. The steel pocket does not affect the readings due to its material properties.

The graph for the sample tested in this mode is shown in Figure 5.3 and again the first peak on the Tan Delta trace shows glass transition temperature at about -36 °C. The material as before shows stability above 0 °C however at around 75 °C a material transition can be seen. In this case it cannot be the fibres' slipping as that is not possible while in the steel pocket therefore it is presumed to be the phenomenon described in literature where the films relax and shrink in the axis they are drawn in [112]. The melting point can also be seen as the trace dips at 166 °C. This gives a working temperature range for the polymer of between -36 °C and 75 °C where at this point the fibre start undergoing physical changes which would adversely affect any devices made using this material.

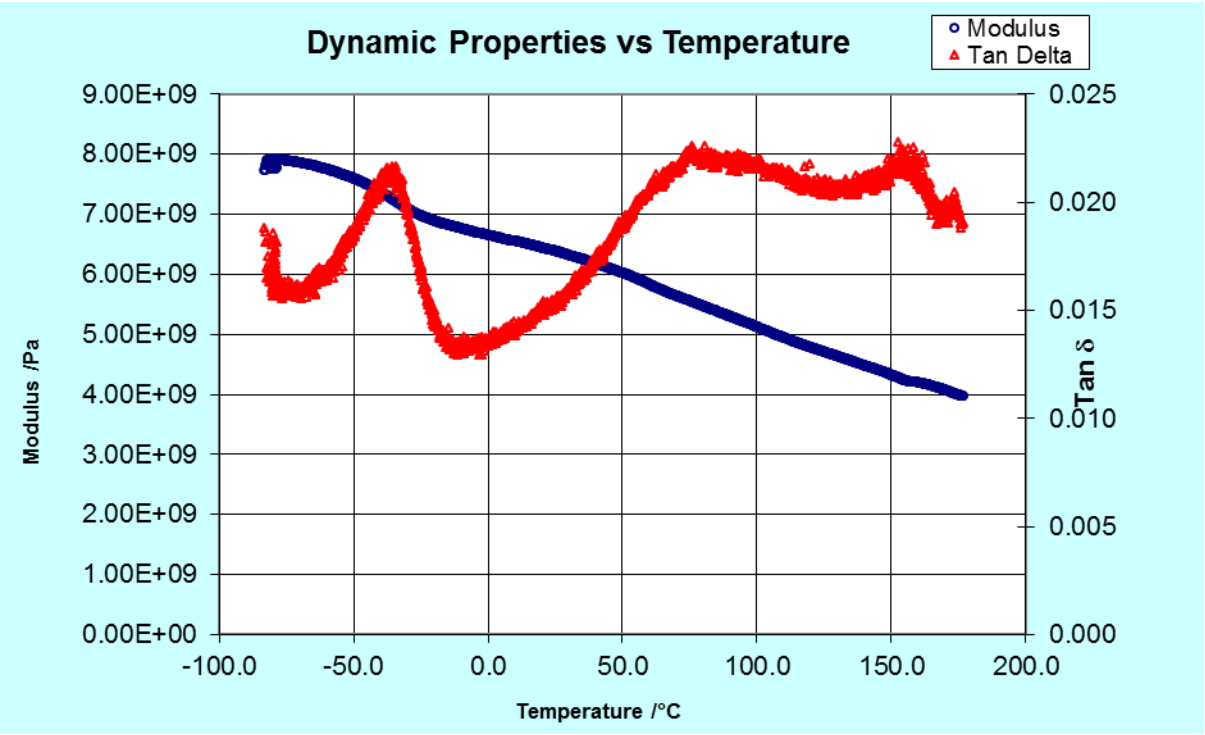

Figure 5.3 –DMA of PVDF film in cantilever mode

5.3 *Substrate Free Film Production and Testing Analysis*

5.3.1 System Overview

The apparatus developed was used together to produce substrate free electrospun PVDF mats with a controlled deposition area. Once dry these mats had electrodes added by painting on conductive silver particulate paint. The produced devices then were tested for piezoelectric response by looking at the produced voltage and also the films resonant frequencies were found where they were producing the greatest voltage output.

The apparatus was tested individually and built up into the full system, the following sections detail and discuss the testing and results from the apparatus used in this system.

5.3.2 Developed Electrospinning Apparatus Tests

5.3.2.1 *Secondary Ring Electrodes*

The secondary ring electrodes were tested using the PVDF solution and experimental setup as described in section 3.3. The collecting substrate used was aluminium foil and a height of 30mm was used between the base electrode and the bottom of the secondary electrode rings.

Experimentation was completed by analysing the use of different diameters of secondary electrode rings and the deposition sizes that were attainable by changing the voltage potential on the rings.

It was found that it was much easier to control the deposition area when using the larger sizes of rings as it allowed a much larger range of deposition sizes. However the potential voltage needed to deposit onto a small area was much greater. There were also issues with electrospinning using smaller secondary electrode rings where the fibres would more readily coat the inside of the rings. The deposition diameter attainable using the secondary electrode rings ranged from greater than 100 mm to a diameter of approximately 10 mm.

Figure 5.4 is an SEM image of the electrospun film produced using the apparatus. It is comparable with the morphology of electrospun films produced in the literature [81, 82]. The image shows randomly orientated fibres with sub-micron diameters. There are also some thicker fibres and nodules present on some fibres. The formation of nodules is known as beading and is common in electrospun films. This shows that the secondary electric field apparatus isn't having an adverse effect on fibre deposition and fibre morphology.

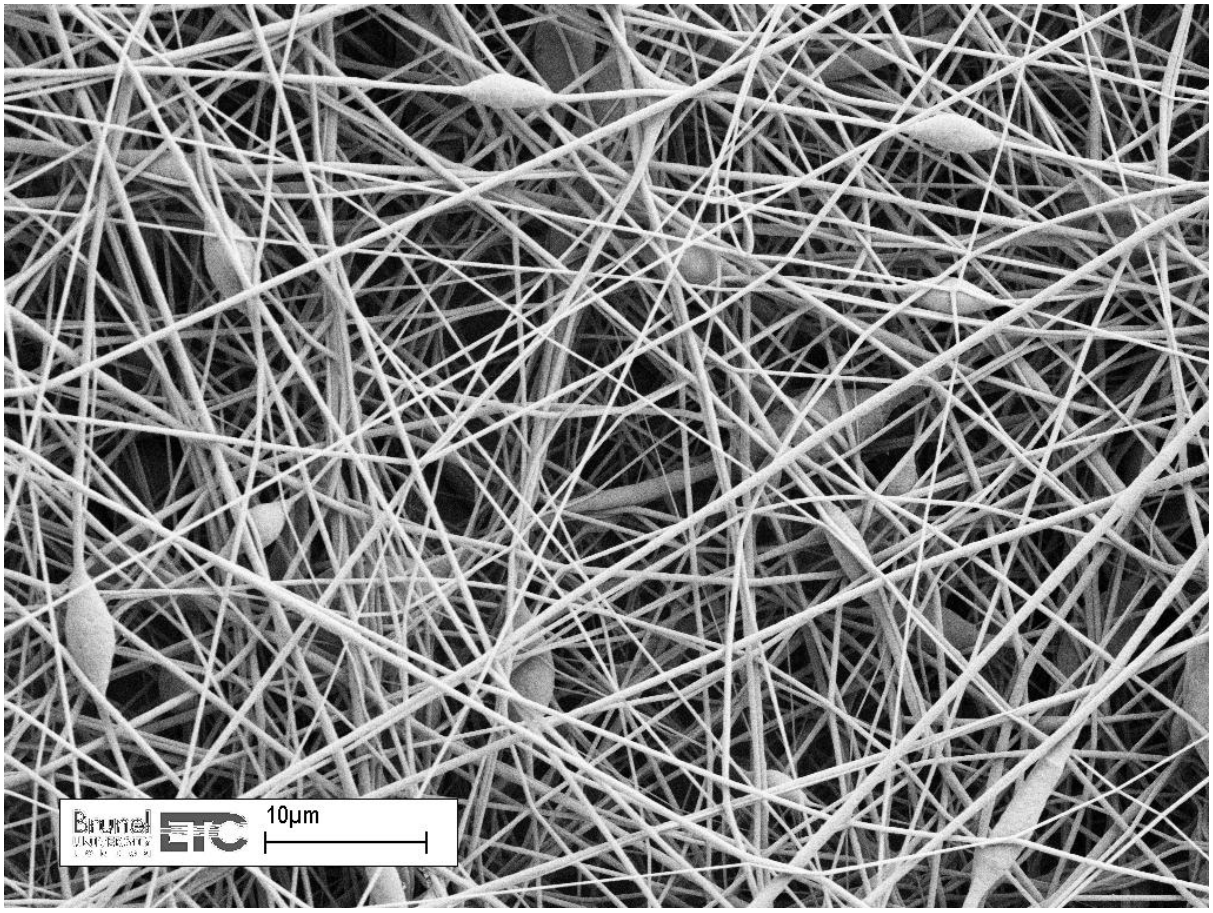

Figure 5.4 - Conventional Electrospun film

5.3.2.2 *Initial Water Bath*

The initial water bath was tested with the inclusion of the secondary ring electrodes so that the fibre deposition could be controlled onto the water's surface. The standardised PVDF solution and experimental parameters were used. In these experiments the secondary electrode rings potential voltage was also changed to produce fibre deposition areas of different diameters.

Again a larger potential voltage produced a smaller deposition area. Figure 5.5 shows an experiment which used a primary voltage of 12 KV and a secondary voltage of 4 KV. The second image, Figure 5.6 shows the same experiment again using 12 KV as the primary electrode voltage and 6 KV for the secondary electrode rings. As can be seen the deposition area is much smaller in diameter for the second image at approximately 40 mm compared to the deposition using the lower secondary potential voltage of approximately 100 mm in diameter.

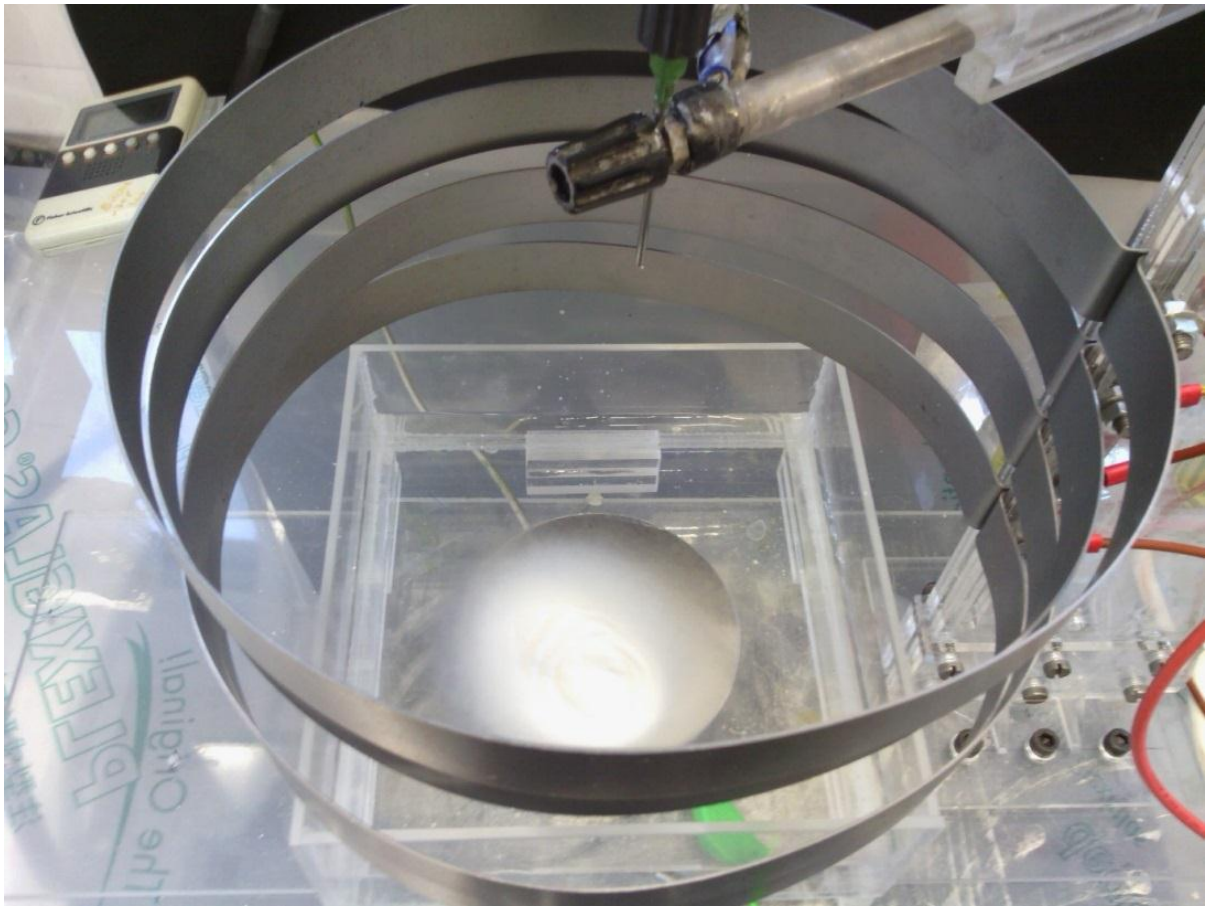

Figure 5.5 - Substrate free film during electrospinning with a low secondary voltage

The problems using this technique can be easily seen from the images where a greater thickness of deposition builds up in the centre of the deposition area which can distort the produced mats. The outer edges of the deposition are made of a very fine layer which cannot be seen on the images, this makes accurately measuring the diameter of the deposited mats difficult.

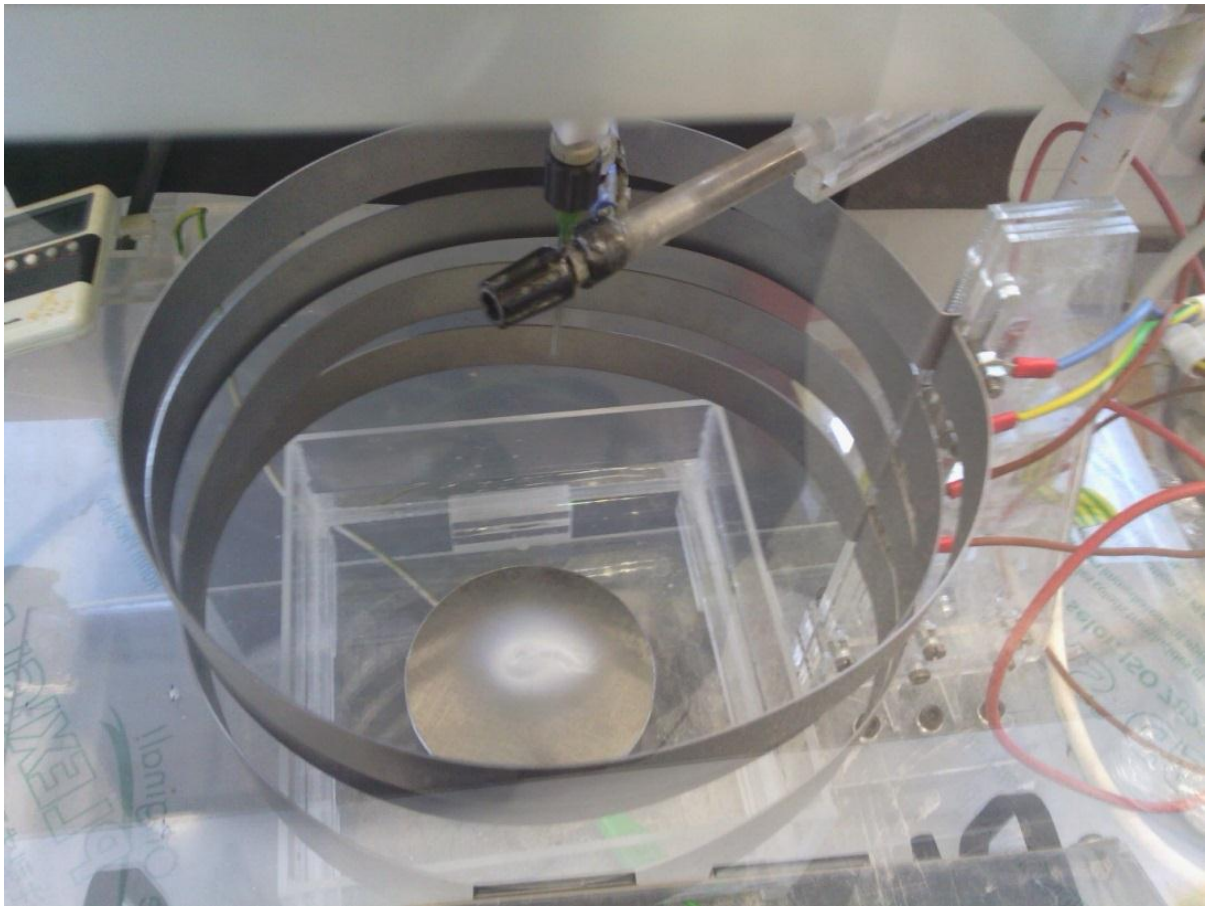

Figure 5.6 -Substrate free film during electrospinning with a high secondary voltage

Other issues found were that the free floating mats often floated around slightly in the water bath often causing oval rather than round depositions. The reasons for the movement is likely because of irregularities in the electric field caused by secondary ring electrodes that were not correctly aligned which the fibre mats then orientate themselves to since they are still carrying some charge.

Another contributing factor to the movement of the mats on the water surface could be due to the cabling connecting the High voltage power supply to the primary electrode electrospinning needle. The multi physics modelling package Comsol was used to visualise the water bath with the wiring in place to see how it affected the electric field. The left image in Figure 5.7 shows a representation of the electric field coming from the needle tip with the cable attached to the needle. The right image shows the same model in an ideal setup where the needle had no wire going to it.

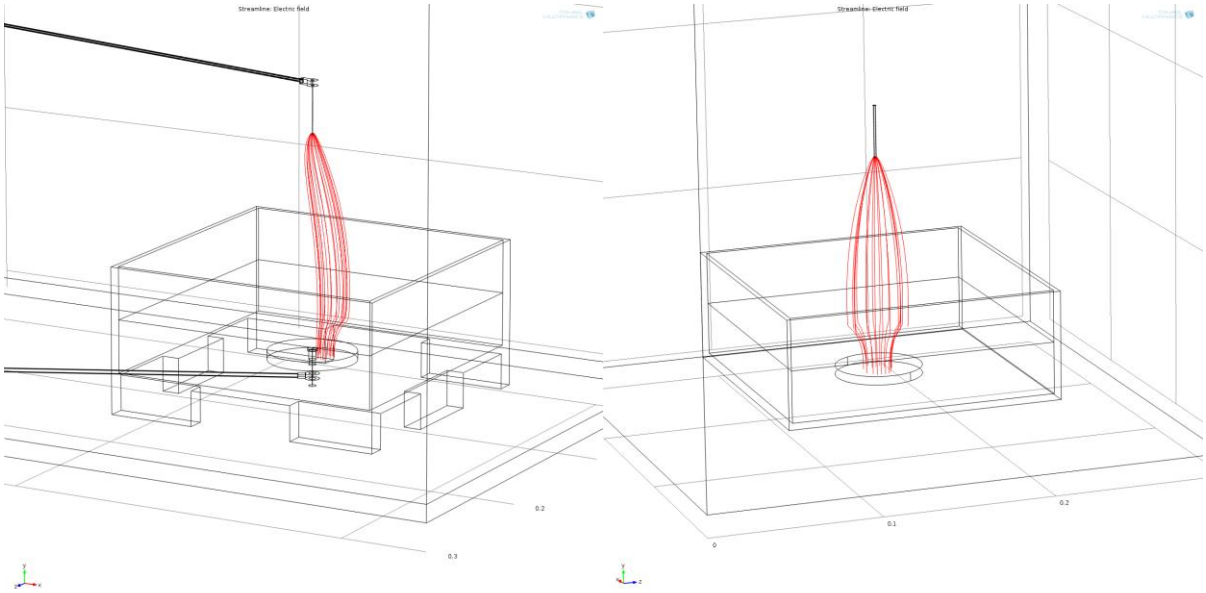

Figure 5.7 - Left image showing model including connecting wires. Right image showing model without wires.

The differences between the two are clear with the cabling affecting the electric field. This modelling does not take into account the secondary electrodes used which will help reduce the effect as they create a secondary interacting electric field.

5.3.2.3 *Improved Water Bath*

The improved water bath was designed so that the base electrode could be moved up to just below the surface of the water. This was done so that there was less depth of water between the base electrode and the surface of the water to reduce the resistance profile and change the electric field so that more uniform depositions could be achieved. From experimentation this was successful as there was noticeable reduction in differences in deposition thickness and less of the fine fibres around the extremities of the deposition area. Figure 5.8 shows the water bath during use.

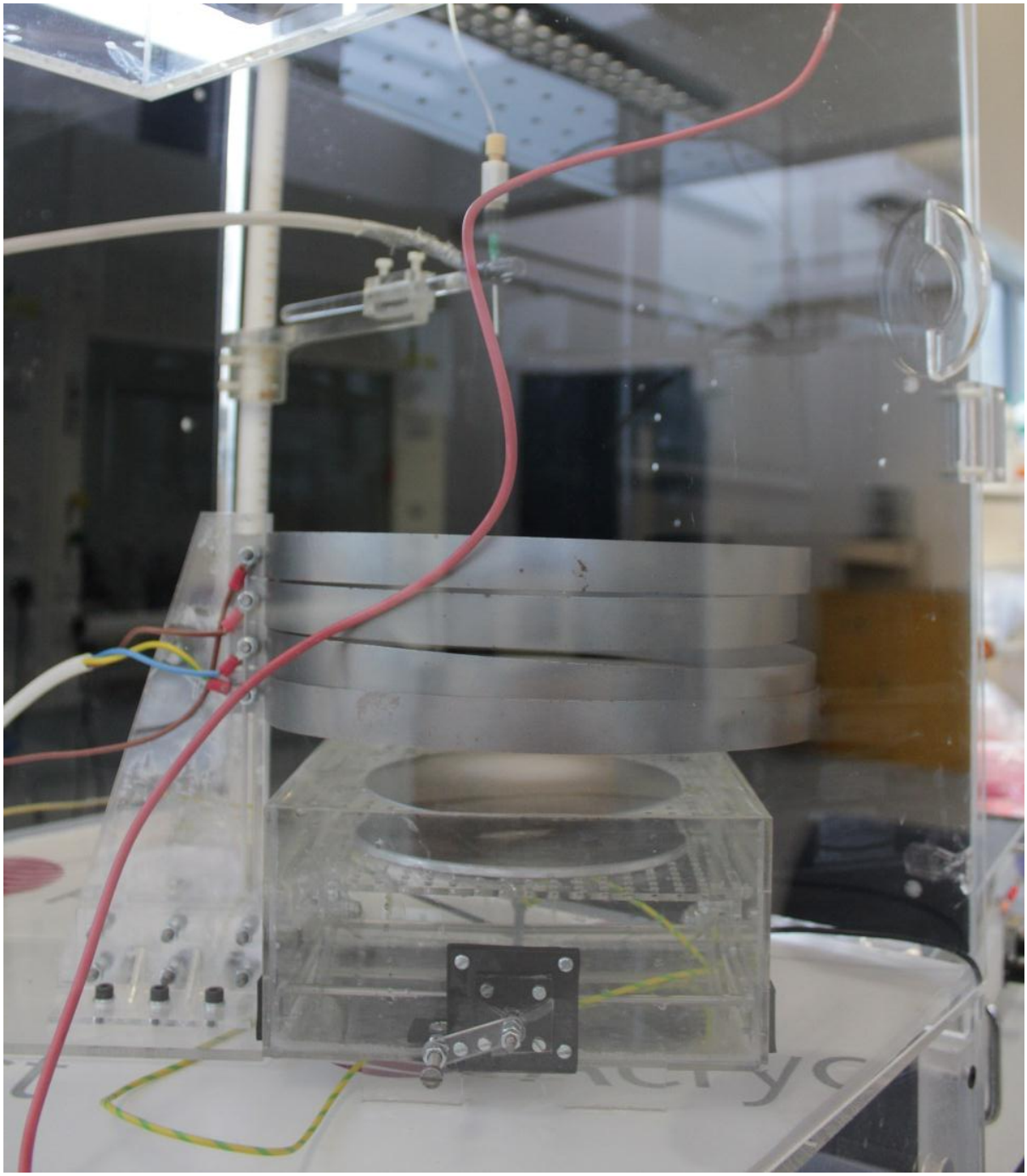

Figure 5.8 - Improved water bath apparatus in use

5.3.2.4 *Substrate Free Film Morphology*

Scanning electron microscopy was used to investigate the fibre morphology of the PVDF electrospun onto the surface of the water and it can be seen in Figure 5.9 that the morphology is different to that of a conventionally electrospun film shown in Figure 5.4.

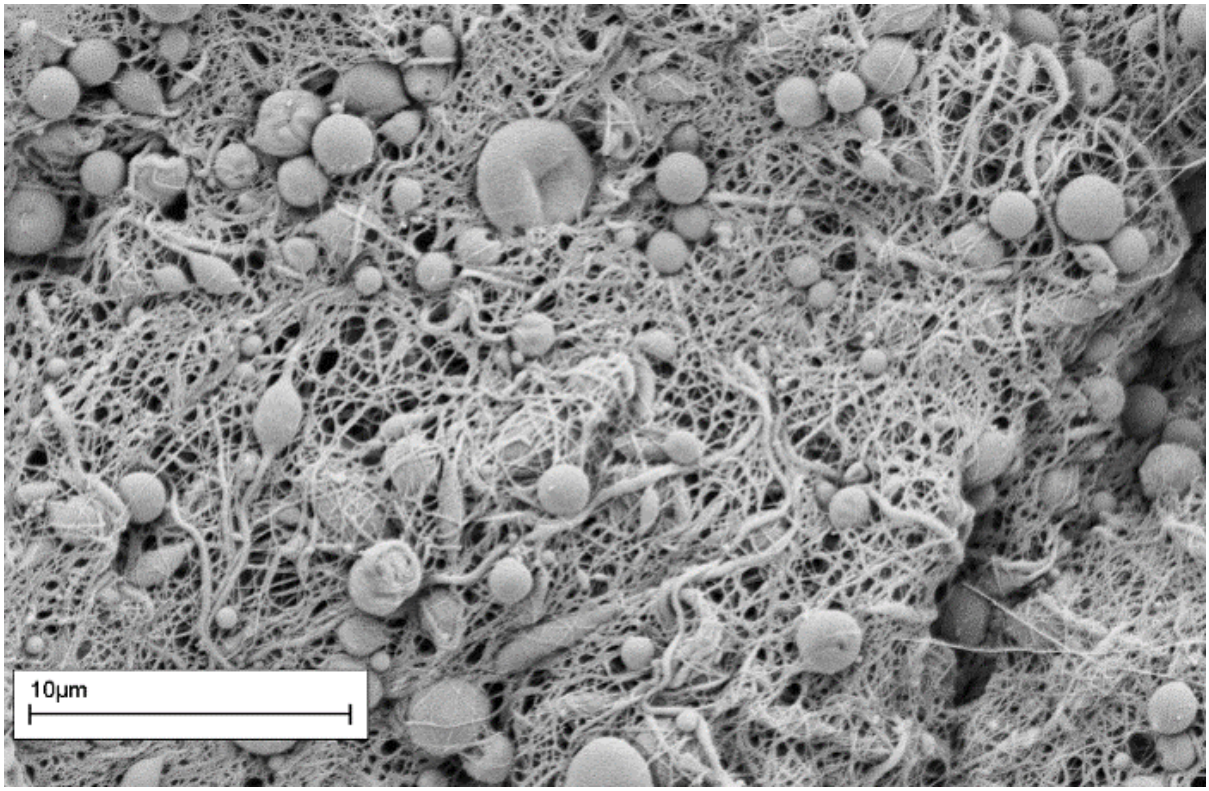

Figure 5.9 - Bottom surface of mat electrospun onto water

The structures seen in some ways resemble beading which is a common phenomenon with electrospinning fibres however this was not seen on the top surface of the films in this manner. Also the large size of the beads in relation to the fibre diameters also suggests that this is not traditional beading.

The balls especially ones of large diameter appear to be mainly on the surface of the electrospun film. This indicates that the structures were in direct contact with the water surface.

The reason for these structures is unknown but it is possible that due to the hydrophobic nature of the polymer there could have been contraction on deposition causing the extra-large beads that can be seen. This would explain why they are seen mainly on the surface of the film because once a number of beads had developed then fibres would be normally deposited spanning across the beads slightly raised from the water's surface.

5.3.3 Testing Apparatus

The produced substrate free fibre mats were collected onto a circular frame and allowed to dry. Square electrodes were then painted onto the top and bottom surface and flying leads attached to a corner on the top and bottom. They were then mounted into the voltage response test rig and the flying leads attached to the circuitry input. The samples were then swept through gradually increasing frequencies produced by an audio transducer. Figure 5.10 is a screen shot from the developed LabVIEW program of a sample being tested. It clearly shows a stable voltage output at the lower frequencies and then an increasing voltage output from the sample being tested showing the sample to be piezoelectric and a potential resonant frequency point at this maximum amplitude.

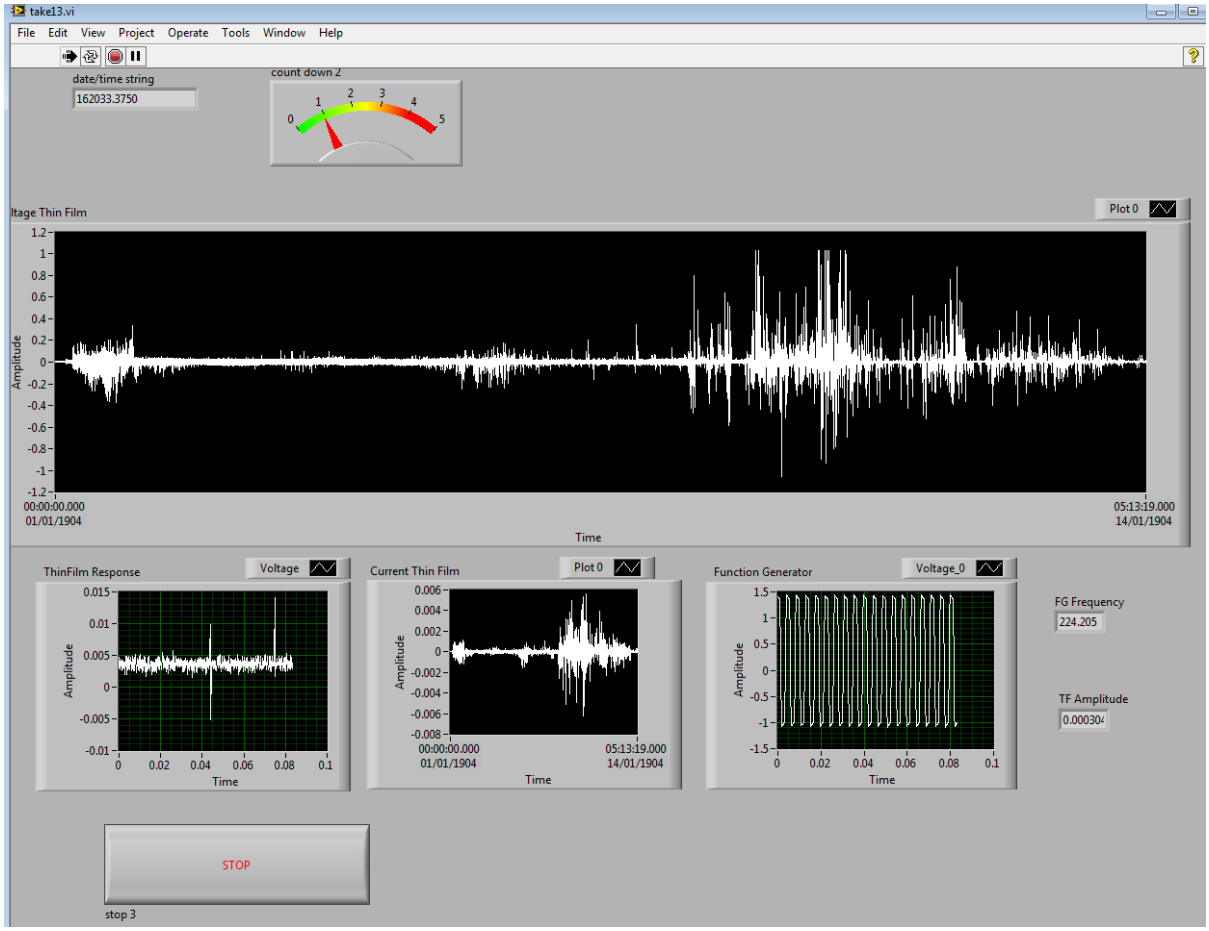

Figure 5.10 - LabVIEW programme user interface during experimentation

The gradual build up and then decrease of piezoelectric output response shown in Figure 5.10 is what would be expected of a sample as it reaches its resonant frequency, where the voltage produced is at its highest. The LabVIEW program developed also recorded the voltage output and the frequency it occurred at and saved it to a spreadsheet which allowed the resonant frequency to be found.

Figure 5.11 is a graph that was created using data recorded from the LabView system. It is a small part of a larger trace as seen in Figure 5.10 and it shows in detail the increase of the piezoelectric output as the frequency increases from 130 Hz up to approximately 135 Hz. Where the output of the film reaches its maximum output at approximately 1.1 v and then decreases gradually past 141 Hz. It would be expected that the voltage output would be mirrored in the negative voltage range however the maximum output is only approximately -0.7 v. This difference in output is due to the mounting of the sample where it can move more in one orientation when oscillating causing a greater voltage to develop and also be because of irregularities in the electrodes.

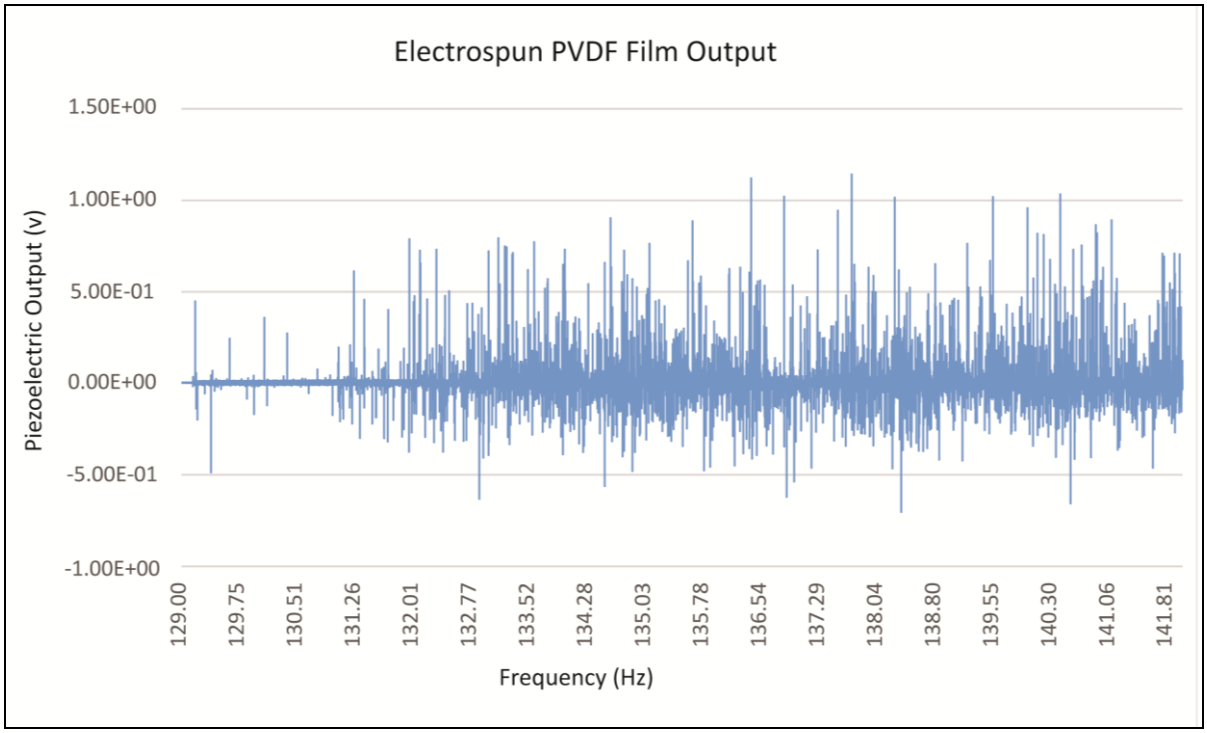

Figure 5.11 - Electrospun PVDF film output

The produced graph shows a gradual increase to a peak output voltage and then a decrease as is expected however the response is over too wide a frequency range showing the sample to have a broadband frequency response. This is because of the poor quality electrodes being used. Painting on electrodes results in an electrode with varying thickness and uniformity which is undesirable as this dampens the material resulting in the broad frequency response profile. The paint layer also excessively stiffened the film which stops the PVDF from being able to deform freely limiting the electrical output. However Figure 5.11 clearly shows a peak in output voltage at approximately 137 Hz which suggests a resonant response at this frequency.

5.3.4 System Evaluation and Conclusion

The system developed has been shown to successfully produce substrate free fibre mats which can be deposited in various thicknesses and diameters utilising a water bath and secondary ring electrodes in conjunction with the conventional electrospinning technique. The electrospun mats are collected from the water using a frame and dried. The fibre mats have electrodes added to them and are then tested for piezoelectricity using an apparatus that vibrates the samples using audio waves at different frequencies. The electrodes added to the fibre mats collect any charge produced by the excitation and the subsequent voltage is recorded using a data acquisition device and a custom program.

The samples produced for this system have been shown through experimentation to be piezoelectric with peak voltages seen of over 1 v. The aim was to also find the resonant frequencies of these samples by looking for the peak voltage output which would correspond to the resonant frequency. However due to the poor electrodes used which dampened the films it was not possible to accurately find the resonant frequency because of their broadband response. The developed apparatus and system worked correctly and as expected, to get better results more suitable electrodes would need to be developed.

5.4 *Novel Advanced Fibre Alignment*

5.4.1 System Overview

The fibre alignment work was based on experimentation found in literature and the first part was to replicate some of the more simple experiments so see the fibre alignment that could be achieved. Apparatus was then developed that allowed greater control of the process allowing more complicated aligned patterns, structures and layers to be developed. In the following sections various experiments and the apparatus developed is evaluated and discussed.

5.4.2 Initial Experimentation

Initial experimentation was completed to see the alignment that had been reported in literature in regards to electrospun fibres in flight automatically aligning across gaps between two base electrodes. The experiments were carried out using the electrospinning parameters detailed in section 3.3.

It was found that the fibres do readily align across gaps between electrodes as can be seen in Figure 5.12. During experimentation these fibres once deposited across the two electrodes can be seen to arc as they are affected by the electric field as shown in right image of Figure 5.12. This may have a positive effect on the formation of beta crystallinity of the fibres, which in turn will increase the piezoelectric output as it has been shown in literature that the stretching of PVDF is a key process for the reordering of the material.

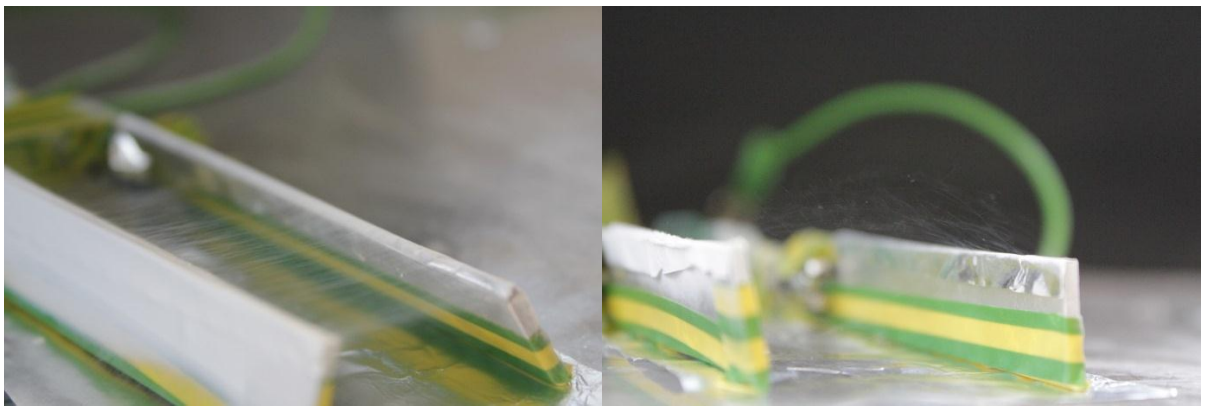

Figure 5.12 - The left image shows aligned fibres between two base electrodes. The right image shows the fibres during electrospinning.

This experimentation showed that good alignment of fibres could be achieved by electrospinning across a gap between electrodes. This was then used to inform the design of more advanced apparatus that could take advantage of this.

5.4.3 Developed Electrospinning Apparatus Tests

5.4.3.1 *Initial Relay apparatus*

The initial apparatus developed, shown in section 4.2.2 was used to see if by selectively switching base electrodes to ground in set patterns different deposition morphologies could be produced.

Figure 5.13 shows an initial test carried out where the electrodes were grounded in two pairs with both electrodes in the pair being grounded at the same time. The pairing was the top left and right electrodes. The other pair was the top left and bottom electrodes. The bottom electrode and top right electrode were never put to a ground state at the same time.

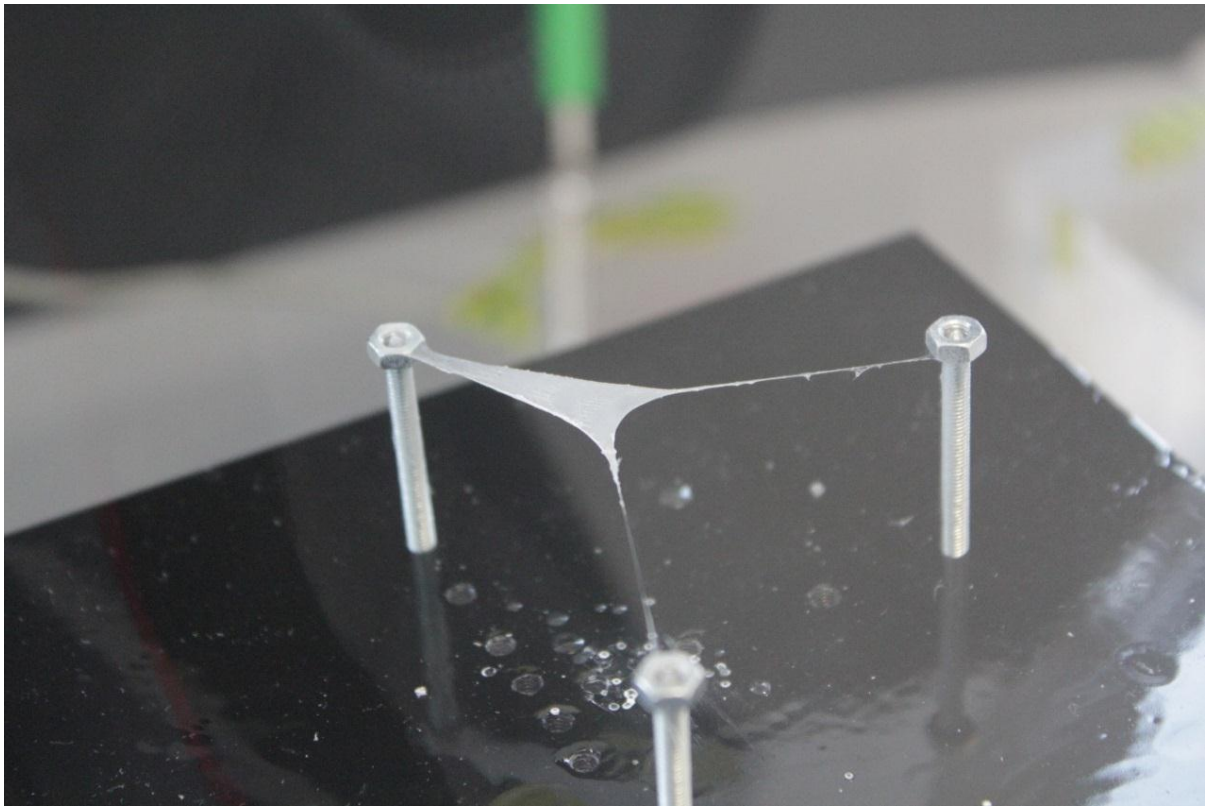

Figure 5.13 – Aligned electrospun structure with matting between electrodes

It can be clearly seen that the fibres readily align between the electrode pairs used. There is no alignment seen between the electrodes not paired together. Most interestingly there is a mat produced spanning across the fibres going between the electrodes. This is because as the fibres are deposited and are grounded fibres inflight are then attracted to the already deposited fibres aligning across them creating the mat.

Figure 5.14 is a Darkfield microscope image showing this with more detail. The more tightly packed fibres shown as the brighter areas at the edges of the structure are the fibres aligned and bundled between the paired electrodes. The lighter area where many individual fibres can be seen is the matting between the aligned bundles. This matting is unwanted as the aim was to produce only aligned bundles of fibres between the paired electrodes.

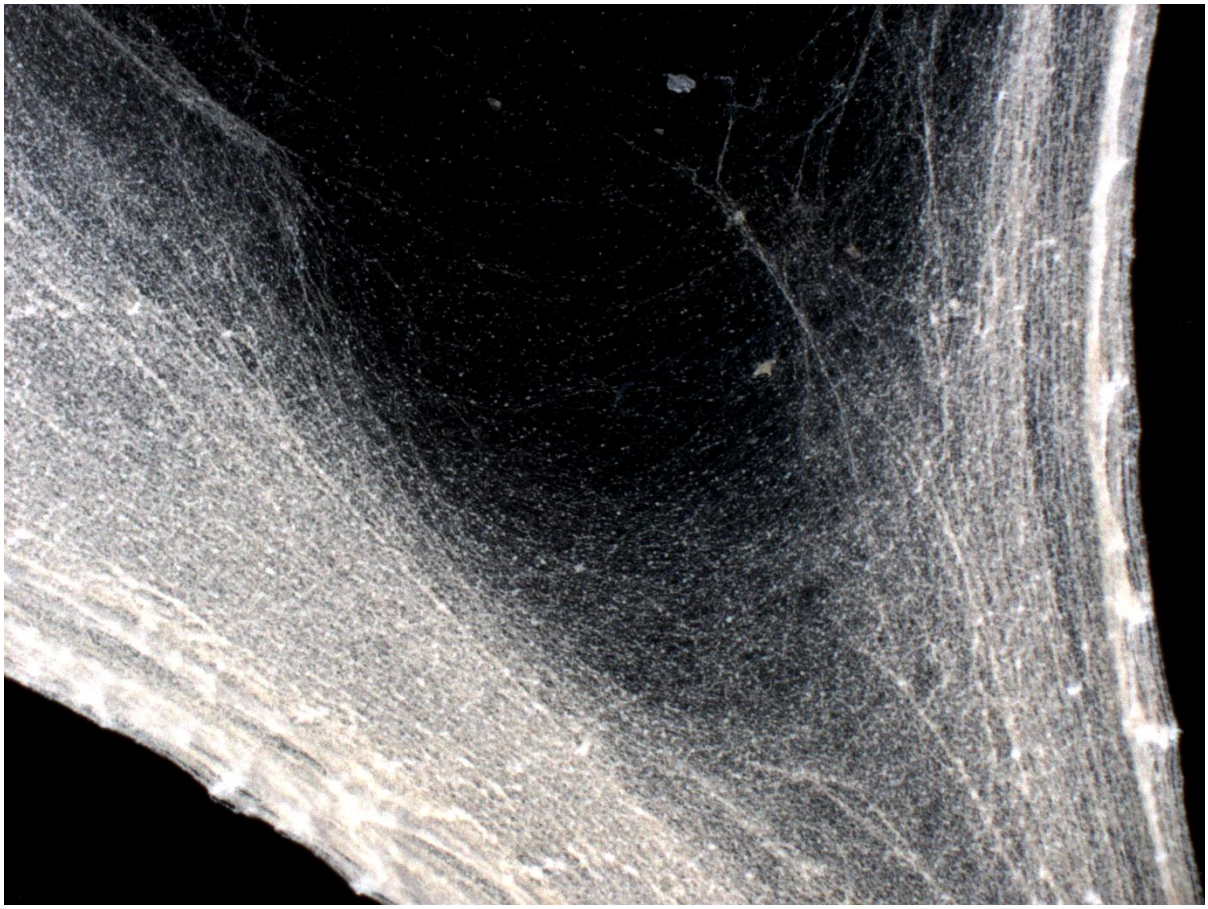

Figure 5.14 - Darkfield microscopy image of the aligned bundles with matting

From the experimentation carried out it was shown that a way to discourage fibres from aligning across the already deposited bundled fibres between electrodes was necessary to take this concept further. The technique itself was shown to work well with the high voltage relays selected being able to be used in pairs to allow selective deposition between multiple electrodes.

5.4.3.2 *Final Relay Apparatus*

The improved apparatus saw the addition of a pull up resistor network that was used to put electrodes that were not switched to ground to a positive potential voltage. This actively repels fibres and encourages deposition between only the desired grounded electrode pairs. The improved apparatus also increased the number of high voltage relays that could be used to seven.

Figure 5.15 shows the results of these improvements. Again as for the initial apparatus test shown electrodes were grounded in pairs. The image clearly shows much better alignment between the electrodes with none of the matting that was seen with the initial experimentation.

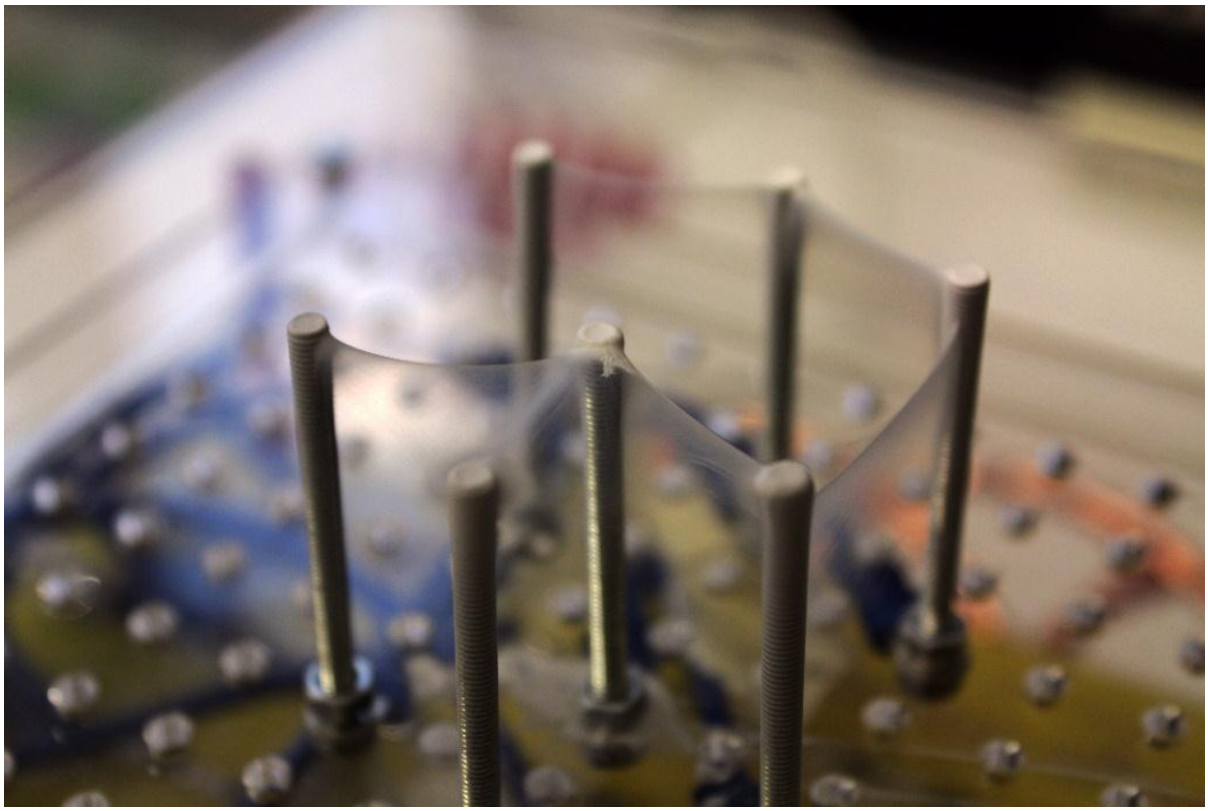

Figure 5.15 - Bundles of aligned fibres between electrodes

The apparatus was also used to investigate a different application where layers of aligned fibres could be built up with different orientation of fibre alignment on different layers. The result of one of the tests can be seen in Figure 5.16 where two pairs of electrodes were used to electrospin two layers at right angles to each other. The image shows this was successful as it can be seen that there is a clear alignment horizontally between the left and right electrode. It is less clear from this image if the bottom layer is well aligned across the top and bottom electrode.

To see if there was any alignment on the bottom layer the sample was imaged using the optical microscope in Brightfield transmission mode which is shown in figure 61.

The image does show some alignment in both horizontal and vertical orientation however it can also be seen that there are unaligned fibres present. It is also not possible to see if the aligned fibres are organised in distinct layers. However when considered in conjunction with Figure 5.17 it is likely that the alignment is organised in layers of different alignment orientation.

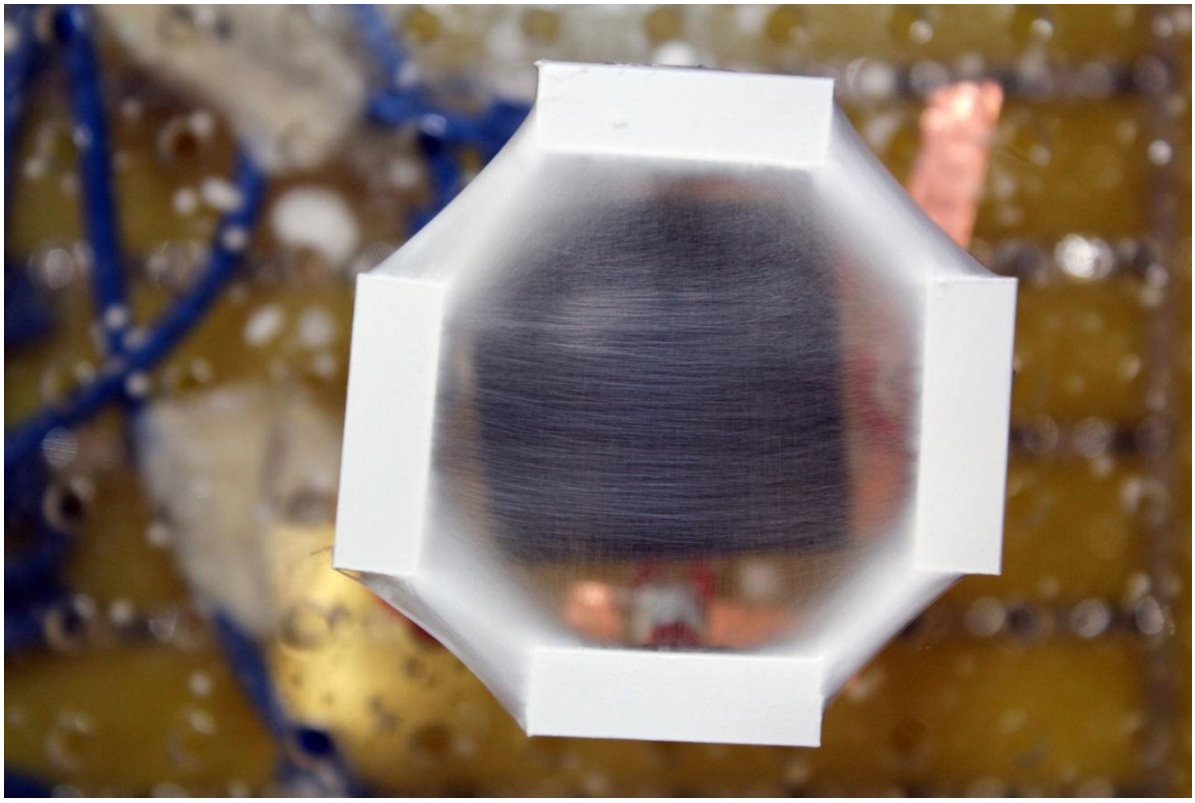

Figure 5.16 - Selectively layered aligned fibres

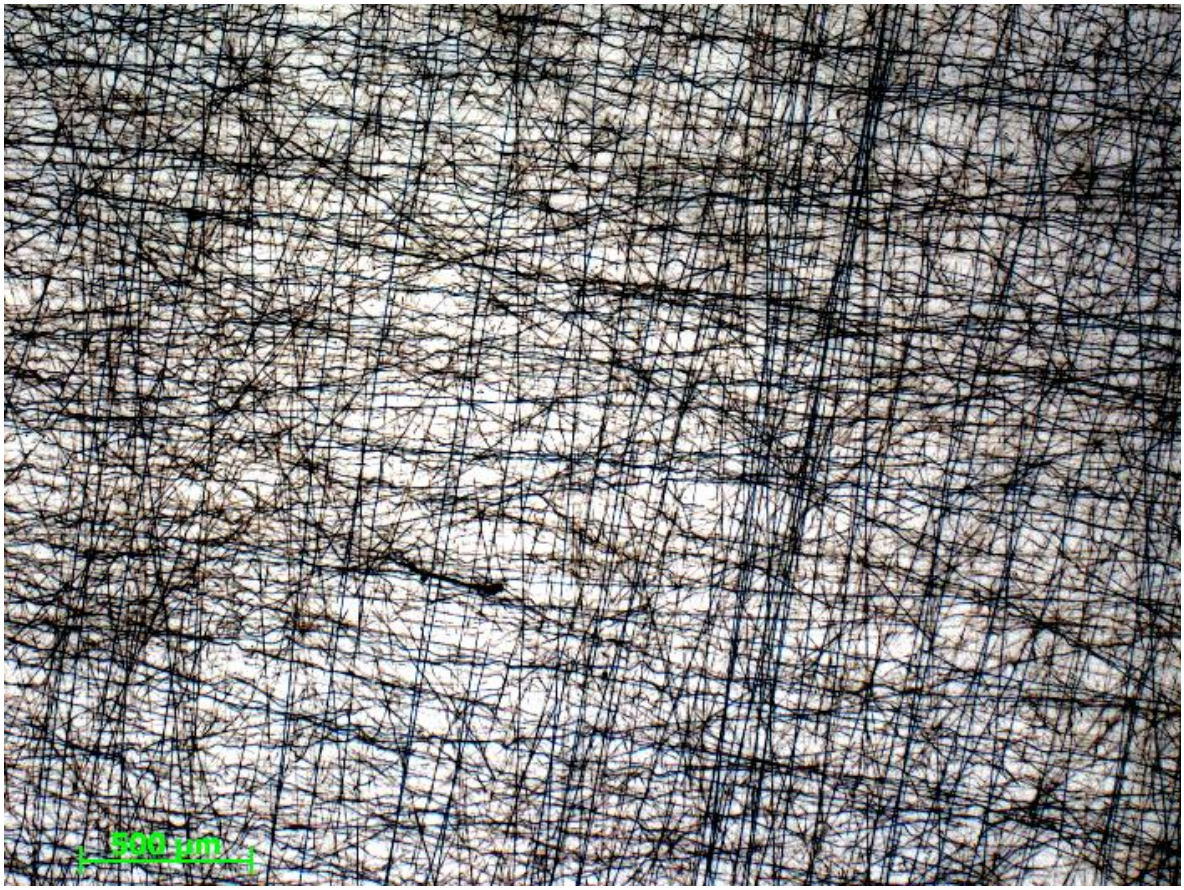

Figure 5.17 - Brightfield transmission microscopy image of multi-layered aligned fibres

5.4.4 System Evaluation and Conclusion

The final apparatus has been shown to successfully allow the production of aligned fibre layers with user selected orientation and also a method of producing bundles of fibres between multiple electrodes with the user choosing which electrodes to electrospin between. The production of aligned layers in this manner has not yet been reported in literature and the next step is to increase the number of paired electrodes and attain aligned layers at more angles since with the work carried out so far only layers with the alignment at right angles has been produced.

5.5 *Patterning Printer*

5.5.1 System Overview

The apparatus is designed as detailed in section 4.3 to allow the deposition of thin tracks of electrospun polymer to be deposited in user defined patterns. This work

was inspired by the earlier work by Bellan and Craighead [83] and Kim [84] who investigated both ways of controlling deposition using various forms of secondary electrodes and also using computer controlled stages. The apparatus designed uses both a focusing second electrode and also a computer controlled stage however the secondary electrode form is very different than the one used by Kim and other innovations have been added in the later development of the apparatus such as the use of a High voltage relay to be able to selectively turn the electrospinning jet on and off as part of the computer controlled deposition process. Being able to switch the electrospinning jet on and off in this way has not been found in the literature.

5.5.2 Initial Observations

As shown in the section 4.3.2 and also shown in Figure 4.17 the initial development of the apparatus had a conical secondary electrode. Figure 5.18 shows the intermediate version of this apparatus when the base electrode was made to move rather than the primary and secondary electrode arrays. The principle reason for the use of a conical electrode was so that whipping of the electrospinning jet would be achieved at the start of the secondary electrode and whipping would then be controlled and reduced by the time the fibre in flight reached the exit of the secondary electrode cone encouraging a smaller deposition diameter.

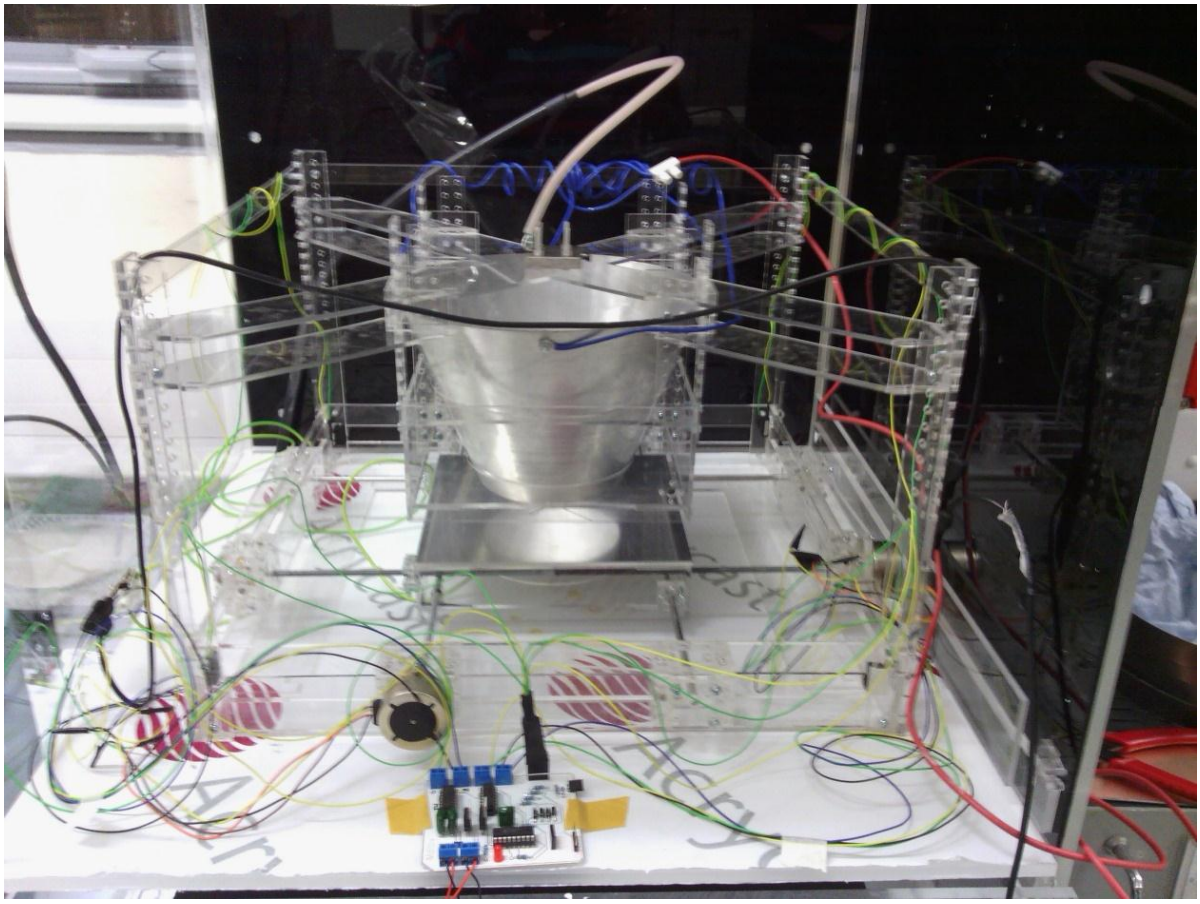

Figure 5.18 - Image of intermediate version of developed patterning apparatus

During experimentation with the apparatus an issue was found; the electrospun fibres would mainly be deposited below the center line of the cone on the base electrode as expected however a much thinner deposition of polymer fibres would also be deposited around this. Figure 5.19 shows this with a clear thick layer of PVDF polymer fibres deposited centrally, with a diameter of approximatly 10 mm and then a finer layer around this which measures approximatly 55 mm in diameter. In the image the substrate being electrospun onto is electrically conductive carbon fibre woven cloth which gives a good contrast to the white PVDF deposition allowing the fibres to be more easily seen.

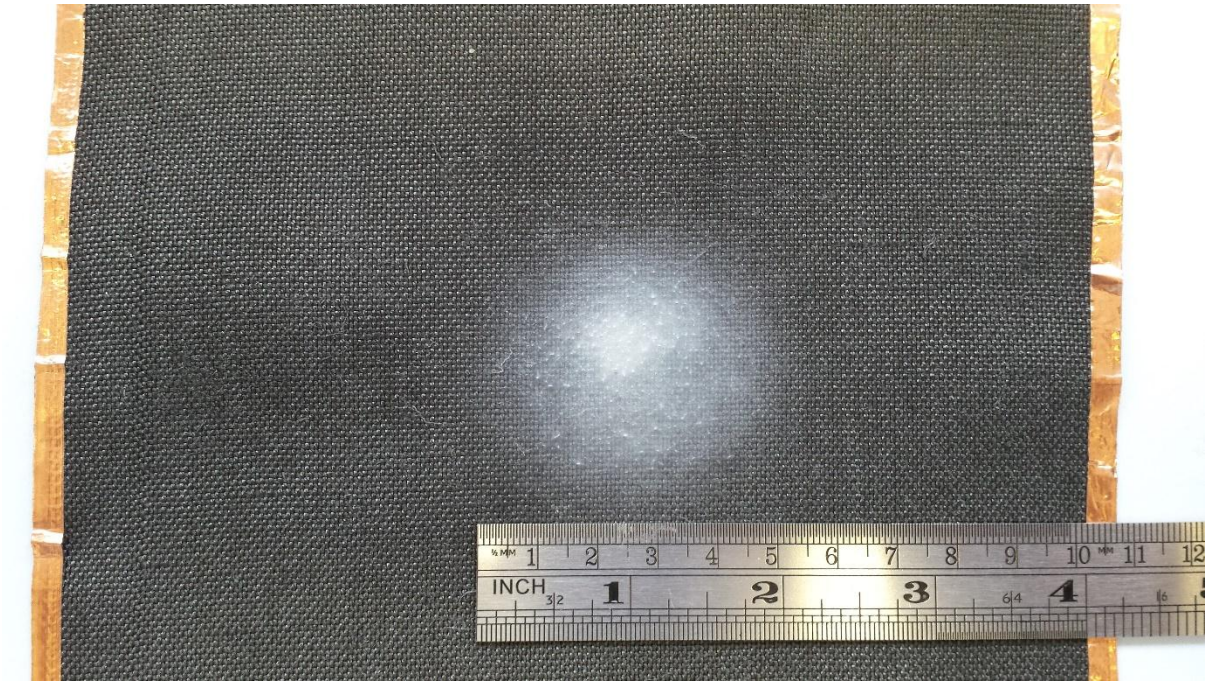

Figure 5.19 – A controlled electrospun deposition showing a thick central and a lighter outer deposit

The main reason for the observed distinct deposition areas is due to the gap between the bottom of the secondary electrode and the base electrode, this gap is necessary to prevent electrical arcing between the two electrodes. However it also is an area where the fibres in flight are no longer contained within the electric field of the secondary electrode and therefore are able to spread out creating the lighter outer deposition seen. It is also thought that a combination of the fibre in flights diameter and residual electrical charge also contributes to how far from the central main deposition area the fibres are deposited to as the fibres in flight are repelled.

The observation led to a necessary redesign of the apparatus to remove the gap between the bottom of the secondary electrode and the base electrode, this was achieved by moving the base electrode and attached moving stage up into within the confines of the secondary electrode. Due to size limitations imposed by the safety casing that the developed apparatus had to fit within, the conical shape of the secondary electrode had to be changed to a cylinder. This was so that the moving stage had a good length of travel. However the maximum travel of the base electrode and stage is reduced by two factors, the first of which is due to the stage now being constrained within the cylinders circular profile. The second reduction is due to the necessary safety distance that needs to be observed between the side of

the secondary electrode cylinder and the edges of the base electrode to prevent arcing.

The testing of the initially developed apparatus also showed some other minor operational issues. An observed issue during operation was that the stage would become jammed intermittently, with the central moving stage no longer being parallel to the track it moves along. This was caused by factors including the loose tolerance between the ball bearing slide assembly's and the track they ran on. Also the initial design did not connect the two slide assemblies on each piece of track together instead leaving them independent, leading to the ability for them to not move in tandem. These are the reasons the jamming could happen however what caused it was also related to the drive mechanism itself, where the drive pressure was on one edge of the stage, which coupled with the issues listed above caused the stage to be able to slightly rotate and then jam. The final design solves these issues by applying the driving force centrally and has guide rails at either edge of each side. The slide assemblies are also fastened together so that the whole movement system is much stiffer and combined with the guide rails the central stage cannot rotate stopping the jamming. The final design iteration is talked about in more detail in section 4.3.3.

5.5.3 Basic Characterisation

The testing of the final iteration of the apparatus showed that the approach was in fact appropriate and that patterns of deposited electrospun fibres could be achieved with a good degree of accuracy. Figure 5.20 shows a simple cross created using this apparatus. As can be seen from this image the track size is approximately 25mm, with a significantly more uniform deposition. However as can be seen the deposition graduates in thickness towards the edges of the tracks created. This over all track width was still comparable to the tracks reported by Kim of around 30 mm in width [84].

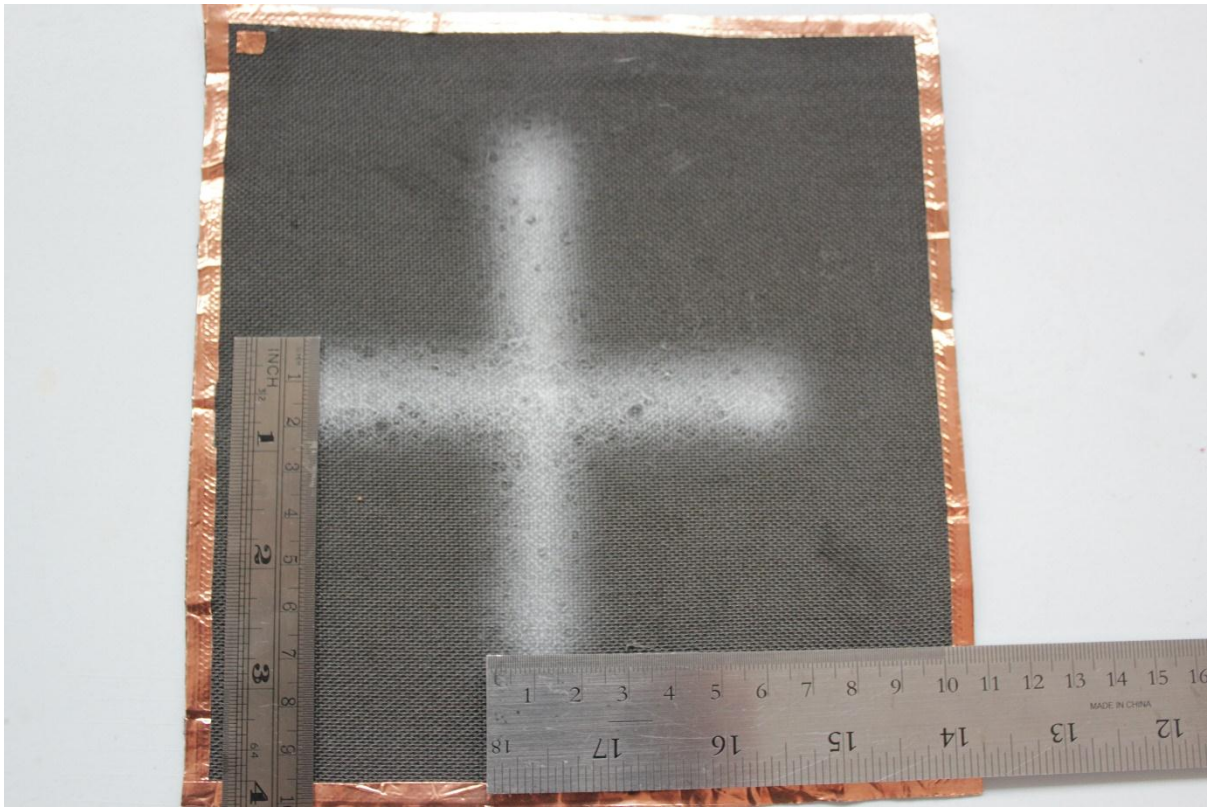

Figure 5.20 - Image of patterned deposition on carbon conductive cloth

Ideally the apparatus would be able to deposit tracks with much lower widths. A reasonable track width would be around 5 mm maximum with a small or non-existent lighter deposition around the outside of the track. To explore exactly the possible minimum deposition diameter and the corresponding lighter deposition sizes a series of experiments were completed where the relationship between the primary voltage that the polymer solution is initially charged to and the potential voltage of the secondary control electrode was investigated.

The balance between the two voltages is essential to optimise since not only a small track diameter is needed but a good consistent Taylor cone must form with a constant jet from it, as this will produce more uniform fibres and therefore depositions.

As discussed earlier a possible cause of the lighter outer deposition could be due to different diameter fibres interacting with the secondary electric field to different extents. To investigate this experiments were completed using different PVDF weights. As shown in literature the larger concentrations of polymer in

electrospinning solutions lead to larger fibre diameters [14]. Therefore by looking at the diameters of the inner and outer deposition areas it can be seen what affect the secondary electrode has on electrospun fibres in flight with different average diameters.

The standard PVDF solution was prepared (see section 3.3.2) however different PVDF weights were used of 0.3 g, 0.4 g, 0.5 g and 0.6 g. The primary voltages investigated were from 10 KV to 14 KV in 1 KV increments. The secondary electrode potential voltage was from 0.5 KV to 10 KV in 0.5 KV increments. Initially it was planned to measure both the inner deposition area and the outer deposition area however it was found in practise that defining where the inner deposition area stopped and the lighter outer deposition area started was difficult to keep consistent leading to poor measurements and an increased likelihood of bias. So the graphs included here are measurements of the total diameter of the deposited electrospun fibres.

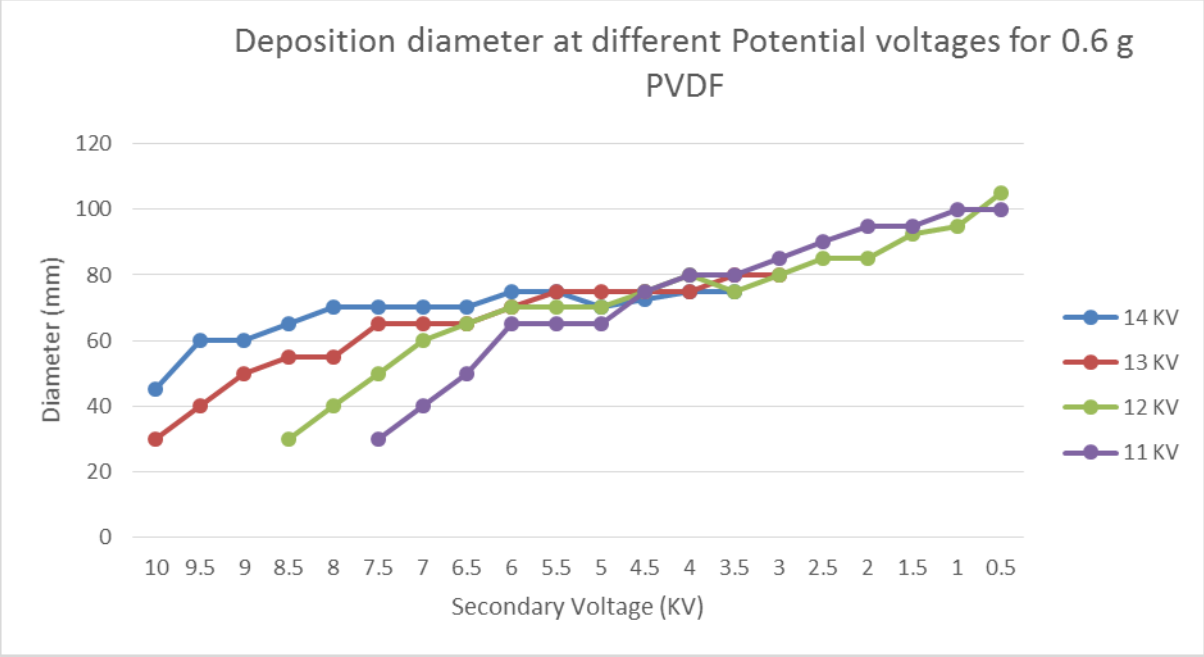

Figure 5.21 - Effect of the primary electrode voltage on deposition diameters for a solution with 0.6g PVDF

The graph shown in Figure 5.21 shows the deposition diameter when different secondary voltages are used. The four data series shown each represent a different

primary voltage. As can be seen from the graph there is a lower limit to the deposition size of approximately 25 mm. The reason that first data point for each series is staggered is that a lower primary electrode voltage means a lower secondary electrode voltage is needed before a stable Taylor cone forms during the electrospinning process. The slope of each data series is consistent with the expectation that as you decrease the voltage on of the secondary electrode then the deposition diameter increases.

This is also shown with different PVDF weights, Figure 5.22 shows the same graph but for 0.5 g of PVDF in the solvent solution, in theory the fibres produced should be thinner on average and therefor interact with the secondary electrodes electric field to a different degree. The graph shown is very similar in form to the previous with the effect on the deposition area being much more sensitive to the primary electrode voltage at higher secondary voltages. From the graph it can be seen that after a secondary electrode voltage of approximately 5.5 KV for both PVDF solutions there is little difference in deposition area using different primary voltages at each secondary voltage level.

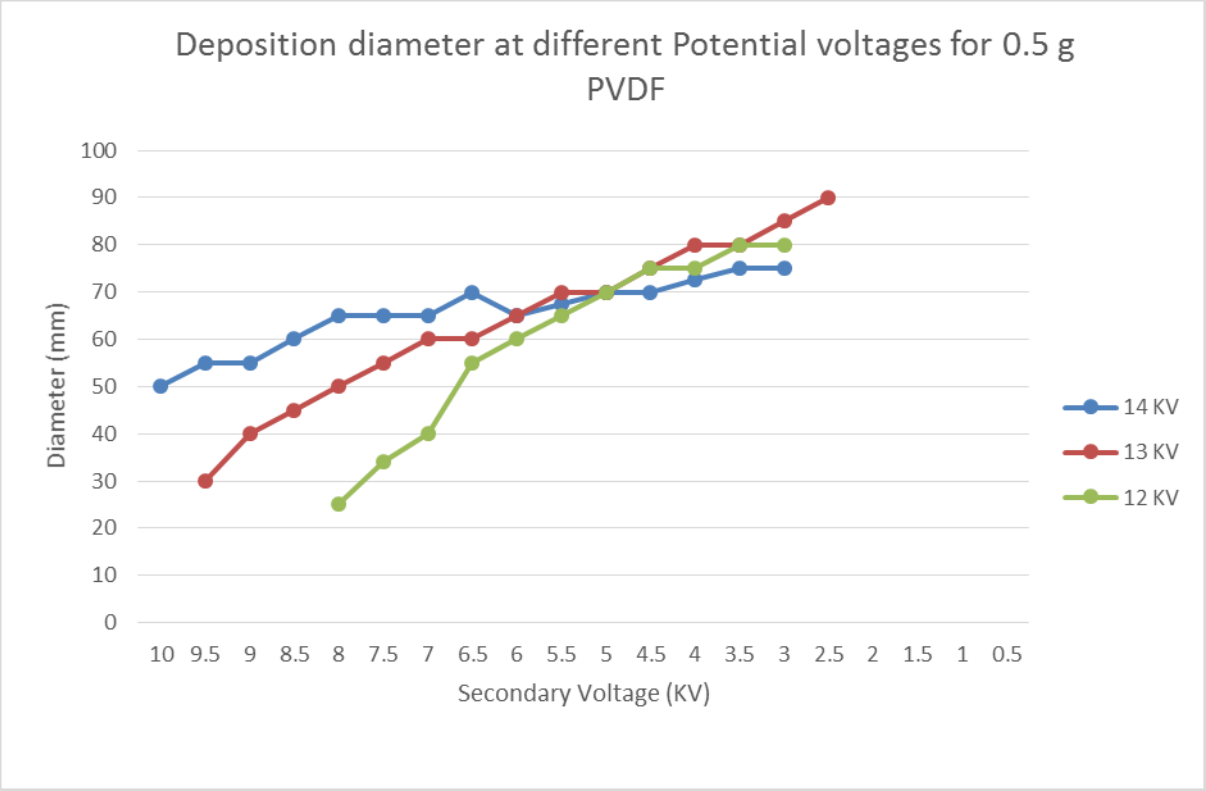

Figure 5.22 - Effect of the primary electrode voltage on deposition diameters for a solution with 0.5g PVDF

When the different PVDF weights are directly compared when electrospun with the same primary electrode voltage there does not seem to be a significant difference in the minimum deposition area. Figure 5.23 is of a graph showing a series of electrospinning samples created with a primary electrode voltage of 12 KV, with the deposition area changing at different secondary electrode potential levels. As can be seen there is no clear pattern in regards to different weights of polymer and the deposition diameters. However it is clear that for all polymer solution weights that an increase in the secondary electrode voltage creates a smaller deposition diameter of deposited polymer fibres.

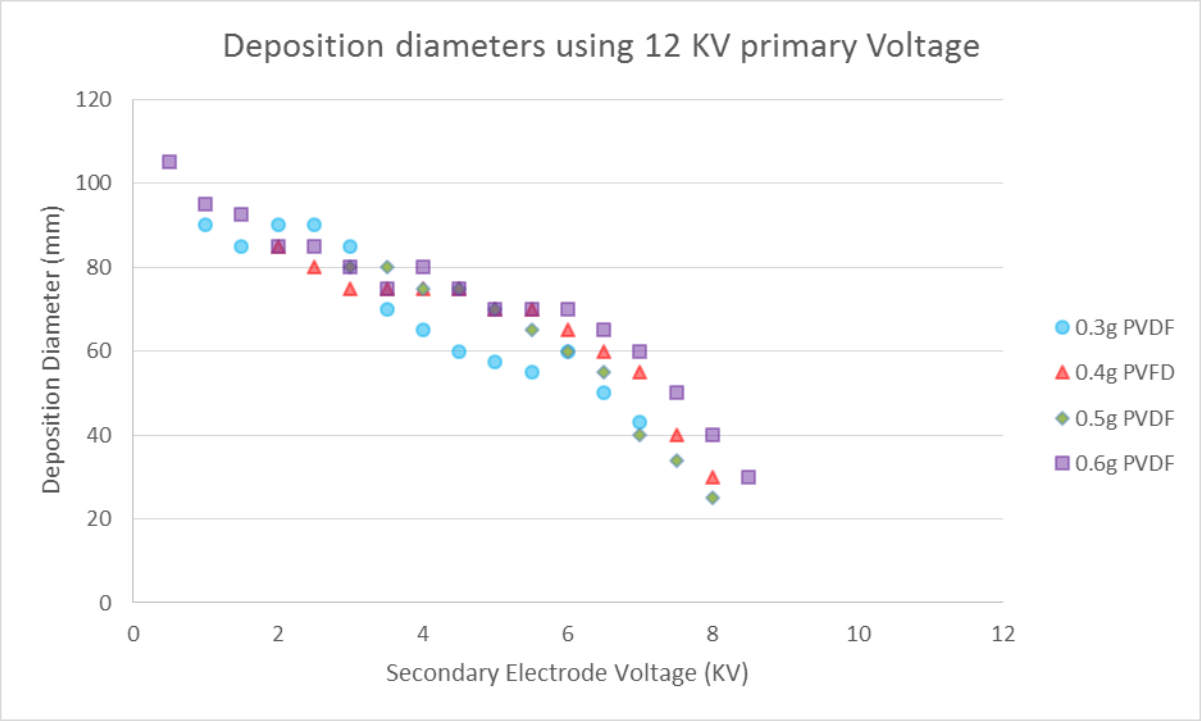

Figure 5.23 - Graph of various PVDF solutions effect on deposition diameter

These results need further investigation and expansion through repetition and analysis using SEM to obtain an average fibre diameter for different areas of the deposition. This would then allow an accurate analysis of what effect the fibre diameter of the fibres in flight have in relation to the secondary electric field and so could help determine the parameters that cause the shown outer deposition area of less thickness and the relatively thicker central deposition. Ultimately it is important for the further development of this apparatus to remove this outer deposition area to allow the creation of tracks of uniform thickness that could then be built up more into three dimensional structures.

5.5.4 System Evaluation and Conclusion

The experiments described in this section have shown that the designed apparatus behaves as was expected with the ability to lay down tracks of polymer in various patterns by electrospinning. With different track widths being achieved by changing the potential voltage of the secondary electrode. The addition of the high voltage relay to allow the control of the electrospinning jet, turning the electrospinning

process on and off using preprogramed timing to allow greater control of the deposition and patterning process was also successful. However the approach used still needs further refinement, the smallest track width were found to be around 25 mm with the apparatus developed. This allows shapes to be patterned successfully however it would be beneficial to be able to produce much smaller diameter tracks that are also free from the lighter deposition observed around the edges of the current deposited tracks. Smaller tracks would allow the development of microelectromechanical systems (MEMS) using polymers such as PVDF due to its piezoelectric properties when electrospun.

The measurement method used to determine the deposition diameter needs changing as it is prone to observational error and parallax errors when measured using a rule. A way to reduce the effect of this would be to repeat the experiments multiple times to obtain average values however this is difficult in this case due to the amount of time needed to create a single data set due to having to clean and then set up the electrospinning apparatus each time for each single data point.

To further expand the apparatus other configurations of electrodes would be first simulated using finite element analysis (Comsol) and then tested to try to achieve smaller diameter deposition areas. Once achieved fine deposited tracks could be built up to produce a larger thickness and potentially three dimensional structures. The process could also be expanded utilising multiple high voltage relays controlling multiple electrospinning jets that would then allow multiple polymers to be deposited during a single electrospinning session allowing the production of composite three dimensional structures.

5.6 *Fibre system*

5.6.1 System Overview

Creating electrospun fibre bundles and core-shell fibres by various techniques has been investigated by other groups as discussed. A different method of core-shell fibre production is investigated in the following sections along with a complimentary system that weaves an outer coating over the core-shell fibres. This outer weave allows the development of three layer piezoelectric fibres to be used as sensors or

energy harvesting devices. With the multilayer devices consisting of a central core electrode, an outer piezoelectric electrospun layer and a woven outer electrode.

5.6.2 Initial Experimentation

Initial experimentation was carried out to coat short lengths of conductive wires with PVDF. Different materials and different diameters were used for the core wire and after they had been produced electrodes were added to create a three layered device. These were then tested to show that the devices created exhibit the piezoelectric effect. This was important to show to give validation for the approach before more advanced experimental apparatus was developed.

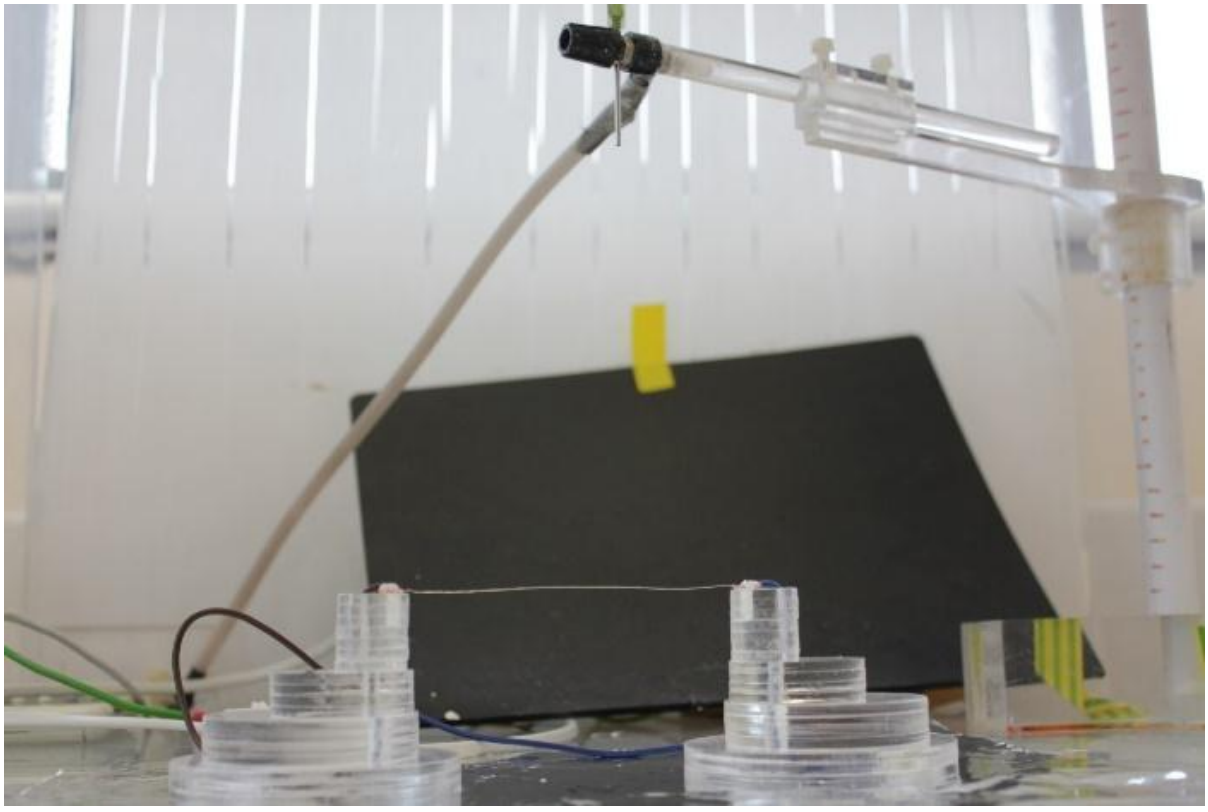

Figure 5.24 - Electrospinning directly onto a wire

The materials used for the wires were aluminium wire, conductive cotton containing silver strands and carbon fibre. All wires were suspended between two posts as shown in Figure 5.24. Each end of the fibre was attached to the high voltage power

supply’s ground connection turning the fibre into the base electrode for the electrospinning process. This limited the choice of materials to those which are conductive however this was beneficial since the developed piezoelectric devices would need an internal electrode for collecting the charge the device generates under strain. The standard PVDF electrospinning technique and solution as shown in section 3.3 was used for all experimentation. The length of the depostion area was 100 mm to 120mm in length.

Fibres were investigated under an optical microscope to look at uniformity in thickness and covering. Figure 5.25 shows one of the coated aluminium core shell fibres with no magnification where it can be seen that one of the main issues with the approach is that the maximum depth of deposition is in the centre of the suspended fibre and the thickness then gets less towards the end of the central core wire.

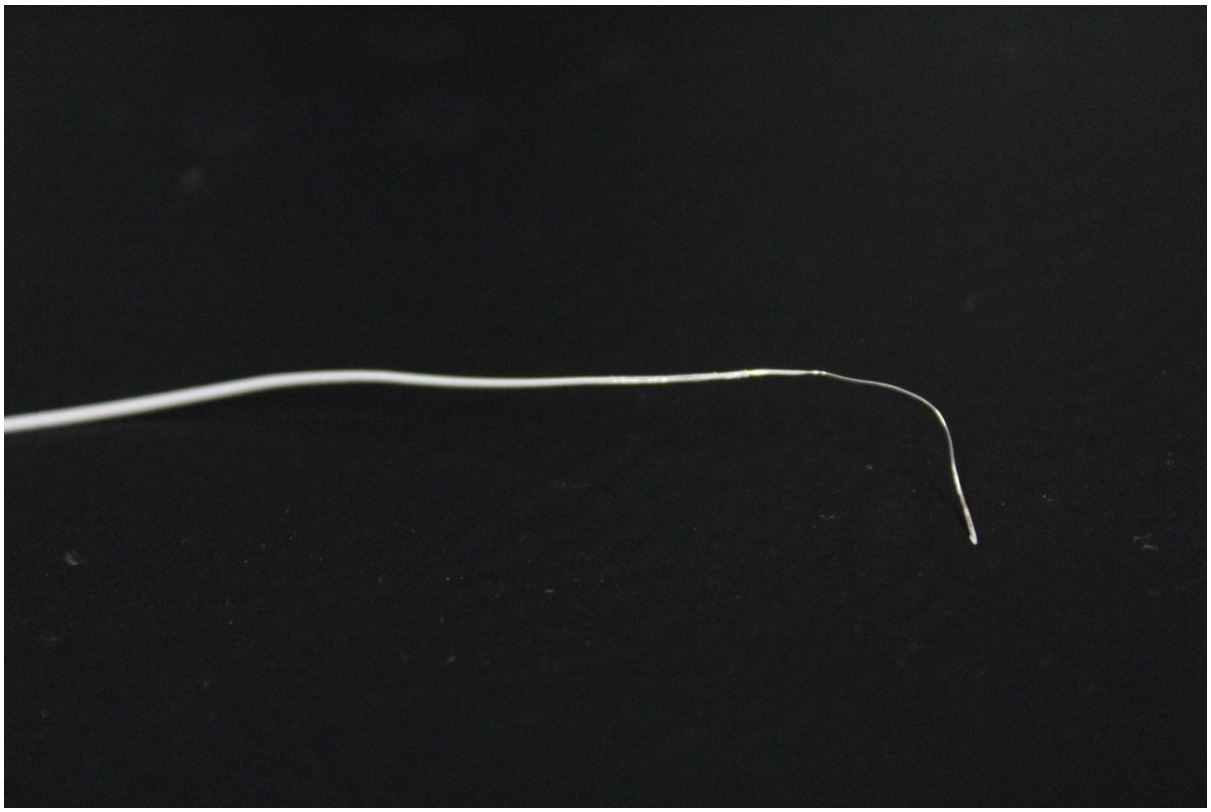

Figure 5.25 - Produced core-shell fibre with the polymer layer thickness decreasing from the left

All the types of fibres were coated cleanly and relatively evenly; this could best be seen on the conductive cotton thread where the PVDF layer followed the twisted contours of the thread as shown in Figure 5.26. There were little or no visible strands or bundles of PVDF attached to the core material and few irregularities in the surface morphology on the microscopy images. The detritus seen on the image in Figure 5.26 is due to the sample being put down on an unclean surface. The residual electrostatic charge and the fibrous structure of the surface of the samples mean they are prone to catch dirt and small particles they come into contact with.

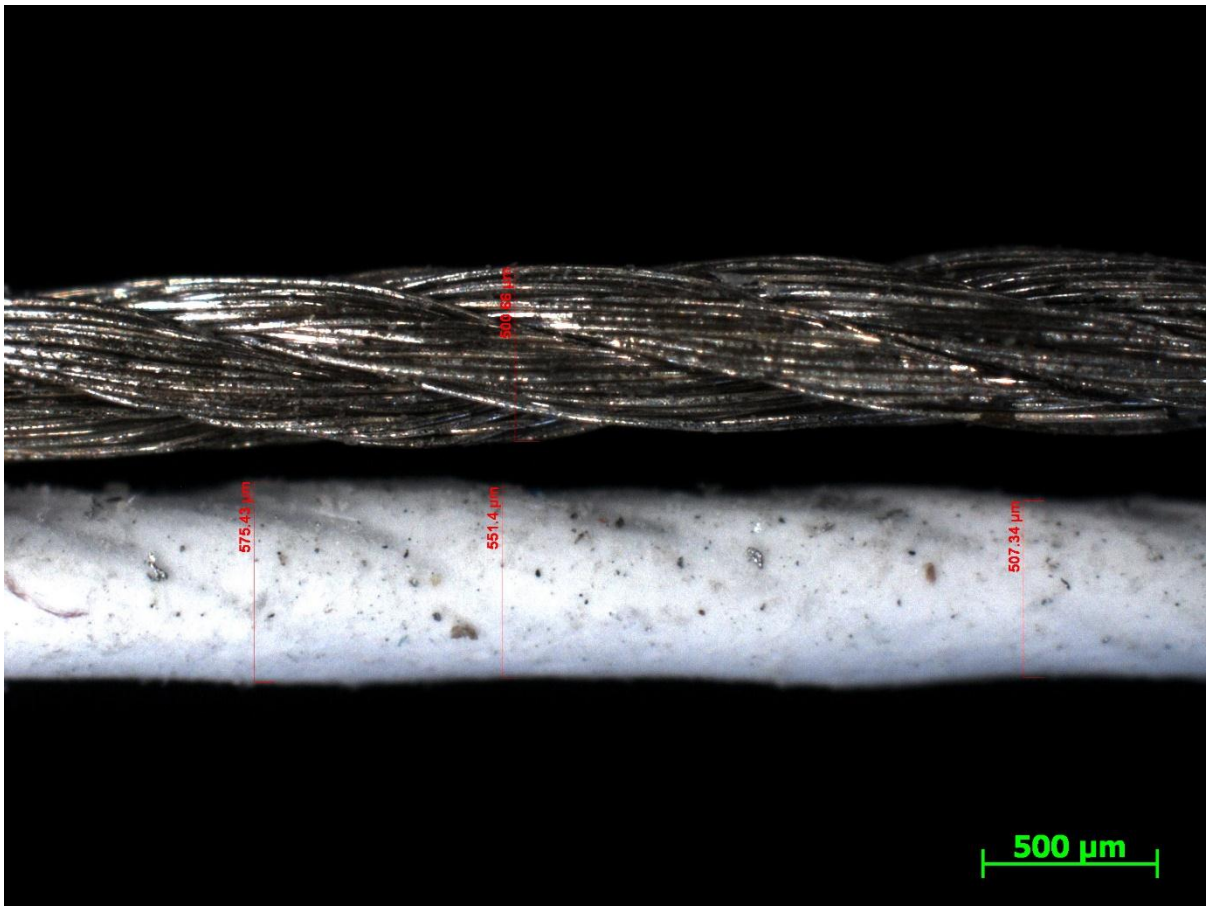

Figure 5.26 - Core-shell fibre produced with conductive thread

The core shell fibres were cut in half to a length of around 50 mm and the cut end was sealed using epoxy resin. This then allowed the core shell fibre to be dip coated in conductive silver paint to create an outer electrode. An area of PVDF coating was left showing to make sure that there was no short circuit between the conductive core fibre and the outer painted silver electrode. A single filament copper wire was

also attached to the painted silver coating at the end sealed with the epoxy resin. This allowed attachment of the outer electrode to the oscilloscope being used to test the device.

The coating process worked as expected however there was issues with the thickness of the PVDF on some of the samples being too low, which meant that the devices short circuited because the outer painted coating short circuit through the thin PVDF layer with the central core which made the devices non-responsive during testing. Another issue found was that the carbon fibre samples were prone to break due to the materials inherent low flexibility.

The surviving samples were tested for piezoelectric response by attaching the exposed end of the core wire to the ground connection of an oscilloscopes probe. The other connection from the oscilloscope was made to the wire attached the bottom of the painted outer electrode. The device was fastened in a cantilever format with one end fixed and the rest of the device hanging down vertically. The free end of the device was then excited by striking using a non-metallic rod and allowed to oscillate freely. The electrical output of the device was collected by the oscilloscope. A sample trace is shown in Figure 5.27, clearly showing a response significantly greater than the noise on each strike. A maximum voltage response between 10mv and 40 mv was achieved for the samples tested.

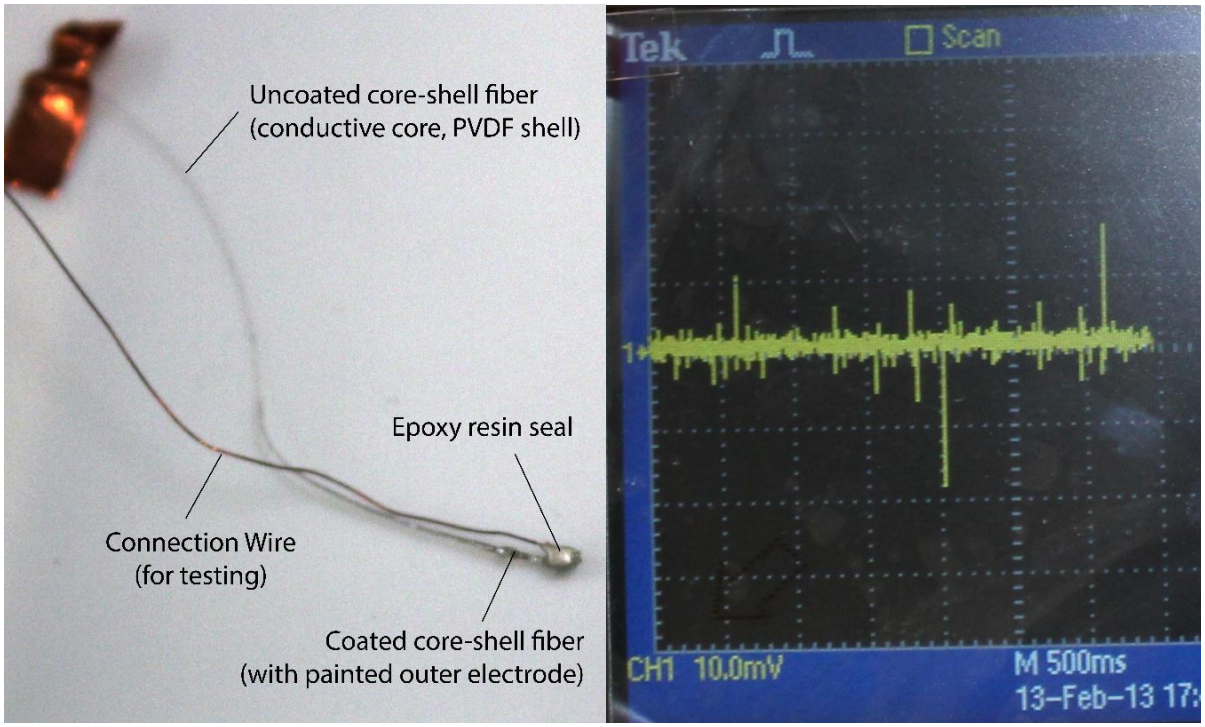

Figure 5.27 - Left image produced three layer device. Right image shows voltage response during testing.

From this very basic experimentation it showed that the fibres developed were piezoelectric; more importantly it showed the limitations of the materials and the processes that had been tried which greatly helped inform the decisions made when developing the apparatus tested in the following sections. The limitations from an electrospinning view point were that the fibres were not of a uniform thickness, as more material was deposited in the centre directly below the electrospinning needle than towards the ends of the conductive core. Also a relatively thick PVDF layer is needed so that the produced core-shell fibres could be handled and undergo post processing, this translates to a longer electrospinning experimentation time.

The dip coated painted outer electrodes that were added to the electrospun core-shell fibres were undesirable as they were of an uneven thickness as can be seen in Figure 5.27. They also added rigidity to the core shell fibre which reduces the flexibility which the PVDF naturally has. Ideally the piezoelectric layer should be mechanically matched with electrodes that have similar material properties so the electrodes don't dampen the piezoelectric materials ability to oscillate and move

freely. The painted surface was also brittle which will have contributed to the fast failure rate of the produced devices. Most devices didn't last more than five tests before a short circuit occurred between the outer painted electrode and the internal conductive core.

5.6.3 Developed Electrospinning Apparatus Tests

5.6.3.1 *Initial Coating Apparatus*

The initial coating apparatus was developed to solve some of the issues identified during the initial experimentation. The conductive core wire could be coated in longer lengths as the process was made reel to reel. On one reel a large length of conductive wire was wound and this wire was then drawn through the electrospinning deposition area and the resulting PVDF coated core-shell fibre was collected on the opposite reel. This made experimentation easier by reducing the set up time and allowing multiple samples to be created without having to reset the equipment.

The downside to using a reel to reel solution was that the core materials had to be flexible enough to be spooled onto the reel. It was found that the Carbon fibre strands used in the initial experimentation was too brittle and therefore were no longer used. Also using this system put a limit on the minimum and maximum diameters of core wire that could be used. By design the central core wire was put under strain to tension it as it was drawn across from reel to reel. Small diameter wires such as 100 µm silver wire that was tested couldn't be used as the strain put on the wire was greater than its ultimate tensile strength and so the wires always failed. This strain was the limiting factor that determined the minimum diameter of material that could be used. The maximum diameter wire that could be used was also dependant on material and was determined by its flexibility, in general the thicker the wire the less flexible it is so once a wire isn't malleable enough to be wrapped onto one of the reels it cannot be used.

Using a reel to reel process made the coating more uniform along the majority of the core-shell fibre because all parts of the core wire went through the middle section of the electrospinning deposition area where the fibre deposition is greatest. Only the

first and last 100 mm of the coated core-shell fibre exhibit the gradual reduction in thickness that could be seen in the initial experimentation with a stationary core wire.

The thickness of the electrospun PVDF layer was controlled in the same manner as conventional electrospinning by adjusting the deposition time, for the drawn core wire this translated into adjusting the feed rate with the lower speed creating a thicker PVDF layer.

Experimentation was done to investigate the feed rate and deposition thickness relationship. During the investigation into feed rates it was found that the core-shell fibres layering were not concentric. It could be visibly seen under optical microscope that even though some of the PVDF fibres in flight were attracted to the bottom of the wire the majority were deposited on the top and sides. Figure 5.28 shows this quite clearly with the central aluminium core wire visible down the centre of the core-shell fibre.

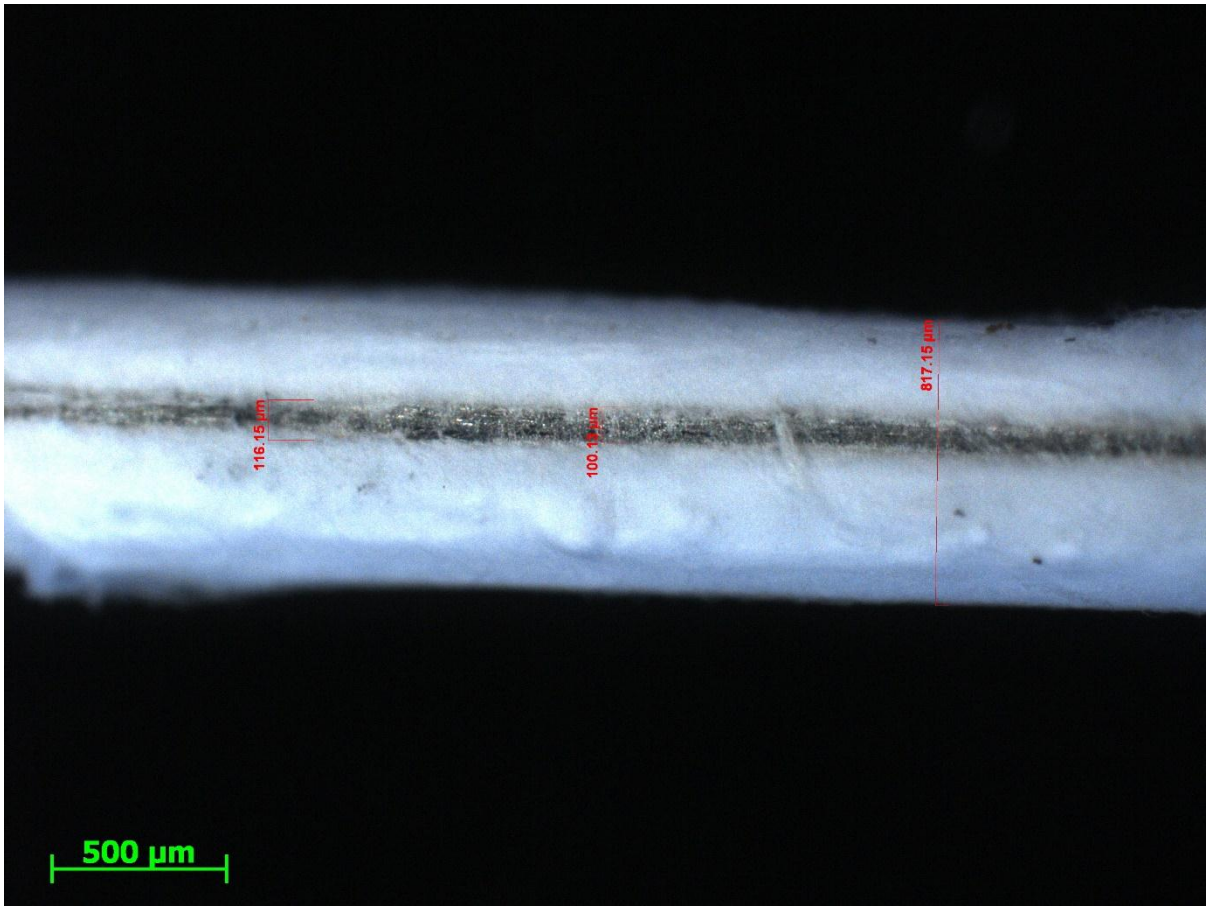

Figure 5.28 - Visible gap on the underside of a core-shell fibre

It is thought that this issue was not identified on the initial experimentation with stationary central cores due to the long experimentation times used for electrospinning and the thinner core wires used. Where the whole central core fibre appeared to be coated concentrically there would have been a thin area with a minimal coating of electrospun PVDF fibres. This would have also contributed to the large failure rate of the devices produced. The finding of this necessitated a full redesign of the apparatus developed.

5.6.3.2 *Final Coating Apparatus*

5.6.3.2.1 *Introduction*

The final apparatus design was by necessity mechanically complex as the central core wire that was to be coated needed to be drawn across the electrospinning deposition area and also rotated at the same time to ensure an even coating of PVDF fibres, as shown in section 4.4.2.3. The following sections give a more in-depth characterisation of the core shell fibres created using this novel approach. Concentricity of the fibre deposition and the uniformity of deposition along the axis of the core wire was investigated.

5.6.3.2.2 *Concentricity Results*

The concentricity of the produced core-shell fibres at different rotational velocities was investigated. Table 5 shows that the standard deviation does decrease as the rotational velocity gets higher with a difference of 11 µm between samples produced with no rotational velocity and those produced at 48 rpm. This suggests that the core-shell fibres produced at 48 rpm are more concentric than those at the lower rotational velocities. Also as can been seen from the table the samples produced at 36, 24 and 12 rpm all have a smaller standard deviation than samples produced at 0 rpm however there is not a clear relationship as there is not a consecutive decrease as the rotational velocity increases.

Rotational velocity (rpm)	Layer thickness Range (µm)	Mean layer thickness (µm)	Median (µm)	Standard Deviation (µm)
48	163.863	131.645	124.715	31.550

36	180.559	119.787	121.641	36.761
24	184.301	141.267	142.800	33.923
12	247.600	126.973	129.187	37.036
0	168.896	138.201	150.014	42.514

Table 5 - comparison of different angular velocities and the effect on concentricity

The experiment was repeated using the 230 µm core wire, with only two rotational velocities of 0 rpm and 48 rpm. Table 6a shows the results for the core-shell fibre with no rotation. There is a large range in the standard deviation however it shows a 29.80 µm variation from the average. When compared to the results shown in Table 6b for the core-shall sample produced at 48 rpm there is a reduced average standard deviation of 13.48 µm. The standard deviation range is also much lower for the core-shell sample rotated at 48 rpm, from 7.53 µm to 23.66 µm compared to between 15.09 µm to 71.52 µm for the sample with no rotation. This clearly shows that the polymer coating around the central core wire at 48 rpm is much more evenly coated than if there is no rotation at all. This can also be seen in Figure 6.28 - a. Sample produced with no rotation b. Sample produced at 48 rpm

b which shows images of the sectioned core-shell fibres.

The core-shell samples produced at 48 rpm as shown in Figure 6.28 - a. Sample produced with no rotation b. Sample produced at 48 rpm

a, have two distinct bulges on opposite sides of the core wire which is likely due to the fact that the deposition area is much wider than the diameter of the core wire so the fibres in air are attracted to the edge of the core. Some fibres whip around the bottom of the core wire which is why there is still deposition on the bottom of the core wire. The white areas that can be seen within the polymer layer on the images shown are where the resin used for sectioning has not fully penetrated the polymer layer.

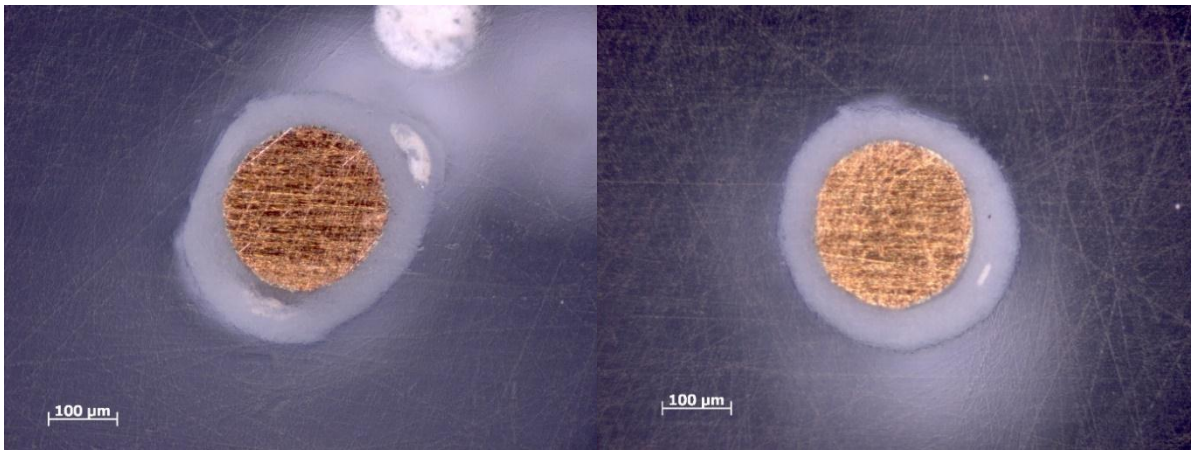

Figure 6.28 - a. Sample produced with no rotation b. Sample produced at 48 rpm

a. 0 rpm Results

Sample no.	Range	Mean	St Dev
1	69.515	68.952	20.557
2	69.921	73.907	26.346
3	106.493	89.666	38.767
4	52.277	64.901	18.373
5	47.355	61.355	15.163
6	62.860	81.547	21.604
7	73.450	61.493	24.037
8	71.483	90.047	24.902
9	55.700	89.218	22.604
10	171.300	86.829	58.661
11	192.398	107.966	71.515
12	50.089	61.331	15.086
Averaged	**85.237**	**78.101**	**29.801**

b. 48 rpm

Sample no.	Range	Mean	St Dev
1	35.626	59.393	14.318
2	33.986	64.191	11.921
3	26.190	59.113	8.048
4	26.770	54.841	7.883
5	23.979	54.953	7.533
6	33.993	62.864	11.010
7	71.039	65.577	23.659
8	43.919	62.177	14.640
9	59.228	70.889	22.350
10	42.800	67.240	14.423
11	54.881	57.067	16.777
12	26.759	58.766	9.146
Averaged	**39.931**	**61.423**	**13.476**

Table 6 - a. 0 rpm - Samples produced with no angular velocity b. 48 rpm - Samples produced with angular velocity of 48 rpm

5.6.3.2.3 *Average Deposition thickness*

The average polymer thickness was investigated at different linear velocities ranging from 0.02 mm/s to 2.0 mm/s for the core wire thickness of 230 µm. Another set of experiments were completed with a core wire of 700 µm with a linear velocity range from 0.1 mm/s to 2.5 mm/s. The thickness of the polymer layer was calculated by taking multiple measurements of the overall diameter of the core-shell fibres and

then subtracting the core wire diameter and dividing by two. Results from both sets of experiments show a clear trend.

Figure 5.30 shows the results of the experiment for the 230 µm core wire. The trend here is very clearly fitting to a power trend line. As expected as the linear velocity is decreased the polymer layer thickness increases. The thickness builds slowly at the higher linear velocities going from 36 µm at 2.0 mm/s to 93 µm at 0.4 mm/s. The deposited thickness is much greater as you reduce the speed by a factor of 10, at 0.04 mm/s the deposition thickness is at 242 µm.

The graph shown in Figure 5.30 also shows results from the same experiment as above with a central core wire of 700 µm. The linear velocity range was from 2.5 mm/s to 0.1 mm/s. Again the thickness increases slowly at first, and then at lower velocities the deposition thickness is much greater. The trend is not as clear as for the experiment using a 230 µm core wire, however is does fit a power trend line. Also due to the thicker central core wire the polymer layer deposited at lower linear velocities is less than for the 230 µm core wire. At 0.1 mm/s the thickness on the 230 µm core wire is 189 µm and at the same linear velocity on the 700 µm core wire the polymer layer thickness is 116 µm. This is because there is a relatively much bigger surface area to cover on the thicker central core wire.

This shows that any thickness of polymer can be deposited from a few tens of microns to over 100 microns on the two core wire diameters tested. This gives a large range of options for creating core-shell fibres for different applications and with potentially different polymers. However it becomes less practical to coat the core wires at lower linear velocities due to the total amount of time it takes to coat long lengths of core wires. As can be seen in the next section there is also problems with uniformity over longer lengths at lower linear velocities.

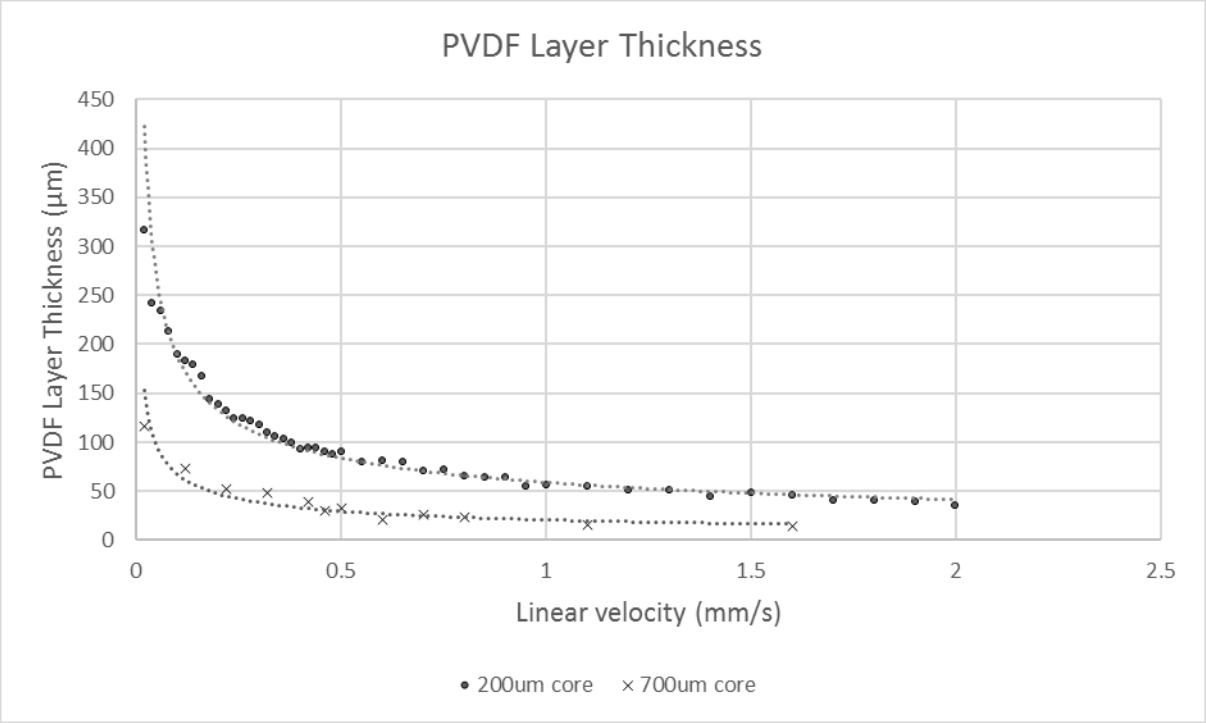

Figure 5.30 -Increasing layer thickness as linear velocity decreases for two diameters of central core.

5.6.3.2.4 *Uniformity along length*

The diameter measurements also allowed the uniformity of the deposition to be measured. The measurements to get the average polymer layer thickness at different linear velocities were taken across a minimum sample length of 60mm. The standard deviation of the measured diameters is a good indication of the uniformity along the 60mm length of sample. Figure 5.31 shows the standard deviation for the averaged diameters with a linear velocity range of 0.02 mm/s to 2.5 mm/s using a 230 µm central core wire.

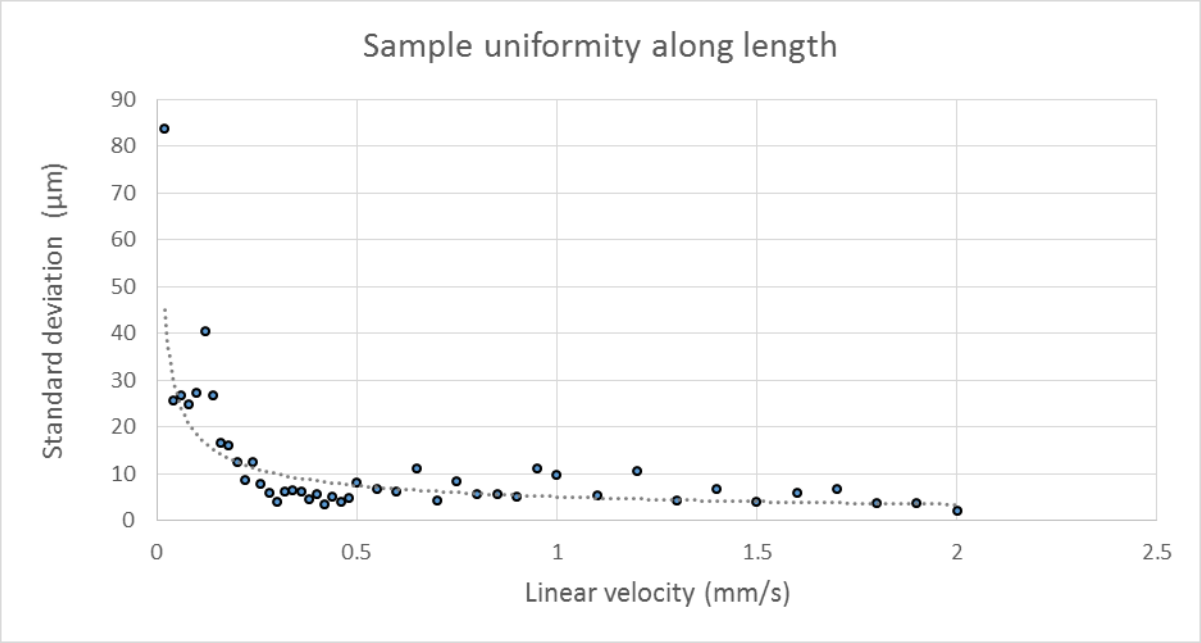

Figure 5.31 - Graph showing the uniformity of sample over a sample length of 60 mm and above.

The standard deviation is below 10 µm for nearly all linear velocities between 2.5 mm/s down to 0.3 mm/s however after this the standard deviation does get gradually greater. The greater the standard deviation the greater the variation in diameters measured and therefore the samples are less uniform along their lengths.

5.6.3.2.5 *General Surface Morphology*

Figure 5.32a and Figure 5.32b shows microscope images at different linear feed rates: 2.0 mm/s and 0.2 mm/s. It is observed that at the higher linear feed rates as shown with the 2.0 mm/s microscope image Figure 5.32a the surface is made up of a uniform polymer coating with regular but randomly distributed areas of polymer build up giving the core-shell fibre a granular texture. These features gradually decrease in number and apparent size as the linear speed decreases and the core-shell fibre diameters get greater.

The theory is that the cause of the polymer build up at higher feed rates is due to the charged nature of the fibres being initially attracted to one spot on the conductive core wire due to small irregularities in the electric field. The polymer fibre in flight then has momentum towards that area creating a build up at that point. This is then

magnified as the electric charge on the polymer fibre dissipates to ground through the conductive core and so then there is a point on the core-shell fibre that is physically higher than the rest of the coating. The fibre then continues to be attracted to that same point because it affects the electric field and forms the shortest physical route for the fibre in flight to travel. Due to the relatively high speed of the feed rate and the angular rotation this spot deposition happens at spaced intervals as the highest area created moves and ceases to be the shortest route for the fibre in flight to be attracted to, giving the uneven morphology result shown in Figure 5.32a.

At lower linear velocities as shown in Figure 5.32b the core-shell fibre morphology is much more uniform, there can be seen some slightly raised areas however they are much fewer and appear smaller in size. This is a trend for all the samples produced with a lower liner velocity right up to 0.02 mm/s. The cause of this is due to the changing electrostatic field as the insulating polymer layer grows in thickness. The insulating properties of the polymer deter spot deposition after a certain depth of polymer has been deposited and so the fibre in flight then becomes attracted to a bare or less covered area on the central core. Therefore a slow feed rate creates a more uniform coating of polymer fibres.

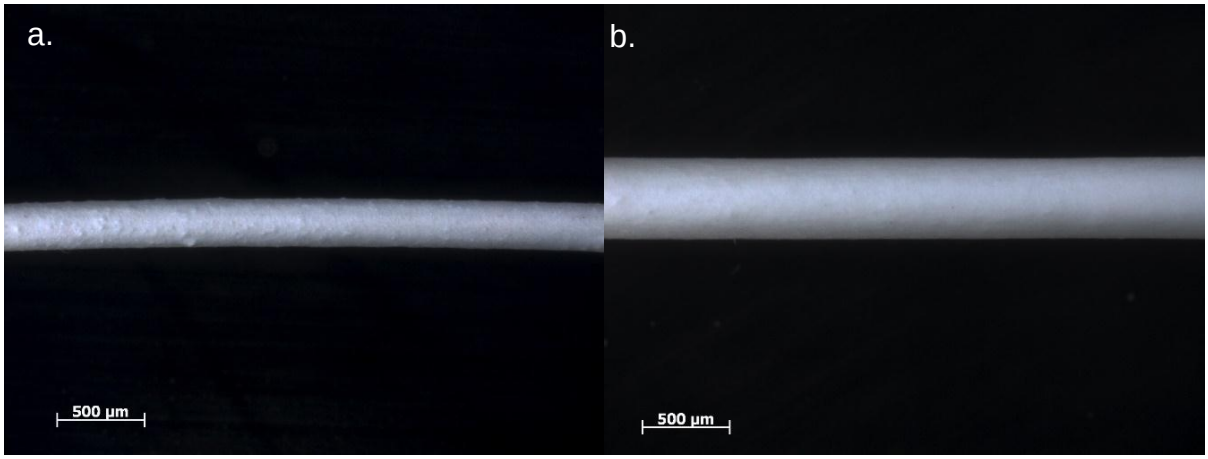

Figure 5.32 - a. Sample produced with 2.0 mm/s linear velocity showing granular texture.

b. A sample produced at a linear velocity of 0.2 mm/s exhibiting a smooth surface morphology.

5.6.3.2.6 *Deposited Fibre Micro Morphology*

The effect of the rotational velocity was investigated using SEM to image the fibrous structure of the deposited PVDF electrospun layer. To make the different images comparable the feed rate, core material and core diameter was kept constant for all samples.

On examination it was found that the rotational velocity introduced an alignment of the electrospun PVDF fibres along the axis of the core fibre and that the degree of rotational velocity affected the order of magnitude of this alignment. Experimentation was completed with rotational velocities of 12, 24, 36, 48 rpm and then multiple SEM images were taken of the produced core-shell fibres. The samples for each different rotational velocity were produced by randomly cutting multiple short lengths (10 - 20 mm) from the longer core-shell fibres and mounting these onto the SEM mounts using carbon tape. During the mounting process it was ensured that the surface to be imaged did not come into contact with any other surfaces to ensure that the surface morphology is not disturbed and that the samples were not contaminated.

Figure 5.33a shows an SEM image of a sample that was rotated at 12 rpm during electrospinning. There is no discernible orientation which was the case with the other images taken for this rotational velocity. At 24 rpm shown in Figure 5.33b there is a clear orientation of the fibres along the length of the sample imaged. Again this orientation was seen on the other images taken by SEM for this rotational velocity. The samples created at 36rpm and imaged showed some alignment but it was very limited and inconclusive as to if the electrospun fibres were aligning at this rotational velocity, a sample image is shown in Figure 5.33c. It is clearer with the 48 rpm samples as all images showed clear fibre alignment however not to the same magnitude as the alignment at 24 rpm. Figure 5.33d shows this rotational velocity's alignment and it can be clearly seen when compared to the 24 rpm sample image directly above the difference in magnitude of the fibre alignment.

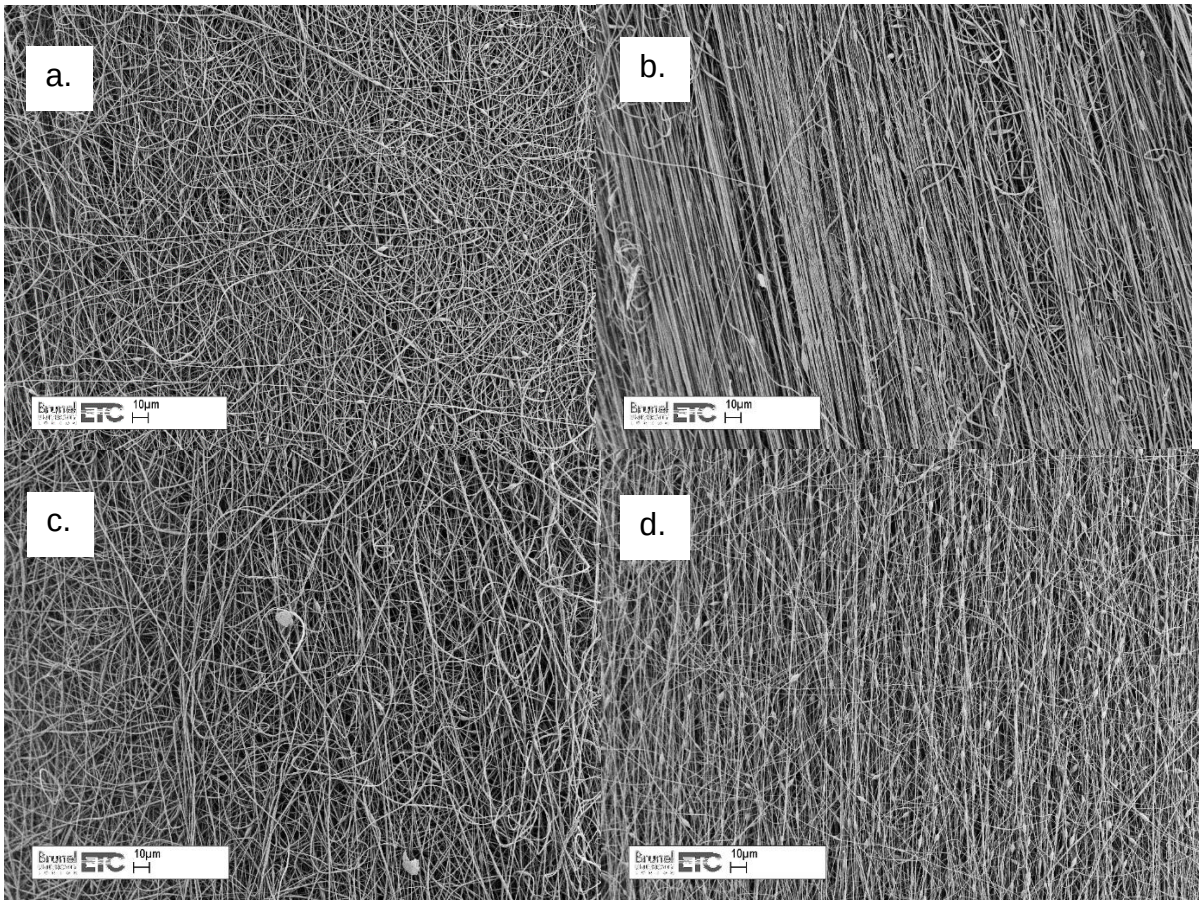

Figure 5.33 - SEM electrospinning images of samples rotated at different angular velocities

Figure 5.34 shows that the fibre alignment is produced along the length of the core-shell fibres, this is counter intuitive since as the fibres are rotating it would expect that the fibres in flight would wrap around the circumference of the core wire during electrospinning. This may indeed be the case at higher rotational velocities however due to the design and choice of motors used for the apparatus developed 48 rpm is the maximum working angular velocity for the central core electrode.

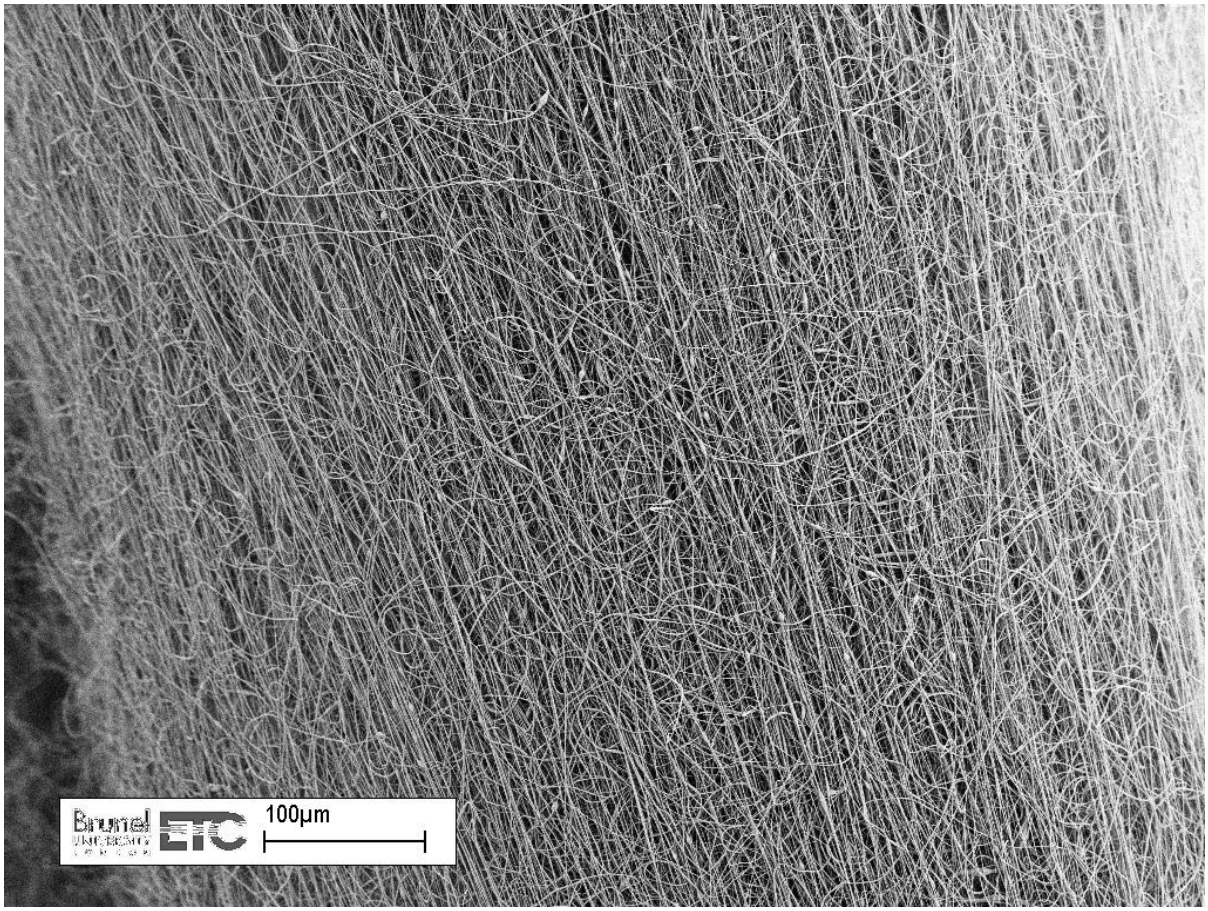

Figure 5.34 - Aligned fibres along length of core fibre

The suggested alignment theory is for this phenomena is as follows. It is known that the positively charged fibre in flight will always be attracted to the highest physical point on any electrode with the lowest potential voltage, in this case 0 v as the core wire is grounded. For the wire core this means that the fibre in flight will align itself along its length at its highest point during deposition. Now as the core wire rotates the area that was just deposited onto is no longer the highest point and so the fibre in flight is now attracted to the new top of the core wire this process is repeated over and over again creating the fibre alignment observed.

This suggested process would be very sensitive to changes in angular velocity as the faster the angular velocity the more the fibres in flight will be aligned around the circumference of the core fibre rather than along the length of the core fibre. This could explain why the deposited fibre alignment is much greater at 24 rpm and then is noticeably less at higher rotational velocities. However this need further

investigation with more intermediate velocities and also with increased velocities over 48 rpm to discern more conclusively the method and reason for alignment.

5.6.3.2.7 *Conclusion*

The final developed apparatus fulfilled the requirements it was designed to operate to, the incremental development shown informs the final design of the apparatus and its operational limitations. The conventional electrospinning process has been extended with this novel apparatus so that any conducive wire can be now be uniformly and concentrically coated with electrospun fibres to a thickness desired by the operator to create core-shell fibres. The current minimum diameter of the conductive core wire is determined by the tensile strength the wire due to mechanical limitations and tolerances in the apparatus design. The current maximum wire diameter is determined by the flexibility of the core wire used as it needs to be easily wrapped around the spool used. This means the maximum diameter is dependent on the material and its inherent properties.

The polymer fibre alignment shown along the axial length of the core wire has not been shown in literature and needs further investigation to see in more detail how this occurs and under what conditions. It could be beneficial for the future development of fibrous sensors and energy harvesting fibres since aligned piezoelectric fibres will be excited in the same orientation giving a greater output compared to if the fibres are randomly orientated.

5.6.4 Post Processing Apparatus

As shown in the early experimentation discussed in section 5.6.2 the outer electrode that is added to the core-shell fibre after electrospinning is an important part of the overall system because of its effects on voltage collection and potential dampening of the piezoelectric material reducing the ability to freely oscillate.

An outer electrode created by dip coating using conductive paint containing silver particles had many downsides including stiffness and brittleness due to its material properties when dry, it also was hard to ensure a thin even coating was applied uniformly on the core-shell fibre. This is problematic when used on a device which by

design must flex repeatedly and with relative freedom of movement to function effectively.

In literature metallic electrodes usually of gold are often deposited by vacuum evaporative or sputter deposition. It was felt that this was not suitable as a solution for coating the produced fibres because achieving a reel to reel solution to would not be possible.

An alternative and inexpensive method of producing an electrode for the outer layer of the devices was developed that aimed to solve some of the issues identified with using the techniques mentioned above. Inspiration was taken from an existing industry technique used for weaving outer sheathing for many applications such as the outer sheathing on some ropes. The apparatus developed is a miniaturised version of industrial machinery that aims to allow the weaving of fine conductive wires with diameters less than 100 µm around the electrospun core-shell fibres. This apparatus was developed to allow the production of three layered fibre devices that can be used for energy harvesting or sensor applications. A benefit of the chosen design is that very long lengths of core-shell fibre can be created since the developed apparatus is reel to reel.

5.6.4.1 *Initial Electrode Weaver*

The initial apparatus developed was mechanical as this was the simplest solution, the operational theory and design of this apparatus is covered in section 4.4.2. As can be seen from the image in Figure 5.35 the developed apparatus was initially tested using cotton instead of fine wire and a piece of string to mimic the central core-shell fibre. The image shows that the process created a uniform weave as expected with the required tightness around the central core.

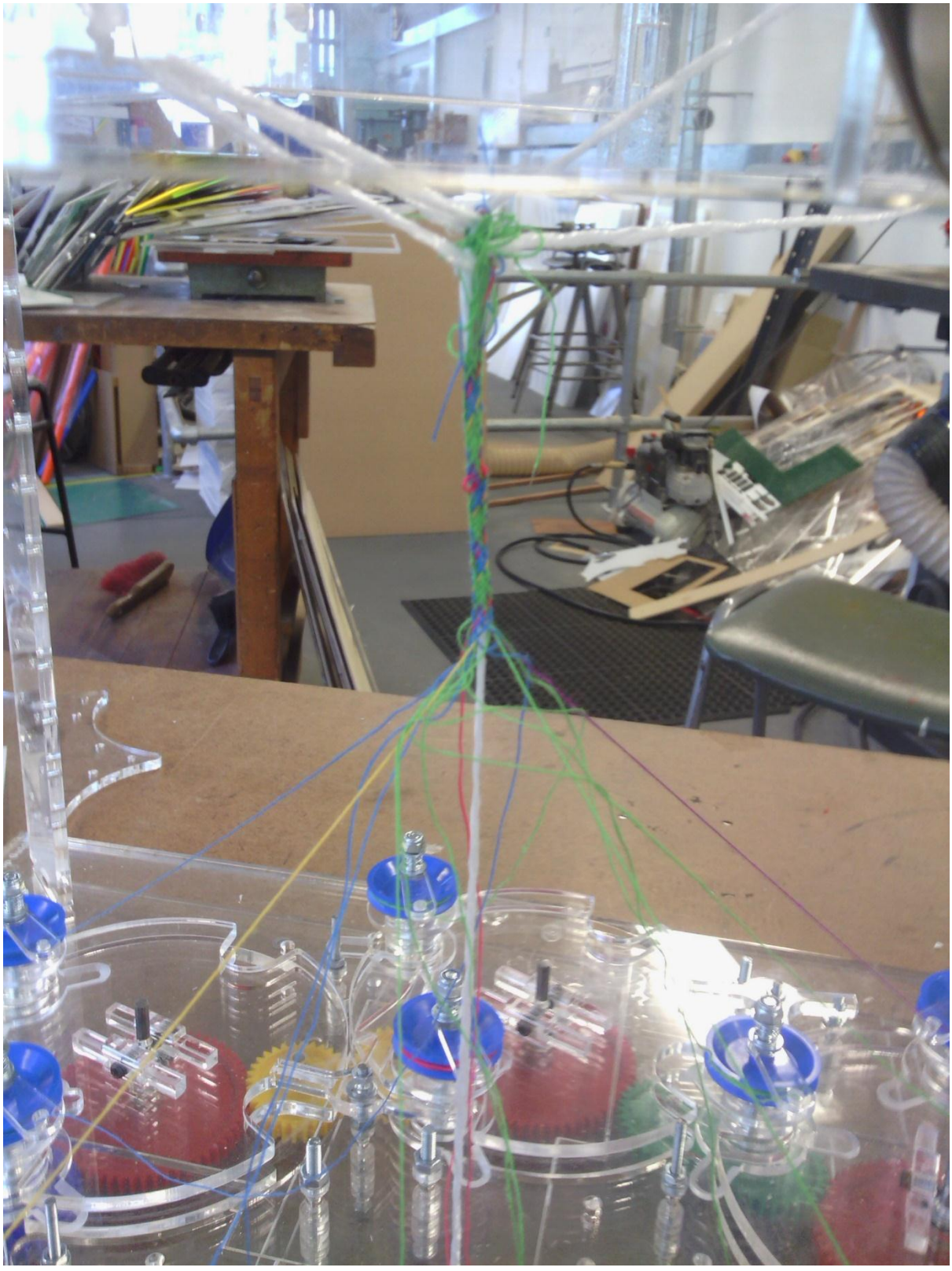

Figure 5.35 - Testing of the initial weaving machine

This validated the method to achieve the weave however there were severe issues with the mechanical approach taken to drive the weaving process. Due to the number of gears used and with only a single gear driven by the motor used there was a problem with the overall friction of the system which meant the motor was not powerful enough to drive the mechanical system. The main issue however was the tolerances between gears as there needed to be some room to allow for the slight differences in the size of the gears themselves and also to ensure that they would still mesh without jamming if the gears were not completely concentric on their shafts. As there were two idle gears between the gears connected to the carousels above, the tolerances magnified so that the carousels would not always align correctly to allow the bobbins to be passed from carousel to carousel. This caused the bobbins to jam on the transfer from carousel to carousel which meant that the bobbins needed to be adjusted continuously stopping any chance of automating the process and driving it using a motor in the apparatus's current form.

5.6.4.2 *Final Electrode Weaver*

Due to the issues with the initial mechanical apparatus a comprehensive redesign and following incremental improvements was needed to create a working apparatus. This process and the final design of the apparatus is explained in detail in section 4.4.3.3.

The operation of the apparatus is automatic and the geared stepper motors and magnetic sensors work in conjunction as envisaged allowing the bobbins to pass from carousel to carousel relatively smoothly. The bobbins do from time to time get caught as they pass from carousel to carousel but this is intermittent and is due to small tolerance issues which are unavoidable due to techniques utilised to build the apparatus, a timeout function is included in the microcontroller code to stop any further movement of any carousels if any of the magnetic sensors are not triggered within a certain time limit. This effectively identifies and stops the apparatus if there is any issues with the bobbins. Other operational issues include the speed of the apparatus, operationally it is very slow and is only capable of weaving an outer layer of approximately 10 mm in length per hour around the central core. This is too slow

for taking advantage of the reel to reel production used to produce the core-shell fibres to which the woven electrodes are being added.

Once the electronic version had been tested and improved so that it could weave effectively with cotton, 100 µm silver wire was then used in place of the cotton. This added more complications due to the difference in flexibility between the two different fibre materials and more improvements needed to be made. Figure 5.36 shows the woven structure achieved with the final apparatus using 100 µm silver wire being woven successfully around the electrospun core-shell fibre. Even though fine silver wire weave was successful showing the designed apparatus to work, there are continuing issues regarding the use of silver wire due its flexibility. It proved difficult to get a tight weave without having the silver wire under relatively large tension to ensure the weave tightened around the central core correctly. This in itself is problematic as the tension can then cause the silver wire to overly compress or cut into the soft electrospun polymer layer, increasing the likelihood of the silver wire coming into contact with the central conductive core fibre and creating a short circuit between the central core and the outer woven electrode.

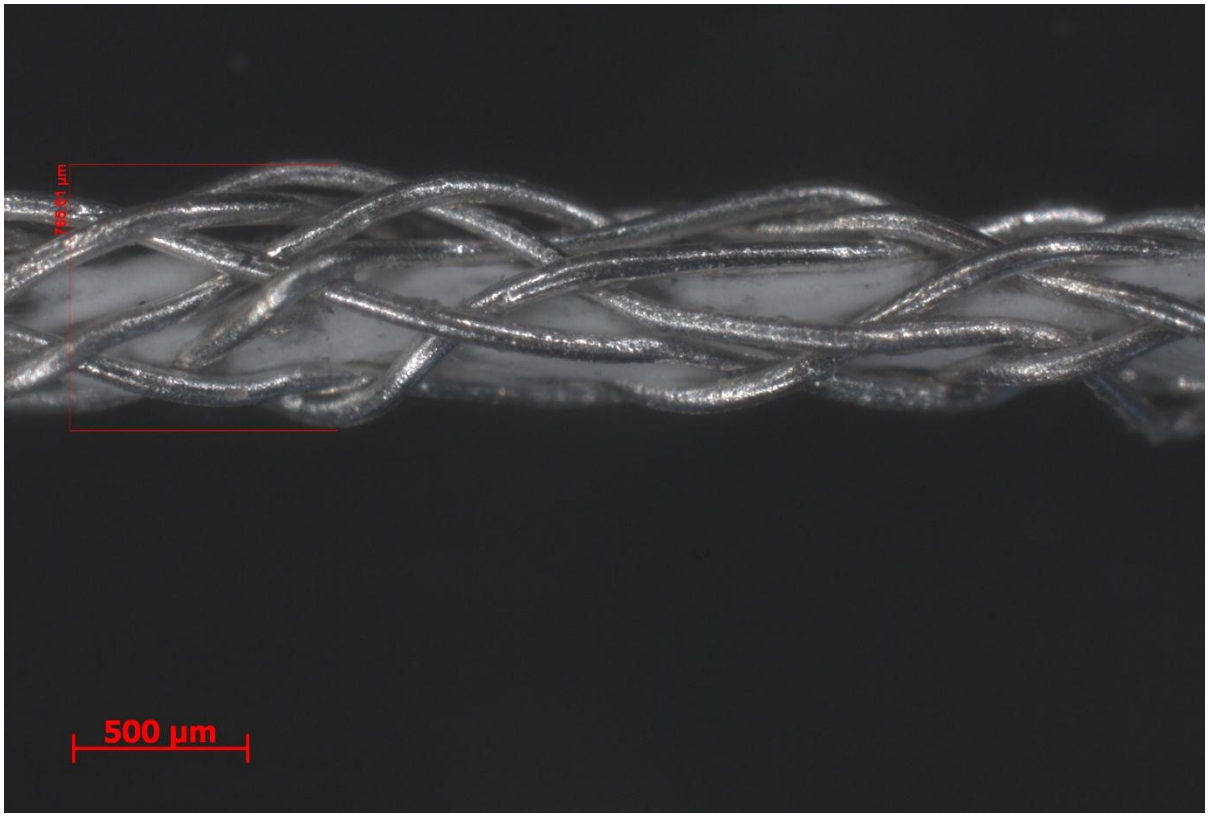

Figure 5.36 - Three layer device with woven outer electrode

5.6.5 System Evaluation and Conclusion

All the individual apparatus used for the system have been shown to work as designed to allow the reel to reel creation of piezoelectric three layer composite fibres for sensor or energy harvesting applications. These fibres consist of a central conductive core covered with electrospun PVDF fibres and a woven outer electrode. Even though the individual systems have been shown to work well and a prototype device created more work needs to be completed to optimise the apparatus to create fully working prototypes and achieve the goal of a complete reel to reel solution.

Due to the tension necessary to achieve a tight well-ordered weave with 100 µm silver wire, experimentation is needed with even thinner wire which should reduce the tension needed and have other benefits such as a smaller final diameter of the produced composite fibres. Other strategies such as using a mix of conductive threads and non-conductive threads for the outer woven electrode need to be tried to increase over all flexibility. This should also help achieve a more even and uniform woven structure.

A relationship needs to be obtained through experimentation to determine what the minimum thickness of the electrospun polymer layer can be for different diameters of conductive fibres used for the woven outer electrode. This is because the tension needed to tighten the outer electrode weave sufficiently differs depending on the diameter of conductive fibre used. Which during the weaving process can compress and cut into the electrospun polymer layer increasing the risk of a short circuit when developing piezoelectric devices.

6 Conclusion

The work that has been completed and described here successfully expands upon the conventional electrospinning technique and fulfils the aim of expanding the electrospinning process to facilitate the future development of advanced devices that utilise polymers and composite materials. The created composite fibres could be used as advanced standalone sensors including microphones. They could also be woven into larger forms to create energy harvesting fabrics or smart fabrics with sensing properties. The aligned fibres deposited in layers could also be used as sensors, however they could also be used as particulate or fluid filters due to the small pore size. By using the inverse piezoelectric effect it may be possible to also change and control the pore size as when a voltage is put across a piezoelectric material it contracts, creating active filters. The alignment of fibres also has other applications especially within the medical sector. Electrospun films are already being investigated as wound dressings and tissue scaffolding [35, 36] so this work could be used to advance these studies.

Some of the techniques and apparatus developed built upon existing experimentation as shown in the literature and the benefits are discussed later in this chapter. Each of the three pieces of apparatus developed that extends the electrospinning technique are all novel due to the differences in approach and the improvements made. Due to the increased complexity and the functionality of the developed electrospinning apparatus it has allowed advanced electrospinning techniques to be developed giving greater control of the whole electrospinning process especially in regards to the control of the electrospun fibres in flight and deposition control. These improvements gave the ability to create novel devices and electrospun morphologies using these newly developed techniques.

For all experiments the samples and devices developed have used the polymer Polyvinylidene fluoride (PVDF) as the electrospun material due to its piezoelectric properties when processed by electrospinning. The developed apparatus can be used with any polymer or other material that can be electrospun however the apparatus was optimised to work with PVDF for the creation of piezoelectric films and composite fibres. Using PVDF added its own challenges into the design and development of the experimental apparatus, methods and systems. This successful

optimisation has led to the development of novel piezoelectric composite fibres and has also worked towards the production of aligned films and printed films for the development of future novel devices. The exact contributions that this work has made are as follows:

The electrospinning apparatus that produced aligned fibre films, described in sections 5.2 and 6.4 is novel because the attraction of the fibres in flight can be changed during the electrospinning process using high voltage vacuum reed relays which is a completely new approach to fibre alignment. Previous work by Ishii et al. had used an electrode switching technique to electrospin a desired number of fibres across a gap between two parralel electrodes [76]. This has been improved upon greatly within this work as by utilising multiple vacuum reed relays more complex morphologies can be produced with up to seven pairs of parrallel elecrodes. The process has also been automated which gives even greater control of the process. This apparatus can also be compared to the work done by Zhang et al. [77] who used a grid of needle electrodes and found that when electrospinning over them fibres aligned between the needles. The apparatus expands on this by allowing the individual needles to be switched using the vacuum reed relays so that patterns can be created within the grid, something that was not possible with the apparatus Zhang et al. used.

The greatest novelty in respect to the apparatus is that by using two or more pairs of parrelel electrodes aligned layers of deposited fibres can be created where the alignment of the layers are orientated differently as shown in section 5.4.3.2. This method of layer alignment has not been shown before in literature.

In summary the process and technologies utilised for this apparatus in conjunction with the electrospinning process have not been reported on before. The apparatus has enabled the production of polymer films with bulk aligned fibres that have multiple layers where the orientation of the alignment is changed for each layer and controlled by the user. This apparatus also allows the patterned deposition of electrospun fibre bundles between point electrodes effectively drawing fibres into desired patterns which has not been achieved using this approach before.

The deposition method and fibre control in conjunction with a moving stage described in sections 4.3 and 5.5 are not a novel approach as similar systems have

been used on different scales in the literature. The work by Kim [84] utilised a modified electric field by adding a shaped secondary electrode around the electrospinning needle to focus the electric field at the needle tip and then used a moving stage to pattern the deposition. The apparatus developed in this work utilises a different secondary electrode morphology by using a drum electrode that controls the deposition area while a moving stage is used to pattern the deposition. The track width achievable with this secondary electrode is comparable with the track width of 30 mm reported by Kim.

The research contribution for this apparatus is the extension to the technique by adding a method to selectively turn the electrospinning jet on and off during the electrospinning process in conjunction with the design of the apparatus itself. This then allows the deposition of piezoelectric fibres into a predetermined pattern with a greater level of control. The apparatus also allows the control over the thickness of a film giving the ability to electrospin films with predetermined and desired areas of different thicknesses.

The apparatus developed for coating conductive fibres is a different approach to the ones that have been shown before in literature, it is similar in its aims and functionality to the other apparatus already shown however. The main difference is it uses a mechanical system to ensure uniformity during electrospinning and uses the central core as the ground electrode rather than other approaches such as using multiple electrospun jets [113]. Some of the coating and bundling techniques created twisted aligned fibres where the polymer being electrospun is stretched as it is collected into long fibres [70, 71, 78, 79]. The apparatus developed here doesn’t collect fibres in this way and so the deposited polymer fibres are not twisted together or put under any force post electrospinning on collection. This could be beneficial depending on the aims of the experimentation. The main contribution that this apparatus makes is the aligned electrospun fibre morphology that is produced by the technique along the axis of the central core fibre. This has not been shown in literature and is of benefit for the future development of sensors and other devices that would benefit from alignment in this axis.

The core-shell fibre coating apparatus is part of a larger system which produces novel three layer piezoelectric fibres. The overall system and production method was

designed from ideation to be reel to reel for both pieces of apparatus developed therefore trying to allow easier transition between research and manufacturability from the outset. Not only is the apparatus developed and the system approach new for this type deposition technique but the three layer piezoelectric fibres themselves are also novel due to the woven outer electrode utilised.

This work has not only expanded the conventional electrospinning technique to make it more versatile and allow more complex samples to be produced. The expansion of the electrospinning technique has also allowed the development of more versatile piezoelectric devices such as the composite fibres described. The future scope for what the developed apparatus can be utilised for is incredibly large. This is because the electrospinning technique can be used with so many different polymer solutions and composite material solutions in conjunction with more post processing and production techniques. This will allow the developments to the conventional electrospinning technique detailed here to be utilised for more cross disciplinary research and the production of devices that touches many different research areas including medical, electronics, filtration and composite material development.

7 Future Work

The areas in which to expand upon the work completed can be split into two distinct areas: further improvement of the developed apparatus and the further exploration of what the apparatus can produce. The following improvements to each of the developed electrospinning apparatus, reasons for the suggested improvements and further necessary characterisation are discussed first. Then potential alternative uses and experimentation utilising the developed apparatus is discussed in the second section.

7.1 *Apparatus Improvement and Further Characterisation*

For the advanced fibre alignment apparatus (sections 4.2 and 5.4) one of the main issues currently is the electrodes being used. Adjustment of the design so that a wider array of electrode with different morphology and spacing could be used would enable more experimentation. The developed system would benefit if it could be made substrate free as currently the electrodes being used become the substrate. A method of stopping the PVDF bonding to any surface on deposition while also keeping the alignment that has been shown in this work would make the process much more versatile and useful for development of advanced aligned meshes and patterned fibre bundles. As to improving the electronics used to enable this apparatus there is still an intermittent issue with resetting of the microcontroller being used when the high voltage relays switch possibly due to EMI spikes. Isolating all the HV relay connections to the microcontroller using optoisolators and incorporating better electrical shielding could help alleviate or remove the issues.

The user interface needs improvement as all input between the host device and the apparatus is text based, being able to predefine graphically the wanted pattern and layer thickness of the deposited aligned layers or fibre bundles would be of great benefit to the usability of the apparatus. To achieve this more experimental characterisation would be needed to build up a comprehensive relationship between deposition layer thickness and timing. Also full characterisation of the relationship between the primary voltage used, secondary voltage used and the degree of alignment of the deposited fibres. This would also be needed to be repeated for different electrospun polymers and solution weights.

The aligned meshes that have been developed need further characterisation; an area of interest identified is the difference in mechanical properties between randomly orientated meshes and aligned meshes of the same thickness and material. To do this different meshes would be tested to their breaking point using a low force tensile testing machine and the results analysed. The level of alignment of the meshes need to be quantified better as well and also an investigation into the possible control of the deposited fibre spacing needs to be done. If an experimental method and relationship could be found that describes the necessary parameters to control the spacing between the fibres advanced aligned meshes could be developed that could be used for filtration. By controlling the mesh spacing the maximum particle size that could travel through the film could be controlled easily and since the fibres produced by electrospinning can be as smaller than a micron in diameter the spacing could be tailored a high degree.

For the apparatus designed to allow the printing patterns of polymer deposition as described in sections 4.3 and 5.5 the following improvements need to be made. As the experiments completed have shown the minimum thickness of the printable tracks is still quite large at around 10 - 30 mm. Improvements need to be made to the core design of the apparatus to do this. Instead of using the moving stage as the ground electrode a fixed ground electrode is placed below the moving stage in the centre of the apparatus. This electrode will be circular and small, the exact size dependant on experimental deduction and simulation. Around the central electrode but with a suitable air gap will be a metal ring that is connected to the secondary high voltage power supply. This new configuration will change the electric field, narrowing it at the bottom of the secondary electrode creating a smaller area for the fibres in flight to whip within. This will reduce the area that the fibres in flight are attracted to and should allow the controlled deposition into a smaller area, therefore allowing smaller tracks to be deposited during printing. It will hopefully also keep the printed tracks more uniform in thickness and stop the spreading that was observed with the current configuration. Other changes such as an improvement to the user interface allowing more complex shapes and geometries to be printed and eventually development of software to allow integration with and design created on CAD software packages to be directly printed.

Another improvement would be to utilise multiple high voltage relays connected to different electrospinning jets. This would allow the use of different polymer solutions to be used in different electrospinning jets facilitating the deposition of different materials during the same experiment creating layered composite polymer structures. With these changes it is hoped that more complex 2D and eventually 3D structures and patterns to be printed in multiple materials.

The fibre coating apparatus detailed in sections 4.4.2 and 5.6 can be improved by increasing the range of speed of the angular rotation by increasing the maximum speed and torque profiles of the motors used. This could necessitate the use of DC motors instead of stepper motors to achieve the increase in speed which would in turn mean a change in the electronic control and feedback system that would monitor the speed. Redesigning some aspects to decrease the manufacturing tolerances, especially between gearing and the change from chain driven gearing to meshed gearing would allow for better control without as such unwanted movement in the mechanical system.

Another important thing to do is to ensure the diameters of both reels are as close to the same diameter as possible by turning them down together on a lathe. As discussed issues with the small difference in diameters of the reels can lead to tension on the central fibre which can lead to the fibre breaking, with the reel diameters identical this would not happen allowing the use of an even finer diameter of core fibre and therefore the production of even smaller multilayer fibre devices.

7.2 *Further Utilisation of the Developed Apparatus*

Within this body of work the only polymer used has been PVDF, repeating all the experiments and characterisation completed with a range of different polymers is necessary to further validate the developed apparatus. This experimentation would identify any future improvements that need to be made and any effects that are polymer specific that could then be investigated further.

The range of polymers that could be tried with the developed apparatus and systems are extensive. However when considering the work that has been completed with PVDF, polymers that support the development of sensors are a priority. Throughout

the whole of the project and as discussed multiple times in previous chapters creating electrodes with a similar material profile to PVDF is essential to the further development of piezoelectric devices. As this would allow the material properties of PVDF to be fully exploited. An option here is to experiment with the creation of electrospun conductive layers using polymers such as PDOT:PSS a conductive polymer that can also be electrospun [114]. This would allow for all polymer piezoelectric devices to be developed. This could be achieved for thin films using the developed printing apparatus, with the substrate free system developed or in multi-layered fibre form using the coating apparatus developed.

Electrospinning has also been shown in literature with polymers doped with colloidal metal particles and using coaxial electrospinning techniques [32] which encapsulate metals or even carbon nanotubes with in fibres [31, 115]. The produced electrospun films then undergo post processing to produce metallic meshes. Using the advanced alignment apparatus it may be possible to develop metallic meshes that are aligned rather than randomly orientated in nature which could have benefit and use for a range of areas including medial applications and filtration.

Within this work the piezoelectric focus has been on sensor development however the inverse piezoelectric effect can also be utilised as an actuator when a voltage is applied across the piezoelectric material. The developed alignment apparatus used with PVDF could be used to create micro actuators, as the actuators would potentially benefit from an aligned structure as all the fibres would contract in the same orientation when a voltage is put across them.

The ultimate goal for both the further characterisation and apparatus improvement would be to merge the developed electrospinning apparatus into a fully integrated multi-functional electrospinning machine that could perform multiple ways of electrospinning by computer numerical control (CNC) in a single unit. Allowing patterning with fibre alignment with the potential to use multiple polymers in a single electrospinning session with no post processing necessary to create three dimensional functional polymer devices.

8 References

[1] D. Reneker, A. Yarin, H. Fong and S. Koombhongse, “Bending instability of electrically charged liquid jets of polymer solutions in electrospinning,” *JOURNAL OF APPLIED PHYSICS,* vol. 87, no. 9, pp. 4531-4547, 2000.

[2] J. Doshi and D. Reneker, “Electrospinning Process and Applications of Electrospun Fibers,” *Journal of Electrostatics,* vol. 35, no. 2-3, pp. 151-160, 1995.

[3] IME Technologies, “Electrospinning equipment,” IME Technologies, [Online]. Available: http://www.imetechnologies.nl/Products/. [Accessed 25 4 2016].

[4] Z. Huang, Y. Zhang, M. Kotaki and S. Ramakrishna, “A review on polymer nanofibers by electrospinning and their applications in nanocomposites,” *COMPOSITES SCIENCE AND TECHNOLOGY,* vol. 63, no. 15, pp. 2223-2253, 2003.

[5] A. Vaseashta, “Controlled formation of multiple Taylor cones in electrospinning process,” *APPLIED PHYSICS LETTERS,* vol. 90, no. 9, 2007.

[6] G. Taylor, “Disintegration of Water Drops in an Electric Field,” *The Royal Society Proceedings A,* vol. 280, no. 1382, 1964.

[7] A. Yarin, S. Koombhongse and D. Reneker, “Taylor cone and jetting from liquid droplets in electrospinning of nanofibers,” *JOURNAL OF APPLIED PHYSICS,* vol. 90, no. 9, pp. 4836-4846, 2001.

[8] A. Yarin, S. Koombhongse and D. Reneker, “Bending instability in electrospinning of nanofibers,” *JOURNAL OF APPLIED PHYSICS,* vol. 89, no. 5, pp. 3018-3026, 2001.

[9] C. S. Kong, W. S. Yoo, N. G. Jo and H. S. Kim, “Electrospinning Mechanism for Producing Nanoscale Polymer Fibers,” *JOURNAL OF MACROMOLECULAR SCIENCE PART B-PHYSICS,* vol. 49, no. 1, pp. 122-131, 2010.

[10] G. Collins, J. Federici, Y. Imura and L. H. Catalani, “Charge generation, charge transport, and residual charge in the electrospinning of polymers: A review of issues and complications,” *JOURNAL OF APPLIED PHYSICS,* vol. 111, no. 4, 2012.

[11] L. M. Guerrini, M. C. Branciforti, T. Canova and R. E. Suman Bretas, “Electrospinning and Characterization of Polyamide 66 Nanofibers With Different Molecular Weights,” *MATERIALS RESEARCH-IBERO-AMERICAN JOURNAL OF MATERIALS,* vol. 12, no. 2, pp. 181-190, 2009.

[12] S.-W. He, S.-S. Li, Z.-M. Hu, J.-R. Yu, L. Chen and J. Zhu, “Effects of Three Parameters on the Diameter of Electrospun Poly(ethylene oxide) Nanofibers,” *JOURNAL OF NANOSCIENCE AND NANOTECHNOLOGY,* vol. 11, no. 2, pp. 1052-1059, 2011.

[13] P. Gupta, C. Elkins, T. Long and G. Wilkes, “Electrospinning of linear homopolymers of poly(methyl methacrylate): exploring relationships between fiber formation, viscosity, molecular weight and concentration in a good solvent,” *Polymer,* vol. 46, no. 13, pp. 4799-4810, 2005.

[14] D. Petras, P. Slobodian, V. Pavlinek, P. Saha and D. Kimmer, “The Effect of PVAc Solution Viscosity on Diameter of PVAc Nanofibres Prepared by Technology of Electrospinning,” *NOVEL TRENDS IN RHEOLOGY IV,* vol. 1375, 2011.

[15] O. Ero-Phillips, M. Jenkins and A. Stamboulis, “Tailoring Crystallinity of Electrospun Plla Fibres by Control of Electrospinning Parameters,” *POLYMERS,* vol. 4, no. 3, pp. 1331-1348, 2012.

[16] A. H. Hekmati, A. Rashidi, R. Ghazisaeidi and J.-Y. Drean, “Effect of needle length, electrospinning distance, and solution concentration on morphological properties of polyamide-6 electrospun nanowebs,” *TEXTILE RESEARCH JOURNAL,* vol. 83, no. 14, pp. 1452-1466, 2013.

[17] B. Ahmad, S. Stoyanov, E. Pelan, E. Stride and M. Edirisinghe, “Electrospinning of ethyl cellulose fibres with glass and steel needle

configurations," *FOOD RESEARCH INTERNATIONAL,* vol. 54, no. 2, pp. 1761-1772, 2013.

[18] C. Zhang, X. Yuan, L. Wu, Y. Han and J. Sheng, "Study on morphology of electrospun poly(vinyl alcohol) mats," *EUROPEAN POLYMER JOURNAL,* vol. 41, no. 3, pp. 423-432, 2005.

[19] X. Yuan, Y. Zhang, C. Dong and J. Sheng, "Morphology of ultrafine polysulfone fibers prepared by electrospinning," *POLYMER INTERNATIONAL,* vol. 53, no. 11, pp. 1704-1710, 2004.

[20] C. Ki, D. Baek, K. Gang, K. Lee, I. Um and Y. Park, "Characterization of gelatin nanofiber prepared from gelatin-formic acid solution," *POLYMER,* vol. 46, no. 14, pp. 5094-5102, 2005.

[21] C. Mit-uppatham, M. Nithitanakul and P. Supaphol, "Ultratine electrospun polyamide-6 fibers: Effect of solution conditions on morphology and average fiber diameter," *MACROMOLECULAR CHEMISTRY AND PHYSICS,* vol. 205, no. 17, pp. 2327-2338, 2004.

[22] R. T. Ogulata and H. I. Icoglu, "Interaction between effects of ambient parameters and those of other important parameters on electrospinning of PEI/NMP solution," *JOURNAL OF THE TEXTILE INSTITUTE,* vol. 106, no. 1, pp. 57-66, 2015.

[23] B. De Schoenmaker, L. Van der Schueren, R. Zugle, A. Goethals, P. Westbroek, P. Kiekens, T. Nyokong and K. De Clerck, "Effect of the relative humidity on the fibre morphology of polyamide 4.6 and polyamide 6.9 nanofibres," *JOURNAL OF MATERIALS SCIENCE,* vol. 48, no. 4, pp. 1746-1754, 2013.

[24] R. M. Nezarati, M. B. Eifert and E. Cosgriff-Hernandez, "Effects of Humidity and Solution Viscosity on Electrospun Fiber Morphology," *TISSUE ENGINEERING PART C-METHODS,* vol. 19, no. 10, pp. 810-819, 2013.

[25] A. Doustgani, "Effect of electrospinning process parameters of

polycaprolactone and nanohydroxyapatite nanocomposite nanofibers," *TEXTILE RESEARCH JOURNAL,* vol. 85, no. 14, pp. 1445-1454, 2015.

[26] X. Zong, K. Kim, D. Fang, S. Ran, B. Hsiao and B. Chu, "Structure and process relationship of electrospun bioabsorbable nanofiber membranes," *POLYMER,* vol. 43, no. 16, pp. 4403-4412, 2002.

[27] O. S. Yoerdem, M. Papila and Y. Z. Menceloglu, " Effects of electrospinning parameters on polyacrylonitrile nanofiber diameter: An investigation by response surface methodology," *MATERIALS & DESIGN,* vol. 29, no. 1, pp. 34-44, 2008.

[28] J. Deitzel, J. Kleinmeyer and D. Harris, "The effect of processing variables on the morphology of electrospun nanofibers and textiles," *POLYMER,* vol. 42, no. 1, pp. 261-272, 2001.

[29] Z. Huang, Y. Zhang, M. Kotaki and S. Ramakrishna, "A review on polymer nanofibers by electrospinning and their applications in nanocomposites," *COMPOSITES SCIENCE AND TECHNOLOGY,* vol. 63, no. 15, pp. 2223-2253, 2003.

[30] F. Ko, Y. Gogotsi, A. Ali, N. Naguib, H. Ye, G. Yang, C. Li and P. Willis, "Electrospinning of continuons carbon nanotube-filled nanofiber yarns," *ADVANCED MATERIALS,* vol. 15, no. 14, pp. 1161-1164, 2003.

[31] K. Ketpang and J. S. Park, "Electrospinning PVDF/PPy/MWCNTs conducting composites," *SYNTHETIC METALS,* vol. 160, no. 15-16, pp. 1603-1608, 2010.

[32] D.-G. Yu, J. Zhou, N. P. Chatterton, Y. Li, J. Huang and X. Wang, " Polyacrylonitrile nanofibers coated with silver nanoparticles using a modified coaxial electrospinning process," *INTERNATIONAL JOURNAL OF NANOMEDICINE,* vol. 7, pp. 5725-5732, 2012.

[33] Z. Dong, S. J. Kennedy and Y. Wu, "Electrospinning materials for energy-related applications and devices," *JOURNAL OF POWER SOURCES,* vol.

196, no. 11, pp. 4886-4904, 2011.

[34] E. Kenawy, G. Bowlin, K. Mansfield, J. Layman, D. Simpson, E. Sanders and G. Wnek, “Release of tetracycline hydrochloride from electrospun poly(ethylene-co-vinylacetate), poly(lactic acid), and a blend,” *JOURNAL OF CONTROLLED RELEASE,* vol. 81, no. 1-2, pp. 57-64, 2002.

[35] P.-o. Rujitanaroj, N. Pimpha and P. Supaphol, “Wound-dressing materials with antibacterial activity from electrospun gelatin fiber mats containing silver nanoparticles,” *POLYMER,* vol. 49, no. 21, pp. 4723-4732, 2008.

[36] L. A. Smith, X. Liu and P. X. Ma, “Tissue engineering with nano-fibrous scaffolds,” *SOFT MATTER,* vol. 4, no. 11, pp. 2144-2149, 2008.

[37] S. Agarwal, J. H. Wendorff and A. Greiner, “Use of electrospinning technique for biomedical applications,” *POLYMER,* vol. 49, no. 26, pp. 5603-5621, 2008.

[38] T. C. Mokhena, V. Jacobs and A. S. Luyt, “A review on electrospun bio-based polymers for water treatment,” *EXPRESS POLYMER LETTERS,* vol. 9, no. 10, pp. 839-880, 2015.

[39] G. Sha-sha, K. Qin-fei, W. Hong, L. Xiong and L. Yun, “Preparation and Characterization of PET Electrospinning-meltblown Composite Nanofiber Mat for Blood Filtration,” *2011 INTERNATIONAL FORUM ON BIOMEDICAL TEXTILE MATERIALS, PROCEEDINGS,* pp. 381-386, 2011.

[40] M. Lackowski, A. Krupa and A. Jaworek, “Nanofabric nonwoven mat for filtration smoke and nanoparticles,” *POLISH JOURNAL OF CHEMICAL TECHNOLOGY,* vol. 15, no. 2, pp. 48-52, 2013.

[41] K. Tonurist, I. Vaas, T. Thomberg, A. Jaenes, H. Kurig, T. Romann and E. Lust, “Application of multistep electrospinning method for preparation of electrical double-layer capacitor half-cells,” *ELECTROCHIMICA ACTA,* vol. 119, pp. 72-77, 2014.

[42] H. Zai-Bo, G. De-Shu, L. Zhao-Hui, L. Gang-Tie and Z. Ji, “P(VDF-HFP)-

based polymer electrolytes prepared by high-voltage electrospinning technology," *ACTA CHIMICA SINICA,* vol. 65, no. 11, pp. 1007-1011, 2007.

[43] H. Cho, S.-Y. Min and T.-W. Lee, "Electrospun Organic Nanofiber Electronics and Photonics," *MACROMOLECULAR MATERIALS AND ENGINEERING,* vol. 298, no. 5, pp. 475-486, 2013.

[44] H. Wu, D. Lin, R. Zhang and W. Pan, "ZnO nanofiber field-effect transistor assembled by electrospinning," *JOURNAL OF THE AMERICAN CERAMIC SOCIETY,* vol. 91, no. 2, pp. 656-659, 2008.

[45] J. Chang, Y. Liu, K. Heo, B. Y. Lee, S.-W. Lee and L. Lin, "Direct-Write Complementary Graphene Field Effect Transistors and Junctions via Near-Field Electrospinning," *SMALL,* vol. 10, no. 10, pp. 1920-1925, 2014.

[46] R. Gonzalez and N. Pinto, "Electrospun poly (3-hexylthiophene-2,5-diyl) fiber field effect transistor," *SYNTHETIC METALS,* vol. 151, no. 3, pp. 275-278, 2005.

[47] C. Yang, Z. Jia and Z. Guan, "Polyvinylidene fluoride membrane by novel electrospinning system for separator of Li-ion batteries," *JOURNAL OF POWER SOURCES,* vol. 189, no. 1, pp. 716-720, 2009.

[48] L. Wang, Y. Yu, P. C. Chen, D. W. Zhang and C. H. Chen, "Electrospinning synthesis of C/Fe3O4 composite nanofibers and their application for high performance lithium-ion batteries," *JOURNAL OF POWER SOURCES,* vol. 183, no. 2, pp. 717-723, 2008.

[49] Y. Xin, Z. H. Huang, L. Peng and D. J. Wang, "Photoelectric performance of poly(p-phenylene vinylene)/Fe3O4 nanofiber array," *ADVANCES IN MATERIALS SCIENCE AND ENGINEERING,* vol. 105, no. 8, 2009.

[50] N. M. Bedford, M. B. Dickerson, L. F. Drummy, H. Koerner, K. M. Singh, M. C. Vasudev, M. F. Durstock, R. R. Naik and A. J. Steckl, "Nanofiber-Based Bulk-Heterojunction Organic Solar Cells Using Coaxial Electrospinning," *ADVANCED ENERGY MATERIALS,* vol. 2, no. 9, pp. 1136-1144, 2012.

[51] S.-S. Kim and C.-D. Kee, “Electro-Active Polymer Actuator based on PVDF with Bacterial Cellulose Nano-whiskers (BCNW) Via Electrospinning Method,” *INTERNATIONAL JOURNAL OF PRECISION ENGINEERING AND MANUFACTURING,* vol. 15, no. 2, pp. 315-321, 2014.

[52] D. Y. Lee, Y. Kim, S.-J. Lee, M.-H. Lee, J.-Y. Lee, B.-Y. Kim and N.-I. Cho, “Characteristics of chemo-mechanically driven polyacrylonitrile fiber gel actuators,” *MATERIALS SCIENCE & ENGINEERING C-BIOMIMETIC AND SUPRAMOLECULAR SYSTEMS,* vol. 28, no. 2, pp. 294-298, 2008.

[53] S. Jiang, F. Liu, A. Lerch, L. Ionov and S. Agarwal, “Unusual and Superfast Temperature-Triggered Actuators,” *Advanced materials,* vol. 27, no. 33, pp. 4865-4870, 2015.

[54] C.-H. Hong, S.-J. Ki, J.-H. Jeon, H.-l. Che, I.-K. Park, C.-D. Kee and I.-K. Oh, “Electroactive bio-composite actuators based on cellulose acetate nanofibers with specially chopped polyaniline nanoparticles through electrospinning,” *COMPOSITES SCIENCE AND TECHNOLOGY,* vol. 87, pp. 135-141, 2013.

[55] V. Vohra, U. Giovanella, R. Tubino, H. Murata and C. Botta, “Electroluminescence from Conjugated Polymer Electrospun Nanofibers in Solution Processable Organic Light-Emitting Diodes,” *ACS NANO,* vol. 5, no. 7, pp. 5572-5578, 2011.

[56] W. Zhao, B. Yalcin and M. Cakmak, “Dynamic assembly of electrically conductive PEDOT:PSS nanofibers in electrospinning process studied by high speed video,” *SYNTHETIC METALS,* vol. 203, pp. 107-116, 2015.

[57] M. Bognitzki, M. Becker, M. Graeser, W. Massa, J. H. Wendorff, A. Schaper, D. Weber, A. Beyer, A. Goelzhaeuser and A. Greiner, “Preparation of sub-micrometer copper fibers via electrospinning,” *ADVANCED MATERIALS,* vol. 18, no. 18, pp. 2384-2386, 2006.

[58] T. T. Wang, S. Y. Ma, L. Cheng, J. Luo, X. H. Jiang and W. X. Jin, “Preparation of Yb-doped SnO2 hollow nanofibers with an enhanced ethanol-gas sensing performance by electrospinning,” *SENSORS AND ACTUATORS*

B-CHEMICAL, vol. 216, pp. 212-220, 2015.

[59] R. Rojas and N. J. Pinto, “Using electrospinning for the fabrication of rapid response gas sensors based on conducting polymer nanowires,” *IEEE SENSORS JOURNAL,* vol. 8, no. 5-6, pp. 951-953, 2008.

[60] “A sensing microfibre mat produced by electrospinning for the turn-on luminescence determination of Hg2+ in water samples,” *SENSORS AND ACTUATORS B-CHEMICAL,* vol. 195, pp. 8-14, 2014.

[61] S. Aydogdu, K. Ertekin, A. Suslu, M. Ozdemir, E. Celik and U. Cocen, “Optical CO(2) Sensing with Ionic Liquid Doped Electrospun Nanofibers,” *JOURNAL OF FLUORESCENCE,* vol. 21, no. 2, pp. 607-613, 2011.

[62] B. Ding, M. Wang, J. Yu and G. Sun, “Gas Sensors Based on Electrospun Nanofibers,” *SENSORS,* vol. 9, no. 3, pp. 1609-1624, 2009.

[63] Y. A. Ismail, J. G. Martinez and T. F. Otero, “Polyurethane microfibrous mat templated polypyrrole: Preparation and biomimetic reactive sensing capabilities,” *JOURNAL OF ELECTROANALYTICAL CHEMISTRY,* vol. 719, pp. 47-53, 2014.

[64] Y. He, X. Liu, R. Wang and T. Zhang, “An Excellent Humidity Sensor with Rapid Response Based on BaTiO3 Nanofiber via Electrospinning,” *SENSOR LETTERS,* vol. 9, no. 1, pp. 262-265, 2011.

[65] B. Sun, Y.-Z. Long, S.-L. Liu, Y.-Y. Huang, J. Ma, H.-D. Zhang, G. Shen and S. Xu, “Fabrication of curled conducting polymer microfibrous arrays via a novel electrospinning method for stretchable strain sensors,” *NANOSCALE,* vol. 5, no. 15, pp. 7041-7045, 2013.

[66] Y. R. Wang, J. M. Zheng, G. Y. Ren, P. H. Zhang and C. Xu, “A flexible piezoelectric force sensor based on PVDF fabrics,” *SMART MATERIALS & STRUCTURES,* vol. 20, no. 4, 2011.

[67] D. Mandal, S. Yoon and K. J. Kim, “Origin of Piezoelectricity in an Electrospun

Poly(vinylidene fluoride-trifluoroethylene) Nanofiber Web-Based Nanogenerator and Nano-Pressure Sensor," *MACROMOLECULAR RAPID COMMUNICATIONS,* vol. 32, no. 11, pp. 831-837, 2011.

[68] J. Chang, M. Domnner, C. Chang and L. Lin, "Piezoelectric nanofibers for energy scavenging applications," *NANO ENERGY,* vol. 1, no. 3, pp. 356-371, 2012.

[69] B. J. Hansen, Y. Liu, R. Yang and Z. L. Wang, "Hybrid Nanogenerator for Concurrently Harvesting Biomechanical and Biochemical Energy," *ACS NANO,* vol. 4, no. 7, pp. 3647-3652, 2010.

[70] P. Dalton, D. Klee and M. Moller, "Electrospinning with dual collection rings," *POLYMER,* vol. 46, no. 3, pp. 611-614, 2005.

[71] J. Joseph, S. V. Nair and D. Menon, "Integrating Substrate less Electrospinning with Textile Technology for Creating Biodegradable Three-Dimensional Structures," *NANO LETTERS,* vol. 15, no. 8, pp. 5420-5426, 2015.

[72] D. Li, Y. Wang and Y. Xia, "Electrospinning of polymeric and ceramic nanofibers as uniaxially aligned arrays," *NANO LETTERS,* vol. 3, no. 8, pp. 1167-1171, 2003.

[73] V. P. Secasanu, C. K. Giardina and Y. Wang, "A Novel Electrospinning Target to Improve the Yield of Uniaxially Aligned Fibers," *BIOTECHNOLOGY PROGRESS,* vol. 25, no. 4, pp. 1169-1175, 2009.

[74] W. A. Yee, A. C. Nguyen, P. S. Lee, M. Kotaki, Y. Liu, B. T. Tan, S. Mhaisalkar and X. Lu, "Stress-induced structural changes in electrospun polyvinylidene difluoride nanofibers collected using a modified rotating disk," *POLYMER,* vol. 49, no. 19, pp. 4196-4203, 2008.

[75] P. Katta, M. Alessandro, R. Ramsier and G. Chase, "Continuous electrospinning of aligned polymer nanofibers onto a wire drum collector," *NANO LETTERS,* vol. 4, no. 11, pp. 2215-2218, 2004.

[76] Y. Ishii, H. Sakai and H. Murata, “A new electrospinning method to control the number and a diameter of uniaxially aligned polymer fibers,” *MATERIALS LETTERS,* vol. 62, no. 19, pp. 3370-3372, 2008.

[77] K. Zhang, X. Wang, D. Jing, Y. Yang and M. Zhu, “Bionic electrospun ultrafine fibrous poly(L-lactic acid) scaffolds with a multi-scale structure,” *BIOMEDICAL MATERIALS,* vol. 4, no. 3, 2009.

[78] E. Smit, U. Buttner and R. Sanderson, “Continuous yarns from electrospun fibers,” *POLYMER,* vol. 46, no. 8, pp. 2419-2423, 2005.

[79] M. Khil, S. Bhattarai, H. Kim, S. Kim and K. Lee, “Novel fabricated matrix via electrospinning for tissue engineering,” *JOURNAL OF BIOMEDICAL MATERIALS RESEARCH PART B-APPLIED BIOMATERIALS,* vol. 72B, no. 1, pp. 117-124, 2005.

[80] W.-E. Teo, R. Gopal and R. Ramaseshan, “A dynamic liquid support system for continuous electrospun yarn fabrication,” *POLYMER,* vol. 48, no. 12, pp. 3400-3405, 2007.

[81] J. Deitzel, J. Kleinmeyer, J. Hirvonen and N. Tan, “Controlled deposition of electrospun poly(ethylene oxide) fibers,” *POLYMER,* vol. 42, no. 19, pp. 8163-8170, 2001.

[82] M. Acharya, G. K. Arumugam and P. A. Heiden, “Dual electric field induced alignment of electrospun nanofibers,” *MACROMOLECULAR MATERIALS AND ENGINEERING,* vol. 293, no. 8, pp. 666-674, 2008.

[83] L. M. Bellan and H. G. Craighead, “Control of an electrospinning jet using electric focusing and jet-steering fields,” *JOURNAL OF VACUUM SCIENCE & TECHNOLOGY B,* vol. 24, no. 6, pp. 3179-3183, 2006.

[84] G. H. Kim, “Electrospun PCL nanofibers with anisotropic mechanical properties as a biomedical scaffold,” *BIOMEDICAL MATERIALS,* vol. 3, no. 2, 2008.

[85] A. Salim, C. Son and B. Ziaie, “Selective nanofiber deposition via electrodynamic focusing,” *NANOTECHNOLOGY,* vol. 19, no. 37, 2008.

[86] Z. Sun, E. Zussman, A. Yarin, J. Wendorff and A. Greiner, “Compound core-shell polymer nanofibers by co-electrospinning,” *ADVANCED MATERIALS,* vol. 15, no. 22, pp. 1929-1932, 2003.

[87] D. Li and Y. (Xia, “Direct fabrication of composite and ceramic hollow nanofibers by electrospinning,” *NANO LETTERS,* vol. 4, no. 5, pp. 933-938, 2004.

[88] G. H. Lee, J.-C. Song and K.-B. Yoon, “Controlled Wall Thickness and Porosity of Polymeric Hollow Nanofibers by Coaxial Electrospinning,” *MACROMOLECULAR RESEARCH,* vol. 18, no. 6, pp. 571-576, 2010.

[89] D. Lukas, A. Sarkar and P. Pokorny, “Self-organization of jets in electrospinning from free liquid surface: A generalized approach,” *JOURNAL OF APPLIED PHYSICS,* vol. 103, no. 8, 2008.

[90] C. Yang, Z. Jia, Z. Xu, K. Wang, Z. Guan and L. Wang, “Comparisons of Fibers Properties between Vertical and Horizontal Type Electrospinning Systems,” *CEIDP: 2009 ANNUAL REPORT CONFERENCE ON ELECTRICAL INSULATION AND DIELECTRIC PHENOMENA,* pp. 514-517, 2009.

[91] G. Jiang and X. Qin, “ An improved free surface electrospinning for high throughput manufacturing of core-shell nanofibers,” *MATERIALS LETTERS,* vol. 128, pp. 259-262, 2014.

[92] N. G. Sahoo, S. Rana, J. W. Cho, L. Li and S. H. Chan, “Polymer nanocomposites based on functionalized carbon nanotubes,” *PROGRESS IN POLYMER SCIENCE,* vol. 35, no. 7, pp. 837-867, 2010.

[93] X. Ren and Y. Dzenis, “Novel continuous poly(vinylidene fluoride) nanofibers,” *Smart Nanotextiles,* vol. 920, pp. 55-61, 2006.

[94] M. G. Broadhurst and G. T. Davis, “PHYSICAL BASIS FOR PIEZOELECTRICITY IN PVDF,” *FERROELECTRICS,* vol. 60, pp. 3-13, 1984.

[95] P. Martins, A. C. Lopes and S. Lanceros-Mendez, “Electroactive phases of poly(vinylidene fluoride): Determination, processing and applications,” *PROGRESS IN POLYMER SCIENCE,* vol. 39, no. 4, pp. 683-706, 2014.

[96] G. Haertling, “Ferroelectric ceramics: History and technology,” *JOURNAL OF THE AMERICAN CERAMIC SOCIETY,* vol. 82, no. 4, pp. 797-818, 1999.

[97] Arkema, “Kynar/Kynar Flex Polyvinylidene Fluoride Performance Characteristics and Data,” 2014. [Online]. Available: http://americas.kynar.com/export/sites/kynar-americas/.content/medias/downloads/literature/2014-kynar-performance-characteristic-brochure.pdf. [Accessed 20 August 2015].

[98] F. Liu, N. A. Hashim, Y. Liu, M. R. M. Abed and K. Li, “Progress in the production and modification of PVDF membranes,” *JOURNAL OF MEMBRANE SCIENCE,* vol. 375, no. 1-2, pp. 1-27, 2011.

[99] A. Jain, K. J. Prashanth, A. K. Sharma, A. Jain and P. N. Rashmi, “Dielectric and piezoelectric properties of PVDF/PZT composites: A review,” *POLYMER ENGINEERING AND SCIENCE,* vol. 55, no. 7, pp. 1589-1616, 2015.

[100] Arkema, “Kynar,” Arkema, [Online]. Available: http://americas.kynar.com/en/. [Accessed 29 9 2015].

[101] Piezotech Arkema Group, “PVDF Active solvents and PVDF Latent Solvents,” Arkema Group, 2015. [Online]. Available: http://www.piezotech.fr/fr/5-technique-piezoelectric-eap-electroactive-polymer/news/news-40-pvdf-active-solvents-and-pvdf-latent-solvents.html. [Accessed 2015 09 21].

[102] H. Liu and Y. Hsieh, “Ultrafine fibrous cellulose membranes from electrospinning of cellulose acetate,” *JOURNAL OF POLYMER SCIENCE PART B-POLYMER PHYSICS,* vol. 40, no. 18, pp. 2119-2129, 2002.

[103] J. Pelipenko, J. Kristl, B. Jankovic, S. Baumgartner and P. Kocbek, “The impact of relative humidity during electrospinning on the morphology and mechanical properties of nanofibers,” *INTERNATIONAL JOURNAL OF PHARMACEUTICS,* vol. 456, no. 1, pp. 125-134, 2013.

[104] W. Rasband, “ImageJ,” U. S. National Institutes of Health, Bethesda, Maryland, USA, 1997 - 2016. [Online]. Available: http://imagej.nih.gov/ij/. [Accessed 15 7 2014].

[105] TA Instruments, “Q2000,” TA Instruments, [Online]. Available: http://www.tainstruments.com/product.aspx?siteid=11&id=15&n=1. [Accessed 29 9 2015].

[106] Perkin Elmer, “DMA8000,” Perkin Elmer, [Online]. Available: http://www.perkinelmer.com/Catalog/Product/ID/N5330101. [Accessed 29 9 2015].

[107] Instruments, Texas, “LM10875 20W Audio Amplifier,” Texas Instruments, May 2004. [Online]. Available: http://www.ti.com/lit/ds/symlink/lm1875.pdf.

[108] “Herzog Braiding Machines,” Herzog, [Online]. Available: http://www.herzog-online.com/_rubric/index.php?rubric=Home+EN. [Accessed 28 09 2015].

[109] Microchip, “PIC16F1789 - 8 - bit PIC Microcontrollers,” Microchip, [Online]. Available: http://www.microchip.com/wwwproducts/Devices.aspx?product=PIC16F1789. [Accessed 09 29 2015].

[110] Texas Instruments, “CD4028B Decoder/Encoder/Multiplexer,” Texas Instruments, [Online]. Available: http://www.ti.com/product/CD4028B/description. [Accessed 29 09 2015].

[111] Texas Instruments, “CD4514B Decoder/Encoder/Multiplexer,” Texas Instruments, [Online]. Available: http://www.ti.com/product/CD4514B/description. [Accessed 29 9 2015].

[112] M. Inoue, Y. Tada, K. Suganuma and H. Ishiguro, “Thermal stability of poly(vinylidene fluoride) films pre-annealed at various temperatures,” *POLYMER DEGRADATION AND STABILITY,* vol. 92, no. 10, pp. 1833-1840 , 2007.

[113] F.-L. Zhou, R.-H. Gong and I. Porat, “ Three-jet electrospinning using a flat spinneret,” *JOURNAL OF MATERIALS SCIENCE,* vol. 44, no. 20, pp. 5501-5508, 2009.

[114] H. D. Nguyen, J. M. Ko, H. J. Kim, S. K. Kim, S. H. Cho, J. D. Nam and J. Y. Lee, “Electrochemical Properties of Poly(3,4-ethylenedioxythiophene) Nanofiber Non-Woven Web Formed by Electrospinning,” *Journal of Nanoscience and Nanotechnology,* vol. 8, pp. 4718-4721, 2008.

[115] Y. Y. S. Huang, E. M. Terentjev, T. Oppenheim, S. P. Lacour and M. E. Welland, “ Fabrication and electromechanical characterization of near-field electrospun composite fibers,” *NANOTECHNOLOGY,* vol. 23, no. 10, 2012.

[116] D. Damjanovic, “Ferroelectric, dielectric and piezoelectric properties of ferroelectric thin films and ceramics,” *REPORTS ON PROGRESS IN PHYSICS,* vol. 61, no. 9, pp. 1267-1324, 1998.

[117] E. Venkatragavaraj, B. Satish, P. Vinod and M. Vijaya, “Piezoelectric properties of ferroelectric PZT-polymer composites,” *JOURNAL OF PHYSICS D-APPLIED PHYSICS,* vol. 34, no. 4, pp. 487-492, 2001.

[118] D. Vatansever, R. L. Hadimani, T. Shah and E. Siores, “An investigation of energy harvesting from renewable sources with PVDF and PZT,” *SMART MATERIALS & STRUCTURES,* vol. 20, no. 5, 2011.

[119] CREE, “C2M1000170D MOSFET Datasheet,” CREE, September 2015. [Online]. Available: http://www.cree.com/~/media/Files/Cree/Power/Data%20Sheets/C2M1000170D.pdf. [Accessed 01 08 2015].

[120] Cynergy3, “Cynergy3 D Series High Voltage Relays Datasheet,” Cynergy3,

2012. [Online]. Available: http://www.cynergy3.com/sites/default/files/product-data-sheets/D%20series%202013.pdf. [Accessed 01 08 2015].

[121] International Rectifier, “IRLU2703 MOSFET Datasheet,” International Rectifier, July 2003. [Online]. Available: http://www.irf.com/product-info/datasheets/data/irlr2703.pdf.

[122] RVFM , “2 Phase Bi-polar Stepper Motor datasheet,” Rapid Electronics/RVFM, 20 02 2007. [Online]. Available: http://www.rapidonline.com/pdf/37-0507.pdf. [Accessed 01 08 2015].

[123] Texas Instruments, “L293D Quadruple Half-H Drivers Datasheet,” Texas Instruments, 2014. [Online]. Available: http://www.ti.com/general/docs/lit/getliterature.tsp?genericPartNumber=l293d&fileType=pdf. [Accessed 01 08 2015].

[124] R. Rottenfusser, E. E. Wilson and M. W. Davidson, “Education in Microscopy and Digital Imaging,” Zeiss, 2015. [Online]. Available: http://zeiss-campus.magnet.fsu.edu/articles/basics/reflectedcontrast.html. [Accessed 21 09 2015].

9 Appendix

9.1 *Piezoelectric Theory*

When a piezoelectric material is put under mechanical stress then the material becomes polarised, this is known as the direct piezoelectric effect. The converse piezoelectric effect occurs when a piezoelectric material is put into an electric field which causes the material to become under strain causing it to contract or expand depending on the orientation of the electric field in relation to the material. There is a linear relationship between stress and polarisation for both the direct and converse piezoelectric effect, the units for the direct piezoelectric effect are C N^{-1} (coulomb per newton applied) and for the converse effect are m V^{-1} (metres per volt applied).

The polarisation of a material when put under stress is due to the type, orientation and symmetry of the crystalline structure. Only non-centrosymmetric crystals can exhibit the piezoelectric effect and there are 20 of these. Within this class of crystals there are 10 types which have a unique polar axis which makes them naturally piezoelectric which means they do not need to be poled in electric field before they will exhibit the piezoelectric effect. All ferroelectric materials fall within these 10 types [116].

Within piezoelectric materials there are many ferroelectric grains which are randomly orientated which means there individual piezoelectric contribution when the material is put under stress cancel each other out so there is no net polarisation across the material and therefore no measurable piezoelectric effect. To rectify this, the material is poled by putting it in a strong electric field up to 100 kV. This doesn't change the orientation or position of the grains themselves but aligns domains within the grain in the direction of the electric field. It is electric dipoles of polar molecules within the ferroelectric grains that are being reoriented. This reorientation means that there is now a net polarisation across the material when it is put under stress and therefore exhibits the piezoelectric effect [116].

Piezoelectric materials with high piezoelectric strain coefficients, piezoelectric voltage coefficients and mechanical compliance and with a low density make the best piezoelectric transducers [117].

9.2 *Piezoelectric Coefficients*

There are numerous piezoelectric coefficients however the d_{33} coefficient is one of the most important coefficient of piezoelectricity, it's a charge coefficient which relates the mechanical stress the material is put under to the amount of charge (charge density) that builds up across the material due to the stress. This would be the d_{33} coefficient of a material exhibiting the direct piezoelectric effect, however the d_{33} value for the converse piezoelectric effect is exactly the same for the same material ($d_{direct} = d_{converse}$) [116]. The maximum voltage produced when the material is put under stress is dependent on the voltage coefficient g_{31} [118]. For sensor applications a high voltage coefficient is usually desirable however charge coefficients are more desirable for energy harvesting applications since it's a high current that's needed for charging batteries and capacitors not high voltage.

The direct piezoelectric effect, where mechanical energy is converted to electrical energy can be described as shown in equation 1.

$$D_i = d_{ijk} X_{jk} \quad (2)$$

Where D_i is the charge density, d_{ijk} is the piezoelectric coefficient and X_{jk} is the applied stress.

The converse piezoelectric effect, where electrical energy is converted to mechanical energy can be described as shown in equation 2.

$$x_{ij} = d_{kij} E_k \quad (3)$$

Where x_{ij} is the deformation, d_{kij} is the piezoelectric coefficient and E_k is the applied polarisation.

The above piezoelectric equations with the tensor subscript notation is based around an orthogonal coordinate system so *x, y, z* directions translate to *1, 2, 3* respectively.

This notation is simplified to produce coefficients with only two subscript notations. The actual piezoelectric coefficient tensors can be put into a matrix following the Voigt convention. This transforms an identical pair of indices such as *ii*, *jj* or *kk* into a single index, *i*, *j* or *k*. So 33 would become 3. Whereas if the pair is different, for example *Ij*, *ik* or *jk* the indices are reduced to a single index *m* which can represent any combination of two of the three original indices *i, j* or *k*. However *ij* is the same as *ji* which means that *m* can be any value from 4 to 6 [116, 117].

The above means that the direct piezoelectric effect equation can be rewritten as equation 3.

$$D_i = d_{im}X_m \qquad (4)$$

Which makes the d_{33} coefficient actually the d_{333} coefficient if the matrix wasn't used or the g_{15} coefficient actually g_{113} or g_{131}. There can be mixed tensors (two stress directions) in piezoelectric coefficients because of shear stress.

For the d_{im} coefficient index *i* is the direction of polarisation, either generated or applied and *m* is the direction of stress either applied or generated. For g_{im} the piezoelectric voltage coefficient *i* is the direction on the electric field and m is the direction of stress [116].

The coefficients are important especially the difference between the d_{33} and d_{31} values as they show to what magnitude a piezoelectric material will produce charge and across which surfaces in relation to the polarisation of the material itself.

9.3 *Information on electronic methods and hardware used*

9.3.1 Microcontrollers

9.3.1.1 *Introduction*

Microcontrollers have been used in the majority of the experimental apparatus developed. The use of microcontrollers especially has allowed the semi-automation of the developed apparatus and much greater control over the electrospinning process in general. As already covered in section 3.3.2 High Voltage Considerations all experiments utilising the electrospinning process have to be carried out in a

locked box for user safety, microcontrollers give the user the ability to react and control any apparatus inside the locked box during experimentation.

The microcontrollers used in all work are from the Microchip PIC range from the 16FXXXX mid-range family of 8 bit microcontrollers with various numbers of pins and working clock speeds. They were chosen depending on the needs of the experimental apparatus being developed.

The following briefly covers the most utilised of the on-board microcontroller technologies leveraged for the experimental apparatus designed without going into depth covering the specific microcontrollers used and their specific structure, coding and limitations.

9.3.1.2 *Analogue to Digital Conversion (ADC)*

Analogue to digital conversion or ADC is the process of converting an analogue or varying voltage to a digital equivalent in binary. An example of this would be a LDR (Light) sensor that gives out a different voltage depending on the level of ambient light. To be able to monitor the light level using a microcontroller the ADC is utilised to calculate the voltage supplied by the sensor.

The ADC takes the incoming voltage and compares it against a reference voltage which is half way between Vss and Vdd, using an internal comparator to see if the incoming voltage is higher or lower than the initial reference voltage, depending on the outcome of the comparison a register bit gets set. The reference voltage then gets changed using a digital to analogue converter (DAC) to be half way between the old reference voltage and either Vss if the previous reference voltage was greater than the incoming voltage or Vdd if the reference voltage was less than the incoming sensor voltage. This cycle keeps happening with a changing reference voltage which accurately finds the sensor voltage by producing a 10 bit binary value (in the case of the microcontrollers used) which is the equivalent of the input voltage compared against the max reference voltage (usually Vdd). The maximum ADC value for the microcontrollers utilised is 1024 (10 bit).

9.3.1.3 *Pulse Width Modulation (PWM)*

Pulse width modulation is used to control the effective voltage and current being supplied to another piece of hardware such as a DC motor in a period of time. This is

done by quickly switching the voltage/current source between two voltage levels at relatively high frequency which is chosen depending on the hardware being driven. So depending on the ratio of time spent at one voltage level compared to the other voltage level the hardware being powered sees an averaged voltage/current level. The proportion expressed as a percentage of time at the higher voltage compared to the lower voltage is known as the duty cycle which can be specified in code and easily mapped to a motors speed or brightness of an LED as examples. This is an important technique which has been leveraged for the apparatus developed as a method of control or for user interfaces. On the microcontrollers chosen the timers used to set the frequency are highly adjustable and the control of the switching output pin are separate hardware blocks so that PWM can be used while the microcontroller does other things, making it a highly versatile technique.

9.3.1.4 *Universal Asynchronous Receiver/Transmitter (UART)*

Another hardware block on some of the microcontrollers used extensively for the apparatus designed is Universal Asynchronous Receiver/Transmitter (UART). It has been used as the communication protocol used for microcontroller to microcontroller communication as well as between microcontroller and the Bluetooth module which has been used extensively in the apparatus developed. It allows two way communication between different pieces of hardware quickly and reliably.

UART is a serial communication protocol that uses either one or two wires to transmit and receive data. There is no separate clock signal used for synchronisation of data between devices instead both devices are told what speed the communication will happen at in bits per second (Baud rate). Data is sent a byte at a time with a start bit before and a stop bit after the data. The hardware block on the microcontrollers used have both send and receive registers which means that data doesn't have to be read as it comes in but can be read after its been received. The PIC16F819 which was used for some projects does not have a USART/UART module and so serial communication of this kind has to be done exclusively through code routines which mean that to receive data the software has to be continuously looking for data being received.

9.3.1.5 *Microcontroller Software Development*

The software routines put on the microcontrollers used to control and interface with the developed apparatus was written in the C programming language. The code development environment used was the microcontroller's manufacturer Microchip's program: MPLAB IDE (Integrated Development Environment). This allowed code to be written to the microcontrollers and also the basic debugging of the microcontrollers in real time from the IDE using a hardware tool produced by Microchip called the PICkit 3. The compiler used to turn the code from the written C code routines to machine code for the microcontroller was CCS C which ran within the MPLAB IDE. CCS C has many built in functions and routines that greatly cut down the development time of the software.

Code routines were produced by identifying necessary functionality and from there developing simple flow charts for different functions. Simple functions were written then tested on the hardware either on the bread-boarded circuits or on the produced PCBs depending on where in the design and development cycle the code was being produced. Once working these simple functions were built into more complex programs and tested until the desired functionality was reached. This cycle of test development went on into the experimentation and testing phases of the finished experimental apparatus as more functionality was identified as desirable or in some cases essential.

9.3.2 Frequently used components

9.3.2.1 *High Voltage Relays*

The ability to control when, if and how the electrospinning process was taking place during experimentation was necessary as the experimental apparatus being developed gained complexity. Due to the very high potential voltages used throughout the electrospinning process hardware that would allow the switching of high voltages was sought after however the technologies available to do this are limited. MOSFET (Metal Oxide Switching Field Effect Transistor) technologies would have been ideal for the applications developed due to their high switch rate, reliability and comparatively low costs however the maximum voltage for an off the shelf part is 1.7kV [119] which is more than a magnitude of ten lower than the required voltage,

multiple units could have been utilised in series however due to the number of parts this approach would have needed (~ 20) it became cost prohibited.

The only hardware technology that could deliver the high voltage requirements needed were High Voltage Vacuum Reed Relays. The relay chosen was the Cynergy3 15kv, 50W High Voltage reed relay [120]. These are rated for switching 10kV at 2A however the isolation between contacts within the relay is 15kV and due to having such a low current during the electrospinning process the relays could be used up to around 12kV allowing electrospinning to take place when combined with slight changes to the experimentation setup and methodology.

Vacuum reed relays consist of a connector switch inside a small vacuum chamber, the vacuum is necessary due to the high voltage isolation needed between the switch contacts. The switch is closed using an electromagnet that is driven by supporting electronics. The speed at which the relays operate is important to the functionality of the designed apparatus, the chosen relays have a turn on time of 3 ms and a release time of 2 ms giving a single cycle time of 5 ms and therefore a frequency of 200 Hz. This is fast enough for the apparatus designed however if a higher frequency was needed MOSFET technologies would have to be used due to their much higher operating frequencies. For the chosen relay an operational voltage of 5v is needed to energise the electromagnetic coil and close the switch terminals, this voltage level was chosen as it matches the microcontroller and other supporting electronics voltage levels. See section 5.2 for circuits and experimental apparatus utilising this component.

9.3.2.2 *Power MOSFETS*

Power MOSFETS (Metal Oxide Field Effect Transistors) are utilised for multiple uses within the electronic circuits developed. They have been used with a microcontroller to switch high current or voltage components, such as the coils on the Vacuum reed relays. The MOSFET most used for the electronics developed is an IRLU20703 HEXFET Power MOSFET and was chosen due to its versatility. Allowing the switching of sources with a maximum current drain of 23A at 10 v or a maximum voltage of 30 V by applying a low logic level to the gate pin. For all the developed electrical circuits the logic level was at 5 v allowing the microcontrollers used to

switch peripherals which required a much higher current draw such as the High voltage relays discussed in the previous section [121].

9.3.2.3 *Stepper Motor*

Stepper motors were used extensively for the development of the experimental apparatus. For many applications they are more suitable than conventional direct current (DC) motors as you can accurately specify using software the rotation angle and angular velocity. The smallest angle of rotation that a stepper motor can do is known as the motor's step angle and the minimum time between steps is known as the maximum slew speed. Stepper motors also generally have good torque characteristics and have what is known as a holding torque due to how they operate. As the step frequency and therefore the rotational velocity increases the available torque decreases which is an important characteristic when designing systems using this type of motor.

The stepper motor used for all the experimental apparatus developed was a 2 phase bipolar stepper motor made by RVFM [122]. It has a step angle of 7.5° which translates to 48 steps per revolution. A maximum speed of 330 pulses per second (pps) gives a revolutions per minute angular velocity as described in equation (5).

$$rpm = \left(\frac{pps}{\left(\frac{360}{sa} \right)} \right) 60 \qquad (5)$$

Where rpm is revolutions per minute, pps is pulses per second and sa is the step angle. This gives a max angular velocity in rpm of 412.5 rpm for the chosen stepper motor, this combined with a good holding torque of 0.107 NM (Newton Meters) and a minimum operational torque of 0.032 NM at 412 rpm means that this stepper motor was well specified as most of the apparatus designed operates at much lower angular velocities. The motor operates at 12v DC and draws a maximum current of around 500 mA.

Bi polar stepper motors operate by alternately energising electromagnetic coils in a set configuration using 4 wires. Energising the coils in the correct sequence leads to

the rotation of the central spindle, this is controlled by supporting electronics such as a H bridge described in the next section.

9.3.2.4 *H Bridge Drivers*

As previously noted stepper motors have to be driven by energising coils in a set configuration using 4 wires however due to the needed current a stepper motor cannot be driven straight from a microcontroller. To allow connection between the output from the microcontroller and the stepper motor the Texas Instruments L293D quadruple half-H drivers [123] were used this allows the microcontroller to switch each of the stepper motors wires between ground and is operating voltage of 12v even though the Microcontroller itself operates at 5v. The chosen driver can be switched much faster than the maximum stepper motor pps rate and can handle currents of up to 600 mA which is more current than a single stepper motor coil draws. The chip switches the outputs using Darlington transistors and also has internal clamping diodes which suppresses EMF developed by the motor coils switching polarity protecting the microcontroller outputs.

9.3.2.5 *Serial Bluetooth Modules*

A challenge presented by having to carry out all experiments and operate all the experimental apparatus developed within a locked plastic box is that there is no way to interact with the experimental equipment after the door to the safety box has been closed. Due to the need to be able to change linear velocities, angular velocities, switching speeds and patterns during the electrospinning process for the majority of the apparatus developed a wireless communication system needed to be built into the developed circuits. Bluetooth modules were chosen due to their ease of integration and their low cost. The modules themselves dealt with all the necessary Bluetooth data packaging and transmission, the interface between the Bluetooth module and a controller was via UART which gave a simple way of allowing 2 way real time interactions with the developed apparatus using a text based interface. Any device such as a smart phone with a Bluetooth connection and a terminal program was able to control the developed apparatus.

9.3.3 PCB Development and Production

For all the electronic circuits developed the design process was as follows. First the desired circuit hardware would be prototyped either in blocks or in its entirety using a breadboard, desired functionality was then checked using the selected components and simplistic coding routines developed to show basic functionality. If necessary this was repeated trying different hardware components and software routines on the used microcontrollers until the desired functionality was attained. For some of the developed apparatus with a large degree of complexity the circuits were prototyped and built up in stages testing functionality at each stage.

Once the desired functionality has been achieved then a schematic is digitally produced incorporating all components and connections this is then used to produce a Printed Circuit Board (PCB) layout. Components are arranged and connections created between component terminals as required by following the schematic previously developed. Once finalised the PCB is produced on FR-4 boards that are made of layered fibre glass set in resin with a thin copper layer bonded on either one or both sides. The usual copper thickness and therefore the final track thickness of the developed PCBs are 34.1 microns.

For all the PCBs produced one of two productions techniques was used; photo-etch, where the desired PCB layout was printed onto tracing paper and then put over the PCB that had been coated in an Ultra Violate (UV) photoresist. The PCB and layout is put under UV light which removes any photoresist that is not covered by the PCB artwork design. This is then put into an acid etching solution which removes the copper from the board leaving only the desired artwork. The etching process is carefully timed to make sure the PCBs were not over or under etched which would degrade the desired tracks and pads. The other manufacturing technique used was PCB routing using a CAD/CAM system where the designed PCB layout was converted to a series of Gerber output files and used with a LPKF Protomat S103 circuit board plotter to CNC mill the desired PCB layout.

Once produced components were soldered by hand onto the PCBs and then rigorously tested, this production process then became iterative if any faults or changes were detected from the testing. Once finalised more complex code could then be developed and tested during the electrospinning process, new software

routines could also be added from the results of the electrospinning tests and experimentation expanding functionality.

9.4 *Supplementary PCBs*

9.4.1 *Pull Up Resistor Network*

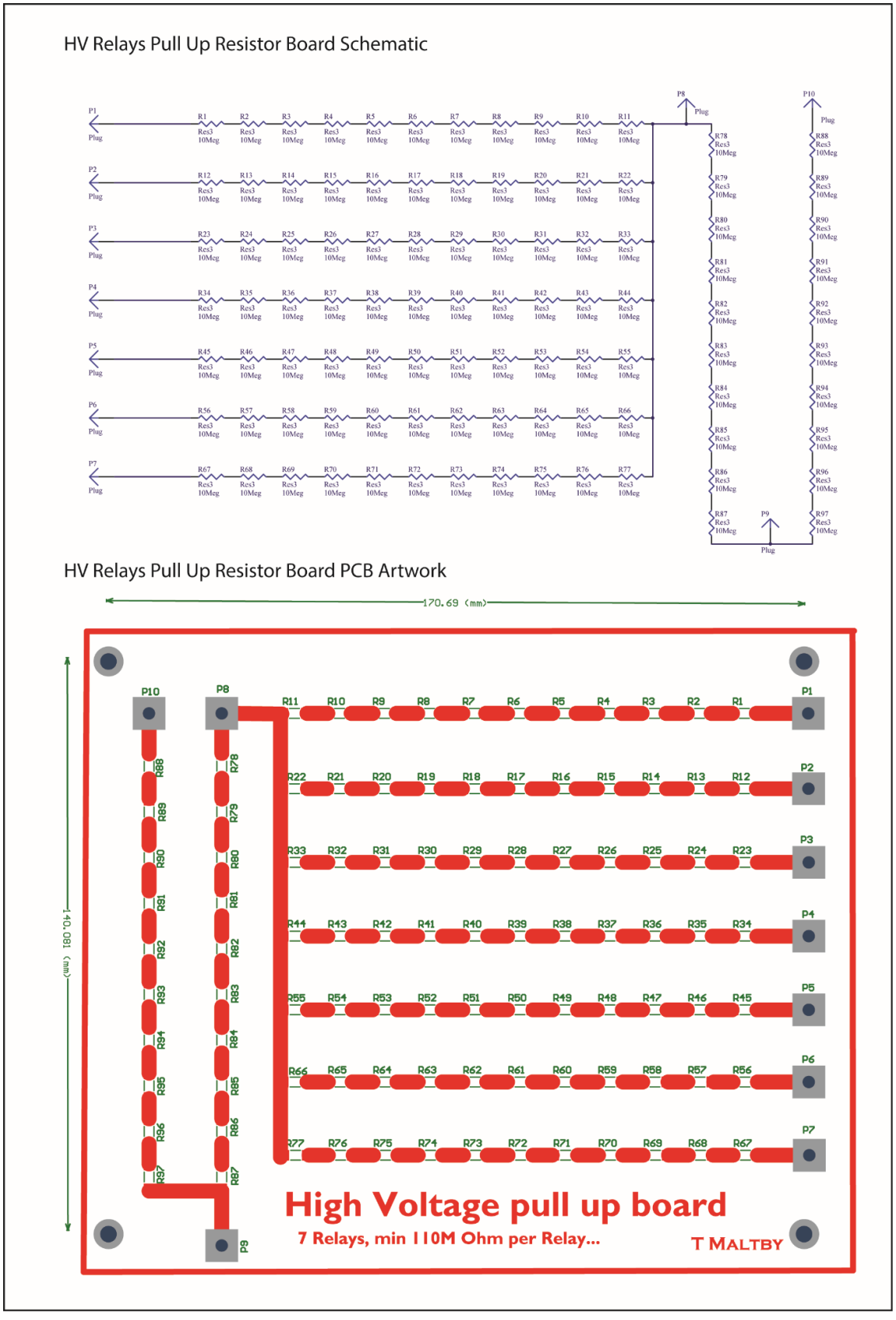

Figure 9.1 - Pull up Resistor Network Schematic and Board Layout

9.4.2 *High Voltage Relay Board*

The high voltage vacuum reed relays were mounted onto custom designed circuit boards with supporting components. This made it easy to transfer the relays between different experimental projects. Each PCB had the following components, the relay, a 1N4007 Diode, an IRLU2703 Power MIOSFET, a 10K resistor and a 3 pin right angled male header. The schematic and PCB artwork is shown in Figure 9.2.

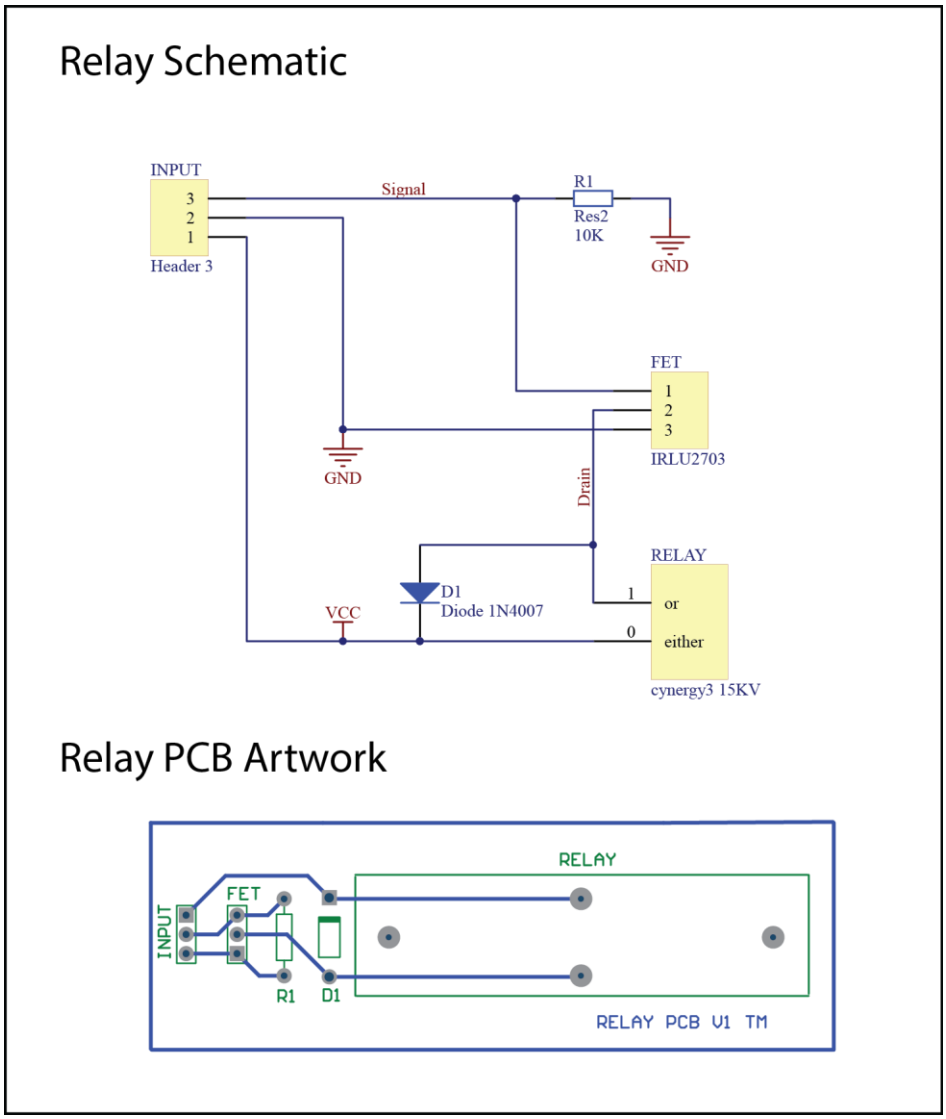

Figure 9.2 - Relay Schematic and Board

9.5 *Optical Microscopy*

All optical microscopy work was completed using a Zeiss microscope. It has 5 objective lenses with the following magnifications 2.5x, 10x, 20x, 40x and 100x. The 40 is an oil immersion lens which was not used in the work. The microscope can be used in reflection mode where the sample is illuminated from above and transmission mode where the sample is illuminated from below. There is an Olympus CCD camera mounted on the microscope which is used to take digital images (micrographs) of the samples to be investigated for analysis. The supporting software allows accurate scale bars to be directly added to the images and also individual measurements of points of interest can be taken.

Both bright field and dark field microscopy was utilised to produce the best possible images with good detail and contrast for analysis. Darkfield reflection microscopy was beneficial for capturing micrographs of electrospun structures as it increases the contrast allowing the individual fibres to be seen in some cases, however not at a magnification large enough to be able to accurately measure the fibres. Reflected dark field microscopy works by illuminating the sample at a large angle compared to the direction of view through the lens. This means the sample is not directly illuminated from above and therefore shows more contrast and detail of the structure being observed as the light reflects off the structure being viewed. It also means that the background of the viewed sample looks black because there is no light reflected back into the lens from any surface that is at a right angle to the lens.

Brightfield microscopy is where a light source is shone directly onto the sample being viewed at the same angle as the viewing angle through the lens. This technique was not used in reflection mode when analysing PVDF films as the fibres themselves are white and so the contrast and detail becomes poor against a light white background. Brightfield microscopy was however used with the microscope in transmission mode where light is shone up from below the sample. This shows the sample with a white background and clearly shows the fibres as dark areas. This technique was useful for looking at fibre alignment [124].

9.6 Code

9.6.1 Novel Advanced Fibre Alignment

9.6.1.1 Initial Version

```
#include <16F819.h>
#fuses INTRC_IO,NOWDT,NOPROTECT,MCLR,NOLVP
#use delay(clock=8000000)

#define button PIN_B0

#define relay1 PIN_A0
#define relay2 PIN_A1
#define relay3 PIN_A7

#define runLED PIN_B1
#define r1LED PIN_B2
#define r2LED PIN_B3
#define r3LED PIN_B4


long timeing=0;                 //1-->7 displayed using binary on LEDs 1->3 timing values 10, 20, 30, 40, 50, 60s
int selection=0;    // 1, 2 03 3 relays used
int i;
long cd=1000;

void flashAll(void);


void main(){
                        output_low(runLED);
                        output_low(r1LED);
                        output_low(r2LED);
                        output_low(r3LED);
            while(input(button)){
                        flashAll();
                        delay_ms(200);
            }
output_low(r1LED);
output_low(r2LED);
output_low(r3LED);
output_high(runLED);
delay_ms(2000);
```

```
        if (input(button)){
                reset_cpu();                    //ultimate in lazy coding...
        }

while (!input(button)){}
delay_ms(200);
while (input(button)){}
output_low(runLED);
timeing=1;
output_high(r1LED);
delay_ms(1000);
        if (!input(button)){
                timeing=2000;
                output_low(r1LED);
                output_high(r2LED);
                delay_ms(1000);
        }
        if (!input(button)){
                timeing=4000;
                output_high(r1LED);
                output_high(r2LED);
                delay_ms(1000);
        }
        if (!input(button)){
                timeing=8000;
                output_low(r1LED);
                output_low(r2LED);
                output_high(r3LED);
                delay_ms(1000);
        }
        if (!input(button)){
                timeing=16000;
                output_high(r1LED);
                output_low(r2LED);
                output_high(r3LED);
                delay_ms(1000);
        }
        if (!input(button)){
                timeing=32000;
                output_low(r1LED);
                output_high(r2LED);
                output_high(r3LED);
                delay_ms(1000);
```

```
        }
        if (!input(button)){
                timeing=60000;
                output_high(r1LED);
                output_high(r2LED);
                output_high(r3LED);
                delay_ms(1000);
        }
while(!input(button)){};
delay_ms(1000);
                output_low(runLED);
                output_low(r1LED);
                output_low(r2LED);
                output_low(r3LED);
                        for (i=0; i<10; i++){
                                output_toggle(runLED);
                                delay_ms(200);
                        }

                while(input(button)){
                        output_toggle(runLED);
                        delay_ms(200);
                };
output_low(runLED);
selection=1;
output_high(r1LED);
delay_ms(1000);

        if (!input(button)){
                selection=2;
                output_high(r1LED);
                output_high(r2LED);;
                delay_ms(1000);
        }
        if (!input(button)){
                selection=3;
                output_high(r3LED);
                delay_ms(1000);
        }

while (input(button)){
                                output_toggle(runLED);
                                delay_ms(200);
```

```
}
                        for (i=0; i<20; i++){
                                output_toggle(runLED);
                                delay_ms(200);
                                output_toggle(runLED);
                                delay_ms(cd);
                                cd=cd-50;
                        }

output_high(runLED);

if (selection==0){reset_cpu();} //error catch

        if (selection==1){
                while(input(button)){
                        output_high(relay1);
                        output_high(relay2);
                        delay_ms (timeing);
                        output_low(relay1);
                        output_low(relay2);
                //      delay_ms (timeing);
                }

        }
                if (selection==2){
                        while(input(button)){
                                output_high(relay1);
                                output_high(relay2);
                                delay_ms (timeing);
                                output_low(relay1);
                                //output_high(relay2);
                                output_high(relay3);
                                delay_ms (timeing);
                                output_low(relay2);
                                output_low(relay3);
                        }
                }


                        if (selection==3){
                                while(input(button)){
                                        output_high(relay1);
```

```
                                        output_high(relay2);
                                        delay_ms (timeing);
                                        output_low(relay1);
                                        output_high(relay3);
                                        delay_ms (timeing);
                                        output_low(relay2);
                                        output_high(relay1);
                                        delay_ms (timeing);
                                        output_low(relay3);
                                    }
                                }

                output_low(runLED);
                output_low(r1LED);
                output_low(r2LED);
                output_low(r3LED);
}

void flashAll(void){
output_toggle(r1LED);
output_toggle(r2LED);
output_toggle(r3LED);
output_toggle(runLED);
}
```

9.6.1.2 *Final Version*

```
////////////////////////////////////////////////////////
//                          RELAY CONTROLLER V2 (7 RELAYS)                  //
//      Advanced menu allows for the following selections:  //
//      1.total no. of relays to be used.                                   //
//      2. if the electrode pattern is sequential with one      //
//      electrode firing after the other OR using paired        //
//      electrode pattern. NB this selection effects the        //
//      following relay timing selection.                                   //
//      3. Relay Timing, selectable for sequential in 5ms       //
//      increments, for Paired electrodes 500ms increments.//
//      4. choose which relays to use, i.e. relays 1,3,4,5      //
//      or choose All relays to reduce menu input time!             //
//      NB this selection is limited by the total no. of        //
//      relays chosen in [1.] so if 1.==4 you can choose        //
//      ANY combination of 4 relays! If All is selected and     //
//      no. of relays chosen in [1.] is below 7 then            //
//      1->n relays will be used in accending sequence.             //
```

```
//
                    //
//                                   Tom Maltby 1/10/13                                   //
//////////////////////////////////////////////////////////

#include <16F819.h>
#fuses INTRC_IO,NOWDT,NOPROTECT,MCLR,NOLVP
#use delay(clock=8000000)
#use RS232 ( XMIT=PIN_B2, STREAM=LCD)

//Global Defines//
#define ButtonMenu PIN_B0
#define ButtonSelect PIN_B1

#define relay1 PIN_A0
#define relay2 PIN_A1
#define relay3 PIN_A2
#define relay4 PIN_A3
#define relay5 PIN_A4
#define relay6 PIN_A6
#define relay7 PIN_A7


#define menuLED PIN_B4
#define countLED PIN_B5
#define activeLED PIN_B4

//Global Variables//
int i,p,x,z,j, Rno,Rused, Rout;
long Rtime;
short ButState, paired;

//Function Prototypes//
void SetupLCD();
void ClearScreen();
void flashAll(long time, int times);
int pushButton();

//Party starting...//
void main(){
SetupLCD();
flashAll(500,5);
ClearScreen();
```

```
fprintf(LCD, "Relay Controller");
delay_ms(1000);
ClearScreen();
fprintf(LCD, "Press button to enter Menu");
while (!input(ButtonMenu)){}
Rno=0;
output_high(menuLED);
ClearScreen();


fprintf(LCD, "No. of relays...");
ButState=0;
        while (!input(ButtonMenu)){                    //Wait for menu button to be pressed again
before selecting final no.
                Rno=Rno+pushButton();
                if (Rno!=p){fprintf(LCD, "%u", Rno);}
                if (Rno>7){Rno=0;}
                p=Rno;
        }
delay_ms(1000);
ClearScreen();


fprintf(LCD, "Sequential or Paired electrodes?");
i=0;
p=0;
while (!input(ButtonMenu)){
        i=i+pushButton();
        if (i==1){
                if (i!=p){
                        ClearScreen();
                        fprintf(LCD, "Sequential Electrodes");
                        }
                paired=0;
        }
        else if (i==2){
                if (i!=p){
                ClearScreen();
                fprintf(LCD, "Paired Electrodes");
                }
                paired=1;
        }
        else {i=0;}
```

```
            p=i;

}
delay_ms(1000);
ClearScreen();

Rtime=0;
ButState=0;
fprintf(LCD, "Relay timing...");
while (!input(ButtonMenu)){

            if (paired==0){                 //timing for sequential electrode style
                                    if (pushButton()==1){Rtime+=5;}
                                    if (Rtime!=p){fprintf(LCD, "%lu ms", Rtime);}
                                    //if (Rno>7){Rno=0;}
                                    p=Rtime;
            }
            else if (paired==1){            //timing for paired electrodes

                                    if (pushButton()==1){Rtime+=500;}
                                    if (Rtime!=p){fprintf(LCD, "%lu ms", Rtime);}
                                    //if (Rno>7){Rno=0;}
                                    p=Rtime;
            }
}
delay_ms(1000);
ClearScreen();


x=0;
z=0;
ButState=0;
fprintf(LCD, "Which relays to be used...");
delay_ms(1000);
ClearScreen();
fprintf(LCD, "use all relays? ");
            while (!input(ButtonMenu)||!input(ButtonSelect) ){}
                        delay_ms(20);

                                    if (input(ButtonSelect)){

                                    bit_set (Rused,0);
                                    ClearScreen();
```

```
                        fprintf(LCD, "Using all relays");
                        delay_ms(500);

                        }
                        else if (input(ButtonMenu)){

                        bit_clear (Rused,0);
                        ClearScreen();
                        fprintf(LCD, "Not using all relays");
                        delay_ms(500);

                                for (i=1; i<=7; i++){
                                        fprintf(LCD, "use relay %u?", i);
                                                while
(!input(ButtonMenu)||!input(ButtonSelect) ){}
                                        delay_ms(20);
                                                if (input(ButtonMenu)){
                                                        bit_clear (Rused,i);
                                                        ClearScreen();
                                                        fprintf(LCD, "Relay %u not
selected", i);
                                                        delay_ms(500);

                                                    }
                                                else if (input(ButtonSelect)){

                                                        bit_set (Rused,i);
                                                        ClearScreen();
                                                        fprintf(LCD, "Relay %u
selected", i);
                                                        delay_ms(500);
                                                        z++;

                                                        }

                                if (z==Rno){
                                        ClearScreen();
                                        fprintf(LCD, "All %u Relays selected", Rno);
                                        break;
                                }
        }
```

```
}
delay_ms(500);
ClearScreen();
output_low(menuLED);
fprintf(LCD, "Ready to go!");

//CODE FOR RUNNING THE RELAYS//


if ( paired==0 && bit_test(Rused,0)==1){      //SEQUENTIAL AND ALL RELAYS USED
ClearScreen();
fprintf(LCD, "Sequential/All Relays");
output_high(activeLED);
        while (!input(ButtonMenu)){
                output_toggle(countLED);
                        for (i=1; i<=Rno; i++){                 //for each relay wanted
                                z=i-1;                                          //take relay # and
convert to Port A Pin out
                                if (z>=5){z+=1;}                //necessary to avoide PIN A5 (MCLR)
since we cant be messing with that one
                                bit_set(Rout,z);                //set bit in Relay output
                                output_a(Rout);                         //output to port a
                                delay_ms(Rtime);                //delay required amount of time
                                //bit_clear(Rout,z);            //clear bit to stop output next time
round
                                Rout=0;                                 //easier/quicker to
clear whole byte???!
                }
        }
}

else if ( paired==1 && bit_test(Rused,0)==1){         //PAIRED AND ALL RELAYS USED
ClearScreen();
fprintf(LCD, "Paired/All Relays");
output_high(activeLED);
        while (!input(ButtonMenu)){
                output_toggle(countLED);
                        for (i=1; i<=Rno; i++){                 //for each relay wanted
                                z=i-1;                                          //take relay # and
convert to Port A Pin out
                                x=i;
                                if (z>=5){z+=1;}                //necessary to avoide PIN A5 (MCLR)
since we cant be messing with that one
                                if (x>=5){x+=1;}                //necessary to avoide PIN A5 (MCLR)
since we cant be messing with that one
```

```
                                        bit_set(Rout,x);                //set 1st bit in Paired Relay output
                                        bit_set(Rout,z);                //set 2nd bit in Paired Relay output
                                        output_a(Rout);                         //output to port a
                                        delay_ms(Rtime);                //delay required amount of time
                                        //bit_clear(Rout,z);            //clear bit to stop output next time
round
                                        Rout=0;                                                 //easier/quicker to
clear whole byte???!
                        }
                }
}

else if ( paired==0 && bit_test(Rused,0)==0){           //SEQUENTIAL AND SELECTED RELAYS USED
ClearScreen();
fprintf(LCD, "Sequential/Selected Relays");
output_high(activeLED);
        while (!input(ButtonMenu)){
                output_toggle(countLED);
                x=1;
                        for (i=1; i<=Rno; i++){

                                        while (bit_test(Rused,x)==0){   //find next wanted relay
                                                x++;
                                        }
                                        z=x-1;                                          //take relay # and
convert to Port A Pin out
                                        if (z>=5){z+=1;}                //MCLR deal
                                        bit_set(Rout,z);                //set required bit in Relay output
                                        output_a(Rout);                         //output to port a
                                        delay_ms(Rtime);                //delay required amount of time
                                        Rout=0;                                         //easier/quicker to
clear whole byte???!
                                        x++;
                                }
        }

}


else if ( paired==1 && bit_test(Rused,0)==0){           //PAIRED AND SELECTED RELAYS USED
ClearScreen();
fprintf(LCD, "Paired/Selected Relays");
output_high(activeLED);
        p=0;
```

```
        while (!input(ButtonMenu)){
                output_toggle(countLED);
                x=1;
                j=1;
                        for (i=1; i<=Rno; i++){

                                if (p==0){
                                        while (bit_test(Rused,j)==0){          //find next 1st
wanted relay
                                                j++;
                                        }
                                        p=j-1;
                                        x=j+1;
                                }

                                while (bit_test(Rused,x)==0){         //find next wanted relay
                                        x++;
                                }
                                z=x-1;                                                  //take relay #
and convert to Port A Pin out

                                if (p>=5){p+=1;}                      //MCLR deal
                                if (z>=5){z+=1;}                      //MCLR deal
                                bit_set(Rout,z);                      //set required bit in Relay output
                                bit_set(Rout,p);                      //set required bit in Relay output
                                output_a(Rout);                               //output to port a
                                delay_ms(Rtime);                      //delay required amount of time
                                Rout=0;                                         //easier/quicker to
clear whole byte???!
                                x++;
                                p=z;                                            //set previous p as z

                        }
        }

}

        else {
                ClearScreen();
                fprintf(LCD, "Error... Restarting!");
                delay_ms(1000);
                reset_cpu();
        }
output_low(activeLED);
```

```
output_low(countLED);
ClearScreen();
fprintf(LCD, "Sequence has been quit. Good bye");
delay_ms(1000);
ClearScreen();

}

//Functions//

void SetupLCD(){
  #define control 0x7C
  #define command 0xFE
  fputc(control, LCD); //Set to 9600 BAUD
  fputc('r', LCD);
  delay_ms(100);
  //fputc(control, LCD); //Set 16 character width
  //fputc(4, LCD);
  //delay_ms(100);
  //fputc(control, LCD); //Set 2 line LCD
  //fputc(6, LCD);
  //delay_ms(100);
  fputc(control, LCD); //Set to brightest display
  fputc(157, LCD);
  delay_ms(100);
  fprintf(LCD, "Display Ready"); //Print Message
  delay_ms(1000); //Wait 1 second
  fputc(command, LCD); //Clear display
  fputc(1, LCD);
  delay_ms(100);
}

void ClearScreen(){
  fputc(command, LCD);
  fputc(1, LCD);
  delay_ms(300);
}

void flashAll(long time,int times){
        for (i=0; i<=times; i++){
                output_toggle(menuLED);
                output_toggle(countLED);
                output_toggle(activeLED);
```

```
                delay_ms(time);
                }
        output_low(menuLED);
        output_low(countLED);
        output_low(activeLED);
}


int pushButton(){
int freshPress=0;
        if (input(ButtonSelect)){                               //button pushed?
                                delay_ms(20);                                   //deals with bounce
                                        if (input(ButtonSelect)&& ButState==0){ //Still pushed and wasnt
pushed last time round?
                                                                freshPress=1;
        //Do some shit
                                                                        ButState=1;
                //flag push
                                                        }
                }else if (input(!ButtonSelect)){ButState=0;}            //no longer pushed? unset flag


return (freshPress);
}
```

9.6.2 Coating Apparatus Code

9.6.2.1 Initial Version

```
#include <16f1827.h>
#fuses NOWDT,INTRC_IO, PLL, PUT, NOPROTECT
#fuses MCLR, NOCPD, BROWNOUT, NOIESO, FCMEN
#fuses CLKOUT, NOWRT, NOSTVREN, BORV25, NOLVP
#DEVICE ADC=10
#use delay(clock=32000000)

#use RS232(STREAM=BT, BAUD=9600,PARITY=N, ERRORS, UART1)
#define cw 0
#define ccw 1

int i;
long time = 8000;
int stepno;
int flag = 0;
int press =0;
```

```
#int_ext
void ISR_EXT(){
	delay_ms(250);
	if (input(PIN_B0)==1){
		delay_ms(1000);
			if (input(PIN_B0)==1){
				output_a(0x00);
				if (flag==1){
					flag=0;
				}
				else{
					flag=1;
				}
			}
	}
	press++;

	if (press>=5){
		press=0;
	}
	if (press == 0){
		time=1000;
		output_low(PIN_A7);
		output_low(PIN_A6);
		output_low(PIN_B4);
		output_low(PIN_B3);
	}
	else if (press == 1){
		time=750;
		output_high(PIN_A7);
		output_low(PIN_A6);
		output_low(PIN_B4);
		output_low(PIN_B3);
	}
	else if (press == 2){
		time=500;
		output_high(PIN_A6);
		output_low(PIN_A7);
		output_low(PIN_B4);
		output_low(PIN_B3);
	}
	else if (press == 3){
		time=250;
```

```
                output_high(PIN_B4);
                output_low(PIN_A7);
                output_low(PIN_A6);
                output_low(PIN_B3);
        }
        else {
                time=10;
                output_high(PIN_B3);
                output_low(PIN_A7);
                output_low(PIN_A6);
                output_low(PIN_B4);
        }

        fprintf(BT, "%Lu\n" time);
        CLEAR_INTERRUPT(INT_EXT);
}

//~~Function prototypes~~
int letsStep(short direc, long steps, long time, int stepno);

//~~Main program~~
void main(){
        enable_interrupts(GLOBAL);
        enable_interrupts(INT_EXT_L2H);
        while(1){
                if (flag==0){
                        stepno = letsStep(ccw, 1, time, stepno);
                }
        }
}


//~~~~~~~Functions~~~~~~~~~~

int letsStep(short direc, long steps, long time, int stepno){
long count;
int currentStep;
currentStep=stepno;

for(count=0; count<steps; count++){
        if (direc==cw){
                currentStep-=1;
        if (currentStep==0){
```

```
                currentStep=4;
        }
        }
        else if (direc==ccw){
                currentStep+=1;
                if (currentStep>4){
                        currentStep=1;
        }
        }
        else{}

        if( currentStep==1){                    //0x06
                output_a (0x06);
        }
        else if( currentStep==2){       //0x05
                output_a (0x05);
        }
        else if( currentStep==3){       //0x09
                output_a (0x09);
        }
        else if( currentStep==4){       //0x0C
                output_a (0x0A);
        }
        else{}

        delay_ms(time);
}
return currentStep;
}
```

9.6.2.2 *Final Version*

9.6.2.2.1 *Linear Movement Controller*

```
//feed rate: v=0.045*2pi*rps


#include <16f1827.h>

#fuses NOWDT,INTRC_IO, PLL, NOPUT, NOPROTECT, MCLR, NOCPD, NOBROWNOUT, NOIESO, NOFCMEN

#fuses NOCLKOUT, NOWRT, NOSTVREN, NOLVP, NODEBUG

#DEVICE ADC=10

#use delay(clock=32000000

#use RS232(STREAM=BT, BAUD=9600,PARITY=N, ERRORS, UART1)
```

```
#include <stdlib.h>

//step size for desired rpm
#define RPM12us 52083
#define RPM24us 26042
#define RPM36us 17361
#define RPM48us 13021

//native linear speed
#define LIN12 1.88496
#define LIN24 3.76992
#define LIN36 5.65488
#define LIN48 7.53984

#define cw 0
#define ccw 1
float mps, linear;
long ms, us, usR, remainder, finalDelay;
long long msHOLD, time0, timeF;
int isr_value;
int stepno;
int value, whole, j=0;
short flag=0, flag2=0;
int direc=2;
char input[6];
int letsStep(short direc, long steps, int stepno);
void menu();
void checkBT();
//***********Interrupts*********************//

#INT_RDA
```

```
void rda_isr(){

isr_value=fgetc(BT);
if(isr_value==13){//return
menu();
checkBT();
}
clear_interrupt(INT_RDA);
}

//********MAIN**********//
void main(){
value=RESTART_CAUSE();
delay_ms(500);

fprintf(BT, "***Reset cause: %x***\r\n\n", value);
while(!kbhit(BT));
fgetc(BT);
menu();
checkBT();

  enable_interrupts(INT_RDA);
  enable_interrupts(GLOBAL);

while(flag==1){
  stepno = letsStep(1, 1, stepno);
  delay_ms(ms);
  delay_us(us);
}
while(flag==0){
  stepno = letsStep(0, 1, stepno);
```

```
  delay_ms(ms);
  delay_us(us);
}
}

//**********Functions**********

int letsStep(short direc, long steps, int stepno){
long count;
int currentStep;

currentStep=stepno;

for(count=0; count<steps; count++)
{
    if (direc==cw)
    {
        currentStep-=1;
        if (currentStep==0)
        {
            currentStep=4;
      }
    }
    else if (direc==ccw)
    {
        currentStep+=1;
        if (currentStep>4)
        {
            currentStep=1;
        }
      }
```

```
  else
  {
}

  if( currentStep==1) //0x06
  {
      output_a (0x06);
  }
  else if( currentStep==2)   //0x05
  {
      output_a (0x05);
  }
  else if( currentStep==3) //0x09
  {
      output_a (0x09);
  }
  else if( currentStep==4) //0x0C
  {
      output_a (0x0A);
  }
  else
     {
     }
    }
    return currentStep;
}

void Menu(){
    fprintf(BT, "Reel to reel\r\n\n");
    fprintf(BT, "Choose direction(L or R:\r\n");
    fprintf(BT, "Choose speed in mm/s(0.01mm/s to 10mm/s)\r\n\n");
```

```
//total range: 0.01mm/s to 9.99mm/s
    fprintf(BT, "Send L or R during to change Direction\r\n\n");
}
void checkBT(){
    while(!kbhit(BT));
   value=fgetc(BT);
    if (value=='R'){
        direc=1;
    }
    if (value=='L'){
        direc=0;
    }
    fprintf(BT, "direction = %u\r\n", direc);
    while(!kbhit(BT));
     fgets(input,BT);
    mps=atof(input);
    fprintf(BT, "input = %1.4fmm/s\r\n", mps);
    while(fgetc(BT)!='r' );
    while(!kbhit(BT));



  value=fgetc(BT);
  if (value =='n'){
       linear=0;
   }
if (value =='1'){
     usR=RPM48us;
      //mps=LIN48-mps;
     linear=LIN48;
}
```

```
if (value =='2'){
     usR=RPM36us;
    linear=LIN36;
}
if (value =='3'){
     usR=RPM24us;
    linear=LIN24;
}
if (value =='4'){
     usR=RPM12us;
     linear=LIN12;
}

if (linear<mps){
    mps=mps-linear;
    flag=1;
}
else{
    mps=linear-mps;
    flag=0;
}
delay_ms(1000);
fprintf(BT, "speed needed = %fus\r\n", mps);
mps=mps/1000;
mps=mps/0.0047124;
mps=mps*48;
mps = 1/mps;
mps = mps*1000;
mps = mps*1000;
msHOLD = (long long)mps;
fprintf(BT, "time between steps = %fus\r\n", mps);
```

```
fprintf(BT, "compensation set\r\n\n");
     ms=msHOLD/1000;
     us=msHOLD%1000;
     fprintf(BT, "ms= %LU\r\n\n", ms);
    fprintf(BT, "us= %lu\r\n\n", us);
}
```

9.6.2.2.2 *Rotational Movement Controller*

```
#include <16f1827.h>
#fuses NOWDT,INTRC_IO, PLL, PUT, NOPROTECT, MCLR, NOCPD, NOBROWNOUT, NOIESO, FCMEN
#fuses NOCLKOUT, NOWRT, NOSTVREN, BORV25, NOLVP, NODEBUG
#use delay(clock=32000000)

#use RS232 (BAUD=9600, UART1, STREAM=BT, ERRORS)

//**********Global Defines**********
//StepMotors
#define M1en      PIN_B4
#define M2en       PIN_B5
//Step Motor
#define brown       PIN_A3
#define black       PIN_A2
#define yellow      PIN_A1
#define orange       PIN_A0

#define relay      PIN_B3
#define LED      PIN_A4
//Direction
#define cw 0
#define ccw 1

#define M1 0
#define M2 1

//**********Global Variables**********

long AllStepsTotal=0;
long i, FRate, time;
int passes, isr_value;
int value=0;
int selection=0;
```

```
//**********Function Prototypes**********
void letsStep(short direc, long steps, long time);

void checkBT();

//************Interrupts*********************//
#INT_RDA
void rda_isr(){
   isr_value=fgetc(BT);
   if(isr_value==114){//r
        reset_cpu();
   }
   clear_interrupt(INT_RDA);
}

//////////////////////MAIN PROGRAM//////////////////////////
void main(){
checkBT();
output_high(PIN_B4);

output_high(PIN_B5);
i=60000;
   while(i>8000){
       letsStep(cw, 1, i);
        i-=100;
        enable_interrupts(INT_RDA);
        enable_interrupts(GLOBAL);
    }

fprintf(BT, "***At Speed***\r\n\n");
   while (1){
      letsStep(cw, 1, time);
   }
}

//**********Functions**********

void letsStep(short direc, long steps, long time){
long count;
int currentStep;
currentStep=currentStepM1;

for(count=0; count<steps; count++)
```

```
{
     if (direc==cw)
    {
       currentStep-=1;
       if (currentStep==0)
      {
           currentStep=4;
      }
    }
   else if (direc==ccw)
  {
       currentStep+=1;
       if (currentStep>4)
      {
       currentStep=1;
      }
  }
 else
 {
 }

 if( currentStep==1) //0x06
 {
     output_a (0x06);
 }
 else if( currentStep==2)   //0x05
 {
     output_a (0x05);
 }
 else if( currentStep==3) //0x09
 {
     output_a (0x09);
 }
 else if( currentStep==4) //0x0C
 {
     output_a (0x0A);
 }
 else
 {
 }
   delay_us(time);
 }
}
```

```
void checkBT(){
  while(value!=114){
     while(!kbhit(BT));
     value=fgetc(BT);
  }
    if(value==114){
        fprintf(BT, "RPM: 1(48) 2(36) 3(24) or 4(12)\r\n\n");
        while(!kbhit(BT));
        selection=fgetc(BT);
         selection-=48;
         fprintf(BT, "Speed: %u\r\n\n", selection);

       if(selection==1){
           fprintf(BT, " 48rpm\r\n\n");
           time=8681;     //us
       }
       if (selection==2){
            fprintf(BT, " 36rpm\r\n\n");
            time=11574;   //us
       }
       if (selection==3){
             fprintf(BT, " 24rpm\r\n\n");
             time=17361;   //us
       }
       if (selection==4){
             fprintf(BT, " 12rpm\r\n\n");
             time=34722;   //us
       }

    }
}
```

9.6.3 Electrode Braiding Apparatus Code - Final Version

```
#include <16F1789.h>
#fuses INTRC_IO, NOWDT, BROWNOUT, BORV25, MCLR
#fuses NOPROTECT,NOLVP, NOCPD, NOCLKOUT, NOVCAP,DEBUG
#use delay(internal=32M)
#USE RS232(baud=9600, xmit=PIN_B6,rcv=PIN_B6, stream=LCD)
#define BCD_A              PIN_B1
#define BCD_B              PIN_B2
#define BCD_C              PIN_B3
#define BCD_D              PIN_B4
```

```
#define LED_A           PIN_D4
#define LED_B           PIN_D5
#define LED_C           PIN_D6
#define LED_D           PIN_D7
#define LED_INHIB       PIN_B7


#define black           PIN_D0
#define orange          PIN_D1
#define brown           PIN_D2
#define yellow          PIN_D3

#define cw                      0
#define ccw             1
//stepper motors
#define smOFF 0x00
#define sm1 0x02
#define sm2 0x04
#define sm3 0x06
#define sm4 0x08
#define sm5 0x0A
#define sm6 0x0C
#define sm7 0x0E
#define sm8 0x10
#define sm9 0x12
//LEDs
#define LED1 0x00
#define LED2 0x10
#define LED3 0x20
#define LED4 0x30
#define LED5 0x40
#define LED6 0x50
#define LED7 0x60
#define LED8 0x70
#define LED9 0x80
#define LED10 0x90
#define LED11 0xA0
#define LED12 0xB0
#define LED13 0xC0
#define LED14 0xD0
#define LED15 0xE0
#define LED16 0xF0
```

```
//~~GLOBAL VARIABLES

int i,j,count;
int firstalign=0;
long triggered = 0; //to hold 16 hall effect trigger values
long oldtrig=0;
int LEDs[]={LED1,LED2,LED3,LED4,LED5,LED6,LED7,LED8,LED9,LED10,LED11,LED12,LED13,LED14,LED15,LED16};
int motors[]={smOFF,sm1,sm2,sm3,sm4,sm5,sm6,sm7,sm8,sm9};
int currentSteps[]={1,1,1,1,1,1,1,1,1,1};
int fooflags[]={0,0,0,0,0,0,0,0};
int reel=0;
short cwccw, aligned;
short fooflag=0;
int timing=0;
int manyTrig=0;

//~~FUNCTION PROTOTYPES
int letsStep(short direc, long steps, int time, int motor);
void enableIOC();
void disableIOC();

//~~ISRs
#INT_EXT                                        //~~Emergency stop button
void isr_EXT(){
        output_b(motors[0]);            //~~Stop motors
        //~~Flash LEDs while button is held
        while(input(PIN_B0)==1){
                output_high(PIN_E0);
                delay_ms(500);
                output_low(PIN_E0);
                output_high(PIN_E1);
                delay_ms(500);
                output_low(PIN_E1);
                output_high(PIN_E2);
                delay_ms(500);
                output_low(PIN_E2);
        }
}

#INT_IOC                                        //~~Interrupt on change
void isr_IOC(){         //~~Process state changes on mag sensors
        int changes;
```

```
        oldtrig=triggered;          //~~Save pervious sensor states

        //~~Look for changes and sort on the whole of port A
        changes = input_change_a();

//~~~~~~~~A0~~~~~~~~~//

        if (bit_test(changes,0)) {
    //~~Here RA0 has changed
                if (input(PIN_A0)&& aligned==1) {
                        //~~ (UNUSED) light LED Corresponding to sensor
                        //output_d(LEDs[16]);
                        bit_clear(triggered, 0);

                }
                else {
                        //~~ (UNUSED) light LED Corresponding to sensor
                        //output_d(LEDs[16]);
                        bit_set(triggered, 0);
                        manyTrig++;
        }
        }

        //~~~~~~~~A1~~~~~~~~~//

        else if (bit_test(changes,1)) {
    //~~Here RA1 has changed
        if (input(PIN_A1)&& aligned==1) {
                        output_d(LEDs[15]);
                        bit_clear(triggered, 1);
                }
        else {
                        output_d(LEDs[15]);
                        bit_set(triggered, 1);
                        manyTrig++;
        }
        }

        //~~~~~~~~A2~~~~~~~~~//

        else if (bit_test(changes,2)) {
    //~~Here RA2 has changed
                if (input(PIN_A2)&& aligned==1) {
```

```
                        bit_clear(triggered, 2);
        }
        else {
                        bit_set(triggered, 2);
                        manyTrig++;
                }
        }

        //~~~~~~~~A3~~~~~~~~~//

        else  if (bit_test(changes,3)) {
        //~~Here RA3 has changed
        if (input(PIN_A3)&& aligned==1) {
                        bit_clear(triggered, 3);
        }
                else {
                        bit_set(triggered, 3);
                        manyTrig++;
        }
        }

        //~~~~~~~~A4~~~~~~~~~//

        else if (bit_test(changes,4)) {
//~~Here RA4 has changed
        if (input(PIN_A4)&& aligned==1) {
                        bit_clear(triggered, 4);
        }
                else {
                        bit_set(triggered, 4);
                        manyTrig++;
                }
        }

        //~~~~~~~~A5~~~~~~~~~//

        else if (bit_test(changes,5)) {
//~~Here RA5 has changed
                if (input(PIN_A5) && aligned==1) {
                        bit_clear(triggered, 5);
                }
                else {
                        bit_set(triggered, 5);
```

```
                manyTrig++;
        }
        }

        //~~~~~~~~~A6~~~~~~~~~~//

        else if (bit_test(changes,6)) {
//~~Here RA6 has changed
                if (input(PIN_A6) && aligned==1) {
                        bit_clear(triggered, 6);
                }
                else {
                        bit_set(triggered, 6);
                        manyTrig++;
        }
        }

        //~~~~~~~~~A7~~~~~~~~~~//

        else if (bit_test(changes,7)) {
//~~Here RA7 has changed
                if (input(PIN_A7) && aligned==1) {
                        bit_clear(triggered, 7);
        }
        else {
                        bit_set(triggered, 7);
                        manyTrig++;
        }
        }


        //~~Same again for PORT C
        //~~Detect changes and then sort through them
        changes = input_change_c();

        //~~~~~~~~~C0~~~~~~~~~~//

        if (bit_test(changes,0)) {
//~~Here RC0 has changed
        if (input(PIN_C0)&& aligned==1) {
                        bit_clear(triggered, 8);
        }
                else {
```

```
                        bit_set(triggered, 8);
                        manyTrig++;
        }
        }

//~~~~~~~~C1~~~~~~~~~//

        else if (bit_test(changes,1)) {
   //~~Here RC1 has changed
                if (input(PIN_C1)&& aligned==1) {
                        bit_clear(triggered, 9);
        }
                else {
                        bit_set(triggered, 9);
                        manyTrig++;
        }
        }

        //~~~~~~~~C2~~~~~~~~~//

        else if (bit_test(changes,2)) {
   //~~Here RC2 has changed
        if (input(PIN_C2)&& aligned==1) {
                        bit_clear(triggered, 10);
                }
        else {
                        bit_set(triggered, 10);
                        manyTrig++;
        }
        }

        //~~~~~~~~C3~~~~~~~~~//

        else if (bit_test(changes,3)) {
   //~~Here RA3 has changed
                if (input(PIN_C3) && aligned==1) {
                        bit_clear(triggered, 11);
        }
        else {
                        bit_set(triggered, 11);
                        manyTrig++;
        }
        }
```

```
        //~~~~~~~~C4~~~~~~~~~//

        else if (bit_test(changes,4)) {
//~~Here RC0 has changed
        if (input(PIN_C4) && aligned==1) {
                        bit_clear(triggered, 12);
        }
        else {
                        bit_set(triggered, 12);
                        manyTrig++;
        }
        }

        //~~~~~~~~C5~~~~~~~~~//

        else if (bit_test(changes,5)) {
//~~Here RC0 has changed
        if (input(PIN_C5) && aligned==1) {
                        bit_clear(triggered, 13);
                }
        else {
                        bit_set(triggered, 13);
                        manyTrig++;
        }
        }

        //~~~~~~~~C6~~~~~~~~~//

        else if (bit_test(changes,6)) {
//~~Here RC0 has changed
        if (input(PIN_C6) && aligned==1) {
                        bit_clear(triggered, 14);
        }
        else {
                        bit_set(triggered, 14);
                        manyTrig++;
        }
        }

        //~~~~~~~~C7~~~~~~~~~//

        else if (bit_test(changes,7)) {
```

```
   //~~Here RC7 has changed
        if (input(PIN_C7) && aligned==1) {
                        bit_clear(triggered, 15);
        }
        else {
                        bit_set(triggered, 15);
                        manyTrig++;
        }
        }

        //~~Check which port should be aligning
        //~~If this is the first state change detected
        if (oldtrig==0 && triggered>0){
                //~~Check which part of the 16-bit word has changed to          //~~determine which
port the state change was on.
                if(triggered < 0x00FF){
                //~~port a first aligned
                        firstalign=1;
                        output_high(PIN_E0);
                }
                else{
                //~~port c first aligned
                        firstalign=2;
                        output_high(PIN_E1);
                }
        }

//~~Interrupts must all be cleared before return to stop multiple triggers per single valid state change

        CLEAR_INTERRUPT(INT_IOC_A0);
        CLEAR_INTERRUPT(INT_IOC_A1);
        CLEAR_INTERRUPT(INT_IOC_A2);
        CLEAR_INTERRUPT(INT_IOC_A3);
        CLEAR_INTERRUPT(INT_IOC_A4);
        CLEAR_INTERRUPT(INT_IOC_A5);
        CLEAR_INTERRUPT(INT_IOC_A6);
        CLEAR_INTERRUPT(INT_IOC_A7);
        CLEAR_INTERRUPT(INT_IOC_C0);
        CLEAR_INTERRUPT(INT_IOC_C1);
        CLEAR_INTERRUPT(INT_IOC_C2);
        CLEAR_INTERRUPT(INT_IOC_C3);
        CLEAR_INTERRUPT(INT_IOC_C4);
        CLEAR_INTERRUPT(INT_IOC_C5);
```

```
	CLEAR_INTERRUPT(INT_IOC_C6);
	CLEAR_INTERRUPT(INT_IOC_C7);
}


void main(){
	fprintf(LCD, "Weaving rig   V2.9.5");

	for (j=0; j<10; j++){
		for (i=1; i<9; i++){
			if (i & 0x01){
				cwccw=ccw;
			}
			else{
				cwccw=cw;
			}
			output_b(motors[i]);
			currentSteps[i] = letsStep(cwccw, 1, 10, currentSteps[i]);
		}
	}
	//~~Enable IOC on port A and C
	input_change_a();
	input_change_c();
	ENABLE_INTERRUPTS(INT_IOC_A0);
	ENABLE_INTERRUPTS(INT_IOC_A1);
	ENABLE_INTERRUPTS(INT_IOC_A2);
	ENABLE_INTERRUPTS(INT_IOC_A3);
	ENABLE_INTERRUPTS(INT_IOC_A4);
	ENABLE_INTERRUPTS(INT_IOC_A5);
	ENABLE_INTERRUPTS(INT_IOC_A6);
	ENABLE_INTERRUPTS(INT_IOC_A7);
	ENABLE_INTERRUPTS(INT_IOC_C0);
	ENABLE_INTERRUPTS(INT_IOC_C1);
	ENABLE_INTERRUPTS(INT_IOC_C2);
	ENABLE_INTERRUPTS(INT_IOC_C3);
	ENABLE_INTERRUPTS(INT_IOC_C4);
	ENABLE_INTERRUPTS(INT_IOC_C5);
	ENABLE_INTERRUPTS(INT_IOC_C6);
	ENABLE_INTERRUPTS(INT_IOC_C7);
	ENABLE_INTERRUPTS(INT_EXT);
	ENABLE_INTERRUPTS(GLOBAL);

	output_low(PIN_B7);
```

```
while(1){
	for (i=1; i<9; i++){
		if (i & 0x01){
			cwccw=ccw;
		}
		else{
			cwccw=cw;
		}
		if (manyTrig > 6){
			timing = 50;
		}
		else{
			timing=6;
		}


	if (bit_test(triggered, (i-1))==0 && bit_test(triggered, (i+7))==0 ){

		output_b(motors[i]);
		currentSteps[i] = letsStep(cwccw, 1, timing, currentSteps[i]);
		output_low(PIN_E0);
		output_low(PIN_E1);
	}

	else if (bit_test(triggered, (i-1))==1 && firstalign ==2 && bit_test(triggered, (i+7))==0){
		cwccw = !cwccw;
		output_high(PIN_E0);
		while(bit_test(triggered, (i+7))==0){
	output_b(motors[i]);
			currentSteps[i] = letsStep(cwccw, 1, 1000, currentSteps[i]);
			output_low(PIN_E0);
			output_low(PIN_E1);
		}
	currentSteps[i] = letsStep(cwccw, 3, 1000, currentSteps[i]);
	}

	else if (bit_test(triggered, (i+7))==1 && firstalign ==1 && bit_test(triggered, (i-1))==0){
		cwccw = !cwccw;
		output_high(PIN_E1);
		while(bit_test(triggered, (i-1))==0){
			output_b(motors[i]);
			currentSteps[i] = letsStep(cwccw, 1, 1000, currentSteps[i]);
			output_low(PIN_E0);
```

```
                                        output_low(PIN_E1);
}
                                currentSteps[i] = letsStep(cwccw, 3, 1000, currentSteps[i]);
                        }

        }

////////////////////////////////////////////////
//~~If all sensors are correctly aligned reset

if(triggered == 0xFF00 || triggered == 0x00FF){
        disableIOC();
        output_low(PIN_E0);
        output_low(PIN_E1);
        fooflag=0;
firstalign=0;
        output_high(PIN_E2);
        delay_ms(1000);
        aligned=1;

        for (j=0; j<15; j++){
                for (i=1; i<9; i++){
                        if (i & 0x01){
                                cwccw=ccw;
                        }
                        else{
                                cwccw=cw;
                        }
                        output_b(motors[i]);
                        currentSteps[i] = letsStep(cwccw, 1, 8, currentSteps[i]);
                }
        }
        triggered=0;
        manyTrig=0;
        output_low(PIN_E2);
        reel++;
        if (reel==8){
                output_b(motors[9]);
                currentSteps[9] = letsStep(cw, 10, 2, currentSteps[9]);
                reel=0;
        }
        enableIOC();
}
```

```
}
}

//~~~~~~~~~~~Functions~~~~~~~~~~~~
//~~ Drive Stepper motor
int letsStep(short direc, long steps, int time, int motor){
	long count;
	int currentStep;

	currentStep = motor;

	for(count = 0; count < steps; count++){
		if (direc==cw){
			currentStep-=1;
		if (currentStep==0){
			currentStep=4;
		}
		}
		else if (direc==ccw){
			currentStep+=1;
		if (currentStep>4){
			currentStep=1;
		}
		}
		else{}

		if( currentStep==1){				//~~0x06
			output_d (0x06);
		}
		else if( currentStep==2){		//~~0x06
			output_d (0x03);
		}
		else if( currentStep==3){		//~~0x09
			output_d (0x09);
		}
		else if( currentStep==4){		//~~0x0C
			output_d (0x0C);
		}
		else{}
		delay_ms(time);
	}
	return currentStep;
}
```

```
//~~Enable inurrupts on state change on port A and C
void enableIOC(){
        ENABLE_INTERRUPTS(INT_IOC_A0);
        ENABLE_INTERRUPTS(INT_IOC_A1);
        ENABLE_INTERRUPTS(INT_IOC_A2);
        ENABLE_INTERRUPTS(INT_IOC_A3);
        ENABLE_INTERRUPTS(INT_IOC_A4);
        ENABLE_INTERRUPTS(INT_IOC_A5);
        ENABLE_INTERRUPTS(INT_IOC_A6);
        ENABLE_INTERRUPTS(INT_IOC_A7);
        ENABLE_INTERRUPTS(INT_IOC_C0);
        ENABLE_INTERRUPTS(INT_IOC_C1);
        ENABLE_INTERRUPTS(INT_IOC_C2);
        ENABLE_INTERRUPTS(INT_IOC_C3);
        ENABLE_INTERRUPTS(INT_IOC_C4);
        ENABLE_INTERRUPTS(INT_IOC_C5);
        ENABLE_INTERRUPTS(INT_IOC_C6);
        ENABLE_INTERRUPTS(INT_IOC_C7);
}

//~~Disable inurrupts on state change on port A and C
void disableIOC(){
        DISABLE_INTERRUPTS(INT_IOC_A0);
        DISABLE_INTERRUPTS(INT_IOC_A1);
        DISABLE_INTERRUPTS(INT_IOC_A2);
        DISABLE_INTERRUPTS(INT_IOC_A3);
        DISABLE_INTERRUPTS(INT_IOC_A4);
        DISABLE_INTERRUPTS(INT_IOC_A5);
        DISABLE_INTERRUPTS(INT_IOC_A6);
        DISABLE_INTERRUPTS(INT_IOC_A7);
        DISABLE_INTERRUPTS(INT_IOC_C0);
        DISABLE_INTERRUPTS(INT_IOC_C1);
        DISABLE_INTERRUPTS(INT_IOC_C2);
        DISABLE_INTERRUPTS(INT_IOC_C3);
        DISABLE_INTERRUPTS(INT_IOC_C4);
        DISABLE_INTERRUPTS(INT_IOC_C5);
        DISABLE_INTERRUPTS(INT_IOC_C6);
        DISABLE_INTERRUPTS(INT_IOC_C7);
        CLEAR_INTERRUPT(INT_IOC_A0);
        CLEAR_INTERRUPT(INT_IOC_A1);
        CLEAR_INTERRUPT(INT_IOC_A2);
        CLEAR_INTERRUPT(INT_IOC_A3);
```

```
        CLEAR_INTERRUPT(INT_IOC_A4);
        CLEAR_INTERRUPT(INT_IOC_A5);
        CLEAR_INTERRUPT(INT_IOC_A6);
        CLEAR_INTERRUPT(INT_IOC_A7);
        CLEAR_INTERRUPT(INT_IOC_C0);
        CLEAR_INTERRUPT(INT_IOC_C1);
        CLEAR_INTERRUPT(INT_IOC_C2);
        CLEAR_INTERRUPT(INT_IOC_C3);
        CLEAR_INTERRUPT(INT_IOC_C4);
        CLEAR_INTERRUPT(INT_IOC_C5);
        CLEAR_INTERRUPT(INT_IOC_C6);
        CLEAR_INTERRUPT(INT_IOC_C7);
}
```